H24/3467

MONASH UNIVERSITY
THESIS ACCEPTED IN SATISFACTION OF THE
REQUIREMENTS FOR THE DEGREE OF
DOCTOR OF PHILOSOPHY
ON..... 4 April 2003 .....
.....[redacted].....
Sec. Research Graduate School Committee

An Antisense Approach to Study the Role of Arginine Decarboxylase and Putrescine *N*-Methyltransferase in Alkaloid Metabolism in *Nicotiana tabacum* L.

A thesis submitted for the degree of
Doctor of Philosophy

Yupynn Chintapakorn
B.Sc. in Pharm., M.Sc. in Pharm. (Pharmacognosy)

School of Biological Sciences
Monash University
Melbourne, Australia

November, 2002

Addendum

It is pleasing that both referees commented very positively on my thesis, its coverage of the topic and the consideration of the results that were obtained. I am grateful for their questions/constructive criticisms and for their recommendations that the thesis be accepted for the degree of PhD without further examination subject to inclusion of minor corrections and consideration of a number of points that were noted. My thanks to J. Arvanitakis and A. Pelosi for their help in preparing this addendum.

Yupynn Chintapakorn
Dept of Botany, Faculty of Science
Chulalongkorn University,
Bangkok, Thailand
28th Feb 2003.

In response to queries from the examiners, the following responses are made.

Query 1. Are standard error bars (eg Figs 3-4, 3-5, 3-18, 4-10) valid when the sample size is less than 3?

For reasons of practicality, it was not feasible to analyse multiple samples at many time points for the relatively large number of root lines and plants that were generated in this study. In many experiments, duplicate samples were analysed to obtain alkaloid levels and/or RNA for northern analysis. In order to provide a measure of the variability in the data obtained, standard errors of the mean were calculated and shown as error bars in figures as presented in this thesis. The validity of this approach was affirmed by consultation with statistical experts at Monash University (Schools of Biological Sciences and also Mathematics & Statistics) who advised that it is possible to generate a standard error of the mean when the sample size is greater than one. It is acknowledged, however, that larger samples sizes are desirable, whenever this is practicable, in order to calculate more accurate standard errors of the mean. Consultation with a statistical expert in the Department of Mathematics at Chulalongkorn University suggests that a sample size of five or greater would be appropriate in such cases.

Query 2. Why is the fresh weight of root inoculum given as 0.8 g (page 68) when growth curves (eg Figs 3-4, 3-21 and 4-17) show lower fresh weights during the early stages of the growth phase?

These apparent differences relate to the 'wet' fresh weight of root tissue that was used to inoculate root cultures as opposed to the 'blotted' fresh weight of cultures that was recorded after harvest and before processing for alkaloids/RNA/enzyme analysis. For practical reasons it is not advisable to blot transformed root tissues to remove all surrounding medium if they are then to be used as inocula. This is because such procedures could lead to damage of root tissues, thus possibly compromising their subsequent growth patterns. Such procedures also tend to greatly increase the chances of fungal contamination of the cultures – even if sterile blotting paper is used.

Query 3. Do growth curves of roots in culture really show evidence of a lag phase as suggested on pages 106 and 124 with reference to Figs 3-21 and 4-17?

This is a good point. Replotting data of these growth curves on semi-log graph paper shows a linear increase in (blotted) fresh weight during the first 12 days of growth. This suggests that the growth rate is exponential during this period and then tapers off during the second half of the growth cycle.

approach appears to be very efficient in silencing endogenous genes (Wesley *et al.*, 2001). The development of these vectors is based upon recent breakthroughs in understanding RNAi, a process by which double stranded RNA is both recognised and then degraded in eukaryotic cells. Though many details remain to be elucidated, clearly this is a sophisticated post-transcriptional gene silencing (PTGS) mechanism that is conserved in plants, animals and fungi. It appears to offer protection against viral infection and possibly also against disruption of the genome by transposable elements. RNAi may also play important roles in regulating expression of genes that are important in development (Waterhouse *et al.*, 2001; Vance and Vaucheret, 2001; Hutvagner and Zamore, 2002). Several genes required for PTGS have been identified. Collectively the proteins encoded by these genes recognise regions of double stranded (ds) RNA and break that RNA into short interfering ds RNA molecules 21– 25 bases in length via the action of an enzyme of the RNA III family referred to as 'DICER' (Zamore *et al.*, 2000). These short interfering RNA molecules then interact with additional proteins to produce a mulitmeric RNase complex referred to as RNA Interference Specificity Complex (RISC). The DICER/RISC complex is used to target homologous RNA molecules by Watson-Crick binding and ATP-dependent cleavage of the ds RNA molecules thus formed prevents translation of the gene in question (Bernstein *et al.*, 2001). RNAi may also lead to methylation of cytosine bases in DNA of the gene in question, so reducing its capacity to be transcribed and, at least in plants, may also mediate a systemic response to silence gene expression in other parts of the plant (Waterhouse *et al.*, 2001; Baulcombe, 2002; Mlotshwa *et al.*, 2002).

RNAi is likely to be responsible for the reduction in endogenous transcript levels observed in this study in transformed roots containing the 1.2 kb *ADC* and also the *PMT*-antisense constructs. Presumably in these cases, antisense transcripts were able to form double stranded RNA molecules with the endogenous *ADC*/*PMT* transcripts and then trigger the RNAi response. The reason(s) why the 460 bp antisense *ADC* transcript of *N. rustica*, though present at high levels, was not apparently capable of reducing levels of endogenous *ADC* transcript in any of the transgenic *N. tabacum* root lines remains unclear. It is possible that secondary structure constraints within the *ADC* transcript and/or its association with ribonucleoproteins (Branch, 1998) prevented sufficiently large regions of double stranded RNA from forming with the 460 bp antisense *ADC* transcript to trigger the RNAi response. This may be a topic that merits further investigation.

Additional References

Baulcombe, D. (2002). RNA silencing. *Current Biology* **12**: R82–R84.

Branch, A. D. (1998). A good antisense molecule is hard to find. *Trends in Biochemical Science* **23**: 45-50.

Bernstein, E., Caudy, A. A., Hammond, S. M., and Hannon, G. J. (2001). Dicer and DNAse III-family nuclease executes the initiation step of RNAi. *Nature* **409**: 363–366.

Hutvagner, G. and Zamore, P. D. (2002). RNAi : Nature abhors a double strand. *Current Opinion in Genetics & Development* **12**: 225–232.

Mizrachi, N., Levy, S., and Goren, Z. (2000). Fatal poisoning from *Nicotiana glauca* leaves: identification of anabasine by gas-chromatography/mass spectrometry. *Journal of Forensic Science* **45**: 736–741.

Mlotshwa, S., Voinnet, O., Mette, M. F., Matzke, M., Vaucheret, H., Ding, S. W., Priss, G., and Vance, V. B. (2002). RNA silencing and the mobile silencing signal. *Plant Cell* **14**: S289–S301.

Query 4. Is it valid to suggest that fresh weights of tissues are highest at day 21 of the growth cycle (page 106, 3rd paragraph) when the S.E. bars of Fig. 3-22 do not suggest a statistical difference between the neighbouring time points?

This is a valid query, particularly in the light of discussion noted above regarding sample sizes. A more accurate description of the data would be to note that the weights of tissues were usually highest between days 18 - 25 of the growth cycle.

Query 5. Why were alkaloid levels in the medium of the root cultures not measured?

Early work conducted by Hamill *et al.*, (1986) showed that a small proportion of alkaloids produced by *Nicotiana tabacum* transformed roots were excreted/leached into the surrounding medium during the early – mid stage of the growth cycle. In terms of calculating absolute levels of alkaloid produced by such cultures, the levels of metabolites in the medium are therefore relevant. In the current study however, the main questions being addressed related to the effects of *ADC* and *PMT* gene antisense manipulations upon the alkaloid profile of *N. tabacum* transformed roots. Every experiment contained several control lines and efforts were focussed upon detailed comparisons of the alkaloid profile of antisense manipulated lines vs that of controls during the growth cycle to determine the effects of each antisense manipulation. It was considered unlikely that the antisense manipulations would in any way change the characteristics or dynamics of alkaloid excretion by such roots. Preliminary analysis of the media of several antisense manipulated lines, compared to controls, confirmed that this was indeed the case – very small amounts of alkaloid with the same characteristics as in controls (ie mainly nicotine, some anatabine) were detectable in the media of these lines.

Query 6. Can a MS spectrum of anatabine standard be included in appendix 3?

As was noted in this thesis, relatively few publications exist in the scientific literature with anatabine as the main focus of the study. A small sample of anatabine standard (gift from Dr Lippiello – p 85) was analysed by GC-MS and the spectrum (Appendix 3-E-i) was found to be extremely similar to that shown in Appendix 3-D. No reports of an anatabine MS spectrum were found in published scientific literature, however a MS spectrum has recently been acquired from a commercial US company (courtesy of Dr Mike Zimmermann, Philip Morris RD and E Center, USA) and is shown in Appendix 3-Eii. Together, these spectra confirm that the elevated peak in line V-26 with RT 15.7 min, as shown in Appendix 3-D, is indeed anatabine. Recently, a commercial supply of pure anatabine has become available via Toronto Research Chemicals Inc. and could be used to corroborate the findings reported here if so desired. It is also noteworthy that MS spectra of nicotine and anabasine were published by Mizrachi *et al.* (2000) and these are also included as Appendices 3-F and 3-Gi , respectively. The small peak with RT of 14.9 mins on the GC chromatograms presented in Appendices 3-A and 3-B was confirmed to be anabasine by comparison of its MS spectrum (Appendix 3-G-ii) with both the HP library database and also the spectrum shown in Appendix 3-G-i.

Query 7. Can a comment on RNAi be included in Chapter 5, with respect to data obtained in this report, in addition to noting it in the future directions (Chapter 5.2)?

Since the inception of this experimental program, approaches for down regulating expression of specific genes via destabilisation of mRNA, have become more sophisticated than the straightforward approach of expressing of antisense sequences as was used here (though the antisense approach remains quite an effective method in many situations). In particular, RNA interference (RNAi) vectors have been designed to express sections of genes as double stranded (ds) RNA molecules in transgenic plants such as the pHANNIBAL and pHELLSGATE vectors, and this

Vance, V. and Vaucheret, H. (2001). RNA silencing in plants – defense and counterdefense. *Science* **292**: 2277–2280.

Zamore, P. D., Tuschl, T., Sharp, P. A., and Bartel, D. P. (2000). RNAi : doublestranded RNA directs the cleavage of mRNA at 21-23 nucleotide intervals. *Cell* **101**: 23–33.

Minor corrections.

piv	line 34:	Replace "his" with "this"
p2	line 10:	"Lycopodium" and "Equisetum" should be italicised
p6	line 17:	Replace "nucleic acid" with "nucleic acids".
p7	line 15:	Replace "alkaloid" with "alkaloids".
p24	line 18:	Should be "...with nicotine being the major alkaloid in roots in 50 out of 60 species"
p25	line 7:	Substitute "*N*-methylpyrrolinium" for "*N*-Methylpyrrolinium".
	line 22:	Delete "in" and read ..."although cell suspension cultures...".
p26		subheading 1.4 should read "The route to the *N*-methylpyrrolinium ring".
p27	line 9:	Italicise "vice versa".
p43	line 9:	Replace "cell culture" with " cell cultures".
p46	line 16:	"*O*-methyltransferases" for "O-methyltransferases".
p48	line 5:	"1,3-diaminopropane" for "1,3-Diaminopropane".
p49		heading 1.4.2.1.5 - "Molecular genetic" should be "Molecular genetics"
p50	line 28:	Replace "cytogenic" with "cytogenetic".
	line 19:	Replace "introgressived" with "introgressive".
p55	line 2:	Insert a space after "(NAD^+)".
p59	line 31:	Replace "effect" with "affect".
p61	line 24:	Insert "that" and read "...studies have shown that both...".
p62	line 5:	Delete "is" and read "...makes it possible...".
p65	line 4:	Insert spaces to read "10 mM" and "1 mM".
p70		subheading 2.4.2: "*Escherichia*" for "*Eschericia*".
p71	line 27:	Insert square brackets to read "...[Speed Vac SC100 (Savant)]...".
p79	line 10:	Substitute "Geiger" for "geiger".
p95	line 2:	Replace "at" with "of" and read "...band of a smaller size...".
p102	line 10:	Delete "were" and read "...reductions observed...".
p103	line 13:	Replace "transcript" with "transcripts".
p108	line 17:	Insert "gene" to read "marker gene *(htp)*.".
p118		subheading 4.2.4: Italicise "N. sylvestris".
p124	line 5:	Delete comma to read "As is clear from this data...".
	line 7:	Insert "be" to read "...likely to be due...".
p126	line 8:	"Data is" should be "Data are"
p129	line 14:	Replace "of" with "by" and read "observations by Sinclair.....".
p130	line 2:	Insert "that" and read "...that the line...".
p131	line 1:	Insert hybridisation to read "...Southern hybridisation...".
p135	line 11:	Should read "...<25% of wild type...".
p136	line 8:	Replace "alkaloid" with "alkaloids".
p139	line 139:	Replace "studies" with "studied".
p140	line 9:	Insert "hybridisation" and read "...northern hybridisation experiments...".
p141	line 16:	Delete space and read "...80%...".
p142	line 13:	Replace "level" with "levels".
	line 22:	Delete "though" and read "...however, it is...".
p165	line 36:	"*O*-methyltransferase" for "O-methyltransferase".
	line 39:	"Practical" for "practical".
Fig. 3-19:		legend (line 8) Replace "sample" with "samples".

Declaration

I declare that this thesis contains no material which has been accepted for the award of any other Degree or Diploma in any university or institute. To the best of my knowledge this thesis contains no material previously published or written by another person, except where due reference is made in the text.

[redacted]

Yupynn Chintapakorn

Acknowledgements

Firstly, I would like to express my sincere gratitude to my supervisor, Professor John D. Hamill, for his support, advice and continual encouragement throughout the course of my study, especially his extreme supervision during the last period of this thesis writing. His assistance in securing a Monash Departmental Scholarship and the Phyllis Hilgrove Scholarship for Research into Agricultural Science during part of my study, was also very much appreciated. I thank him also for the proverbs I learnt from him in various situations of the dissertation.

I would also like to acknowledge Dr. Patrick M. Lippiello and Dr. Elisa Lovette (Pharmacology Laboratory Research & Development, RJ Reynolds Tobacco Company) for kindly supplying their authentic standard of anatabine. I would like to thank the staff members of Monash University, Dr. Kathy Walsh for the GC-MS analysis to identify the anatabine peak, Dr Aidan Sudbury for statistic analysis of the data, and Mrs. Nga Dang-Lien for looking after my transformed plants while I was away.

I wish to thank all the lab members for their support and technical assistance. In particular, I would like to thank Dr. Eugene and Dr. Dale Fredericks for their company, warm friendship, and generous guidance in helping me understand the Australian way of life as well as to correct my written English and speech. Their nice and cosy home that has accommodated me during the last month of my thesis writing will be a lifelong memory. Special thanks also go to Elaine, Assunta, Penny, Joyce, and Foong for our enjoyable girl talk. Thanks to Steve for reading part of this thesis and another thanks to Assunta for reading the whole thesis as a final check. Also another huge special thanks to Euge for answering all questions I always had during the thesis write up. Thank-you also to Karen for being my messenger during the past year when I was back in my home country. I would also like to give a warm thanks to all my young Thai friends I met at Monash University: Seng, Bee, Poom, Tuk, Kit, Nuj, Noi, Tum, Orh, Oai, Chan, and Kay for their friendship, opened ears, and showing me how various computer programs worked. All of them made me feel as though I had never left home.

I would like to acknowledge the Thai Government for the scholarship I received during my first few years. I am also deeply grateful to Monash International, Phyllis Hilgrove Scholarship, for supporting my stipend and the university fees in the years after the financial crisis occurred in my country. I also thank the Faculty of Science at Chulalongkorn University for giving me study-leave for all these years.

Last but not least, I would like to extend my deep indebtedness and grateful thanks to my family, my late Dad, my Mum and my brother, Vichit, for their unconditional love, unlimited patience, and thoughtful understanding.

List of Abbreviations

ADC	arginine decarboxylase
BAP	6-benzylaminopurine
bp	base pair
cDNA	complementary deoxyribonucleic acid
DFMA	DL-α-difluoromethylarginine
DFMO	DL-α-difluoromethylornithine
DMSO	dimethyl sulphoxide
DTT	dithiothreitol
GUS	β-glucuronidase
IAA	indole-3-acetic acid
LB	left broader
mins	minutes
mRNA	messenger ribonucleic acid
MS	mass spectrometry
ODC	ornithine decarboxylase
PCR	polymerase chain reaction
RACE	rapid amplification of cDNA ends
RB	right broader
Ri T-DNA	root-inducing transferred DNA
RT	retention time
RT-PCR	reverse transcription- polymerase chain reaction
SAM	S-adenosylmethionine
SAMDC	S-adenosylmethionine decarboxylase
SAMS	S-adenosylmethionine synthase
SPDS	spermidine synthase
SPMS	spermine synthase
T-DNA	transferred DNA
Term	CaMV35S terminator
UR	upsteam enhancer of CaMV35S promoter

Abstract

Nicotiana tabacum L. produces a number of pyridine alkaloids, with nicotine representing approximately 80-85% and anatabine representing approximately 10-15% of the total alkaloid fraction. This thesis describes experiments using an antisense approach to down-regulate the expression of two key genes encoding enzymes involved in alkaloid biosynthesis in *N. tabacum*, namely arginine decarboxylase (ADC) and putrescine *N*-methyltransferase (PMT).

In the first part of the study, transformed roots were generated containing a construct possessing either a 460 bp fragment or a 1.2 kb fragment of *Nicotiana ADC* coding sequence (full-length 2.8 kb) in an antisense orientation under control of the CaMV35S promoter. Although antisense transcripts were detected representing the 460 bp fragment, no decrease in endogenous *ADC* transcript levels were observed and no alterations in alkaloid content of tissues were apparent. In contrast, the 1.2 kb fragment did reduce endogenous *ADC* transcript levels in actively growing lines (by 70-80% in some cases) and also ADC activity (by 50-60% in some cases). The latter lines possessed normal alkaloid profiles during the early-to-mid stages of the growth cycle but were characterised by a slight reduction in nicotine content, with some also possessing a slight increase in anatabine content, when analysed at the latter part of the growth cycle. Plants regenerated from these root lines possessed alkaloid profiles that were very similar to controls.

In the second part of the study, transformed root lines were generated containing a construct possessing the full-length *Nicotiana PMT* coding sequence (1.4 kb) in an antisense orientation, also under control of the CaMV35S promoter. Several lines contained markedly reduced PMT activity compared to controls (10- to 40-fold lower than controls at day 12 of the growth cycle) with a concomitant reduction in nicotine content. No negative effects on growth were observed. Interestingly, several antisense *PMT* root lines and also leaf tissues of regenerated plants showed a substantial increase in anatabine content relative to controls. Northern blotting, involving several transformed root lines, indicated that the antisense *PMT* manipulation had little or no effect on the transcript levels of a number of genes encoding enzymes involved in alkaloid metabolism, including quinolinic acid phosphoribosyltransferase (QPT). The latter enzyme plays a key role in regulating the synthesis of nicotinic acid which supplies the pyridine ring necessary for both nicotine and anatabine synthesis. Thus, elevated anatabine levels appear to be a consequence of a relative oversupply of nicotinic acid in antisense *PMT* lines which, in the absence of adequate levels of *N*-methylpyrrolinium (the ultimate product of PMT activity), is used to synthesise anatabine directly. As is discussed, no species or varieties of *Nicotiana* have been reported in the literature that typically produce high levels of anatabine in root tissues, meaning that the antisense *PMT* transgenics produced in his study have no natural counterpart.

Together, these *ADC* and *PMT* antisense experiments, involving transformed roots of *N. tabacum*, contribute to a greater understanding of the *in vivo* factors that control pyridine alkaloid metabolism in plants. A series of further experiments are identified, also employing strategies to down-regulate gene expression, which may further enhance our understanding of this area of plant secondary metabolism.

Table of Contents

Chapter 1

Introduction

1.1 Alkaloids

Alkaloids are nitrogen-containing organic compounds and often display physiological activity in animals (Kutchan, 1995; Roberts and Wink, 1998). They are produced primarily in higher plants but also to a lesser extent in some lower organisms and animals. About 10,000 compounds have been listed in the Dictionary of Alkaloids (Southon and Buckingham, 1989). They exhibit a great variety of structures, resulting from many different biosynthetic pathways and have a wide range of pharmacological activities.

The term "alkaloid" was coined in 1819 by the pharmacist W. Meissner and meant simply, "alkali-like" (from the Arabic "*al kaly*" = soda, and the Greek "*eidos*" = appearance) (Pelletier, 1983; Bruneton, 1995). Today this alkaline character is no longer regarded as being a necessary property of an alkaloid. For example colchicine, piperine, amine oxides such as indicine N-oxide and quarternary salts such as laurifoline chloride are all classed as alkaloids despite their lack of basicity (Pelletier, 1983). There is, however, a fine line between describing a chemical as an alkaloid as opposed to other natural nitrogen-containing metabolites. With this in mind, Pelletier (1983) suggested defining alkaloids as cyclic organic compounds containing nitrogen in a negative oxidation state, which are of limited distribution among living organisms.

1.1.1 Occurrence and distribution

Alkaloids are the most diverse group of secondary metabolites formed in living organisms. As has been noted, the Dictionary of Alkaloids (Southon and Buckingham, 1989) contains information on about 10,000 alkaloids, whilst 12,000 structures of alkaloids have been described (De Luca and St Pierre, 2000) and approximately 16,000 alkaloids have been listed in the data bank "NAPRALERT" (Verpoorte, 1998). Some

alkaloids have a wide distribution in nature. Caffeine, lycorine and berberine occur in the largest number of families, genera and species, respectively (Wink, 1998b). The major source of alkaloids is the Angiospermae (flowering plants) where about 20% of all species surveyed are found to contain one or more of these compounds (Wink, 1998b). Families of higher plants known to be particularly rich in alkaloids include the Apocynaceae, Asclepiadaceae, Berberidaceae, Boraginaceae, Leguminosae, Papaveraceae, Ranunculaceae, Rubiaceae, Rutaceae, Solanaceae, and Liliaceae (Wink, 1997). In contrast, species in the Labiatae and Rosaceae are almost devoid of alkaloids (Tyler *et al.*, 1981). Alkaloids also occur in more primitive groups within the plant kingdom, such as Lycopodium and Equisetum (Wink, 1997) as well as more rarely in the gymnosperms (Tyler *et al.*, 1981).

The ability to produce alkaloids, however, is not restricted only to plants. In recent years an increasing number and diverse arrays of alkaloids have been isolated from other organisms including microorganisms, fungi, marine and non-marine animals. Interestingly, whereas higher plants are the richest and most important group of alkaloid producers in the terrestrial environment, relatively few alkaloids have been found in marine plants. The vast majority of marine alkaloids identified to date have been isolated from the numerous invertebrates that are sessile or slow moving such as sponges, bryozoans and holothurians (Proksch and Ebel, 1998). These marine invertebrates lack effective morphological defense mechanisms. The frequent occurrence, and in many cases high yields, of alkaloids formed in these marine invertebrates is considered to reflect the evolution of chemically mediated defense mechanisms that protect these soft-bodied organisms from predators (Proksch and Ebel, 1998). A capacity for alkaloid synthesis in some non-marine animals has also been reported, such as Salamanders (*Salamandra* spp.), toads (*Melanophrynicus* spp.), frogs (Dendrobatidae), millipedes (Diplopoda), beetles (Coleoptera) and ants (Hymenoptera) (Braekman *et al.*, 1998).

Despite the large diversity of alkaloids in nature, the distribution of particular alkaloids is often confined within taxonomic groups, since the alkaloid pattern of each organism is defined by its genetics. Consequently, alkaloids have provided many valuable insights into the unraveling of taxonomic relationships (Waterman, 1998). In

some instances, particular alkaloids have proved useful as chemical characters in systematic taxonomy and phylogeny of plants. For example, benzylisoquinoline alkaloids are typical of species in the Papaveraceae, Berberidaceae and Ranunculaceae which seem to be phylogenetically related to one another (Wink, 1997). Colchicine and hyoscyamine are normally confined to a number of genera within specific plant families, the Liliaceae and Solanaceae, respectively (Tyler *et al.*, 1981; Bruneton, 1995). Other alkaloids are characteristics of a group of species within one genus such as thebaine in the genus *Papaver*, and some are more highly specific, such as morphine in *P. somniferum* (Bruneton, 1995).

Interestingly, some specific alkaloids are synthesised by systematic units that are not closely related. Examples here include ergot alkaloids which occur in some fungi (*Claviceps*) but also in members of the Convolvulaceae. Also quinolizidine alkaloids which are typically found in some species in Leguminosae, but have also been detected in species of the Berberidaceae (Wink, 1997). This may be because the mechanism of alkaloid biosynthesis involves a Schiff base plus Mannich condensation and is therefore a rather conservative process at the biosynthetic level (Waterman, 1998). Thus, although there are many different classes of alkaloids evolutionary changes seem to have occurred primarily through variation in the substrate utilized for alkaloid synthesis rather than in the mechanism of alkaloid formation. Given this underlying degree of conservation, genetic information encoding enzymes governing alkaloid synthesis is likely to be conserved, and may be present, although silent, in many non-alkaloid-producing species (Waterman, 1998). Recent data from the *Arabidopsis thaliana* genome sequencing program supports this view with the existence of homologues of tropinone reductase detected on chromosome 2 (Lin *et al.*, 1999). This enzyme plays an important role in the biosynthesis of tropane alkaloids but these alkaloids have not been reported to occur in *Arabidopsis* or other genera within the Brassicaceae.

1.1.2 Roles

In contrast to the past when the likelihood of alkaloids having a particular purpose in nature was questioned, prevailing views generally regard them to be part of an elaborate

system of chemical defense in plants (Wink, 1998b). The same seems to be true of alkaloids found in other sources, such as vertebrates, invertebrates and marine organisms. As has been noted, many alkaloids are physiologically active compounds having a variety of toxic effects on microorganisms, insects and animals so it is not surprising that they serve as defense compounds against microbes, virus, and herbivores (Wink, 1998b). The bitter taste of many alkaloids may also be of importance as a feeding deterrent (Wink, 1997). Nearly all structural types of alkaloids have also been reported to exhibit allelopathic activities, being inhibitory to the growth of competitors in the vicinity of plants that produce them (Hartmann, 1991; Lambers *et al.*, 1998; Lovett and Hoult, 1998; Wink, 1998b).

The location of alkaloids within plants is an important part of their role in conferring chemical defense to the plant. For optimal protection, alkaloids may be stored predominantly in tissues which are important for survival and reproduction, such as actively growing tissues, photosynthetically active tissues, roots, stem bark, flowers (especially seeds) and seedlings (Wink, 1997). For example, Aerts *et al.* (1991) studied the distribution of alkaloids in different parts of six months-old saplings of *Cinchona ledgeriana*. They found that young, partially expanded leaflets, which are most attractive to predators, had the highest alkaloid content of tissues sampled from the whole plant with levels being about five times higher than in older leaves. Many alkaloids, such as berberine, cinchonine and quinine, are located in root or stem bark tissues which are likely to be strategically important sites for deterrence of intruders at the first opportunity (Wink, 1998b). In legume species, lupin alkaloids are preferentially stored in the epidermal, subepidermal and hypodermal tissues of stems and leaves (Wink, 1983a, b; Wink *et al.*, 1984). The alkaloid barrier in these storage tissues are thought to protect against small herbivores and pathogens that could otherwise enter the plants via injury to the epidermis (Wink, 1998b).

As many alkaloids can absorb UV radiation, Lambers *et al.* (1998) suggested that another possible functional role of alkaloids may be in providing protection against UV induced cellular damage. To date, however, convincing evidence for such a role is lacking. Indeed, Baldwin and Huh (1994) found that nicotine supplied exogenously to

Datura stramonium did not result in increased UV protection, even though nicotine has a high molar extinction coefficient (2695 M^{-1} cm^{-1}) at 262 nm.

1.1.3 Classification

There are many different systems of alkaloid classification, since these compounds are greatly varied in their chemical structures and are also variable in botanical and biochemical origin, as well as in their pharmacological activity. A convenient approach to classification is to group them according to their biochemical origins, a concept which has been used in the Dictionary of Alkaloids (Southon and Buckingham, 1989) and in a recent comprehensive treatise on alkaloids (Roberts and Wink, 1998).

The nitrogen atom in most alkaloids originates from an amino acid. The carbon skeleton of the particular amino acid precursor, in general, is also largely retained intact in the alkaloid structure, though the carboxylic acid carbon is often lost due to decarboxylation. Thus most alkaloids can be classified according to their amino acid precursors. Relatively few amino acid precursors are actually involved in alkaloid biosynthesis, the principal ones being, lysine, tyrosine, tryptophan, histidine, and the non-protein amino acids ornithine, nicotinic acid, and anthranilic acid.

The nitrogen atoms of a number of alkaloids, however, are acquired via transamination reactions in which only the nitrogen atom from the amino acid is incorporated into the alkaloid structure. In such cases, the rest of the alkaloid molecule may be derived from a non-amino acid origin via acetate, shikimate or mevalonate pathway(s).

Therefore it is possible to group alkaloids into:

A. <u>Alkaloids derived from amino acids</u>.

At present, the majority belong to this group and involve mainly:

- those derived from ornithine or arginine including the pyrrolizidine and tropane alkaloids and the pyridine alkaloids nicotine and nornicotine, these latter two also involving nicotinic acid.
- those derived from lysine including the piperidine, quinolizidine, and indolizidine alkaloids and the pyridine alkaloid anabasine which also involves nicotinic acid.
- those derived from tyrosine including the tetrahydroisoquinoline, benzyltetrahydroisoquinoline, terpenoid tetrahydroisoquinoline and phenethylisoquinoline alkaloids.
- those derived from tryptophan including indole, β-carboline, quinoline, pyrroloindole and ergot alkaloids.
- those derived from histidine including imidazole alkaloids.
- those derived from nicotinic acid including pyridine alkaloids which also may involve ornithine, arginine or lysine as noted above.
- those derived from anthranilic acid including quinazoline, quinoline and acridine alkaloids.

B. Purine alkaloids:

The origins of alkaloids in this category are very closely linked with the purine bases adenine and guanine which are fundamental components of nucleic acid. A well-known example here is caffeine.

C. Alkaloids derived by amination reactions:

Alkaloids in this class are synthesized primarily from non-amino acid precursors such as terpenoids, steroids and polyketides. The nitrogen atom is inserted into the structure at a relatively late stage in biosynthesis, mostly through a transamination reaction. Alkaloids classed as belonging to this group are increasing in number as more insects and marine organisms are further investigated. Consistent with their metabolic origins, sub-divisions of alkaloids in this class are terpenoid alkaloids, steroidal alkaloids, acetate-derived alkaloids and phenylalanine-derived alkaloids.

1.1.4 Pharmacological activity

Many alkaloids have been used for hundreds of years as poisons. Before and during the Middle Ages, several alkaloids, such as aconitine, atropine, colchicine, coniine and strychnine were used for murder and executions (Wink, 1998a). Some alkaloids that interfere with the nervous system in muscles have played a significant role as arrow poisons for hunting and warfare in ancient times (Neuwinger, 1998). Examples of alkaloids constituting these arrow poisons are aconitine, ajmaline, atropine, physostigmine, reserpine, toxiferine, and d-tubocurarine. Now, ironically, some of these alkaloid poisons have provided mankind with effective medicines and have been also applied as tools in biomedical research. Examples here are physostigmine for the treatment of glaucoma and myasthenia gravis; d-tubocurarine as a muscle relaxant in anesthesia; reserpine as an antihypertensive and psychotropic drug; and ajmaline for cardiac rhythm disturbances (Neuwinger, 1998).

Due to their pharmacological activities and their effects on many systems in humans, some plants containing alkaloid have had a long history of medicinal use. For example, *Atropa belladonna*, *Mandragona officinarum*, and *P. somniferum* are documented in 4000 year old Assyrian clay tablets (Wink, 1998a). During the first decade of the 19th century, Serturner was the first investigator to purify an alkaloid, using dried latex of the opium poppy to identify morphine (Kutchan, 1995; Roberts and Wink, 1998). Numerous modern drugs used today still contain plant-derived alkaloids or their analogues (Table 1-1) and a number of research programs currently underway continue to search for new pharmacological active alkaloids from natural sources.

Table 1-1 Utilization of alkaloids in modern medicine (summarized from data presented by Schmeller and Wink,.1998).

Group	Source	Alkaloid	Usage
Tropane alkaloid	*Duboisia myoporoides*, *D. leichhardtii*, *Hyoscyamus muticus*, *H. niger* (Solanaceae)	Atropine, Hyoscyamine	Anticholinergic, antispasmodic, mydriatic, cycloplegic, as a premedicant before general anesthesia
		Hyoscine (Scopolamine)	Antispasmodic, motion sickness, as a premedicant before general anesthesia
	Erythroxylon coca (Erythroxylaceae)	Cocaine	Local anesthetic
Piperidine alkaloid	*Lobelia inflata* (Lobeliaceae)	Lobeline	Bronchial asthma, chronic bronchitis, emphysema, discourage smoking
Quinolizidine alkaloid	*Cytisus scoparius* (Leguminosae)	Sparteine	Cardiac arrhythmias
Tetrahydro-isoquinoline alkaloid	*Cephaelis acuminata* (Rubiaceae)	emetine	Severe intestinal and hepatic amoebiasis, expectorant
	Peumus boldo (Monimiaceae)	Boldine	Cholelithiasis, stomachic disorders, vomiting, constipation and dyspepsia
Tetrahydrobenzyl-isoquinoline alkaloid	*Chondodendron tomentosum* (Menispermaceae)	Tubocurarine	Muscle relaxant
	Papaver somniferum (Papaveraceae)	Codeine	Cough suppressant, analgesic
		Narcotine	Cough suppressant
		Morphine	Strong analgesic
	Berberis vulgaris (Berberidaceae)	Berberine	Antiamoebic, eye infections
Benzylisoquinoline alkaloid	*P. somniferum*	Papaverine	Vasodilator
Benzyophenan-thridine-isoquinoline alkaloid	*Sanguinaria canadensis* (Papaveraceae)	Sanguinarine	Antiplaque agent and expectorant
Phthalide-isoquinoline alkaloid	*P. somniferum*	Noscapine (Narcotine)	Cough suppressant
	Hydrastis canadensis (Berberidaceae)	Hydrastine	Gastrointestinal disorders

Group	Source	Alkaloid	Usage
Phenethyl-isoquinoline alkaloid	*Colchicum autumnale* (Liliaceae)	Colchicine	Acute gout
Indole alkaloid	*Rauwolfia serpentina* (Apocynaceae)	Reserpine, Rescinnamine	Antihypertension
	R. serpentina, *R. vomitoria* (Apocynaceae)	Raubasine (Ajmalicine)	Peripheral and cerebral vascular disorder
	R. vomitoria, *Catharanthus roseus* (Apocynaceae)	Ajmaline	Antiarrhythmia
	R. vomitoria	Yoimbine	Aphrodisiac, urinary incontinence
	Strychnos nux-vomica (Loganiaceae)	Strychnine	Optic nerve atrophy, eye disorders
	Vinca minor (Apocynaceae)	Vincamine	Cerebral disorder
	C. roseus	Vinblastine Vincristine	Hodgkin's disease and other lymphomas
Quinoline alkaloid	*Cinchona succirubra* (Rubiaceae)	Quinidine	Antiarrhythmia
		Quinine	Malaria, babesiosis, myotonic disorders
Ergot alkaloid	*Claviceps purpurea* (Clavicipitaceae)	Ergotamine	Migraine
	C. paspali (Clavicipitaceae)	Ergometrine	Postpartum or postabortal hemorrhage
Pyrroloindole alkaloid	*Physostigma venenosum* (Leguminosae)	Physostigmine (Eserine)	Glaucoma
Imidazole alkaloid	*Pilocarpus microphyllus*, *P. jaborandi*, *P. racemosus*, *P. pennatifolius* (Rutaceae)	Pilocarpine	Glaucoma
Pyridine alkaloid	*Nicotiana tabacum*, *N. rustica* (Solanaceae)	Nicotine	Used in gum and transdermal patches as aids to stop smoking

Group	Source	Alkaloid	Usage
Purine alkaloid	*Coffea arbica* (Rubiaceae) *Paullinia cupana* (Sapindaceae) *Cola nitida*, *C. acuminata* (Sterculiaceae)	caffeine	Neonatal apnea, atopic dermatitis
	Theobroma cacao (Sterculiaceae)	Theobromine	Antiasthma
Terpenoid alkaloid	*Aconitum napellus* (Ranunculaceae)	Aconitine	Rheumatism, neuralgia
Diterpenoid alkaloid	*Taxus brevifolia* (Taxaceae)	Taxol	Treatment of mamma and ovary carcinoma and several other malignancies
Phenylalanine derived alkaloid	*Catha edulis* (Celastraceae)	Cathine	Anorectic
	Ephedra sinica, *E. shunnungiania* (Ephedraceae)	Ephedrine	Nasal decongestant

Wink (1998c) has summarized modes of action of alkaloids, considering subcellular targets and interactions with particular organs along with their effects on the physiology of complete organisms. Important subcellular targets include DNA, RNA, and the enzymes involved in their synthesis. Other enzymes involved in protein biosynthesis, in maintaining membrane integrity and ion channels, electron transport chains and signal transduction pathways are also important targets. At the organ level, alkaloids may affect the function of the brain, muscles, heart and the circulatory system, lungs, kidneys, liver, bones and the process controlled by these organs such as digestion, diuresis, respiration, blood circulation, hormonal interactions and reproduction, or the maintenance of homeostasis. Wink *et al.* (1998) have discussed comparative *in vitro* assays to elucidate the modes of action of about 70 different alkaloids, which represent most structure types and most biochemical properties.

1.2 Identification of genes and manipulation studies involving transgenic plants tissues

1.2.1 Isolation of genes in alkaloid biosynthesis

Kutchan *et al.* (1988) were the first group to clone a gene encoding an enzyme specific to an alkaloid biosynthetic pathway - strictosidine synthase (SSS) from *Rauvolfia serpentina*. SSS catalyzes the stereospecific condensation of tryptamine and seco-loganin to form 3α(S)-strictosidine, a key intermediate in indole alkaloid biosynthesis. Since then, many genes involved in alkaloid metabolism have been cloned (Table 1-2). Most cDNAs have been isolated by a strategy involving either purification of enzyme protein, amino acid sequencing and screening libraries with synthetic oligonucleotide probes or by immuno-screening an expression library with an antibody (Saito and Murakoshi, 1998). Differential screening of libraries prepared from mutants or induced cells, and genetic complementation in other organisms, have also been useful strategies to identify cDNAs without enzyme purification (Vetter *et al.*, 1992; Noji *et al.*, 1993, 1994; Hibi *et al.*, 1994). The isolated genes were then expressed as proteins in heterologous cells, generally *E. coli*, to verify their identity.

Table 1-2 Cloned genes involved in the biosynthesis of alkaloids in plants.

Type of metabolite	Enzyme / gene	Species	Details on DNA recovered	Cloning strategy	Reference
Mono-terpenoid indole alkaloid	Tryptophan decarboxylase (TDC or TryDC)	*Catharanthus roseus*	cDNA	Antibody screening	De Luca *et al.*, 1989
			Genomic DNA	cDNA probe	Goddijn *et al.*, 1994
		Camptotheca acuminata	cDNA *(TDC1)*	partial genomic clone used as probe	Lopez-Meyer and Nessler, 1997
			Genomic DNA (*TDC2)*	cDNA probe	
	3-Hydroxy-3-methylglutaryl CoA reductase (HMGR)	*Catharanthus roseus*	cDNA	PCR product used as probe	Maldonado-Mendoza *et al.*, 1992
	Strictosidine synthase (STR or SSS)	*Rauwolfia serpentina*	cDNA	Oligonucleotide probe	Kutchan *et al.*, 1988
		R. serpentina *R. mannii*	Genomic DNA (*STR1* and the promoter)	cDNA probe	Bracher and Kutchan, 1992
		C. roseus	cDNA	Oligonucleotide probe	McKnight *et al.*, 1990
			(SSS)	Antibody screening	Pasquali *et al.*, 1992
			Genomic DNA (*STR1* and the promoter)	cDNA probe	Pasquali *et al.*, 1999
	Strictosidine beta-D-glucosidase (SGD)	*C. roseus*	cDNA (*SGD*)	PCR product used as probe	Geerlings *et al.*, 2000
	Polyneuridine aldehyde esterase (PNAE)	*R. serpentina*	cDNA	PCR product used as probe	Dogru *et al.*, 2000

Type of metabolite	Enzyme / gene	Species	Details on DNA recovered	Cloning strategy	Reference
	Tabersonine 16-hydroxylase (T16H)	*C. roseus*	cDNA	PCR product used as probe	Schroder *et al.*, 1999
	Desacetoxyvindoline-4-hydroxylase (D4H)	*C. roseus*	cDNAs (*cD4H-1*, *cD4H-2*, *cD4H-3*)	PCR product used as probe	Vazquez-Flota *et al.*, 1997
			Genomic DNA (*gD4H-8*)	cDNA probe	
	Acetyl CoA:deacetyl-vindoline 4-*O*-acetyl-transferase (DAT)	*C. roseus*	Genomic DNA		St-Pierre *et al.*, 1998
Isoquinoline alkaloid	Tyrosine/3,4-dihydroxy-phenylalanine (dopamine) decarboxylase (TyDC/DODC)	*Papaver somniferum*	cDNA (*cTyDC1*)	PCR product used as probe	Facchini and De Luca, 1994
			cDNAs (*cTyDC2*, *cTyDC3*)	Heterologous cDNA probe	
			Genomic DNAs (*gTyDC1*, *gTyDC4*)	cDNA probe	
			Genomic DNA (*TyDC5*)	PCR product used as probe	Maldonado-Mendoza *et al.*, 1996
	S adenosyl-L-methionine: norcoclaurine 6-*O*-methyl-transferase (6-OMT)	*Coptis japonica*	cDNA	Oligonucleotide probe	Morishige *et al.*, 2000
	Coclaurine N-methyltransferase (CNMT)	*C. japonica*	cDNA	RACE products cloned	Choi *et al.*, 2002
	Berbamurine synthase (CYP80A1)	*Berberis stolonifera*	cDNA	Oligonucleotide probe	Kraus and Kutchan, 1995

Type of metabolite	Enzyme / gene	Species	Details on DNA recovered	Cloning strategy	Reference
	(*S*)-*N*-methylcoclaurine 3'-hydroxylase (CYP80B1)	*Eschscholtzia californica*	cDNA	Oligonucleotide probe	Pauli and Kutchan, 1998
		P. somniferum	cDNA	PCR product used as probe	Huang and Kutchan, 2000
	S adenosyl-L-methionine: 3'-hydroxy-*N*-methyl-coclaurine 4'-*O*-methyl-transferase (4'-OMT)	*C. japonica*	cDNA	Oligonucleotide probe	Morishige *et al.*, 2000
	Berberine bridge enzyme ((*S*)-reeticuline:oxygen oxidoreductase, BBE)	*E. californica*	cDNA	Oligonucleotide probe	Dittrich and Kutchan, 1991
			Genomic DNA (*BBE1* and the promoter)	cDNA probe	Hauschild *et al.*, 1998
		P. somniferum	Genomic DNA		Facchini *et al.*, 1996
	S adenosyl-L-methionine: scoulerine 9-O-methyl-transferase (SMT)	*C. japonica*	cDNA	Oligonucleotide probe	Takeshita *et al.*, 1995
	Codeinone reductase	*P. somniferum*	cDNAs (*COR1.1, COR 1.2, COR 1.3, COR 1.4*)	PCR product used as probe	Unterlinner *et al.*, 1999
Tropane alkaloid	Ornithine decarboxylase (ODC)	*Datura stramonium*	cDNA	PCR product used as probe	Michael *et al.*, 1996

Type of metabolite	Enzyme / gene	Species	Details on DNA recovered	Cloning strategy	Reference
	Putrescine N-methyltransferase (PMT)	*Atropa belladonna*	cDNAs (*AbPMT1, AbPMT2*)	cDNA probe	Suzuki *et al.*, 1999
		Hyoscyamus niger	cDNA (*HnPMT*)		
	Tropinone reductase I (TRI)	*D. stramonium*	cDNA	Oligonucleotide probe	Nakajima *et al.*, 1993a
		H. niger	cDNA	RACE products cloned	Nakajima *et al.*, 1999
			Genomic DNA		
	Tropinone reductase II (TRII)	*D. stramonium*	cDNA	Oligonucleotide probe	Nakajima *et al.*, 1993a
		H. niger	cDNA	Oligonucleotide probe	Nakajima *et al.*, 1993b
	Hyoscyamine 6β-hydroxylase (H6H)	*H. niger*	cDNA	Antibody screening	Matsuda *et al.*, 1991
			Genomic DNA	cDNA probe	Kanegae *et al.*, 1994
Pyridine alkaloid	Ornithine decarboxylase (ODC)	*Nicotiana tabacum*	cDNA	Differential screening	Imanishi *et al.*, 1998a, b
			Genomic DNA (*gNtODC-1*)	cDNA probe	Imanishi *et al.*, 2000
	Arginine decarboxylase (ADC)	*N. tabacum*	cDNA	Subtractive hybridization screening	Wang *et al.*, 2000
	S-adenosylmethionine synthetase (AdoMet)	*Lycopersicon esculentum*	cDNAs (*SAM1*)	Differential screening	Espartero *et al.*, 1994
			cDNAs (*SAM2*, *SAM3*)	cDNA probe	
	Quinolinic acid phosphoribosyltransferase (QPT)	*N. tabacum*	cDNA (*TQPT*)	PCR product used as probe	Sinclair *et al.*, 2000
		N. rustica	cDNA (*RQPT*)		

Type of metabolite	Enzyme / gene	Species	Details on DNA recovered	Cloning strategy	Reference
	Putrescine N-methyltransferase (PMT)	*N. tabacum*	cDNA	Differential screening	Hibi *et al.*, 1994
		N. tabacum cv Xanthi	Genomic DNA (*PMT1a , PMT 2 , PMT 3, PMT 4*)	cDNA probe	Riechers and Timko, 1999
		N. sylvestris	Genomic DNA (*NsPMT1, 2, 3*)	cDNA probe	Hashimoto *et al.*, 1998a
		N. attenuata	cDNA (*NaPMT1, 2*)	PCR product used as probe	Winz and Baldwin, 2001
Pyrrolizidine alkaloid	Homospermidine synthase (HSS)	*Senecio vulgaris*	cDNA	PCR product used as probe	Kaiser, 1999
				PCR product used as probe	Ober and Hartmann, 1999
Acridone alkaloid	α subunit (α1 and α2) of anthranilate synthase (AS)	*Ruta graveolens*	cDNAs (*ASα1, ASα2*)	A fragment of yeast *ASα* as probe	Bohlmann *et al.*, 1995
	Acridone synthaseI	*R. graveolens*	cDNA	Oligonucleotide probe	Junghanns *et al.*, 1995
	Acridone synthaseII	*R. graveolens*	cDNA	a fragment of heterologous chalcone synthase gene as probe	Lukacin *et al.*, 1999
Ergot alkaloid	4-(Gamma gamma-dimethylallyl) trytophane synthase (DMATS)	*Claviceps fusiformis*	cDNA (*dmaW*)	PCR product used as probe	Tsai *et al.*, 1995
		C. purpurea 1029 strain P1	Genomic DNA (*cpd1*)	cDNA from *C. fusiformis* used as heterologous probe	Tudzynski *et al.*, 1999
	Lysergyl peptide synthetase1 (LPS1)	*C. purpurea* 1029 strain P1	Genomic DNA (*cpps1*)	Chromosome walking downstream of *cpd1*	Tudzynski *et al.*, 1999
	Chanoclavine cyclase	*C. purpurea* 1029 strain P1	Genomic DNAs (Two putative oxidase genes; *cpox1, cpox2*)	Chromosome walking upstream of *cpd1*	Tudzynski *et al.*, 1999

Type of metabolite	Enzyme / gene	Species	Details on DNA recovered	Cloning strategy	Reference
Heterocyclic amino acid	β-Pyrazolealanine	*Citrullus vulgaris*	cDNA	Genetic complementation	Noji *et al.*, 1993, 1994
General or unknown	Cytochrome P450	*Catharanthus roseus*	CDNA (*Cros1*, *Cros2*)	PCR product used as probe	Vetter *et al.*, 1992 Meijer *et al.*, 1993b
			CDNA (*Cros1*)	cDNA probe	Mangold *et al.*, 1994
			Genomic DNA (*Cros3*)	cDNA probe	
	Cytochrome P450 reductase	*P. somniferum* *E. californica*	cDNA	PCR product used as probe	Rosco *et al.*, 1997
	NADPH:cytochrome P450 reductase	*C. roseus*	cDNA	Antibody screening	Meijer *et al.*, 1993a
			Genomic DNA		

1.2.2 Expression of recombinant DNA encoding enzymes involved in alkaloid biosynthesis in transgenic plants

The availability of cloned genes involved in alkaloid metabolism has allowed the investigation and manipulation of the biosynthesis of plant alkaloids at the molecular level. Altering the expression of these genes can be used to manipulate the metabolic pathways in transgenic plants and in tissues cultured *in vitro*. This can be performed in the same species as the genes were derived from, or across wide phylogenetic distances. Over-expression of only one gene encoding an enzyme in the multi-step biosynthesis pathway, however, does not usually result in a significant increase in the amount of end product of the pathway. Sometimes it leads to only a marginal increase in the end product, even though the activity of the encoded enzyme or its immediate metabolite has been increased (Hashimoto and Yamada, 1994). Table 1-3 lists examples of some plant species which have been successfully transformed using genes from plants (either the same or different species), microorganisms or animals to modify the amount or pattern of alkaloid production (modified and updated from Saito and Murakoshi, 1998).

Table 1-3 Examples of manipulation of alkaloid biosynthesis by gene transfer.

Enzyme (source)	Host	*Phenotype of transformants*	Reference
Terpenoid indole and quinoline alkaloids			
Tryptophan decarboxylase (TDC) (*Catharanthus roseus*)	*Nicotiana tabacum* plants (CaMV35S promoter)	Increase in levels of the enzyme, tryptamine and tyramine without significant effects on anthranilate synthase and chorismate mutase, the chorismate-utilizing enzymes which function as branch point enzymes in the shikimate pathway	Songstad *et al.*, 1990, 1991; Poulsen *et al.*, 1994; Thomas *et al.*, 1995
		TDC was targeted to either the chloroplast, endoplasmic reticulum or cytosol of transgenic plants. Targeting to the chloroplast resulted in the highest level of tryptamine but also led to a lesion-mimic phenotype in transgenics.	Di Fiore *et al.*, 2002
	Brassica napus plants (CaMV35S promoter)	Redirected tryptophan pools away from indole glucosinolate production. Thus mature seeds accumulated tryptamine and contained reduced level of indole glucosinolates to increase palatability in animal feed.	Chavadej *et al.*, 1994
	Solanum tuberosum (potato) plants (CaMV35S promoter)	Accumulated tryptamine, the immediate product of the TDC reaction. The redirection of tryptophan into tryptamine also resulted in a dramatic decrease in the levels of tryptophan, phenyl-alanine and phenylalanine-derived phenolic compounds as well as polyphenolic compounds, such as lignin, in transgenic tubers compared with nontransformed controls.	Yao *et al.*, 1995
	Peganum harmala suspension cell and root cultures (CaMV35S promoter)	Increased the levels of enzyme activity (up to 11-fold in the callus and 20-fold in the cultured roots) and serotonin (hydroxylated tryptamine) (up to 10-fold) but the level of tryptamine was unchanged.	Berlin *et al.*, 1993
	Catharanthus roseus crown gal calluses (CaMV35S promoter)	Increase in TDC protein level, TDC activity and tryptamine content but no significant increase in indole alkaloid production.	Goddijn *et al.*, 1995

Enzyme (source)	Host	Phenotype of transformants	Reference
	Catharanthus roseus crown gall calluses containing the *TDC* antisense construct (CaMV35S promoter)	Decrease in levels of TDC activity	Goddijn *et al.*, 1995
Strictosidine synthase (*C. roseus*)	*N. tabacum* plants (CaMV35S promoter)	Targeting to vacuole to obtain high levels of the enzyme activity (3- to 22-fold).	McKnight *et al.*, 1991
Tryptophan decarboxylase and strictosidine synthase (*C. roseus*)	*N. tabacum* cell cultures (CaMV35S promoter)	Accumulated tryptamine and produced strictosidine upon feeding of secologanin, In contrast to *C. roseus*, the tobacco cells excreted this alkaloid. This demonstrated the functionality of the two transgene-encoded enzymes in vivo.	Hallard *et al.*, 1997
	N. tabacum plants (CaMV35S promoter)	Being introduced with both genes on a single transforming plasmid, 33% of the transgenic plants expressed and accumulated the transcripts of both transgenes.	Leech *et al.*, 1998
	C. roseus cell cultures (CaMV35S promoter)	Alkaloid accumulation by highly productive transgenic lines showed considerable instability. High transgene-encoded tryptophan decarboxylase activity was unnecessary for increased productivity. In contrast, high strictosidine synthase activity appeared to be necessary to sustain high rate of terpenoid indole alkaloid biosynthesis	Canel *et al.*, 1998
	Cinchona officinalis transformed root cultures (CaMV35S promoter)	High levels of the enzymes and quinidine accumulated in the root cultures. After 1 year, however, tryptophan decarboxylase and the capacity to accumulate alkaloids had been completely lost.	Geerlings *et al.*, 1999
Isoquinoline alkaloid A promoter fragment (-2060) of tyrosine/3,4-dihydroxy-phenylalanine decarboxylase (TyDC5) (*Papaver somniferum)*	*N. tabacum* plants (*TyDC5* promoter::GUS)	GUS activity transiently appeared in all parts of the seedling during germination, but was limited to the roots in older plants. Experiments suggest that *TyDC5* expression is transcriptionally regulated and the enzyme may play an important role in alkaloid biosynthesis in the roots and germinating seedlings of opium poppy.	Maldonado-Mendoza *et al.*, 1996

Enzyme (source)	Host	Phenotype of transformants	Reference
Scoulerine 9-O-methyltransferase (SMT) (*Coptis japonica*)	*Eschscholtzia californica* cell cultures	Expression of *Coptis* SMT transcript, protein and activity in transgenic cells, whereas none of them expressed in the wild type cells. Change of the metabolic flow of scoulerine to a new branch for columbamine resulted in a modified metabolite profile with several novel metabolites not present in the wild type cells. On the other hand, sanguinarine, a major alkaloid in the wild type cells, was markedly decreased in transgenic cells.	Sato *et al.*, 2001
	Coptis japonica 156-1 cell cultures (high berberine producers) (CaMV35S promoter with duplicated enhancer)	An increase in SMT transcript (30-50%), activity (20%), and berberine and columbamine (15%).	Sato *et al.*, 2001
Berberine bridge enzyme (BBE) and N-methylcoclaurine 3'-hydroxylase (CYP80B1) (*E. californica*)	*E. californica* cell cultures	The antisense constructs of *BBE* and *CYP80B1* were introduced separately into the cell cultures. The transformed cell lines showed reduced accumulation of benzophenanthridine alkaloids compared with control cultures. The growth rate of the cultures was reduced. The transformed cells contained larger cellular pools of several amino acids.	Park *et al.*, 2002
<u>Tropane alkaloids</u> Hyoscyamine 6β-hydroxylase (H6H) (*Hyoscyamus niger*)	*A. belladonna* plants, transformed root cultures and regenerated plants (CaMV35S promoter)	Elevated levels of enzyme activity and scopolamine in both plants and root cultures. Leaves of the regenerated plants showed further-enhanced conversion to scopolamine.	Yun *et al.*, 1992; Hashimoto *et al.*, 1993
	N. tabacum plants (CaMV35S promoter)	Hyoscyamine bioconversion. Upon feeding of l-hyoscyamine or its 6-hydroxy derivative, scopolamine could be detected in the leaves.	Yun *et al.*, 1993

Enzyme (source)	Host	Phenotype of transformants	Reference
<u>Pyridine alkaloids</u> Ornithine decarboxylase (ODC) (*Saccharomyces cerevisiae*)	*N. rustica* transformed root cultures (CaMV35S promoter)	Enhanced ODC activity, and increase in nicotine accumulation up to 2- to 3-fold compared to controls (see also Table 1-6).	Hamill *et al.*, 1990
Lysine decarboxylase (LDC) (*Hafnia alvei*)	*N. glauca* transformed root cultures (CaMV35S promoter)	Increased LDC activity (10-fold) resulted in an accumulation of cadaverine (10-fold) and anabasine (2-fold). The levels of nicotine were (slightly) decreased whereas the levels of anatabine were increased 4- to 6-fold.	Fecker *et al.*, 1992
	N. tabacum plants (under *rbcS* promoter from potato)	Increased cadaverine accumulation in the chloroplasts.	Herminghaus *et al.*, 1991
	N. tabacum transformed root cultures (CaMV35S promoter)	Increased the levels of LDC activity, cadaverine (14-fold) and anabasine (3-fold).	Fecker *et al.*, 1993
	N. tabacum transformed root cultures (CaMV35S promoter and fused to small subunit *rbcS* transit peptide)	The enhanced effects resulting from this promoter on the levels of enzyme activity, cadaverine and anabasine accumulation were stronger than CaMV35S promoter alone. Over-production of cadaverine also led to the formation of hydroxycinnamoyl-cadaverine, new metabolite which have not yet been described as natural constituents of tobacco.	Herminghaus *et al.*, 1996; Berlin *et al.*, 1998
Putrescine N-methyltransferase (PMT) (*N. tabacum*)	*A. belladonna* plants and transformed root cultures (CaMV35S promoter with duplicated enhancer)	Unchanged alkaloid profiles in transgenic plants and root cultures, despite an increase in *PMT* transcript levels compared to the controls, (1.3- to 3.3-fold for transgenic plants and 5-fold for transformed roots). The transgenic plants were phenotypically normal.	Sato *et al.*, 2001

Enzyme (source)	Host	Phenotype of transformants	Reference
	N. sylvestris plants (CaMV35S promoter with duplicated enhancer)	-Transgenic plants with over-expression of *PMT* exhibited/possessed an increase in nicotine (40%) and an accumulation of methylputrescine in leaves, whereas, the spermidine and spermine contents were decreased. The phenotypes of transgenic plants were normal. -The cosuppression line accumulated a very low level of nicotine (2% of that of wild type) and increased amounts of putrescine and spermidine. This suggests that the efficient inhibition of PMT activity shifted the nitrogen flow from nicotine to polyamine synthesis. The reduction of PMT activity in roots caused the accumulation of polyamines in leaf. Several distinct phenotypes in the T0 and T1 generation were observed: a continuous spiral sheet along the stem, branched inflorescent stems, fruits with a small seed set from self-pollinated flowers.	Sato *et al.*, 2001
	N. sylvestris plants	The sequence was expressed in an antisensense orientation in *N. sylvestris*. The leaf material of the transformed plants was fed to *Manduca sexta* larvae. Larvae consumed more leaf area and gained more mass on the foliage of plants with low *PMT* expression and low nicotine levels as compared to plants with high *PMT* expression and high nicotine levels and wild type plants.	Voelckel *et al.*, 2001
<u>Pyrrolizidine alkaloid</u> Homospermidine synthase (HSS) (*Rhodopseudomonas viridis*)	*N. tabacum* plants (CaMV35S promoter)	Free spermidine content in transgenic plants was significantly decreased while the pool of conjugated spermidine was not affected. A range of abnormal phenotypes such as dwarfness and stunted growth was also observed.	Kaiser *et al.*, 2002

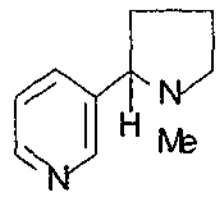

Nicotine

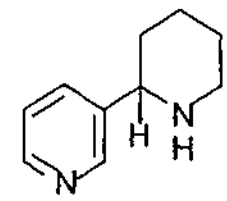

Anabasine

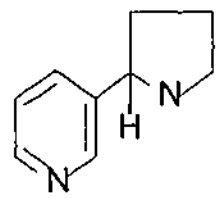

Nornicotine

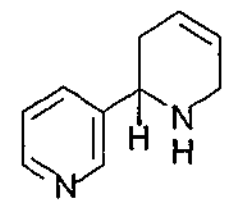

Anatabine

Fig. 1-1 Chemical structures of four principal alkaloid, nicotine, nornicotine, anbasine and anatabine, in *Nicotiana* species.

1.3 *Nicotiana* alkaloids

The presence of pyridine alkaloids is a characteristic of *Nicotiana* species (Dawson, 1962) with the most widely and abundantly distributed members of the group being nicotine, nornicotine, anabasine and anatabine (Fig. 1-1). Saitoh *et al.* (1985) determined the quantity of these four alkaloids in leaves and roots of 60 *Nicotiana* species representing the 3 subgenera and 12 sections within the genus. In a subsequent study, Sisson and Severson (1990) reported the alkaloid content and composition in greenhouse-grown and also field-grown plants of 66 *Nicotiana* species representing almost all of the recognized *Nicotiana* species at that time. Nicotine and nornicotine were detected in all *Nicotiana* species analysed by Saitoh *et al.* (1985) and Sisson and Severson (1990) whereas some species either did not produce anabasine and/or anatabine, or had trace levels of these alkaloids. These studies, taken together with previous investigations, showed that wild *Nicotiana* species predominantly contain a single alkaloid type, mostly either nicotine or nornicotine, with anabasine being a major constituent of the alkaloid fraction in a limited number of species (e.g. *N. glauca* and *N. debneyi*). The distribution between predominantly nicotine producers and predominantly nornicotine producers in leaf tissues is approximately equal (Sisson and Severson, 1990). However, the situation in root tissues appears to be different from that in leaf tissues with nicotine being as the major alkaloid in roots of 50 out of 60 species analysed (Saitoh *et al.*, 1985). Differing from other reports in which anatabine was never found to be the predominant alkaloid, Saitoh *et al.* (1985) also reported anatabine to be the predominant alkaloid in leaves of *N. otophora* though overall levels of alkaloid were extremely low compared to most other species in the genus.

While one alkaloid was found to be predominant within a given species, often a second alkaloid accounted for a significant portion of the remainder of the alkaloid fraction (Sisson and Severson, 1990). The most frequent combinations of primary and secondary alkaloids detected were nicotine-nornicotine followed closely by nornicotine-nicotine (Sisson and Severson, 1990). Nicotine-anabasine and nicotine-anatabine were other combinations that also occurred commonly (Saitoh *et al.*, 1985; Sisson and Severson, 1990). Anabasine and anatabine did not occur together in a predominant

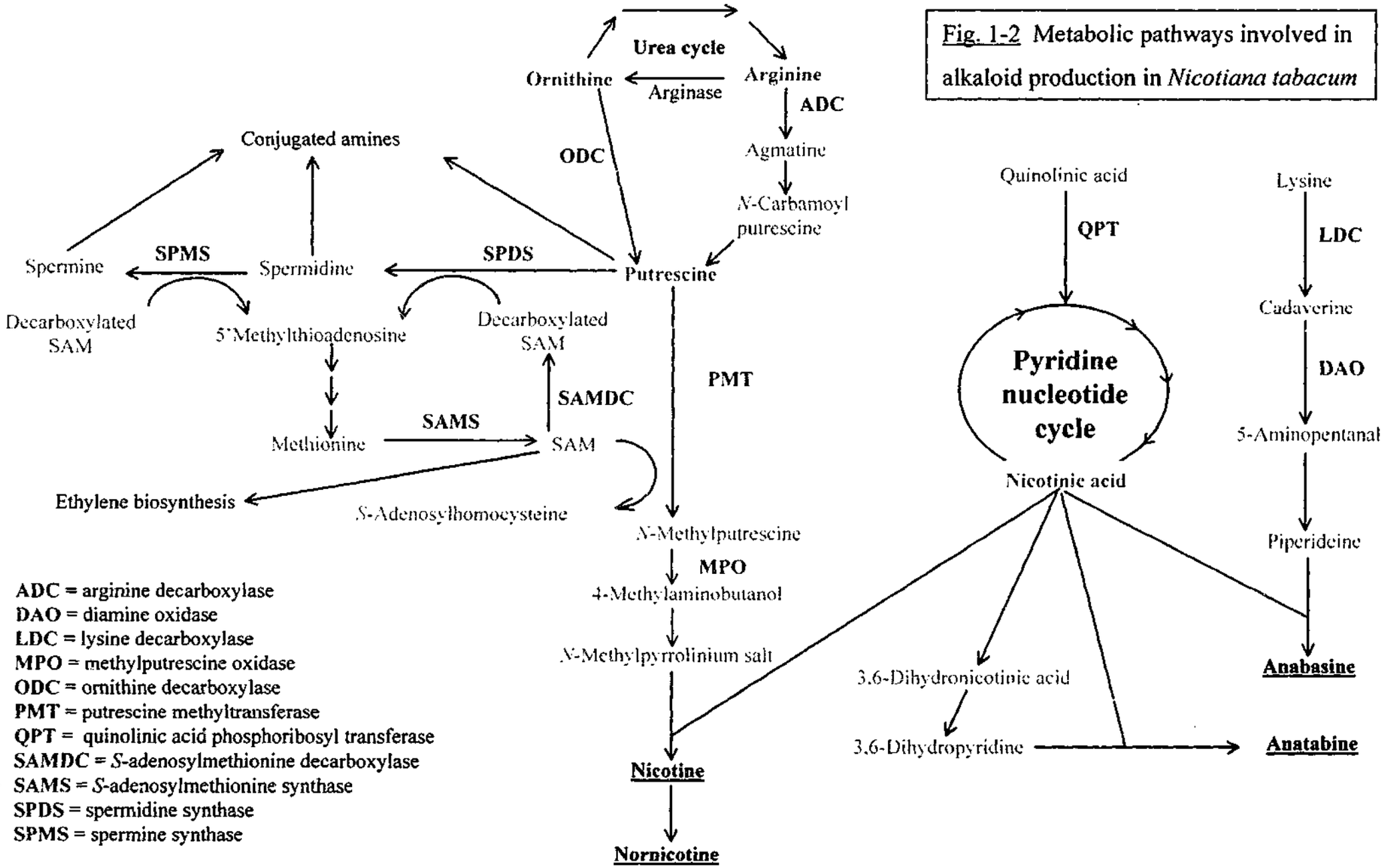

Fig. 1-2 Metabolic pathways involved in alkaloid production in *Nicotiana tabacum*

combination in any of the species studied (Saitoh *et al.*, 1985; Sisson and Severson, 1990).

A diagram of the biosynthetic pathway leading to the synthesis of the four most common *Nicotiana* alkaloids, and the main enzymes involved is illustrated in Fig. 1-2. The synthesis of nicotine, the structure of which contains a pyrrolidine ring as well as a pyridine ring, occurs in the roots of *Nicotiana* through the condensation of two metabolites obtained from separate areas of primary metabolism. *N*-Methylpyrrolinium is derived either from the amino acid ornithine or from arginine via putrescine, an important component of polyamine metabolism. The second metabolite, nicotinic acid, is provided by the pyridine nucleotide cycle (Leete, 1983). Key enzymes involved in the synthesis of these precursors are putrescine methyltransferase (PMT) and quinolinic acid phosphoribosyltransferase (QPT), respectively (Wagner *et al.*, 1986c) (details in section 1.4 and 1.5).

Nornicotine is the irreversible demethylation product of nicotine (Leete, 1979). The site of demethylation of nicotine has been found mostly to be the leaves (Waller and Nowacki, 1978). Experiments involving *Nicotiana rustica* lacking roots showed that approximately 40% of nicotine that was taken up and translocated to shoots was demethylated to produce nornicotine (Griffith and Griffith, 1964). Consistent with these observations, Saito *et al.* (1989) showed that shooty teratoma tissues of *N. tabacum* were unable to synthesise nicotine or nornicotine due to the absence of roots, but were able to efficiently biotransform exogenously supplied nicotine to nornicotine. Separate studies showed that although in cell suspension cultures of *N. plumbaginifolia* lacked detectable tobacco alkaloids, they retained an ability to demethylate exogenous supplied nicotine to nornicotine (Manceau *et al.*, 1989). Light appeared to enhance this catalytic activity of the cells suggesting that this particular metabolic step may be bound to photodependent systems (Manceau *et al.*, 1989). The enzyme catalyzing nicotine *N*-demethylation was partially characterized subsequently in a microsomal preparation from *N. otophora* (Chelvarajan *et al.*, 1993). More recent studies involving cell-free preparations from suspension cultures of *N. tabacum* provided some tentative evidence for the involvement of cytochrome P-450 in the *N*-demethylation of nicotine to form nornicotine (Hao and Yeoman, 1996, 1998). The study also supported the view that

nicotine *N*-demethylation is likely to be an enzymatically oxidative demethylation rather than a transmethylation (Hao and Yeoman, 1998).

Anabasine is derived from the condensation of piperideine and dihydronicotinic acid (Fig. 1-2). Its structure comprises a pyridine ring, as in nicotine and nornicotine, and a piperidine unit which arises from lysine, via a piperidinium cation (Dawson, 1962; Leete, 1983; Luckner, 1990). Several studies indicate that low levels of lysine decarboxylase are primarily responsible for the very low levels of anabasine that are found in *Nicotiana hesperis, N. rustica* and *N. tabacum* (Walton and Belshaw, 1988; Walton *et al.*, 1988; Fecker *et al.*, 1993).

Anatabine, like anabasine, also contains a pyridine ring and a piperideine unit. However, there is strong evidence that both rings in anatabine are derived from nicotinic acid units (Leete and Slattery, 1976; Leete, 1979). Biosynthesis of anatabine is thought to proceed via the conversion of nicotinic acid to 3,6-dihydronicotinic acid. This is decarboxylated to produce 3,6-dihydropyridine which then dimerizes with nicotinic acid to produce an intermediate which is converted to anatabine by dehydrogenation (Fig.1-2) (Leete and Slattery, 1976; Leete, 1979). Despite the similarity of their structures, there is apparently no interconversion of anatabine and anabasine in tobacco (Leete, 1979). It is not yet clear whether the same enzyme/enzyme complex that condenses *N*-methylpyrrolinium and nicotinic acid to produce nicotine, is also involved in the synthesis of anabasine and /or anatabine. Previous work of Walton and Belshaw (1988) and more recent work of Sinclair and Hamill (2002) suggest that this may indeed be the case, at least for anabasine.

1.4 The route to the *N*-Methylpyrrolidine ring

Experiments with radioactive labeled precursors have enabled the unraveling of many complex biogenic pathways. Studies conducted since the early 1970s have provided insight into enzymes associated with alkaloid formation, with cell culture techniques also playing an important role in the elucidation of the enzymes involved.

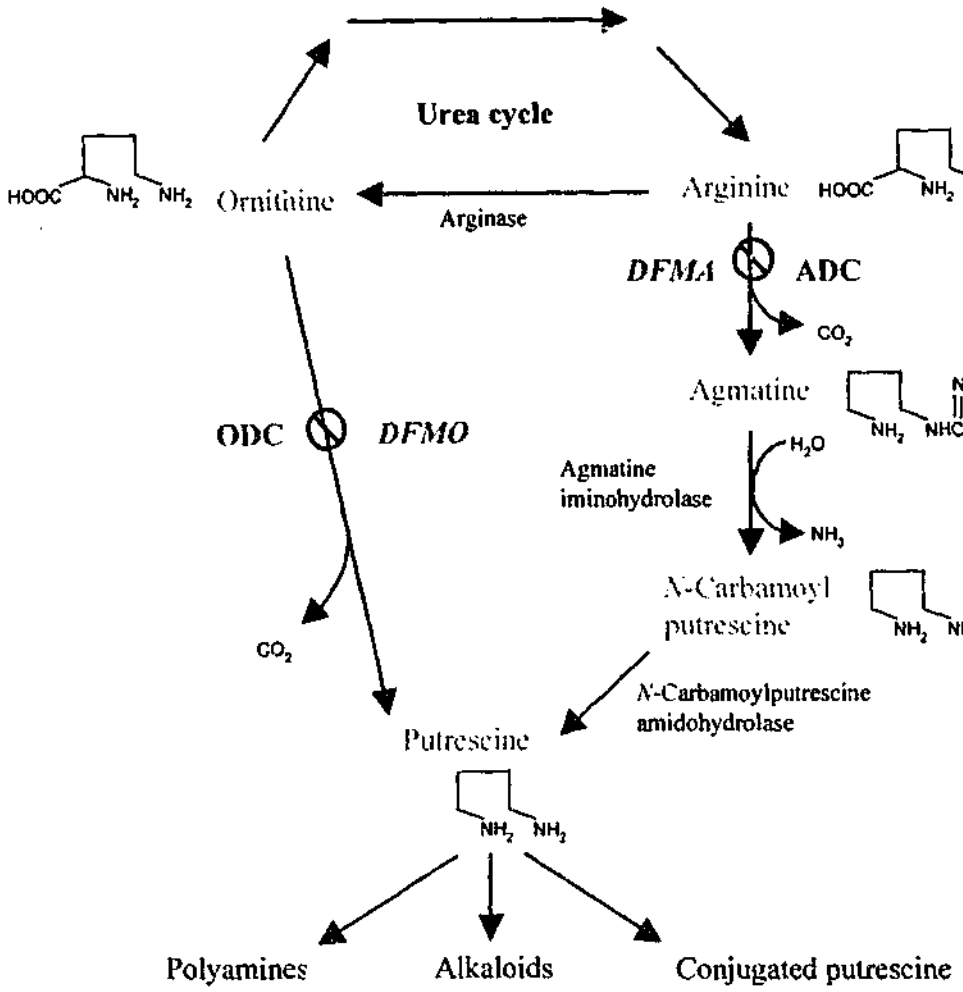

ADC = arginine decarboxylase
ODC = ornithine decarboxylase
DFMA = DL-α-difluoromethylarginine
DFMO = DL-α-difluoromethylornithine
⊘ = specific biochemical inhibition

Fig. 1-3 Metabolic pathway of putrescine in *N. tabacum*.

Since the late 1980s, some of the genes encoding enzymes involved in alkaloid metabolism have been isolated and characterized at the molecular level.

1.4.1 The route to putrescine used for alkaloid biosynthesis

In higher plants it has been shown that putrescine is formed by two independent routes (Fig. 1-3). One is by the direct decarboxylation of ornithine, which is under the influence of ornithine decarboxylase (ODC, EC 4.1.1.17). The second route is from arginine via agmatine and *N*-carbamoylputrescine, following decarboxylation with arginine decarboxylase (ADC, EC 4.1.1.19) (Leete, 1979, 1983). In cell cultures of *N. tabacum*, ADC was found not to be inhibited by a 100-fold excess of ornithine and vice versa, demonstrating that the enzymes, ADC and ODC, were not competing for the same substrate (Berlin, 1981). In some cell types arginine and ornithine are interconvertable, with arginine being produced from ornithine via the urea cycle, whilst arginine can be hydrolyzed by arginase to form ornithine (Fig. 1-3) (Berlin, 1981). In tobacco plants the formation of ornithine from arginine appears to be negligible, whereas a small fraction of ornithine might be converted into arginine (Yoshida, 1969). There was little interconversion of the two amino acids, ornithine and arginine, in tobacco cell cultures over the course of a 5-day incubation (Berlin, 1981).

1.4.1.1 Inhibition of ODC and ADC activities in plant tissues

The most effective inhibitors of ODC and ADC are the irreversible inhibitors, α-difluoromethylornithine (DFMO) and difluoromethylarginine (DFMA), respectively (Berlin, 1981; Flores *et al.*, 1989). They are highly specific and effective in plant cells *in vivo* and *in vitro* (Flores *et al.*, 1989) and each has the same basic mechanism of action as an inhibitor of enzyme activity. Upon decarboxylation a highly reactive, unstable nucleophile is formed which enables the halogen atom of the reaction product to bind covalently to a cysteine residue at the active site of the enzyme, thereby irreversibly inactivating it (Flores *et al.*, 1989; Robins *et al.*, 1994).

In most cases, DFMO and DFMA do not seem to be further metabolised by plant cells (Flores *et al.*, 1989), except in tissues possessing high arginase activity (Slocum *et al.*, 1988). In such tissues, DFMA is partially metabolised to urea and DFMO, thereby indirectly inhibiting ODC. For example, Slocum and Galston (1985a) observed a significant inhibition of ODC activity in tobacco ovary tissues treated with DFMA *in vivo*. They also demonstrated that bovine and tobacco arginases hydrolyse DFMA *in vitro*, using an assay based on the production of urea and DFMO (Slocum and Galston, 1985b). Accumulation of DFMO resulting from arginase-mediated hydrolysis of DFMA has been shown in tobacco ovary tissues *in vivo* and, *in vitro* with purified bovine arginase using radio-actively labeled substrate, [3,4-^{3}H]DFMA (Slocum *et al.*, 1988). In contrast to animal systems, DFMO treatment did not reduce the putrescine pool in tobacco cell cultures. suggesting that the cells compensated by increasing the synthesis of putrescine from arginine (Berlin, 1981).

Activity of both decarboxylases in plants may also be inhibited by the products of decarboxylation; ODC by putrescine and ADC by agmatine (Berlin, 1981). In general, ADC appears to be more sensitive to feedback inhibition than ODC. Experiments involving tobacco cell cultures showed that rather high concentrations of putrescine were necessary to cause an inhibition of ODC activity (Berlin, 1981). However, there have been some contradictory studies concerned with the inhibitory effects of these amines. Robins *et al.*, (1991c) demonstrated that feeding either agmatine or putrescine at 1 mM repressed the activity of ADC in *D. stramonium* transformed root cultures. In contrast, the level of ODC activity was not affected by feeding 2 mM putrescine, but was decreased by the 2 mM agmatine treatment. Hiatt *et al.* (1986) demonstrated that ADC activity in tobacco cell cultures was rapidly diminished by exogenously added putrescine, agmatine, spermidine or spermine. In contrast, ODC activity was less affected by putrescine and agmatine (50% reduction in activity) and was unaffected by the presence of spermidine and spermine. Similarly, activity of the purified ADC from soybean hypocotyls was inhibited by 70% in the presence of 0.5 mM agmatine or putrescine (Nam *et al.*, 1997a). In a study of the role of putrescine metabolic pathways in the differentiation of maize meristematic callus the activities of both ADC and ODC were found to be considerably lower in tissues fed with exogenous putrescine compared

to non putrescine treated controls (Bernet *et al.*, 1998). A study involving grapevine cell suspension cultures also showed that the addition of 5 mM putrescine caused a 4-fold decrease in ADC activity (Primikirios and Roubelakis-Angelakis, 1999). Together, these results appear to indicate that product feedback inhibition is greater for ADC than for ODC. However, in other studies, an apparent lack of ADC inhibition by agmatine, except at very high concentrations, has been interpreted as suggesting that feedback inhibition of this enzyme might not be significant under physiological conditions (Slocum, 1991).

1.4.1.2 Ornithine and arginine in alkaloid biosynthesis

The relative importance of ornithine and arginine in providing putrescine for alkaloid biosynthesis is not clear. Several studies have suggested that both sources may be utilised. For example, it has been demonstrated, via the use of radio labeled precursors, that arginine and the intermediates, agmatine and *N*-carbamoylputrescine, were effective precursors of nicotine when applied to excised tobacco root tissues. However, it was noted that ornithine was also an efficient precursor when fed to tissues under the same conditions (Yoshida and Mitake, 1966; Yoshida, 1969). Similarly, the relative contribution of these precursor amino acids to the biosynthesis of tropane alkaloid(s), another putrescine-derived alkaloid, is also not conclusive. Hashimoto *et al.* (1989b) observed that in *Hyoscyamus albus* root cultures, the tropine moiety of tropane alkaloids was biosynthesized from both ornithine and arginine via putrescine. They found that exogenously applied L-[2,3-^{3}H]arginine was converted to diamines (putrescine and N-methylputrescine) much more efficiently than was DL-[5-^{14}C]ornithine; however, the incorporation of labeled arginine into alkaloids was only marginally higher than that of ornithine. Potassium deficiency is known to lead to increased putrescine content of several plant species (Evans and Malmberg, 1989; Flores, 1991). Khan and Harborne (1991) found that in *Atropa acuminata* plants grown on medium deficient in potassium, the levels of putrescine and tropane alkaloid, as well as the activities of both ODC and ADC were increased compared to controls. These results raise the possibility that in potassium-deficient plants of *A. acuminata*, ODC and ADC may both be responsible for the increase in tropane alkaloid level via putrescine.

A number of studies have suggested that the ODC route is an important source of putrescine used for alkaloid synthesis. For example, Mizusaki *et al.* (1973) observed an excellent correlation between the accumulation of nicotine and the increase in ODC activity in the roots of decapitated tobacco. However, as ADC activity was not reported in this study, it is difficult to conclude whether ADC activity also was elevated by decapitated treatment. A more recent study involving the induction of nicotine biosynthesis in tobacco cell cultures treated with mJA found that the level of ODC transcript was rapidly increased, whereas the level of ADC transcript was not affected (Imanishi *et al.*, 1998b). It is important to note, however, that ADC is known to be subject to post-translational and/or post-transcriptional control in plants (Malmberg *et al.*, 1992; Rastogi *et al.*, 1993). Thus, the possibility of an increase in ADC activity without a concomitant increase in transcription can not be ruled out in the experiment reported by Imanishi *et al.* (1998b). In addition to nicotine biosynthesis in *Nicotiana*, tropane alkaloid production also incorporated [U-^{14}C]ornithine more efficiently than [U-^{14}C]arginine in aseptic roots of intact plants and in homogenous suspension cultured cells of *A. belladonna* (Nyman, 1994).

On the other hand, several studies have suggested that ADC rather than ODC might provide the principal source of the putrescine which is incorporated into alkaloids. For example, Tiburcio *et al.* (1985) observed that changes in ADC activity, but not ODC, corresponded to increased alkaloid levels in tobacco callus grown on media optimal for alkaloid biosynthesis. In addition, they also found that L-[U-^{14}C]arginine was more efficiently incorporated into nicotine than was L-[U-^{14}C]ornithine. Furthermore, inhibition of ADC activity by both DFMA and D-arginine was more effective than inhibition of ODC by DFMO, in inhibiting alkaloid formation in tobacco callus (Tiburcio and Galston, 1986, Tiburcio *et al.*, 1987). Together these observations convinced these researchers that arginine is the preferred origin of putrescine-derived tobacco alkaloids. A study by Feth *et al.* (1986) also claimed support for this postulate. These researchers showed that there was no change in the ornithine content of tobacco callus cultures after the induction of nicotine production by transfer to a medium with altered hormonal composition. Therefore, the ornithine level in the calli is not directly linked to fluxes of metabolites in the direction of nicotine. Another study from the same

laboratory showed that the steady state level of the ornithine pool did not reveal any correlation with the nicotine-producing capacity of tobacco plants. Furthermore, the ornithine pools in tomato roots and tobacco roots were at similar levels, despite the lack of nicotine synthesis capacity in tomato (Feth and Wagner 1989). However, it is important to note that these studies did not determine the levels of either ADC activity or the arginine pool in the tissues under examination, making it impossible to judge the relative importance of ADC in the synthesis of nicotine in these tissues.

Evidence from plant species belonging to other genera has also suggested that arginine supplies most of the putrescine that is consumed in alkaloid biosynthesis. For example, hyoscyamine production, together with free and conjugated putrescine, were substantially inhibited by feeding transformed roots of *D. stramonium* with DFMA, whereas only minimal reduction in levels of these metabolites was observed by feeding with DFMO (Walton *et al.*, 1990; Robins *et al.*, 1991b). These observations led the researchers involved to conclude that the arginine → putrescine route is more important than the ornithine → putrescine route, in providing putrescine for tropane alkaloid production (Walton *et al.*, 1990; Robins *et al.*, 1991b). It should be noted, however, that feeding DFMA also decreased ODC activity in these experiments, since DFMA can be converted to DFMO by arginase (Slocum *et al.*, 1988). Thus, the severe decrease in alkaloid biosynthesis in response to DFMA feeding may not have been solely due to inhibition of ADC activity. In addition, it was noted that in DFMO-fed *D. stramonium* roots, the level of ADC activity was increased which may have compensated for the loss of ODC activity due to the inhibitor. This in turn may have prevented a significant depletion of amine metabolites and alkaloid pools in DFMO-fed roots. Another point is that the levels of spermidine and spermine in these studies (Walton *et al.*, 1990; Robins *et al.*, 1991b) were maintained constant regardless of which inhibitor was present. Thus, it indicated that putrescine was probably metabolised to those compounds preferentially, irrespective of its original source.

Similar DFMO/DFMA feeding experiments involving *Heliotropium angiospermum* and *H. indicum* shoots as well as *Senecio vulgaris* root cultures have been interpreted as providing strong evidence that L-arginine is the main or sole source of putrescine for pyrrolizidine alkaloid formation in these species (Birecka *et al.*, 1987; Hartmann *et al.*,

1988). However, a subsequent study involving *S. riddellii*, *S. longilobus* along with *Crotalaria retusa*, indicated that endogenous ornithine is the main precursor of putrescine converted into the aminoalcohol moiety of pyrrolizidine alkaloid. In these experiments DFMA treatment of the shoots of these plants exposed to ^{14}C-labeled CO_2 had no effect on ^{14}C incorporation into the alkaloid necine, whereas DFMO treatment reduced ^{14}C incorporation into necine significantly (Birecka *et al.*, 1988).

It should be noted that the biosynthesis of putrescine from arginine, involves not only ADC activity, but also the co-ordinated activity of agmatine iminohydrolase and N-carbamoylputrescine amidohydrolase. Burtin and Michael (1997) examined the effects of over-expressing the oat *ADC* cDNA in tobacco plants. Despite a markedly elevated ADC activity (6- to 16-fold), and elevated agmatine levels (16-fold increase) in the second-generation offspring of the transgenic plants, no effect on nicotine, putrescine, spermidine or spermine levels as well as the polyamine conjugate pool could be detected in transgenics compared to controls. Thus, the capacity of elevated ADC alone to influence polyamine and alkaloid biosynthesis appears to be limited (Burtin and Michael, 1997).

Pinol *et al.* (1987) suggested that in tobacco plant tissues the relative contribution of ADC and ODC to the biosynthesis of putrescine, and consequently of nicotine, is dependent upon the type of tissue and growth process conditioned by the medium.

If putrescine produced by either the ODC or the ADC route is preferentially utilised either for growth or for alkaloid biosynthesis, the question arises as to how both pools of putrescine are distinguished *in vivo*. One mechanism may be by ensuring that the key biosynthetic enzymes are localised in separate subcellular compartments. An immuno-histochemical study of oat ADC showed that this enzyme was present in the thylakoids of the chloroplasts and was not found in root sections of oat seedlings (Borrell *et al.*, 1995). It is not yet clear whether ADC is localised in the plastid of roots of alkaloid producing species in which its activity has been measured, e.g. in cultured roots of *H. albus* (Hashimoto *et al.*, 1989a), *D. stramonium* transformed roots (Walton *et al.*, 1990; Robins *et al.*, 1991a, 1991b, 1991c; Michael *et al.*, 1996) and *Nicotiana* transformed roots (Hamill *et al.*, 1990, and this study Chapter 3). In contrast to the localisation of

ADC in plastids, ODC activity has been detected in the vacuole, nucleus and cytoplasm (Galston *et al.*, 1997). Thus, it is possible that these two biosynthetic pathways leading to putrescine formation might be physically separated within plant cells (Kumar *et al.*, 1997; Walden *et al.*, 1997). Interestingly, analysis of the deduced proteins from *N. tabacum ODC* and *ADC* cDNAs (Table 1-5), using the PSORT program (Prediction Of Protein Localisation Sites, version 6.4, http://psortnibb.ac.jp: 8800; Nakai and Kanehisa, 1992) suggests that ADC may be targeted to the chloroplast whereas ODC is likely to be cytosolic, or possibly ER-membrane targeted in tobacco (Table 1-4).

Table 1-4 Predicted subcellular localisation of deduced proteins using PSORT (NC = not computed).

***N. tabacum* ODC**	**Certainty**	***N. tabacum* ADC**	**Certainty**
ER (membrane)	55%	ER (membrane)	NC
ER (lumen)	10%	ER (lumen)	NC
Peroxisome	13%	Peroxisome	33%
Chloroplast (stroma)	NC	Chloroplast (stroma)	85%
Chloroplast (thylakoid)	NC	Chloroplast (thylakoid)	46%
Mitochondria	NC	Mitochondria	NC

1.4.1.3 Molecular biology of ODC and ADC

In animal systems, ODC is regulated at a number of different levels of gene expression; including transcription, mRNA stability and degradation, translation and enzyme stability and degradation (Hayashi and Murakami, 1995). Moreover, its activity is regulated in a complex manner by a specific antizyme protein (reviewed in Hayashi and Murakami, 1995). In mammalian cells and yeast, the presence of polyamines exerts a strong negative feedback regulation upon ODC, which involves changes in rates of the synthesis as well as the degradation of the enzyme (Hayashi and Murakami, 1995; Toth and Coffino, 1999; Wallstrom and Persson, 1999). In contrast, increasing the exogenous supply of polyamines did not suppress ODC activity in tobacco cell cultures

(Hiatt *et al.*, 1986), raising the possibility that feedback control of ODC activity by polyamines may not be as important a control step in plants as it is in animal systems. This may, at least in part, be due to the capacity of plant tissues to sequester excess polyamines in the form of phenolic conjugates (reviewed in Martin-Tanguy, 1985, 1997).

ODC has been extensively studied at the molecular level in mammalian systems, as the synthesis of putrescine in such cells is solely through the decarboxylation of ornithine (Flores and Galston, 1982; Leete, 1983; Tiburcio *et al.*, 1997). In plants, however, the molecular regulation of ODC has been less well characterized (Kumar *et al.*, 1997; Tiburcio *et al.*, 1997). Sequence analysis of the first plant *ODC* cDNA to be cloned from *D. stramonium*, revealed that the encoded protein does not possess an equivalent C-terminal amino acid extension which is known to be involved in the rapid turnover of mammalian ODC (Michael *et al.*, 1996). No evidence for a specific ODC antizyme protein has been found in plants, unlike the situation in animal cells. Interestingly, a recent report by Hanfrey *et al.* (2001) suggests that plants may not be reliant upon possession of a functional ODC enzyme. In their study, Hanfrey *et al.* (2001) report a lack of an intact or degraded *ODC* sequences, as well as the absence of *ODC* expressed sequence tags in the *Arabidopsis* genome, making *Arabidopsis* the only plant characterised to date that lacks ODC activity.

In comparison to plant ODC, the molecular and biochemical regulation of plant ADC has been more thoroughly investigated. Evidence suggests that ADC activity seems likely to be regulated at multiple levels by different stimuli (Malmberg *et al.*, 1998). A cDNA for oat *ADC* was cloned by Bell and Malmberg (1990). Further studies showed that oat ADC is synthesized as a proenzyme, which is cleaved to produce the active enzyme (Malmberg *et al.*, 1992; Malmberg and Cellino, 1994). This post-translational processing is inhibited by addition of spermine (Borrell *et al.*, 1996). Nam *et al.* (1997a) demonstrated that the activity of purified ADC from soybean is very sensitive to agmatine and putrescine whereas application of 0.5 mM spermidine or spermine inhibited ADC activity by only 10-20% (see also section 1.4.1.1).

Several studies have shown correlations in transcript levels and enzyme activity in different types of tissue or in different developmental stages of plants (reviewed by Malmberg *et al.*, 1998). In soybean for example, an increase in ADC activity after acid treatment was preceded by a corresponding increase in *ADC* transcript levels (Nam *et al.*, 1997b). Furthermore, ADC activity in different soybean tissues was found to be correlated with transcript levels (Nam *et al.*, 1997b). On the other hand, some studies have shown that changes in transcript and protein levels cannot account for the observable changes in enzyme activity (Malmberg *et al.*, 1998). Rastogi *et al.* (1993) reported a lack of correlation between ADC activity and transcript levels in the fruit of ripening tomato. This suggests that ADC may be subject to translational and/or post-translational regulation during the process of fruit ripening in tomato. Similar conclusions have been drawn from studies involving pea (Perez-Amador *et al.*, 1995) and *Arabidopsis* (Watson and Malmberg, 1996). A similar study in *Vitis minifera* found that levels and/or activity of ADC is post-translationally regulated (Primikirios and Roubelakis-Angelakis, 2001). Changes in ADC activity during early fruit development in pea (Perez-Amador *et al.*, 1995) or due to potassium deficiency stress in *Arabidopsis* (Watson and Malmberg, 1996) did not appear to correlate with transcript or protein abundance. In contrast to the situation of oat ADC (Malmberg and Cellino, 1994; Malmberg *et al.*, 1992), however, evidence of ADC regulation by post-translational proteolysis of a precursor protein could not be detected in *Arabidopsis* (Watson and Malmberg, 1996). Thus, a variety of mechanisms may be involved in regulating ADC in different plant species and tissues, in response to a range of stimuli (Tiburcio *et al.*, 1997).

Many of the plant decarboxylase genes involved in polyamine biosynthesis are developmentally regulated (Kumar *et al.*, 1997). For example, the *Datura ODC* gene (Michael *et al.*, 1996) and the potato *SAMDC* gene (Taylor *et al.*, 1992; Mad Arif *et al.*, 1994) all appear to be expressed preferentially in rapidly growing tissues (Kumar *et al.*, 1997). These results are consistent with reports that ODC appears to be associated with actively dividing cells in meristematic and reproductive tissues. ADC has been reported to be the primary enzyme for putrescine synthesis in non-dividing elongating cells and

in cells exposed to various stress conditions (Slocum *et al.*, 1984; Evans and Malmberg, 1989; Tiburcio *et al.*, 1997; Walden *et al.*, 1997).

In recent years, DNA sequences encoding ODC and ADC have been cloned from various plants as listed in Table 1-5.

Table 1-5 Cloned sequences encoding plant ODC and ADC

Enzyme encoded	Source of plant species	Reference
ODC	Datura (*Datura stramonium*, cDNA)	Michael *et al.*, 1996
	Tobacco (*Nicotiana tabacum*, cDNA and genomic DNA)	Imanishi *et al.*, 1998a, b, 2000; Wang *et al.*, 2000
	Tomato (*Lycopersicon esculentum*, cDNA)	Alabadi and Carbonell, 1998
ADC	Oat (*Avena sativa*, cDNA)	Bell and Malmberg, 1990
	Tomato (*L. esculentum*, cDNA)	Rastogi *et al.*, 1993
	Pea (*Pisum sativum*, cDNA)	Perez-Amador *et al.*, 1995
	Soybean (*Glycine max*, cDNA)	Nam *et al.*, 1996
	Arabidopsis thaliana (two cDNAs)	Watson and Malmberg, 1996; Watson *et al.*, 1997
	Tobacco (*N. tabacum*, cDNA)	Wang *et al.*, 2000
	Grapevine (*Vitis vinifera*, cDNA)	Primikirios and Roubelakis-Angelakis, 1999
	Carnation (*Dianthus caryophyllus*, genomic DNA)	Chang *et al.*, 2000

Each clone encodes a protein containing a conserved putative substrate-binding site found in all reported eukaryotic ADCs or ODCs (Walden *et al.*, 1997). Furthermore, they also have residues similar to those described as functional binding sites for pyridoxal 5'-phosphate and DFMO, suggesting a similar catalytic mechanism of eukaryote ADCs and ODCs (Tiburcio *et al.*, 1997; Walden *et al.*, 1997). The structure and the evolution of both decarboxylases have been reviewed by Malmberg *et al.* (1998). ADC in plants is typically encoded by a single or low copy nuclear gene, which appears to lack introns (Galloway *et al.*, 1998). Two copies of the *ADC* genes, *ADC1* and *ADC2*, are found in *Arabidopsis* (Watson *et al.*, 1997) and in all other members of

the Brassicaceae so far examined except the basal genus *Aethionema* (Galloway *et al.*, 1998). Comparison of *ADC* gene sequence between different species within the Brassicaceae has also been used to determine phylogenetic relationships (Galloway *et al.*, 1998). Ruiz *et al.* (2000) have identified five different molecular forms of oat ADC and have shown that all of them are immunoreactive and have enzymatic activity.

Mutants deficient in ADC activity have been isolated from *A. thaliana* by Watson *et al.* (1998). Genetic analysis of these mutants indicated that the alleles fell into two complementation groups named *spe1* and *spe2*. These mutants exhibited 20% to 50% of wild type ADC activity. The most striking phenotypes of the individual *spe* mutants were in root development, where decreased ADC activity was correlated with increased lateral root branching and root growth (Watson *et al.*, 1998). Soyka and Heyer (1999) have isolated an *A. thaliana* mutant line carrying an insertion of the *EN-1* transposable element at the *ADC2* locus which caused a knockout of the gene. ADC activity in this mutant is reduced by 44% relative to wild type without obvious changes to phenotype or developmental processes. In this case, *ADC2* seems to play a predominant role in the osmotic stress response, since unlike the wild type, no induction of ADC expression or activity by the osmotite sorbitol could be observed in the homozygous mutant.

Experiments involving altered *ODC* and *ADC* expression in transgenic plants, or cell and tissue cultures, have also been attempted to provide further insights into function or regulation. A summary of these activities and the main conclusion obtained is presented in Table 1-6.

Table 1-6 Manipulations of *ODC* and *ADC* in plants and cultures

Species of plant and cell types used for study	Procedure	Main effect	Reference
Induction of ODC			
Nicotiana rustica transformed root cultures	Over-expressed yeast *ODC* (CaMV35S promoter)	Altered ODC activity profile with an increase up to 3-fold at day 10 of growth cycle (peak ODC activity in control tissues) and persistence of ODC activity thoughout growth cycle such that ODC activity of transgenic tissues were 30-fold greater than that of controls at day 26 of growth cycle. Nicotine levels of transgenic tissues increased up to 2-3 fold relative to controls. Some changes in putrescine content but no alteration in spermine/spermidine content of transgenic tissues.	Hamill *et al.*, 1990
N. tabacum cv. Xanthi whole plants and generated callus	Over-expressed mouse *ODC* (either truncate or full-length) (CaMV35S promoter)	Increased putrescine accumulation in both leaves (2- to 3-fold) and callus cells (4- to 12-fold). Effects on alkaloids metabolism not assessed.	DeScenzo and Minocha, 1993
Daucus carota cell cultures (carrot)	Over-expression of 3'-truncated sequence of mouse *ODC* (CaMV35S promoter)	Increased putrescine levels which correlated with the induction of a high degree of somatic embryogenesis under *in vitro* conditions. The induction in putrescine production via the ODC pathway has no compensatory effects on the ADC pathway since labeled arginine fed to both transgenic and nontransgenic cells were decarboxylated and converted into labeled putrescine at similar rates. In addition, higher rates of putrescine production in the transgenic cells are accompanied by higher rates of putrescine conversion into spermidine and spermine as well as catabolism putrescine.	Bastola and Minocha, 1995; Andersen *et al.*, 1998
Oryza sativa whole plants	Over-expressed human *ODC* (with either CaMV35S or seed-specific promoters)	Significant alterations in titres of putrescine, spermidine and spermine, in seeds, leaves, and roots.	Lepri *et al.*, 2001

Species of plant and cell types used for study	Procedure	Main effect	Reference
Induction of ADC			
N. tabacum cv. Wisconsin38 whole plants	Over-expressed oat *ADC* (Inducible promoter, the Tet-repressor system)	Increased the levels of ADC transcript and activity, together with putrescine and spermidine contents (mainly conjugated forms), following Tet induction. Stunted growth with altered phenotype, characterized by short internodes, thin stems and leaves, leaf chlorosis and necrosis, and reduced root growth. Effects on alkaloids metabolism not assessed.	Masgrau *et al.*, 1997
N. tabacum cv. Xanthi whole plants	Over-expressed oat *ADC* (CaMV35S promoter)	Increased ADC activity (10- to 20-fold) and agmatine level (20- to 65-fold). No increase in the levels of the polyamines, putrescine, spermidine or spermine, was observed. No diversion of polyamine metabolism into hydroxycinnamic acid-polyamine conjugate pool or into the tobacco alkaloid nicotine was detected.	Burtin and Michael, 1997
O. sativa callus and whole plants	Over-expressed oat *ADC* (CaMV35S promoter)	Increased putrescine levels in transgenic callus and regenerated plants (up to 4-fold). The ability/capacity of the callus to regenerate plants or to differentiate were inhibited.	Capell *et al.*, 1998
O. sativa callus and whole plants	Over-expressed oat *ADC* (maize ubiquitin 1 promoter)	Significantly increased the levels of ADC transcript and activity, together with polyamine contents in transgenic callus but were not maintained in vegetative tissue. Only one in 16 independent transgenic lines showed very significant increases in putrescine preferentially in seeds (up to 10 times compared to controls).	Noury *et al.*, 2000
O. sativa whole plants	Over-expressed oat *ADC* (with an ABA-inducible promoter)	Stress-induced up-regulation of ADC activity and accumulation of polyamines in plants.	Roy and Wu, 2001
Cajanus cajan cell lines	Over-expressed oat *ADC*	Increased titres of putrescine in all lines analysed, whereas spermidine and spermine levels were increased in only some of the lines.	Sivamani *et al.*, 2001

Species of plant and cell types used for study	Procedure	Main effect	Reference
Down-regulation of ADC			
Oryza sativa callus and plants	Expressed oat *ADC* in an antisense orientation (CaMV35S promoter)	Exhibited up to 95% and 80% reduction in ADC and ODC activities, respectively, in cell lines. These reflected in a marked decrease in the levels of putrescine (up to a 30-fold reduction) and spermidine (up to a 28-fold reduction), but not spermine. In contrast, the vegetative tissue of transgenic plants did not show a reduction in polyamines levels. However, seeds derived from three out of five plant lines analysed possessed significant reductions in putrescine levels (up to 5-fold reduction).	Capell *et al.*, 2000

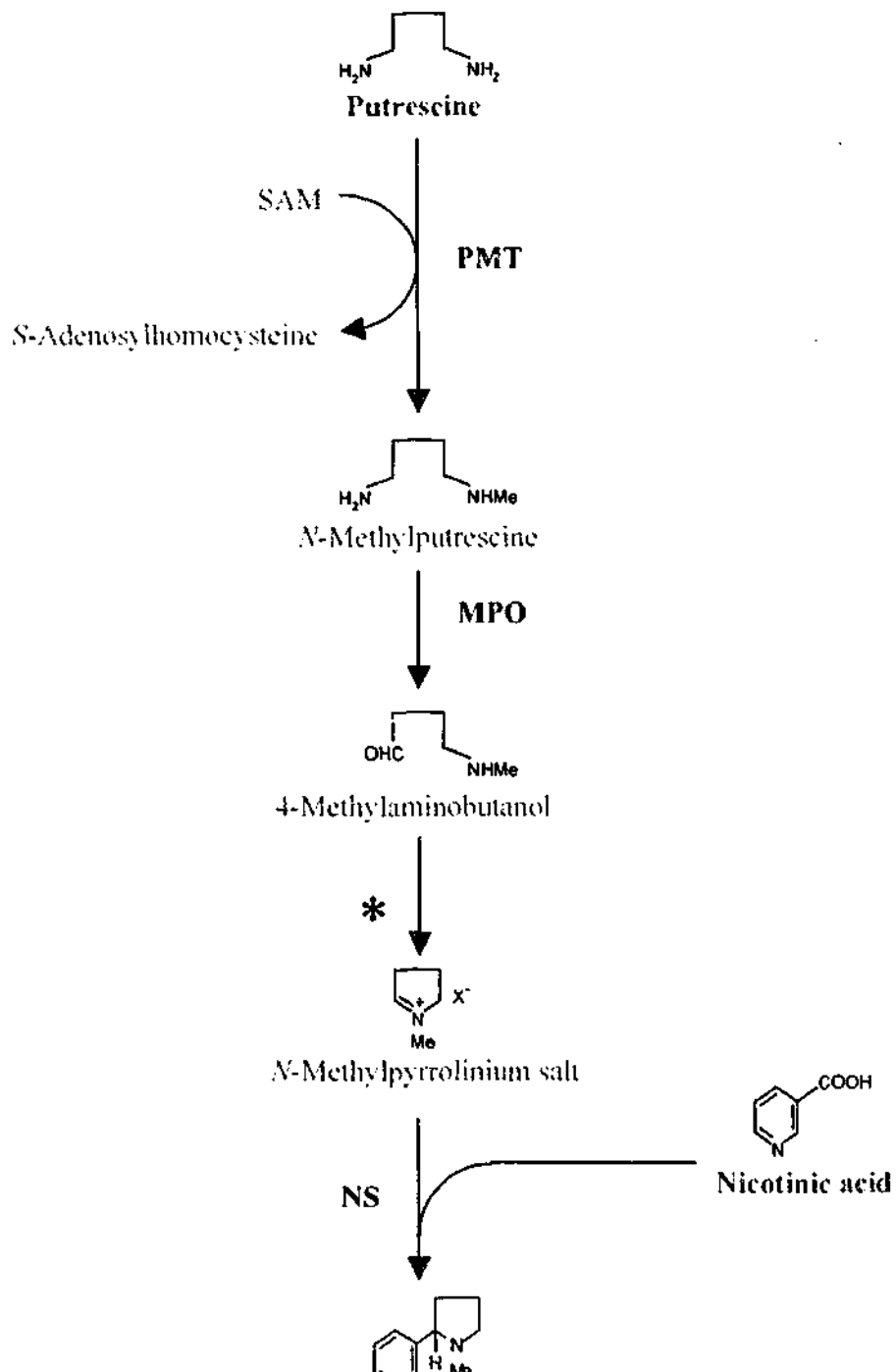

SAM = *S*-adenosylmethionine
PMT = putrescine methyltransferase
MPO = methylputrescine oxidase
NS = nicotine synthase (not characterised to date)
* = spontaneous reaction

Fig. 1-4 Biosynthetic pathway of nicotine from putrescine and nicotinic acid.

1.4.2 The route from putrescine to *N*-methylpyrrolinium salt

Putrescine is probably found in all living cells (Galston and Kaur-Sawhney, 1995) and is metabolised to conjugated forms or to the cell function-regulating polyamines, spermidine and spermine (Slocum *et al.*, 1984; Tiburcio *et al.*, 1997). As has been noted, in some plants, however, putrescine is also metabolised to alkaloids such as nicotine (pyrrolidine alkaloid), hyoscyamine (tropane alkaloid) and serecionin (pyrrolizidine alkaloid). Turburcio *et al.* (1985) have suggested that bound putrescine, particularly in the perchloric acid (PCA)-soluble fraction, may act as a pool for pyrrolidine alkaloid formation in tobacco callus when grown on optimal media for alkaloid biosynthesis. The demonstration that both putrescine conjugates and pyrrolidine alkaloid (nicotine plus nornicotine) titers were effectively reduced by polyamine inhibitors has supported this view (Turburcio *et al.*, 1987). Similarly, a significant decrease in the content of PCA-soluble putrescine conjugates that may supply free putrescine for tropane alkaloid formation was observed at the onset of active alkaloid biosynthesis in *H. albus* root cultures (Hashimoto *et al.*, 1989a). Robins *et al.* (1991c) also suggested that putrescine conjugates may act as a pool of putrescine for tropane alkaloid biosynthesis in transformed root cultures of *D. stramonium*. A more recent study of the utilization and accumulation of ^{15}N labeled metabolites in *D. stramonium* transformed root cultures, using ^{15}N–nuclear-magnetic-resonance, also found that putrescine could be stored as putrescine conjugates prior to its utilization in other pathways (Ford *et al.*, 1998). In addition, the lack of stimulation of hyoscyamine production in *D. stramonium* transformed root cultures by exogenously supplied putrescine indicates that subsequent reactions may be saturated and/or rate-limiting in alkaloid biosynthesis (Walton *et al.*, 1990).

Putrescine *N*-methyltransferase (PMT, EC 2.1.1.53) is the first enzyme specific to the pathway of nicotine and tropane alkaloid biosynthesis and directs the flow of nitrogen away from polyamine biosynthesis to alkaloid biosynthesis (Fig.1-4). Evidence for this is apparent from the reverse relationship that is observed between the contents of putrescine and tropane alkaloids caused by the inhibition of PMT. Both *H. albus* and *D. stramonium* root cultures treated with N-butylamine, a PMT inhibitor,

resulted in a decrease in the combined total content of alkaloids plus methylputrescine together with an approximately equal degree of increase in the combined total contents of putrescine plus polyamines (Hibi *et al.*, 1992).

PMT catalyses the formation of *N*-methylputrescine, an intermediate in the pathway of nicotine and tropane alkaloid biosynthesis, by transferring a methyl group from *S*-adenosyl-L-methionine (SAM) to an amino group of putrescine (Mizusaki *et al.*, 1971; Leete, 1979, 1983; Kutchan, 1998) (further details relating to PMT are in section 1.4.2.1).

In the next step, *N*-methylputrescine is oxidatively deaminated to 4-methyl-aminobutanol by *N*-methylputrescine oxidase (MPO) (Mizusaki *et al.*, 1972). This compound undergoes spontaneous ring closure to form the *N*-methylpyrrolinium cation (Fig. 1-4) (Leete, 1979). MPO has been isolated and characterised from *N. tabacum* and has been demonstrated to catalyze the oxidative deamination of the primary amino group of *N*-methylputrescine (Mizusaki *et al.*, 1972; Davies *et al.*, 1989). In *N. tabacum*, MPO activity was found only in the roots (Mizusaki *et al.*, 1973) which is consistent with the site of nicotine biosynthesis (Waller and Nowacki, 1978). Moreover, the level of MPO activity was increased by prior decapitation (topping) of tobacco plants (in conjunction with ODC and PMT activities) and the enzyme level reached a maximum 24 hours after decapitation (Mizusaki *et al.*, 1973). Cadaverine is also oxidized to piperideine, an important intermediate in the synthesis of the alkaloid anabasine (Fig. 1-2), by MPO whereas other primary amines, such as histamine, tyramine and hexylamine, are not suitable substrates for the enzyme (Leete, 1983).

The *N*-methylpyrrolinium cation is a reactive compound which couples with nicotinic acid to form nicotine (Leete, 1983). Nicotine synthase, the enzyme responsible for producing nicotine from *N*-methylpyrrolinium cation and nicotinic acid, has been reported in cell-free extracts from roots of *Nicotiana glutinosa* and *N. tabacum* and from seedlings of *N. tabacum*, though it has not been characterized in any detail (Friesen and Leete, 1990). Other laboratories have reported difficulties in measuring nicotine synthase in cell free extracts of *Nicotiana* (Hashimoto and Yamada, 1994).

1.4.2.1 Enzymatic and molecular genetics of PMT

1.4.2.1.1 Enzyme properties

PMT was first reported in *N. tabacum* roots, where it was noted that the catalytic reaction of PMT has no requirement for other cofactors (Mizusaki *et al.*, 1971). Subsequently, the enzyme has been purified and characterized from root cultures of *H. albus* and *D. stramonium* (Hibi *et al.*, 1992; Walton *et al.*, 1994). PMT activity was found in *Nicotiana* cell suspension cultures that produced nicotine but was absent in cell lines that did not produce nicotine (Ohta and Yatazawa, 1980). The enzymology of PMT has been extensively studied in cell culture and roots of tropane and pyrrolidine alkaloid producing species, the main studies involving PMT being summarized in Table 1-7 and Table 1-8.

Table 1-7 Summaries of the PMT purification and properties from *N. tabacum* var. Bright Yellow, (Mizusaki *et al.*, 1971) *H. albus* (Hibi *et al.*, 1992) and *D. stramonium* (Walton *et al.*, 1994)

PMT properties	Plant species		
	N. tabacum var. Bright Yellow roots	*H. albus* root cultures	*D. stramonium* transformed root cultures
Purification (fold)	30	13	697
Final yield (%)	26.8	22	3.0
Final specific activity (pkat/mg protein)	854	385	7386
Molecular weight (kDa)	60	62	40
Optimum pH in Tris buffer	8-9	9	8-9
K_m for putrescine (mM)	0.4	0.277	0.31
K_m for SAM (mM)	0.11	0.203	0.1

Table 1-8 PMT activities assay conducting from various sources

Plant	Tissue	PMT activity (pkat/mg protein)	Reference (Analytical procedure)
Nicotiana tabacum var. Bright Yellow	Root	2.4	Mizusaki *et al.*, 1973 (Radioactive product assay)
	Leaf	0	
	Callus	0	
(Decapitated Plant)	Root	36.7	Mizusaki *et al.*, 1973 (Radioactive product assay)
	Leaf	0	
N. tabacum var. Samsun	Root	14	Feth *et al.*, 1985 (HPLC)
		22.5	Wagner *et al.*, 1986c (HPLC)
		35	Feth and Wagner, 1989 (HPLC)
	Cultured root	10	Wagner *et al.*, 1986c (HPLC)
	Callus	0.55	Wagner *et al.*, 1986c (HPLC)
	Suspension culture	0.05	Wagner *et al.*, 1986c (HPLC)
N. tabacum cv. Bursa (nicotine-rich)	Root	18.6	Wagner *et al.*, 1986c (HPLC)
cv. Bursanica (nicotine-poor)	Root	2.8	Wagner *et al.*, 1986c (HPLC)
N. glutinosa	Root	18.3	Feth and Wagner, 1989 (HPLC)
N. debneyi	Root	2.8	Feth and Wagner, 1989 (HPLC)
Atropa belladonna	Root	35.8	Mizusaki *et al.*, 1973 (Radioactive product assay)
Datura stramonium	Root	7.8	Mizusaki *et al.*, 1973 (Radioactive product assay)
		2.7	Feth *et al.*, 1985 (HPLC)
		2.8	Wagner *et al.*, 1986c (HPLC)
	Cultured root	9	Feth *et al.*, 1985 (HPLC)
		8.8	Wagner *et al.*, 1986c (HPLC)
	Transformed root	10.6	Walton *et al.*, 1994 (Radioactive product assay)
Hyoscyamus albus	Cultured root	29	Hibi *et al.*, 1992 (HPLC)
Lycopersicon esculentum (Tomato)	Root	0	Mizusaki *et al.*, 1973 (Radioactive product assay)
		Not detectable	Feth and Wagner, 1989; Wagner *et al.*, 1986c (HPLC)
Barley	Seedling	0	Mizusaki *et al.*, 1973 (Radioactive product assay)

NB PMT activities in tissue and cell cultures of various species studied by Hashimoto *et al.* (1989a) have not been included in this table since they were reported in pkat/g fresh weight.

In an additional study, Hibi *et al.* (1992) have determined PMT activity in root cultures of 17 species representing six tropane alkaloid producing genera from the Solanaceae (*Atropa*, *Datura*, *Duboisia*, *Hyoscyamus*, *Physalis* and *Physochlaina*) and one tropane alkaloid producing species from the Convolvulaceae (*Calystegia sepium*). They found that PMT activity varied substantially among species (ranging from 0.03 to 1.3 pkat/mg dry weight). Despite this variation, a correlation between PMT activity and total alkaloid content was found in the cultured roots that contained hyoscyamine-type alkaloids. The correlation coefficient was 0.745 ($n = 12$, $P < 0.01$) (Hibi *et al.*, 1992).

1.4.2.1.2 Distribution of PMT among plant organs

In *Hyoscyamus niger*, *Datura innoxia*, *A. belladonna*, and *N. tabacum*, PMT activity is strictly localized in the root (Mizusaki *et al.*, 1971; Hibi *et al.*, 1992). This is consistent with the fact that nicotine and tropane alkaloids are synthesized in the roots of these species (Waller and Nowacki, 1978). No PMT activity was detected in the leaf, stem, flower or cultured cells of those tropane alkaloid-producing plants (Hibi *et al.*, 1992). Similarly, in *N. sylvestris PMT* transcript was detected in root tissue but not in flower, leaf or stem tissue (Shoji *et al.*, 2000a). In addition, activity in the branch roots was higher than the main ones consistent with localisation primarily in the metabolically dynamic region of the root tip (Hibi *et al.*, 1992).

1.4.2.1.3 Inhibition of PMT activity

Mizusaki *et al.* (1973) found that the administration of 0.05 mM nicotine to tobacco roots partially prevented the increase in PMT, MPO and ODC activities that would normally be promoted by decapitation. Application of nicotine at a 5 mM concentration completely prevented a rise in these enzyme activities in decapitated plants. However, PMT activity in cell free extracts was not affected by the addition of nicotine. Therefore, the researchers concluded that the capacity to increase PMT activity *in vivo* following decapitation is sensitive to nicotine levels of tissues.

Various amines have been tested for inhibitory effects on PMT *in vitro* (Hibi *et al.*, 1992; Walton *et al.*, 1994). In both investigations, the monoamines: cycloheximine, *exo*-2-aminonorbornane and *n*-butylamine exhibited strongest inhibition. Kinetic analysis indicated that these monoamines are competitive inhibitors of PMT with respect to putrescine (Hibi *et al.*, 1992). Interestingly, the inhibition by cadaverine (a diamine intermediate precursor of anabasine) was moderately effective and was approximately competitive with respect to putrescine (Walton *et al.*, 1994). *N*-methylputrescine also showed inhibition approximately competitive with respect to putrescine though it is not a substrate for the methylation (Walton *et al.*, 1994). *N*-carbamoylputrescine (the immediate precursor of putrescine from agmatine) and agmatine (the metabolic precursor of *N*-carbamoylputrescine and the decarboxylation product of arginine) have no appreciable inhibitory effect on PMT activity in *in vitro* assays (Robins *et al.*, 1991c; Walton *et al.*, 1994). Unlike many methyltransferases, sulfhydryl reagents such as *p*-chloromercuribenzenesulfonic acid, *N*-ethylmaleimide and iodoacetamide, inhibited PMT activity in *H. albus* root cultures only at relatively high concentrations (Hibi *et al.*, 1992). This is not likely to be because O-methyltransferases require Mg^{2+} for maximum activity, whilst no such requirement for Mg^{2+}, or inhibition by EDTA was observed for *H. albus* PMT (Hibi *et al.*, 1992).

Exogenously applied *n*-butylamine, a strong PMT inhibitor, did not severely suppress the growth of *H. albus* cultured roots, although some growth inhibition was apparent at elevated concentrations (more than 6 mM) of the inhibitor (Hibi *et al.*, 1992). At all tested concentrations of *n*-butylamine, (1-10 mM) the content of tropinone, tropine, pseudotropine and hyoscyamine in the cultures was decreased whereas the content of 6β-hydroxy-hyoscyamine and scopolamine remained relatively constant relative to untreated controls (Hibi *et al.*, 1992). These changes suggest that most of the intermediates leading to tropane alkaloid biosynthesis exist in metabolically active pools and that the synthesis of the two hyoscyamine-derivatives, 6β-hydroxy-hyoscyamine and scopolamine, is not controlled primarily by the size of the cellular hyoscyamine pool.

Treatment of *H. albus* root cultures with *n*-butylamine also caused a large increase in both free and conjugated putrescine, 5-fold in the free pool and 2-fold in the conjugated pool (Hibi *et al.*, 1992). The patterns of the increase in putrescine were mirror images of the decrease in total alkaloids of the root cultures with the magnitude of the increase in total putrescine pools being large enough to account for the decrease in the total alkaloid pools. As expected, addition of *n*-butylamine, the inhibitor of PMT, lead to a drastic decrease in the *N*-methylputrescine content of tissues. After the same treatment, in both free and conjugated fractions, the spermine content slightly increased, whereas the spermidine content slightly decreased. This may indicate that *n*-butylamine also inhibited spermidine synthase (Hibi *et al.*, 1992). There was evidence for the inhibition of spermidine synthase and the stimulation of spermine synthase in protoplasts from Chinese cabbage leaves treated with cyclohexylamine (Greenberg and Cohen, 1985). It has been suggested that cyclohexylamine causes an increase in decarboxylated SAM, which is then utilized for the conversion of spermidine to spermine. *n*-Butylamine may have the same function as cyclohexylamine due to the similarity of their structures (Hibi *et al.*, 1992).

Unlike *H. albus* cultured roots, the growth of *D. stramonium* root cultures was partially inhibited by *n*-butylamine feeding (13% at 1 mM) (Hibi *et al.*, 1992). Therefore, the effect of the inhibitor on alkaloid production in *D. stramonium* root cultures was studied only at low concentrations (0.5 and 1 mM). Treatment with 1 mM *n*-butylamine resulted in a clear reduction of the combined total content of alkaloids plus *N*-methylputrescine as well as an increase in the combined total content of putrescine plus spermidine and spermine. This reverse relationship between polyamine and tropane alkaloid levels, plus *N*-methylputrescine levels, was essentially the same as that observed in *H. albus* root cultures, although of a lower magnitude (Hibi *et al.*, 1992). These studies also provide further evidence that PMT is the first enzyme functioning specific to tropane alkaloid biosynthesis in *H. albus* and *D. stramonium* root cultures.

1.4.2.1.4 Substrate specificity

PMT enzymes from root cultures of *H. albus* and *D. stramonium* have been reported to be active against some putrescine derivatives, particularly 1,4-diaminobutane and 1,4-diaminocyclohexane (Hibi *et al.*, 1992; Walton *et al.*, 1994). The highest activity was, however, obtained with putrescine itself. In contrast, 1,3-Diaminopropane, 1,5-diaminopentane (Cadaverine) and 1,6-diaminopentane were virtually inactive as substrates (Hibi *et al.*, 1992; Walton *et al.*, 1994). The essential requirements for appreciable substrate activity were found to be the presence of at least two amino groups in a *trans* conformation, separated by four carbon atoms. According to Walton *et al.* (1994), the requirements for substrate activity are appreciably more stringent than for inhibitory activity. For example, cadaverine as well as its chain-methylated derivatives and monoamine counterpart, amylamine, are active inhibitors, but are not substrates for PMT.

Hibi *et al.* (1992) proposed a model for the active site of PMT comprised of three subsites, one to accommodate the hydrocarbon unit in the substrate and the others for binding the amino groups. One of the amino group binding subsites has a negative charge, whereas the other one where the methylation takes place has a positive charge. This positive charge may be provided by bound SAM, the methyl group donor. This model would explain why the monoamines are good competitive inhibitors of putrescine, but poor substrates since their sole amino group would be placed at the negatively charged subsite, leaving the catalytic subsite empty. The model is also consistent with the higher affinity of the enzyme for monoamine inhibitors than for the diamines since the positive charge at the catalytic subsite would dispel the incoming amino group of the substrate. Furthermore, the model is consistent with the relatively high pH optimum for PMT, since it may help to reduce the positive charge and also to deprotonate the amino groups of the diamines (Hibi *et al.*, 1992). Interestingly, the model of the active site of *H. albus* PMT is also very similar to the model reported for spermidine synthase (SPDS) (Hibi *et al.*, 1992). SPDS catalyzes the transfer of an aminopropyl moiety from decarboxylated *S*-adenosylmethionine to putrescine (Slocum *et al.*, 1984; Tiburcio *et al.*, 1997). Moreover, the inhibitory effects of various

monoamines on *H. albus* PMT are remarkably similar to their inhibitory effects on SPDS (Hibi *et al.*, 1992).

1.4.2.1.5 Molecular genetic of PMT

A cDNA for *PMT* was first isolated by differential screening between the cultured roots of high and low alkaloid varieties of *N. tabacum*, Burley 21 and LA Burley 21 respectively (Hibi *et al.*, 1994). These near-isogenic lines differ in two non-linked loci, A and B, which control nicotine biosynthesis in tobacco (Legg *et al.*, 1969; Legg and Collins, 1971). These loci have been referred to as *NIC1* and *NIC2* by Hibi *et al.* (1994). Using the tobacco PMT cDNA as a probe, *PMT* cDNAs have also been isolated from *A. belladonna* and *H. niger* (Suzuki *et al.*, 1999). Genomic clones of *PMT* also have been isolated from *N. sylvestris* (Hashimoto *et al.*, 1998a), *N. tabacum* (Riechers and Timko, 1999) and *A. belladonna* (Suzuki *et al.*, 1999). Recently, a *PMT* cDNA was cloned also from *N. attenuata* (Winz and Baldwin, 2001).

Deduced amino acid identity between *N. tabacum* PMT and SPDSs from *N. sylvestris*, *H. niger* and *A. thaliana* ranges between 64-68%. This level of conservation is higher than that between mammalian SPDSs and plant SPDSs (47-59% identity) (Hashimoto *et al.*, 1998b). Despite the similarity in amino acid sequence, *N. tabacum* PMT showed no SPDS activity when it was expressed in spermidine synthase-deficient *Escherichia coli* (Hibi *et al.*, 1994). The proposed phylogenetic tree from these data suggests that *PMT* probably evolved from plant *SPDS* after plant and animal *SPDS*s diverged (Hashimoto *et al.*, 1998b). This evolution of *PMT* may have opened up the possibility of alkaloid biosynthesis pathways, which may have been extended by evolutionary mechanisms to enable the synthesis of more complex alkaloids in some plant genera (Hashimoto and Yamada, 1994). In addition, the wide distribution of nicotine (Leete, 1983) and many tropane alkaloids in several taxonomically unrelated genera, albeit at very low levels in most cases (Romeike, 1978) suggests that the evolution of functional PMT from spermidine synthase may have occurred independently in some genera (Hashimoto and Yamada, 1994).

In addition to the portion that is homologous to spermidine synthase, the deduced protein from the *N. tabacum PMT* gene possess an *N*-terminal extension that is not present in spermidine synthase (Hibi *et al.*, 1994). This portion is highly hydrophilic and contains putative glycosylation signals along with tandem repeats of an eleven amino acid element in the first exon (Hibi *et al.*, 1994; Hashimoto *et al.*, 1998a). All five *PMT* nuclear genes in *N. tabacum* have this repeat array with the number of repeats varying from 2 to 8 (Hashimoto *et al.*, 1998a; Riechers and Timko, 1999). *PMT* genes in *N. sylvestris*, *N. tomentosiformis* and *N. attenuata* also have varying numbers of this tandem array in their first exon (Hashimoto *et al.*, 1998a; Winz and Baldwin, 2001). This repeat array in *Nicotiana PMT* is not necessary for enzymatic activity, since a truncated tobacco *PMT* in which this repeat array was entirely removed still retained full enzymatic activity when expressed in *E. coli* (Hashimoto *et al.*, 1998a). In fact, these tandem repeats are absent in *H. niger* and *A. belladonna PMT*s, even though these genes encode fully functional enzymes (Hashimoto *et al.*, 1998a; Suzuki *et al.*, 1999). Analysis of PCR fragments amplified from the genome of *N. tabacum* and its two probable progenitors, *N. sylvestris* and *N. tomentosiformis*, indicates that tandem repeats were added to the ancestral PMT gene, and that the tandem repetition has contracted and expanded during evolution of the *Nicotiana* genus (Hashimoto *et al.*, 1998a).

Genomic DNA blot analysis suggested that *PMT* genes exist as small gene families in *N. tabacum, N. sylvestris, N. attenuata, A. belladonna* and *H. niger* (Hashimoto *et al.*, 1998a; Winz and Baldwin, 2001). Three genes are present in the genome of *N. sylvestris* whereas five are present in *N. tabacum* and all are expressed (Hashimoto *et al.*, 1998a; Riechers and Timko, 1999). Sequence analysis has revealed that three members of the *N. tabacum PMT* gene family were most similar to the three *PMT* genes present in *N. sylvestris* (Hashimoto *et al.*, 1998a; Riechers and Timko, 1999). The two remaining *N. tabacum PMT* genes were similar to *PMT* genes present as single copies in *N. tomentosiformis* and *N. otophora* (Riechers and Timko, 1999). These results support the hypothesis, derived initially from a molecular cytogenic study, which suggested that one haploid set of the *N. tabacum* genome may have originated from ancestral *N. sylvestris* and the other genome set may derive from an introgressived hybrid between *N. tomentosiformis* and *N. otophora* (Kenton *et al.*, 1993). All five *PMT* genes in *N.*

tabacum are highly homologous except for the number of tandem repeats encoded at the *N*-terminus (Riechers and Timko, 1999). The location of the seven introns within the *PMT* genes is identical and appears to be conserved among *PMT* genes from different *Nicotiana* species (Riechers and Timko, 1999). Very little variation in the nucleotide sequences at the exon-intron splice junctions in the various *PMT* genes in *N. tabacum* was reported (Riechers and Timko, 1999).

1.4.2.1.6 Role of PMT enzyme in alkaloid biosynthesis

As has been noted, PMT is the first committed enzyme in the biosynthesis pathway of nicotine and tropane alkaloids and diverts putrescine from polyamine metabolism to alkaloid synthesis (Hashimoto *et al.*, 1989a, b; Kutchan, 1995, 1998). Studies have consistently provided evidence that PMT plays a key role in controlling the synthesis of nicotine and tropane alkaloids.

Initial studies by Mizusaki *et al.* (1973) as well as Saunders and Bush (1979) demonstrated that PMT activity in tobacco root increased and reached a peak 24 hours after the decapitation of the shoot. The increase in PMT activity is followed by a marked rise in nicotine content of wounded plants during subsequent days. A low alkaloid variety of *N. tabacum,* unable to increase nicotine levels substantially following decapitation, also did not show an elevation in PMT activity following decapitation (Saunders and Bush, 1979). Later Hibi *et al.* (1994) found the induction of *PMT* transcript in the roots of the decapitated wild type tobacco, but not the low alkaloid variety.

Experiments undertaken in the mid-late 80's in the laboratory of Wagner involved direct comparisons between PMT activity in the roots of different tobacco cultivars, in different organs of tobacco, together with in dedifferentiated and differentiated tobacco cultures and in the roots of different plant species. Together, these experiments provided evidence that PMT plays a key role in the regulation of nicotine production (Wagner *et al.*, 1986c; Feth and Wagner, 1989).

Further evidence for PMT having a key role in alkaloid production comes from studies of enzyme activity in *N. tabacum* callus, along with *N. rustica* and *D. stramonium* transformed root cultures which were treated with plant growth regulators (Feth *et al.*, 1986; Rhodes *et al.*, 1989; Robins *et al.*, 1991a). For example, in nicotine-stimulating medium, PMT activity in tobacco callus was strongly increased compared to that observed in callus grown under non-nicotine-stimulating conditions (Feth *et al.*, 1986). Similarly, hormonal treatment of *N. rustica* and *D. stramonium* transformed root cultures leads to a very rapid reduction in PMT activity which correlates with a cessation of nicotine and hyoscyamine biosynthesis, respectively (Rhodes *et al.*, 1989; Robins *et al.*, 1991a). Continued growth of transformed roots of *D. stramonium* in hormone enriched medium produced a cell suspension which had very low levels of PMT activity and alkaloid synthesizing capacity. Upon removal of exogenous hormones, root tissues were able to regenerate which was accompanied by an increase in PMT activity and a capacity to synthesize high level of tropane alkaloids (Robins *et al.*, 1991a). These finding(s) are compatible with the hypothesis that the overall ability to biosynthesize either nicotine or hyoscyamine is dependent upon the presence of PMT activity, (since PMT is more sensitive to factors that stimulate or repress nicotine synthesis than other enzymes in the pathway (see also section 1.6)) and the synthesis and inactivation of PMT are rapidly and tightly regulated.

Northern and *in situ* analyses, using the *PMT* coding sequence as a probe, have shown that the predominant site of PMT transcript accumulation is in root tissues of tobacco and *A. belladonna* (Hibi *et al.*, 1994; Suzuki *et al.*, 1999). This is consistent with previous studies showing these tissues to be the primary site of nicotine and tropane alkaloid biosynthesis (Waller and Nowacki, 1978; Wink and Roberts, 1998). Decapitation (topping) of wild type tobacco plants leads to a marked rise in *PMT* transcript abundance in roots within 24 hours (Hibi *et al.*, 1994). Moreover, the accumulation of *PMT* transcript is much lower in the roots of low-alkaloid mutant tobacco than in those of wild type, which correlates with the nicotine production capacity of these plants (Hibi *et al.*, 1994). These observations are consistent with earlier studies into the wound inducibility of PMT activity in roots of the wild type and low alkaloid mutant (Saunders and Bush, 1979). Detailed studies from the laboratory of

Baldwin have shown that nicotine is stimulated in roots of *N. sylvestris* by damage to aerial tissues and that jasmonates are a key component of the signaling mechanism between damaged leaves and roots (Baldwin *et al.*, 1994, 1997; Zhang and Baldwin, 1997). Exogenous application of mJA induces PMT expression in tobacco cell cultures and the intact root tissue as well as in *N. sylvestris* hairy root culture along with inducing nicotine production in these tissues (Imanishi *et al.*, 1998b; Shoji *et al.*, 2000a). Interestingly, mJA treatment did not up-regulate the *PMT* transcript level in *A. belladonna* roots (Suzuki *et al.*, 1999). Histochemical analysis of transgenic *A. belladonna* expressing β-glucuronidase (GUS) fused to the *AbPMT* promoter showed that GUS was expressed specifically in root pericycle cells and is not up-regulated by mJA treatment (Suzuki *et al.*, 1999). A similar experiment conducted in *N. sylvestris* revealed that the *NsPMT* promoter enabled GUS expression in cortex, endodermis and xylem of root tissues (Shoji *et al.*, 2000a).

PMT is thought to be regulated directly, or indirectly by separate genes that were identified initially by Legg *et al.* (1969), Legg and Collins (1971) and subsequently designated *NIC1* and *NIC2* by Hibi *et al.* (1994). Both the enzyme activity of PMT and transcript levels of *PMT* were reduced by mutation in either of the two mutations with the lowest level of *PMT* transcript and enzyme being found in the double mutant *nic1/nic2* (Saunders and Bush, 1979; Hibi *et al.*, 1994).

Auxin is thought to play an important role in the regulation of *PMT* gene expression. Decapitation of tobacco, which may cause a reduced auxin supply from the aerial parts to the roots, not only increased PMT activity as previously mentioned but also rapidly induced *PMT* transcripts in the root (Hibi *et al.*, 1994). Application of auxin to the severed apex after decapitation prevented the rise in *PMT* transcript levels in root tissues (Hibi *et al.*, 1994). Expression of *PMT* in cultured tobacco roots was also down-regulated by the exogenous supply of auxin (Hibi *et al.*, 1994). This is consistent with previous studies showing a rapid decrease in PMT activity in transformed roots of *N. rustica* following treatment with auxin (Rhodes *et al.*, 1989).

It is also possible that PMT may be subject to feed-forward regulation. Elevated levels of PMT activity were observed in transformed roots of *N. rustica* over-expressing

the yeast ODC gene which produced elevated levels of putrescine in these tissues (Hamill *et al.*, 1990). In *D. stramonium* transformed roots treated with DFMA and, to a lesser extent DFMO, PMT activity was diminished in a concentration-dependent manner (Robins *et al.*, 1991b). The diminished PMT activity might be due to an extreme reduction in agmatine content which is caused by DFMA-treatment. When roots were treated with 5 mM DFMA, the addition of 2 mM to 3 mM agmatine caused a substantial stimulation of PMT activity, restoring the levels normally present in the absence of DFMA (Robins *et al.*, 1991b). More detailed studies are necessary to determine whether these alteration in PMT activity are due to change in *PMT* transcript levels.

Alteration of the calcium levels in culture medium also affects the expression of PMT. Without affecting the growth of *D. stramonium* transformed roots, decreasing calcium ion-concentrations from the normal level of 1.0 mM to 0.25 mM in B5 liquid medium significantly decreased *PMT* transcript levels and the enzyme activity. This resulted in markedly reduced tropane alkaloid levels in these tissues (Pinol *et al.*, 1999).

1.5 The route to the pyridine ring

The precursor of the pyridine ring in *Nicotiana* alkaloids is nicotinic acid which is synthesized as part of the pyridine nucleotide cycle (Dawson, 1962; Mann and Byerrum, 1974; Leete, 1983; Wagner *et al.*, 1986a, 1986b). In plants, the biosynthetic pathway for the formation of nicotinic acid, which is involved in primary metabolism as well as alkaloid biosynthesis, differs from the route established in animals and microorganisms (Luckner, 1990). The primary precursor of nicotinic acid in animals is tryptophan (Leete, 1983; Luckner, 1990). In plants the primary precursors of nicotinic acid formation are considered to be aspartic acid and 3-phospho-D-glyceraldehyde or closely related metabolites. These are condensed and then undergo a series of reactions to form quinolinic acid, a key intermediate in nicotinic acid biosynthesis (Luckner, 1990).

In the nicotinic acid biosynthetic pathway in *N. tabacum* root (Fig. 1-5), quinolinic acid is converted to nicotinic acid mononucleotide (NaMN) before entering the pyridine

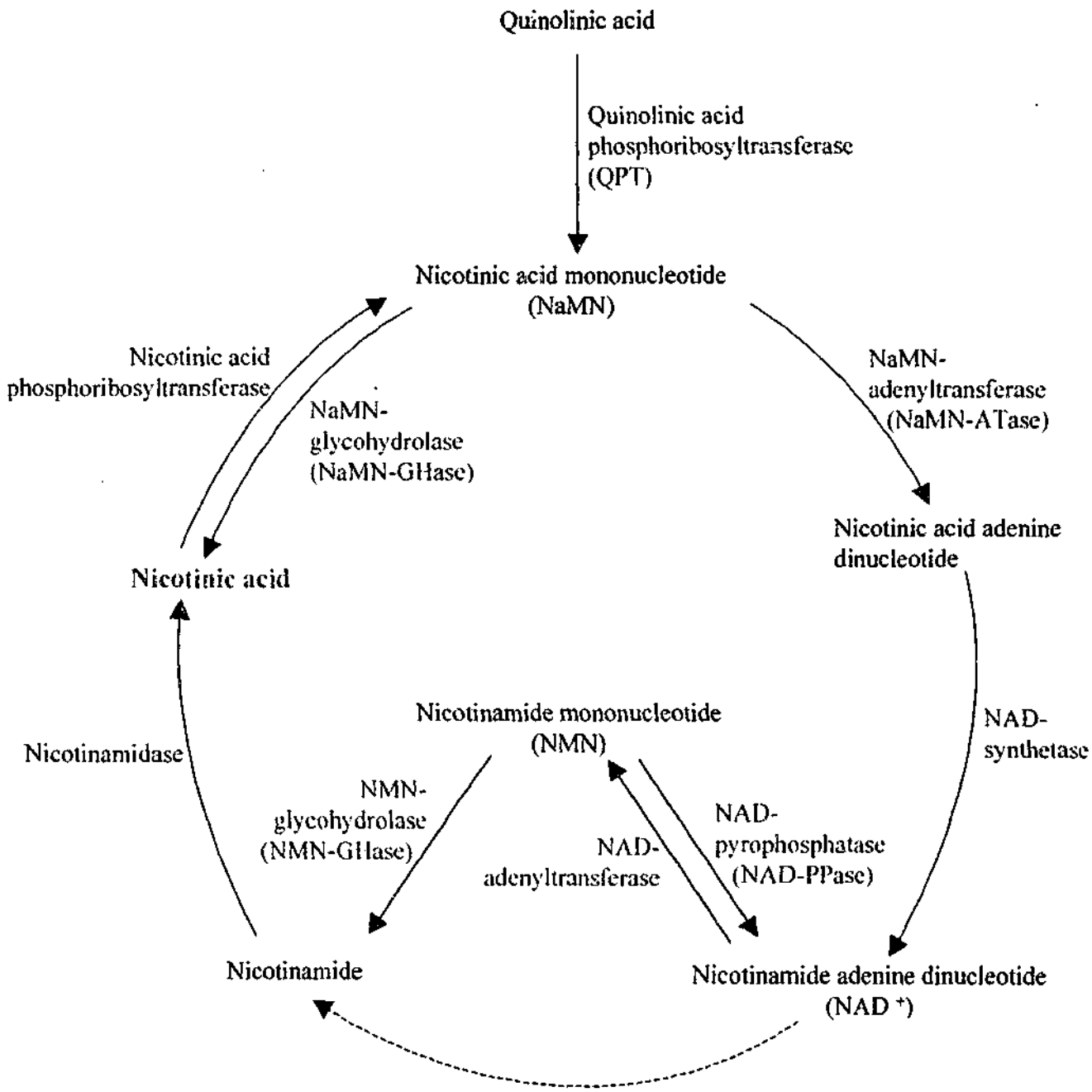

Fig. 1-5 The pyridine nucleotide cycle in *Nicotiana* (adapted from Wagner *et al.*, 1986c)

nucleotide cycle, the recycling pathway of nicotinamide adenine dinucleotide (NAD^+)(Wagner and Wagner, 1985; Wagner *et al.*, 1986a, 1986c; Lucker, 1990; Sharma *et al.*, 1998). NAD^+ is an essential cofactor of many hydrogen-transferring oxidoreductases in all organisms (Wink, 1997). Quinolinic acid phosphoribosyl-transferase (QPT, EC 2.4.2.19) is the enzyme that catalyzes this conversion by transfer of a phosphoribosyl group from 5-phosphoribosyl-1-diphosphate to quinolinic acid, forming NaMN. From this point, NaMN can be directed to nicotinic acid via two routes (Wagner *et al.*, 1986a, 1986b, 1986c). On the one hand, it may be converted either directly to nicotinic acid via the catalytic reaction of NaMN glycohydrolase (NaMN-GHase). Alternately, it may also be converted via NAD^+ as a component of the pyridine nucleotide cycle (Wagner *et al.*, 1986a, 1986c; Lucker, 1990).

The pyridine nucleotide cycle has been studied and several enzymes in the cycle have been characterized in different tobacco tissues and tomato roots by Wagner and co-workers (Wagner and Wagner, 1985; Wagner *et al.*, 1986a). Despite the existence of several possible different versions of the pyridine nucleotide cycle in nature, their data favoured the existence of the so-called pyridine-nucleotide cycle VI which includes six component members (Fig. 1-5) (Wagner *et al.*, 1986a).

In the formation of NAD^+, NaMN-adenyltransferase (NaMN-Atase) converts NaMN into nicotinic acid adenine dinucleotide (NaAD) which then is converted into NAD^+ by NAD synthetase (Wagner and Wagner, 1985). NAD^+ is then amidated into nicotinamide mononucleotide (NMN) which is cleaved to nicotinamide. The enzymes in these two steps are NAD pyrophosphatase (NAD-PPase) and NMN glycohydrolase (NMN-GHase), respectively. It is also possible that NAD^+ is directly converted into nicotinamide, although this enzymatic activity has not yet been determined in tobacco (Wagner *et al.*, 1986a). Deamidation of nicotinamide by nicotinamidase leads to nicotinic acid which is then transformed via NaMN and NaAD back into NAD (Wagner *et al.*, 1986a). Thus, the pyridine nucleotide system has two possible routes leading to nicotinic acid. One enzymatic route takes advantage of the fact that NAD^+ is rather rapidly turned over in living cells. The second route is a direct one using one enzymatic step which transforms NaMN to nicotinic acid (Fig. 1-5).

There is considerable evidence that together with PMT, QPT (the enzyme feeding the pyridine nucleotide cycle) is also of key importance in nicotine synthesis. For example, the activity of *N. tabacum* QPT is much greater in the roots where nicotine is produced, than in the leaves (Saunders and Bush, 1979). In addition, as for PMT, the level of QPT activity was observed to increase in root tissues after the decapitation of shoots and in callus cultures grown in nicotine-induction medium, at 3- and 5-fold, respectively (Saunders and Bush, 1979; Wagner *et al.*, 1986b). The levels of QPT activity in four Burley21 tobacco genotypes with different nicotine-producing capacities: high (AABB), high intermediate (AAbb), low intermediate (aaBB) and low (aabb) nicotine levels, have been reported (Saunders and Bush, 1979). These genotypes were nearly isogenic except for the loci which controls nicotine production (A = *NIC1* and B = *NIC2*, section 1.4.2.1.6). It was observed that QPT activity in roots of these varieties correlated with genotype. QPT activity in the low genotype was very low compared to activity found in the high genotype. In addition, QPT activity in this low alkaloid genotype was not induced significantly following decapitation, whereas activity in the high alkaloid variety was increased 3-fold. Thus, a ceiling on QPT activity in the low-nicotine-producing genotype may limit nicotine synthesis (Saunders and Bush, 1979). Moreover, comparison of enzyme activities in tobacco tissues with different capacities of nicotine synthesis showed that QPT activity was strictly correlated with nicotine content (Mann and Byerrum, 1974; Wagner and Wagner, 1985).

Work reported by Wagner *et al.* (1986c) also demonstrated that the pathway providing nicotinic acid for nicotine production is predominantly regulated by QPT. The activities of the enzymes in the route from quinolinic acid to nicotinic acid, together with nicotine content, were determined in a variety of tobacco tissues. It was observed that all samples with high nicotine contents also showed high levels of QPT activity whilst tissues with low or zero capacity to synthesise nicotine possessed low QPT activity. Recent identification of cDNA sequences representing *Nicotiana* QPT will facilitate further experimentation to determine the link between transcript abundance and enzyme activity in nicotine synthesis (Sinclair *et al.*, 2000).

Regulation of other enzymes in the pyridine nucleotide cycle, particularly NaMN-glycohydrolase and also NaMN-ATase, NAD-PPase, NMN-GHase and NaMN-GHase,

are likely to play a role in regulating the supply of nicotinic acid for nicotine synthesis (Wagner *et al.*, 1986b).

Nicotinic acid also serves as a precursor for anatabine and anabasine synthesis in tobacco (Leete, 1983). Thus, it is likely that the biosynthesis of these *Nicotiana* alkaloids might compete for the common intermediate, nicotinic acid. Feeding nicotinic acid to *N. rustica* transformed roots enhanced the levels of both nicotine and anatabine, with a markedly greater proportion of anatabine being produced (Robins *et al.*, 1987). In contrast, feeding cadaverine to transformed root cultures of *N. rustica* led to an increase in anabasine levels at the expense of nicotine (Walton *et al.*, 1988). Recent work by Sinclair and Hamill (2002) has shown that *QPT/PMT* transcript levels in wounded leaves of *N. glauca* seem to follow patterns expected for anabasine biosynthesis.

1.6 Co-ordinated relation of the enzymes from both branches of metabolism involved in nicotine biosynthesis

As has been described, the nicotine biosynthesis pathway is bifurcated and is closely connected with primary metabolism (Wagner *et al.*, 1986b). The routes from ornithine/ arginine, on the one hand, and from quinolinic acid and the enzymes in the pyridine nucleotide cycle on the other hand must be regulated co-ordinately in order to ensure nicotine levels can be increased in response to environmental stress. As yet, the mechanisms controlling this co-ordinated regulation are poorly understood, though progress is being made toward this goal. Both routes of the pathway are strictly regulated and obviously tuned to each other. For the route leading to *N*-methylpyrrolinium, it is the activity of PMT which is very stringently controlled, whereas with the pyridine nucleotide cycle it is the anaplerotic enzyme, QPT. In both routes, however, additional enzyme activities (such as MPO, and NaMN-adenyltransferase) appear to be co-regulated, although in a less stringent way (Wagner and Wagner, 1985; Wagner *et al.*, 1986b). Changes in the levels of these enzymes involved in nicotine biosynthesis following the alteration of nicotine production capacity have been investigated as presented below.

The work of Mizusaki *et al.* (1973) and Saunders and Bush (1979) showed that nicotine synthesis as well as activity levels of the enzymes ODC, PMT, MPO and QPT were co-ordinately increased in roots following 24-48 hours after the decapitation of tobacco shoots. ODC, PMT and MPO activities all reached their peaks within 24 hours after the decapitation, whilst QPT activity peaked somewhat later at 40 hours. Nicotine levels continued to rise in plants 7-10 days after wounding and it was suggested that the decline in enzyme activities may be due, in part, to repression of enzyme synthesis by the accumulated nicotine. Simultaneous changes in the activities of these enzymes suggest that they may be under the control of a common regulatory system, which is specifically concerned with nicotine biosynthesis.

Comparison of PMT, MPO and QPT activities in four tobacco genotypes, that are near isogenic but differing at A (*NIC1*) and B (*NIC2*) loci, suggested that all three enzymes are co-ordinately regulated by one or both loci in a complex association (Saunders and Bush, 1979). The recessive allele at either locus affected levels of all three enzymes in roots. The data of Saunders and Bush, (1979), together with the data of Legg and Collins (1971) indicated that effects of both regulatory loci are additive and cumulative upon nicotine levels and associated enzymes, PMT, MPO and QPT. Saunders and Bush (1979) suggested that such regulation could be direct with either or both loci serving as regulatory loci or, alternatively, indirect regulation involving metabolic products of other enzymes coded for by the A (*NIC1*) or B (*NIC2*) loci. These authors also studied QPT activity in leaves of these four genotypes. Whilst QPT levels were low compared to roots of wild type, there was no significant difference in activity between genotypes, suggesting that neither the A (*NIC1*) nor B (*NIC2*) loci is operative in the leaves.

Changes in the levels of enzyme activities involved from both areas of metabolism leading to nicotine biosynthesis have also been studied in tobacco callus (Feth *et al.*, 1986; Wagner *et al.*, 1986b). The induction of nicotine production in tobacco callus by a reduction of the auxin concentration stimulated the activities of PMT, MPO and QPT rather early in the growth cycle. The strong stimulation of these enzyme activities indicates that induction of nicotine synthesis is correlated to the increased activities of these control enzymes. However, in contrast to the situation in decapitated tobacco,

ODC activities were very similar in such callus under nicotine-stimulating and non-stimulating conditions. Another difference from studies involved in plants was that the peak of QPT activity in the callus was slightly in advance of those of PMT and MPO, rather than lagging behind, as in roots of decapitated tobacco. The fact that the enzyme activities declined during the later stages of growth may be due to turnover and degradation of the enzymes together with reduced rates of enzyme synthesis.

Rhodes *et al.* (1989) and Robins *et al.* (1991a) have also studied the relationship of the enzyme activities in transformed roots of *N. rustica* and *D. stramonium* transferred to NK medium where the alkaloid production in both species ceased promptly. In this medium, in contrast to B5 medium lacking phytohormones, the PMT and MPO activities were dramatically reduced, while the activities of ODC and ADC were much less reduced.

The induction of genes encoding enzymes involved in nicotine synthesis by the application of mJA has been studied in tobacco cell cultures. Imanishi *et al.* (1998b) have reported that mJA sequentially induces expression of a series of genes involved in nicotine biosynthesis by multiple regulatory mechanisms. Together with a marked increase in PMT activity and transcript levels (as mentioned in section 1.4), mJA also induced the accumulation of *SAMS*, *ODC* and *QPT* transcript levels in tobacco cell cultures. These mJA-inducible accumulated mRNAs were significantly repressed by auxin (with the exception of *QPT*, which was not mentioned). Unlike the mJA-induction of the *ODC* mRNA, which occurred in the presence of cycloheximide, mJA-induction of *SAMS*, *PMT* and *QPT* mRNAs were blocked by cycloheximide. This indicates that *de novo* synthesis of functional protein(s), possibly one or more transcription factor/protein(s), might be required after mJA treatment to up-regulate expression of SAMS, PMT and QPT. As expression of ODC occurred in the presence of cycloheximide, mJA-induced accumulation of *ODC* mRNA might be mediated via the activation of pre-existing protein(s). Another difference between the regulation of these genes is that the level of *ODC* mRNA declined after 1 to 4 hours following mJA treatment, while the transcript levels of *SAMS* and *PMT* continued to increase. In addition, mJA treatment also led to an increase in the level of *N*-methylputrescine along with a slow increase in putrescine level. In contrast, mJA treatment did not effect the

levels of spermidine, spermine, nor *ADC* and *SAMDC* transcripts. Thus, mJA seems to induce expression of genes encoding enzymes involved in nicotine biosynthesis selectively, while genes involved in the synthesis of higher polyamines from putrescine are unaffected. A subsequent study found that when transformed roots of *N. sylvestris* were treated with natural ethylene precursor, the capacity of *PMT* and *ODC* genes to be induced by jasmonate was completely suppressed (Shoji *et al.*, 2000b). This suppressive effect was abolished when ethylene perception was blocked by feeding silver cations. These results, together with additional immunoblot studies suggested that the jasmonate signal in nicotine biosynthesis is antagonized by the ethylene signal (Shoji *et al.*, 2000b). Similar results were also recently observed in *N. attenuata* plants (Winz and Baldwin, 2001).

Taken together, information presented in this section and section 1.5, suggests that a complex association exists, involving the co-ordinated regulation of enzymes noted above, by one or more regulatory genes, probably encoding transcription factor(s).

1.7 Aims of this study

1.7.1 Down-regulation of *ADC* by antisense methodology

As mentioned in section 1.4.1.2 questions remain regarding the contribution of ADC to the biosynthesis of putrescine, which is required for alkaloid formation. Conclusions from previous studies have been based largely upon correlations between enzyme activity and alkaloid production or following treatment with the irreversible biochemical inhibitors of ODC and ADC, namely DFMO and DFMA respectively. The latter, whilst useful, may have variable effects upon metabolism and show different levels of stability in plant cells (Kumar *et al.*, 1997) leading to varied results in different plant systems. In addition, feeding of these inhibitors at mM concentrations is also detrimental to the growth of transformed root cultures, such as *D. stramonium* (Walton *et al.*, 1990). Moreover, application of these inhibitors to living plant tissues may not be strictly inhibitory to the target enzymes, especially DFMA which can be converted to DFMO by arginase (Slocum *et al.*, 1988). Arginase activity was found to be low in tobacco

callus tissues (Tiburcio and Galston, 1986) but was high in transformed root tissues of both *D. stramonium* and *A. belladonna* (Walton *et al.*, 1990). Interestingly, whilst the inclusion of DFMA in culture media was more effective than equivalent concentrations of DFMO, DFMA at 10 mM reduced growth relative to untreated control tissues by more than 50%, whereas DFMO at 10 mM reduced growth by only about 25% (Walton *et al.*, 1990). The data of Robins *et al.* (1991b) also shows that whilst 1-10 mM DFMA is more effective than equivalent concentrations of DFMO at reducing putrescine and *N*-methylputrescine levels of *D. stramonium* transformed roots, it also significantly reduced ODC as well as ADC activity of roots compared to untreated controls. Paradoxical effects of these inhibitors on polyamine levels also have been reported in *Hevea brasiliensis* (El Hadrami and D'Auzac, 1992). Thus, biochemical inhibitor experiments are sometimes difficult to interpret.

In the current project, experiments described in chapter 3 were undertaken with the intention of down-regulating ADC activity using antisense methodology to study effects upon alkaloid levels of *N. tabacum* transformed root cultures. Down-regulation of ADC specifically was considered a useful way of determining whether a correlation exists between reduced ADC activity and reduced alkaloid content of tobacco transformed roots as is suggested by the various studies noted above which have involved the use of DFMA in callus tissues of *N. tabacum* (Tiburcio and Galston, 1986; Tiburcio *et al.*, 1987), in addition to root cultures of other species including *H. angiospermum* and *H. indicum* (Birecka *et al.*, 1987), *S. vulgaris* (Hartman *et al.*, 1988) and *D. stramonium* (Walton *et al.*, 1990; Robins *et al.*, 1991b).

1.7.2 Down-regulation of *PMT* by antisense methodology

As has been noted, previous studies have shown both PMT and QPT levels are elevated in wild type *N. tabacum* relative to the low alkaloid variety carrying a mutation in both regulatory genes *Nic1* and *Nic2* (Saunders and Bush, 1979; Wagner *et al.*, 1986c). Recent results in this laboratory have demonstrated that the expression of *PMT* together with *QPT* in roots of wild type *N. tabacum* and also *N. sylvestris* are up-regulated 12-24 hours after wounding of aerial tissues. In contrast, the expression of

both genes in a low-alkaloid-producing variety tobacco, LAFC53 are low relative to the closely related high alkaloid-producing line NC95 and are not up-regulated by wounding (Sinclair *et al.*, 2000).

The isolation of a cDNA encoding *PMT* (Hibi *et al.*, 1994) in conjunction with antisense methodology, makes it is possible to study the effects of specifically diminishing expression of *PMT* in transgenic plant tissues containing wild type versions of *NIC1* and *NIC2* genes. This would be distinct from the *in vivo* situation involving the low alkaloid variety of tobacco where PMT and QPT are both down-regulated by the *nic1/nic2* mutations (Saunder and Bush, 1979; Wagner *et al.*, 1986c). It would also be expected to differ from the situation of tobacco callus growing in media with altered auxin concentrations where PMT and QPT activities both are affected (Fetch *et al.*, 1986; Wagner *et al.*, 1986b).

Previous experiments showed that transformed roots of *N. rustica* were sensitive to the addition of low level of nicotinic acid to the medium, with growth being totally inhibited by 2.5 mM nicotinic acid (Robins *et al.*, 1987). Moreover, roots treated in this manner were observed to contain high levels of anatabine, normally a minor alkaloid in *N. rustica* and *N. tabacum*.

Experiments described herein seek to address the question as to whether down-regulation of PMT activity would be possible, using an antisense approach, due to the possible build up of nicotinic acid *in vivo* to levels which would prove toxic to growth. If lines strongly down-regulated for PMT were capable of being recovered, it would be of interest to assess the extent to which their alkaloid content was altered by the manipulation. Additionally, it would be of interest to assess whether expression of other genes in this area of metabolism was affected by the manipulation.

Chapter 2

Materials and Methods

2.1 Solutions, reagents, and media

2.1.1 General solutions

All solutions, reagents, and media were made using high quality Milli-Q water unless otherwise stated and were made according to the protocol of Hamill and Lidgett (1997).

- **Agarose gels for separation of DNA and RNA by electrophoresis.** 0.8% (w/v) to 1% (w/v) agarose gel powder dissolved in 1 X TBE buffer containing 3 µl EtBr stock solution per 100 ml of molten agarose.
- **Ammonium acetate.** A 10 M stock was made and sterilised by filtration.
- **Chloroform/IAA.** 24 parts chloroform with 1 part isoamyl alcohol.
- **Cell lysis buffer.** 0.2 M NaOH, 10% (w/v) SDS.
- **Denaturer.** 0.5 M NaOH, 1.5 M NaCl. pH adjusted until over 12.
- **Denhardt's solution.** A 50X stock was made and filtered; 1% (w/v) Ficoll (Type 400), 1% (w/v) soluble polyvinylpyrrolidone, 1% (w/v) BSA (bovine serum albumin) fraction V.
- **EtBr stock solution.** A 1% (w/v) stock was made and stored in the dark at 4°C.
- **Extraction buffer for plant genomic DNA.** 0.1 M Na_2EDTA, 0.1 M sodium diethylthiocarbonate in 3 X SSC (pH = 8).
- **Formaldehyde denaturing agarose gel for separation of RNA by electrophoresis.** 1.5% (w/v) agarose, 5% (v/v) formaldehyde, 1 X MOPS buffer and 0.67 mg/L ethidium bromide.
- **Gel loading dye.** A 6X stock was made; 0.25% bromophenol blue, 0.25% xylene cyanol FF, 15% ficoll type 400.

- **Luria Bertani broth (LB).** 1% (w/v) tryptone, 0.5% (w/v) yeast extract, and 1% (w/v) NaCl. pH adjusted to 7.5 with 1 M NaOH before autoclaving. (For solid media, 1.5% (w/v) agar was added to the liquid media before autoclaving.)
- **MOPS RNA buffer.** A 5X stock was made; 1 M 3-(N-morpholino) propanesulfonic acid (MOPS), 0.25 M sodium acetate, 0.05 M EDTA.
- **Neutraliser.** 1 M Tris-HCl, 1.5 M NaCl. pH adjusted to 8 with concentrated HCl.
- **Phenol/chloroform.** Equal volumes of phenol and chloroform/IAA solutions were combined.
- **Phenol for DNA purification**. 500 g of high quality phenol crystals were melted and washed in 500 ml TE and stirred for 15 min. The supernatant was discarded and the extraction repeated until the pH of the supernatant was 7.5–8.0.
- **Phenol for RNA purification.** As above, except that TE of pH 4.5 was used to extract and store the phenol.
- **Plasmid isolation buffer.** 50 mM glucose, 25 mM Tris HCl (pH 8.0) and 10 mM Na_2EDTA (pH 8.0).
- **Potassium acetate.** A 3 M solution was made and the pH adjusted to 4.8 with glacial acetic acid before autoclaving. The resulting solution is 3 M with respect to K^+ and 5 M with respect to acetate.
- **RNase A.** A 10 mg/ml stock was made in 10 mM Tris HCl (pH 7.5) and 15 mM NaCl. The solution was boiled for 15 minutes and cooled to room temperature before storage at -20°C.
- **Salmon/herring sperm DNA (100 ml).** A 5 mg/ml stock of salmon or herring testes DNA was made. The solution was passed through a fine gauge needle (23G) several times to shear the DNA and was stored at -20°C.
- **Sodium acetate.** A 3 M solution was made and the pH adjusted to 6.0 with glacial acetic acid before autoclaving.
- **Sodium phosphate buffer.** A 1 M stock was made and the pH adjusted to 7.0 with orthophosphoric acid.
- **SSC.** A 20X stock was made. 3 M NaCl and 3 M sodium citrate (or sodium acetate). The pH was adjusted to 7.0 with 10 M NaOH before autoclaving.

• **SSPE.** A 20X stock was made. 175.3 g NaCl and 31.2 g $NaH_2PO_4.H_2O$ was dissolved in 800 ml H_2O. The pH was adjusted to 7.7 with NaOH before the addition of 40 ml of 0.5 M Na_2EDTA (pH = 8.0) and then autoclaved.

• **TE.** 10mM Tris, 1mM EDTA. pH adjusted to 7.5 before autoclaving.

• **TLES buffer for RNA extraction from plant tissue.** 100 mM Tris HCl (pH = 8), 100 mM LiCl, 10 mM EDTA (pH = 8), 1% (w/v) SDS.

• **Tris-Borate buffer (TBE).** A 10X stock was made. 0.09 M Tris-Borate, 0.002 M EDTA. pH should be 8.3 with adjustment.

• **Tryptone Yeast broth (TY).** 0.5% (w/v) tryptone, 0.3% (w/v) yeast extract. pH adjusted to 7.0 with 1 M NaOH before autoclaving. (For solid media, 1.5% (w/v) agar was added to the liquid media before autoclaving.)

• **Transformation and storage buffer (TSB).** LB broth (pH = 6.1) with 10% (w/v) PEG [MW = 6000], 10 mM $MgCl_2$, 10 mM Mg_2SO_4 and 5% (v/v) DMSO which was added prior to resuspension.

• **X-Gluc solution.** A 20 mM stock was prepared in *N,N*-dimethylformamide in 100 mM sodium phosphate buffer (pH = 7) containing 0.1% (v/v) Triton X-100, 10 mM EDTA, and 1 mM each of potassium ferri-and ferrocyanides.

• **Yeast mannitol broth (YMB).** 0.05% (w/v) K_2HPO_4, 0.2% (w/v) $MgSO_4.7H_2O$, 0.1% (w/v) NaCl, 0.4% yeast extract and 1% (w/v) mannitol. pH adjusted to 7.0 with 1 M NaOH before autoclaving. (For solid media, 1.5% (w/v) agar was added to the liquid media before autoclaving.)

2.1.2 Tissue culture media, hormones, and antibiotic solutions

• **Ampicillin.** (As ampicillin sodium) A 25 mg/ml stock solution was made in Milli-Q water and filter-sterilised with a 0.2 μm sterile disposable filter before storage at –20°C in 1 ml aliquots. Ampicillin was added to media to give a final concentration of 50 μg/ml for plasmid selection in *E. coli* or 250 μg/ml – 500 μg/ml for root cultures.

• **B5 medium** (Gamborg *et al.*, 1968). 0.3875% (w/v) B5 plant medium powder (ICN-Biomedical), 3% (w/v) sucrose, pH = 5.8-6.0 after autoclaving. 0.27% (w/v) Phytagel (Sigma) was added to prepare solid B5 medium.

• **BAP.** A 1 mg/ml stock solution was made in 1 N NaOH and filter-sterilised with a 0.2 µm sterile disposable filter.

• **IAA.** A 1 mg/ml stock solution was made in ethanol and filter-sterilised with a 0.2 µm sterile disposable filter.

• **Kanamycin.** (As kanamycin monosulfate) A 25 mg/ml stock solution was made in Milli-Q water and filter-sterilised with a 0.2 µm sterile disposable filter before storage at –20°C in 1 ml aliquots. Kanamycin was added to media to give a final concentration of 50 µg/ml for plasmid selection in bacteria or 30 µg/ml for selection of transformed root cultures containing binary vector T-DNA.

• **MS medium (Murashige and Skoog, 1962).** 0.471% (w/v) MS plant medium powder (ICN-Biomedical), 3% (w/v) sucrose, pH = 5.8-6.0 after autoclaving. 0.27% (w/v) Phytagel (Sigma) was added to make solid medium.

• **MSRI solid medium.** 0.471% (w/v) MS plant medium powder (ICN-Biomedical), 3% (w/v) sucrose, 0.27% (w/v) Phytagel (Sigma), pH = 5.8-6.0 after autoclaving. IAA and BAP stock solutions were added to medium after autoclaving to give a final concentration of 2 mg/L and 1 mg/L respectively.

2.2 Plant material and greenhouse growth conditions

Seeds of *N. tabacum var.* NC95 (a high alkaloid variety) and LAFC53 (a low alkaloid variety isogenic with NC95 apart for genes regulating alkaloid biosynthesis) were obtained from Assoc. Prof. Verne Sisson, NC State University, USA. Seeds of *N. sylvestris* were obtained from a commercial seed company (Fothergills, UK). Wild type and transgenic plants were grown in a greenhouse under a regime of 25°C with a 16 hour photoperiod (150 µmol m^{-2} s^{-1}). All plants were potted in a soil mixture comprising two parts seed raising mixture (Debco) and one part perlite. 100 g of slow release complete fertiliser (Osmocote) was added per 6 L of soil mix.

2.3 *In vitro* growth conditions

2.3.1 Initiation and establishment of transformed root cultures

Agrobacterium rhizogenes LBA9402, or *A. rhizogenes* containing the appropriate binary vector construct were isolated from a single colony grown on solid YMB medium and inoculated into 10 ml YMB broth. The bacteria culture was incubated at 28°C for 48 hours prior to use. Young, healthy, and fully expand leaves were excised from 8-12 week old *N. tabacum* plants (pre-flowering) and surface sterilised by immersion in 10% (v/v) Domestos, a commercial bleach, for 20-30 minutes. The leaves were then thoroughly rinsed three times in sterile water. Leaf sections were cut to approximately 6 cm in length and 4 cm to 5 cm in width, with the leaf midrib remaining intact. Transformed root cultures were initiated by inoculating the midrib and lateral veins with a hypodermic needle containing the *A. rhizogenes* culture. Infected leaf sections were then placed petiole-first into a jar containing B5 solid medium.

Roots appeared from the wound sites after three to four week incubation in a culture room with 16 hours artificial illumination per day and a constant temperature of approximately 20°C. When roots reached approximately 10 mm in length, tissues bearing emergent roots were excised and placed in a 60-ml glass jar containing 20 ml of B5 liquid medium supplemented with 500 μg/ml ampicillin. After three days incubation on a rotary shaker in a culture room, roots were transferred to fresh media containing 500 μg/ml ampicillin. To ensure that transformed lines possessed a binary vector construct with the neomycin resistance gene, the culture media was also supplemented with kanamycin at 30 μg/ml. After ten days of growth, an individual root line was established from a single root tip taken from each cluster of emergent roots.

2.3.2 Maintenance of root cultures

Transformed root cultures were grown in 250 ml polypropylene pots containing 50 ml of B5 media supplemented with 500 μg/ml ampicillin. For root cultures transformed with binary vector, kanamycin at the final concentration of 30 μg/ml was also added to

the media. Root cultures were routinely subcultured at three-to-four weekly intervals by transfer of approximately 0.5 g root tissue into fresh media. Cultures were maintained in the dark on a rotary shaker (80 rpm) at 21±2°C.

2.3.3 Growth analysis and harvesting of root cultures

Experimental samples were set up using 0.8 g of root tissue taken from the most active growing part of 17 day-old healthy root cultures and inoculated into 50 ml fresh B5 medium. At each time point, root tissues were harvested, blotted on absorbent paper towel with gentle pressure to remove surface liquid, weighed, and then wrapped in aluminium foil. Samples were immediately snap frozen in liquid nitrogen and stored at -70°C for subsequent analysis.

2.3.4 Regeneration of plants from root cultures

A cluster of root tips, approximately 1 cm in length, was placed onto MSRI medium and incubated in a culture room with a 16 hour photoperiod and a constant temperature of 21±2°C. After four-to-six weeks shoots appeared from the callused tissue. The base of each new plantlet was trimmed to remove excess callus tissue before transfer to solid MS media. Shoot cultures were incubated in the culture room under the conditions described above. After two-to-three weeks, root growth was observed at the base of plantlets.

2.4 Molecular analysis

2.4.1 Large scale isolation of plasmid DNA

The method used to obtain high quality plasmid DNA (from *E. coli*) was modified from that of Sambrook *et al* (1989). A loopful of bacterial culture was inoculated into 500 ml LB broth containing the appropriate antibiotic(s) and incubated overnight. Cells were pelleted by centrifugation at 6,000 rpm for 30 minutes at 4°C in a Sorvall GSA

rotor and then resuspended in a few drops of the supernatant by vortexing. 10 ml of plasmid extraction buffer containing 50 mg of lysozyme was added to the suspension. The sample was chilled on ice for 5 minutes, after which 20 ml of freshly prepared cell lysis buffer was added. The solution was then gently mixed by inversion and returned to chill on ice for a further ten minutes before the addition of 15 ml of ice-cold 5 M potassium acetate (pH = 4.8). The sample was mixed by inversion and centrifuged at 9,000 rpm at 4°C for 30 minutes in a Sorvall SS-34 rotor to remove cellular DNA and bacterial debris. The supernatant was filtered through nylon mesh and approximately 0.6 volumes of isopropanol was added. The solution was mixed and allowed to stand for 15 minutes before being centrifuged at 8,000 rpm for 30 minutes. The DNA pellet was washed with 70% ethanol and briefly dried in a vacuum desiccator. The combined DNA pellets were dissolved in 8 ml of TE and the pH was adjusted to 8 with 2 M Tris HCl. The volume was then made up to 10 ml with TE.

Purification of plasmid DNA on a caesium chloride gradient was performed by the addition of 10 g caesium chloride and 1.1 ml of 10 mg/ml ethidium bromide. The solution was transferred to an opaque Beckmann quick-seal tube and centrifuged at 40,000 rpm for 64 hours at 18°C in an ultracentrifuge, model L8-80M, using a 80Ti rotor. Under UV exposure, the lower band representing closed-circular plasmid DNA, was removed using a sterile needle and syringe. Ethidium bromide was removed by several extractions with an equal volume of water-saturated butanol. DNA was precipitated by the addition of two volumes of sterile water, 1/10 the volume of 3 M sodium acetate (pH = 6) and two volumes of 95% ethanol. The DNA was pelleted in a Corex tube by spinning at 10,000 rpm at 4°C in a Sorvall SS-34 rotar for 30 minutes, before being dissolved in 0.5 ml TE. The solution was transferred to a 1.5 ml capacity microcentrifuge tube and 50 µl of 3 M sodium acetate and 1 ml ice-cold ethanol were added, and the tube placed in liquid nitrogen for ten minutes. The DNA was pelleted by centrifugation at 10,000g for ten minutes. The pellet then was washed with ice-cold 70% ethanol, dried in a vacuum centrifuge (Speed Vac SC100 [Savant]), and resuspended in 200 µl of TE.

2.4.2 Plasmid DNA miniprep procedure from *Eschericia coli*

The method used is based on that described by Chowdhury (1991). 750 µl of a mixture of phenol: chloroform:isoamylalcohol (25:24:1) was added to a microcentrifuge tube containing 750 µl of an overnight bacterial culture. The sample was mixed by vortexing at maximum speed for one minute and spun at 14,000 rpm for five minutes. Leaving the interphase undisturbed, the upper aqueous phase (approximately 650 µl) was transferred to a new microcentrifuge tube containing 750 µl of isopropanol. The sample was mixed well by inversion and then centrifuged at 14,000 rpm for five minutes. The resulting pellet was washed twice with ice-cold 70% ethanol, dried in a vacuum centrifuge (Speed Vac SC100, Savant) and resuspended in 50 µl –100 µl of TER buffer (TE with 20 mg/ml RNase).

2.4.3 Extraction and isolation of genomic DNA from plant tissues

Approximately 5 g of plant tissue was ground to fine powder under liquid nitrogen using a mortar and pestle. The frozen powder was transferred into a 50 ml Oakridge tube containing 10 ml extraction buffer and 2 ml 10% SDS which was preheated to 65°C. The mixture was homogenised by vortexing for 30 seconds before the addition of 10 ml phenol-chloroform. The cellular debris was pelleted by centrifugation in a Sorvall SS-34 rotor at 10,000 rpm for 15 minutes at 4°C. The supernatant was transferred to a clean tube and two volumes of ethanol was added and the tube incubated at 4°C overnight. Crude DNA was recovered from the solution by centrifugation in a Sorvall SS-34 rotor at 10,000 rpm for 20 minutes at 4°C. The DNA pellet was dissolved in 9 ml TE and then 9 g caesium chloride ($CsCl_2$) and 500 µl EtBr stock solution were added before the solution was transferred into an opaque Beckman quickseal centrifuge tube. The tube was sealed and centrifuged in an ultracentrifuge (model L8-8OM) using an 80Ti rotor at 40,000 rpm for 64 hours at 18°C. A fluorescent band of DNA was visualised under long wave UV light, and removed with an 18 or 19G needle. To remove the EtBr from the DNA solution, 6-8 ml of water-saturated butanol was added to the solution vigorously mixed. The resulting butanol layer was removed with a Pasteur pipette. The butanol extraction was repeated until the DNA solution was

colourless, and then the solution was made up to a volume of 5 ml with sterile water. The solution was transferred to a 30 ml glass Corex tube and 0.5 ml of 3 M sodium acetate (pH = 6) and 11 ml ethanol were added, and the solution allowed to cool at -20° C for at least 1 hour. After this time, the solution was centrifuged in a Sorvall SS-34 rotor at 10,000 rpm for 20 minutes at 4°C. The DNA pellet was dissolved in 0.5 ml sterile water and transferred to a microcentrifuge tube. 50 µl of 3 M sodium acetate (pH = 6) and 1 ml ethanol were added and the solution incubated at -20°C overnight. DNA was recovered by centrifugation at 14,000 rpm for 30 minutes. The pellet was then carefully rinsed with 70% ethanol and allowed to dry before being dissolved in 100 µl TE.

2.4.4 Extraction of total RNA from plant tissues

This method is based on that of Verwoerd *et al.* (1989). 0.5 g of plant tissue was ground to a fine powder using a mortar and pestle under liquid nitrogen. Whilst frozen, the powder was transferred to an Oakridge tube containing 750 µl TLES and 750 µl phenol (pH = 8.0) which was preheated to 70°C. The sample was immediately vortexed for 30 seconds to homogenise the solution. 750 µl of chloroform:isoamylalcohol (24:1) was added and the sample was again vortexed. The mixture was then divided into two microcentrifuge tubes and centrifuged at 14,000 rpm for five minutes. The supernatant was then transferred to new microcentrifuge tubes before the addition of an equal volume of 4 M lithium chloride. After mixing, samples were incubated at 4°C overnight to allow the precipitation of RNA. Following incubation, the RNA was pelleted by centrifugation at 14,000 rpm for 30 minutes and resuspended in 250 µl of sterile Milli-Q water. 25 µl of sodium acetate (pH = 6.0) and 500 µl of ethanol was then added and the RNA was precipitated, either at -70°C for one hour, or at -20°C overnight. Again, the RNA pellet was collected by centrifugation at 14,000 rpm in a microfuge for 20 minutes. The resulting pellets were washed with 70% ethanol, partially dried either at room temperature or in a vacuum centrifuge (Speed Vac SC100 (Savant)) and then resuspended in 50 µl of sterile Milli-Q water. 5 µl of the RNA solution was taken for UV spectrophotometry (see section 2.4.5). The RNA was then precipitated by the addition of sodium acetate and ethanol, as described above, and

resuspended in sterile Milli-Q water to achieve a final concentration in the range of 4-5 μg/μl. RNA samples were stored at -70°C until required.

2.4.5 Quantification of nucleic acids

DNA and RNA samples were quantified using a Perkin-Elmer Lamda 1 UV/VIS spectrophotometer. A 5 μl aliquot of the nucleic acid solution was made up to 1 ml with Milli-Q water and the absorbance was measured at a wavelength of 260 nm. A reading of 1.0 corresponds to 50 μg/ml for double-stranded DNA or 40 μg/ml for RNA (Sambrook *et al.*, 1989). Readings were also taken at wavelengths of 230 nm and 280 nm in order to check the quality of the preparation. DNA of sufficient quality exhibited approximately equal readings at wavelengths of 230 nm and 260 nm, and had a ratio of readings at 260 nm to 280 nm of approximately 1.8 to 1.

2.4.6 Restriction enzyme digestion

Approximately 1-10 μg of DNA was digested with restriction endonucleases purchased from either Toyobo or Promega under conditions recommended by the respective manufacturers. Digestion of plasmid DNA was performed in a total volume of 30–50 μl with the presence of required restriction enzyme(s) at 1-1.5 unit per μg of DNA, as well as the appropriate enzyme buffer. Typically, for the restriction of genomic DNA, 3-5 units of restriction enzyme(s) was added per μg of genomic DNA in combination with spermidine (Sigma) at a level of 1 mM. BSA (Promega) at a final concentration of 1% (w/v) was also added to the reaction. The mixture was incubated at 37°C for three hours for plasmid DNA or overnight for genomic DNA. The digestion was stopped by the addition of one-sixth the volume of 6X gel-loading dye.

2.4.7 Gel electrophoresis

DNA fragments were separated by electrophoresis on a horizontal agarose gel. Electrophoresis was performed with TBE buffer in a Pharmacia gel tank, using a current ranging from 25 mA to 50 mA for 1 to 16 hours depending on the purpose of

separation. 250 ηg of λ DNA digested with *Bst*EII (generating fragment in the size range of 700 bp to 14 kb) or ϕx174 DNA digested with *Hae*III (generating fragments in the size range of 600 bp to 1.35 kb) were used during electrophoresis for determining sizes of linearised DNA fragments. Uncut λ DNA at different known concentrations was used for estimating DNA quantity.

RNA samples were denatured prior to electrophoresis as described by Sambrook *et al.* (1989). 20 μg of total RNA was mixed with 50% (v/v) deionised formamide, 15% (v/v) formaldehyde and 0.5 X MOPS buffer and incubated at 65°C for 15 minutes prior to chilling on ice. After 2 μl of loading buffer was added, the sample was subjected to electrophoresis on a formaldehyde denaturing gel with 1 X MOPS buffer. Electrophoresis was performed in a Pharmacia gel tank using a current of 25 mA and run overnight, allowing the dye front to migrate approximately 8 cm to 10 cm from the wells.

Gels were examined on an UV transilluminator and photographed with a Polaroid LP-4 camera using Polaroid 667 positive film, or using a camera control unit (UVP) and a Mitsubishi videospacecopy processor with a thermal printer.

2.4.8 Isolation of DNA fragments from agarose gels

DNA bands were excised from electrophoretic gels whilst under UV transillumination using a sterile blade. As much gel was removed from the excised band, and the DNA fragment purified either by phenol-freeze extraction or using a BRESAspin Gel Extraction Kit (Bresatec) as directed by the manufacturer. For phenol-freeze extractions, gel fragments were thoroughly crushed in a microcentrifuge tube before the addition of 0.5 ml phenol. The tube was vortexed and left either at -70°C for 30 minutes or at -20°C overnight. After centrifugation at 14,000 rpm for 30 minutes, the upper aqueous layer was transferred to a fresh microcentrifuge tube. 200 μl of TE buffer was added to the remaining bottom layer and the mixture vortexed and centrifuged at 14,000 rpm for 15 minutes. The upper layer was removed and combined with the previous upper layer. An equal volume of chloroform:isoamylalcohol (24:1)

(v/v) was added to the tube, and the sample briefly vortexed and centrifuged at 14,000 rpm for ten minutes. The top layer was removed carefully to a new tube and the DNA was recovered from the aqueous phase by the addition of $1/10^{th}$ the volume of sodium acetate and two volumes of ethanol. The sample was mixed and allowed to stand at room temperature for 30 minutes before incubation at either -70°C for 30 minutes or at -20°C overnight. The DNA was then pelleted by centrifugation at 14,000 rpm for 30 minutes. The resulting pellet was washed with 70% ethanol, dried and resuspended in 10 µl of sterile Milli-Q water. DNA concentration and purity was checked by electrophoresis of a 1 µl aliquot of the sample on a minigel.

2.4.9 Polymerase chain reaction (PCR)

2.4.9.1 DNA amplification

All PCR amplifications used a Promega Taq DNA Polymerase Kit (Promega) containing 25 mM magnesium dichloride, 10 X Taq DNA reaction buffer (500 mM potassium chloride, 100 mM tris-HCl (pH 9), 1% Triton X-100) and Taq DNA polymerase (5 units/µl). In addition, dNTPs (from 2 mM stock of dATP, dTTP, dCTP, dGTP [Promega]) were added to a final concentration of 200 µM. Each PCR amplification was carried out in a 50 µl reaction volume which was overlaid with approximately 100 µl of light mineral oil (Selby Scientific) to prevent evaporation. A Hybaid HB-TR1 Thermal Reactor set at tube control temperature was used for all amplifications. Amplification of DNA by PCR was performed using repeated cycles to denature the DNA, anneal the primers, and finally to extend the primers. At the end of the last cycle in all amplifications, a further 10 minutes extension step was included before the reaction was allowed to cool to ambient room temperature. Routinely, 10 µl to 20 µl of each amplified sample was subjected to electrophoresis to identify positive amplification products, and then the gel blotted and probed if required. When necessary, PCR products were re-amplified by diluting a small aliquot (typically 1/100th) of the amplified mixture directly into new PCR buffers containing the same primers and constituents.

2.4.9.2 Colony boil PCR

Colony boil PCR amplifications were performed to test for the presence of recombined plasmids in cells from a bacterial colony. A sterile toothpick was touched to a single colony and dipped into 10 µl of sterile Milli-Q water in a 0.5 ml microcentrifuge tube. The tube was incubated at 99°C for five minutes in a preheated Hybaid HB-TR1 Thermal Reactor before the temperature was reduced to 92°C. 40 µl of PCR mix (final concentration of 1 X Taq DNA polymerase buffer, 200 µM each dNTP, 1.5 mM magnesium dichloride, 1 ηg of both forward and reverse primers, and 0.5 units of Taq DNA polymerase) was added to the tube. The mix was pulse-centrifuged to collect condensation and the tube returned to the cycling machine at 92°C. Approximately 100 µl of light mineral oil (Selby Scientific) was immediately added and the tube subjected to a thermocycling regime of 95°C for one minute for the denaturation of DNA, 55°C for two minutes for the annealing of primers, and 75°C for two minutes for the extension of the primer. In total, 30 such cycles were used, including a final extension step as described above. 20 µl of the amplified mix was then electrophoresed on an agarose gel and subsequently blotted and probed to identify positive transformants.

2.4.10 Ligation of DNA

Ligation of insert DNA into vector DNA was carried out according to instructions of the vector manufacturer (Promega). Briefly, 100 ηg – 200 ηg of linearised vector and insert DNA were mixed in a 0.5 ml microcentrifuge tube. The insert-to-vector ratios used, in molar amounts, were 1:1, 1:3, and 3:1, while control reactions used either vector or insert DNA only. Sterile Milli-Q water was added to the tube to made up the volume to 7.5 µl. The sample was warmed to 45°C for five minutes before chilling on ice. After this time BSA (at final concentration of 50 ηg/µl), 1 µl of T4 DNA ligase 10 X buffer (300 mM tris-HCl pH 7.8, 100 mM $MgCl_2$, 100 mM DTT and 10 mM ATP) and 1 weiss unit T4 ligase (Promega) were added with sterile Milli-Q water to make a final volume of 10 µl. The ligation reaction was incubated at 15°C for four hours and then at 4°C overnight. After heat inactivation at 70°C for ten minutes, the ligation

product was used to transform *E. coli*. For direct cloning of PCR products, a pGEM-T vector kit (Promega) was used and ligation was carried out according to the instruction of the manufacturer.

2.4.11 Bacterial transformation

2.4.11.1 Transformation of E. coli

Transformation of *E. coli* was performed as described by Chung and Miller (1988) using strain DH5α. 50 µl of an overnight culture of DH5α was inoculated into 100 ml of LB broth and grown to early log phase (OD_{600} = 0.3 to 0.6) which required approximately three hours on a shaking incubator at 37°C. Cells were pelleted by centrifugation in a microcentrifuge at 3,000 rpm for five minutes at 4°C and resuspended in $1/10^{th}$ the original volume of ice-cold transformation and storage buffer (TSB). The suspended cells were then left on ice for approximately 30 minutes. Transformation was carried out by the addition of DNA, ranging from 100 pg to 50 ηg of DNA, or 5 µl of the ligation mix, to a 100 µl aliquot of competent cells in a pre-chilled test tube. The cells were then returned to ice for approximately 30-45 minutes. After addition of 0.9 ml of TSB, containing filter-sterilised glucose to a final concentration of 20 mM, the cells were grown on a shaker at 37°C for one hour to allow expression of antibiotic resistance gene. Aliquots of 20-100 µl of the transformed cell mix were then spread onto LB plates supplemented with antibiotics. When blue-white selection was employed, LB plates were also supplemented with 0.5 mM IPTG and 40 µg/ml X-gal. Bacterial colonies that were white in colour represented cells possessing recombinant plasmids, whereas blue colonies signified cells transformed with plasmids lacking insert DNA. Putative positive colonies were analysed for the presence of recombinant plasmids following transfer to growth plates for subsequent colony blotting, or following growth in broth for isolation of plasmid DNA or for colony boil PCR amplification.

2.4.11.2 Transformation of A. rhizogenes via triparental mating

A single colony of the recipient *A. rhizogenes* wild type strain LBA9402 was inoculated and grown in antibiotic-free YMB broth at 28°C for approximately 48 hours. After 24 hours, a single colony of donor *E. coli* containing a correct construct of the binary vector, and a single colony of *E. coli* helper strain containing pRK2013 were separately inoculated into LB broths, with appropriate antibiotic, and grown overnight at 37°C. 100 µl of each of the *E. coli* cultures and 200 µl of the recipient strain were mixed and centrifuged at 6,000 rpm for 30 seconds. Cells were then resuspended in 50 µl of antibiotic-free LB broth and spread onto an LB:YMB (1:1) plate. Such a triparental mating plate was incubated at 28°C for approximately 48 hours. One loopful of bacteria was streaked onto a YMB plate containing 100 mg/L rifampicin and the appropriate antibiotic to select the plasmid, and then incubated at 28°C for approximately 72 hours. Single colonies were selected and re-streaked. This step was then repeated using solid YMB supplemented with the appropriate antibiotic to select the plasmid. The presence and integrity of the desired vector in the transformed *A. rhizogenes* culture was tested prior to use for plant transformations.

2.4.12 Southern blot analysis

2.4.12.1 Colony blotting

The method used was based on the protocol supplied by the Amersham company. Single putative positive colonies were patched onto two identical plates of solid medium containing the appropriate antibiotic and incubated overnight. A Hybond-N^+ (Amersham) membrane was cut to size and placed on the agar surface of one plate. After one minute, the membrane was carefully lifted from the plate and placed with the bacterial colonies facing upwards, onto two sheets of blotting paper soaked in denaturing solution for seven minutes. The membrane was then neutralised twice for three minutes each on two sheets of blotting paper soaked in neutralising buffer. Finally, the membrane was rinsed in 2 X SSC and air-dried with the colony-side up.

2.4.12.2 DNA blotting

Following electrophoresis, the agarose gel was depurinated in 0.25 M hydrochloric acid for 20 minutes with gentle agitation. The gel was then briefly rinsed twice in distilled water and soaked in denaturing solution for 40 minutes with gentle shaking. After a brief rinse in distilled water, the gel was neutralised for 30 minutes with gentle agitation in neutralising buffer. A capillary blot was prepared as described in Sambrook *et al* (1989). A wick was made from two sheets of blotting paper saturated with blotting buffer consisting of 20 X SSC and laid flat on a perspex plate with each end of the wick immersed in blotting buffer. The gel was then placed upside down on the wick. A sheet of Hybond-N^+ (Amersham) membrane was cut to the appropriate size and placed on the gel, ensuring that the top of the membrane was aligned with the wells of the gel. Two sheets of blotting paper saturated with blotting buffer were layered over the membrane. Air bubbles were removed by gently rolling a glass pipette over the surface of each layer. A stack of dry paper towel was placed on the top and pressed down with a light weight, approximately 700 g. DNA transfer was allowed to proceed for 16-40 hours.

2.4.12.3 Alkaline fixation of DNA to nylon membrane

Blotted membranes were placed DNA-side up on two sheets of blotting paper soaked in 0.4 M sodium hydroxide for 15 minutes. Membranes were subsequently rinsed in 2 X SSC with gentle agitation for approximately one minute, after which they were either directly used in the DNA:DNA hybridisation or allowed to air dry prior to storage at room temperature.

2.4.12.4 Preparation of radiolabelled probes

Radiolabelled double-strand DNA probes were prepared by random primer extension in the presence of ^{32}P-dATP using a Gigaprime DNA Labelling Kit (Bresatec) according to the manufacturer's instruction. Approximately 100-200 ηg of double-strand DNA was denatured in a screw-capped tube in a volume of 6 µl by boiling for

five-to-ten minutes, followed by chilling on ice. The tube was then briefly pulse-centrifuged to bring down the condensation before addition of 6 µl decanucleotide solution, 6 µl nucleotide buffer cocktail, 5 µl ^{32}P-ATP (Bresatec) and 1 µl Klenow DNA polymerase. The mixture was incubated at 37°C for at least 15 minutes. The radiolabelled DNA fragments were then separated from the unincorporated nucleotides by passage through sephadex G-50 (medium grade, Amersham Pharmacia Biotech AB) equilibrated with TE buffer and packed in a short Pasteur pipette used as a column. After labelling, the reaction mix was eluted from the column with TE buffer and the eluent was collected as a series of 8-drop fractions, the radioactivity of which were monitored with a geiger counter.

2.4.12.5 Synthesis of single-strand DNA probe by asymmetric PCR

This method was based on that of Taylor (1991). Unlabelled double-strand DNA fragments were firstly synthesised as described in section 2.4.9.1. A single-strand DNA probe was produced by taking a small aliquot (1 µl) of the PCR product without purification and repeating the temperature cycling process using one primer only. This process dilutes the other primer to approximately less than one-fiftieth of the normal level, which is quickly used up as the amplification reaction progresses, producing a relatively small amount of double-stranded DNA together with single-strand DNA. In the repeated PCR, a dNTP stock solution was used lacking dATP. Immediately before the reactions were allowed to proceed, ^{32}P-dATP was added to each amplification reaction. The radiolabelled single-stranded DNA fragments in the PCR product were separated from the unincorporated nucleotides as described above.

2.4.12.6 Prehybridisation and hybridisation

Membranes were treated with prehybridisation solution in a volume of 10-50 ml depending on their size. The hybridisation solution consisted of 5 X SSC, 5 X Denhardt's solution, 0.5% (w/v) SDS and 200 µg/ml salmon sperm DNA or herring sperm DNA which had been denatured by boiling for ten minutes and then chilled on

ice. The incubation was carried out at 65°C in either a shaking water bath or a rotating hybridisation oven for at least three hours prior to addition of probe.

Labelled probe was denatured at 100°C for 10 minutes and chilled on ice before addition to the prehybridisation mix. The hybridisation was carried out overnight at 65°C. To remove non-specifically bound probe after hybridisation, membranes were subjected to a high stringency wash (0.1 X SSC, 0.5% w/v SDS) at 65°C for 15 minutes. Additional washes were performed if background signals gave high geiger counter readings. Moist membranes were sealed in plastic before exposure to Fuji X-ray film with an intensifying screen at -70°C. The duration of exposure varied according to the strength of signal. Autoradiographs were developed using an Agfa Gevaert Gavanamic-60 X-ray machine.

2.4.13 Northern blot analysis

Following electrophoresis, formaldehyde-agarose gels were rinsed twice with 10 X SSC for 20 minutes. The blotting procedure was essentially the same as described above for Southern blotting; except that 10 X SSC was used as the blotting buffer. Capillary transfer of RNA was allowed to proceed over 24 hours. For fixation of RNA, the blotted Hybond N^+ membranes were placed RNA-side up for five minutes onto two sheets of Whatmann chromatography paper soaked in 0.05 M sodium hydroxide and then briefly rinsed in 2 X SSC. Prehybridisation and hybridisation were performed using Expresshyb solution according to the manufacturer's instructions (Clontech Laboratory Inc.). Membranes were placed in pre-heated hybridisation tubes containing 5 ml of Expresshyb solution and incubated in a rotary hybridisation oven at 65°C for 30 minutes. Radioactively-labelled probes were prepared as described for Southern blot analysis. For hybridisation, the prehybridising solution was discarded and 3 ml of pre-heated fresh Expresshyb solution, containing the denatured probe, was added to the hybridisation tube and incubated for a further one-to-two hours at 65°C. Membranes were washed four times at room temperature with a low stringency wash solution (2 X SSC, 0.05% w/v SDS), with each wash lasting for eight-to-ten minutes. If required, membranes were then washed once or twice with a high stringency wash solution (0.1 X

SSC, 0.1% w/v SDS), for 20 minutes each at 65°C. To prevent drying, moist membranes were mounted on Whatmann chromatography paper dampened with 2 X SSC and sealed in plastic film before exposure for up to one week at -70°C using Fuji X-ray film with an intensifying screen. Autoradiographs were developed as described above.

To standardise the amount of total RNA fractionated on each lane, membranes were exposed to a phosphor screen (Dynamic, Kodak) for 16-72 hours as required. Signal intensities were quantified with either a Fujix bio-imaging analyser (BAS1000, Mac BAS software) or Storm Phosphor-FluorImager (Image Quant software). To further standardise signals, membranes were stripped as described above and reprobed with a radiolabelled sequence of the 'housekeeping' gene ubiquitin from *Antirrhinum majus*. (The sequence was kindly supplied in plasmid pJAM293 by Dr. Cathie Martin, John Innes Institute, Norwich, U.K.) Again, signal intensities were quantified using a phosphorimager, and standardised by calculating the ratios of mRNA signals from the band of interest to those of the ubiquitin signal. The lowest relative ratio was assigned a value of 1, and other samples on the same membrane adjusted accordingly.

2.4.14 Membrane stripping

Probes were removed from membranes by gentle agitation in freshly boiled 0.5% (w/v) SDS and the solution allowed to cool to room temperature. Complete removal of the radioactive bound probe was assessed by autoradiography. Membranes were stored dry or further hybridised immediately with a freshly prepared radiolabelled probe.

2.4.15 DNA Sequencing

Sequencing of double-stranded DNA was performed using an ABI PRISM Dye Terminator Cycle Sequencing Ready Reaction Kit (Perkin Elmer) according to the manufacturer's instructions. Approximately 1 μg of purified DNA and 3.2 pmol of primers were mixed with 9.5 μl of reaction premix containing A,T,G, and C dideoxy terminators, DNA polymerase buffer, and Ampli Taq DNA polymerase in a 0.5 ml

microcentrifuge tube. Final reaction volumes were adjusted to 20 µl with sterile Milli-Q water and overlaid with 40 µl of light mineral oil. Amplification/sequencing cycles were carried out in a Corbett Research FTS-1 Thermocycling machine preheated to 96°C. A standard amplification/sequencing regime consisted of 25 cycles of denaturation at 96°C for 30 seconds (90 seconds for the first cycle), annealing at 50°C for 15 seconds, and primer extension at 60°C for four minutes. Reaction products were then purified by phenol-chloroform extractions. The reaction mixes were transferred to a fresh tube and 80 µl of sterile Milli-Q water was added to each tube. Extractions were performed twice by addition of 100 µl of phenol:water:chloroform (68:18:14), followed by vortexing and centrifugation at 14,000 rpm for 5 minutes. 15 µl of 2 M sodium acetate (pH = 4.5) and 300 µl of ethanol were added before the tube was incubated on ice for 15 minutes. DNA was pelleted by centrifugation at 14,000 rpm for 15 minutes. Pellets were washed with 70% ethanol and vacuum dried. DNA sequence determination was undertaken using an ABI 373A Automated Sequencer by the Microbiology Department at Monash University, Clayton. Sequence data obtained were analysed using the ABI SeqEd program and the Australian National Genomic Information Service (http://www.angis.org.au/).

2.5 Biochemical analysis

2.5.1 Histochemical localisation of β-glucuronidase (GUS) activity

Plant tissue was covered with 100-200 µl of X-Gluc solution in a microcentrifuge tube which was incubated at 37°C overnight. The tissue was then soaked in 95% ethanol to remove chlorophyll if necessary. GUS-expressing cells were visualised by blue staining under a low powered dissecting microscope.

2.5.2 Enzyme assay

2.5.2.1 ADC and ODC

Extraction and assay procedures were based on those described by Robins *et al.* (1990). Tissues were harvested, weighed, immediately frozen in liquid nitrogen and stored at -70°C until required for enzyme activity determinations. Both ADC and ODC activities were determined simultaneously using the same extract. Approximately 0.5 g of frozen tissue was ground with 100 mg/g insoluble polyvinylpyrrolidone (PVP) under liquid nitrogen using a chilled mortar and pestle. The fine powder was immediately added to 3 volumes of buffer A containing 100 mM tris-HCl (pH = 8), 20 mM EDTA (pH = 8), 10 mM dithiothreitol (DTT), and 2 mM pyridoxal phosphate. After vortexing, the sample was centrifuged at 15,000 g for 20 minutes at 4°C to remove insoluble debris. The supernatant was transferred to a clean centrifuge tube and volumes were adjusted to 3.5 ml with buffer A. To remove low molecular-weight contaminants, a prepacked PD-10 desalting column (Pharmacia) equilibrated in one-tenth-strength buffer A was used according to the manufacturer's instructions. Soluble proteins were eluted from the column using one-tenth-strength buffer A and were then used for ADC and ODC enzyme assays as well as protein quantification. Protein concentrations were determined by the protein-dye binding method using Bradford reagent (Biorad) according to the manufacturer's instructions (Bradford, 1976). Bovine serum albumin (BSA) (Promega) was used as a standard.

Activity of ADC was determined by measuring the amount of $^{14}CO_2$ released from L-(U-^{14}C)-arginine (Amersham; specific activity 12.7 GBq/mol) diluted with non-radioactive L-arginine-HCl (Sigma) to produce a 2.5 mM stock with a specific activity 103 MBq/mmol. The incubation mixture used contained 200 µl of enzyme extract and 50 µl of arginine stock in a de-capped microcentrifuge tube within a 20 ml scintillation vial containing 100 µl of 20% (w/v) KOH. Vials were sealed with subaseals before incubation at 37°C in a shaking water bath. At designated time points, reactions were terminated by the injection of 200 µl of 5% (v/v) perchloric acid into the microcentrifuge tubes. Vials were incubated at 37°C for a further 50 minutes. Tubes

were removed and their outsides were rinsed into the vials with 0.9 ml of sterile water. After addition of 9 ml of scintillant (Ready Value, Beckman) vials were shaken until the solution was clear, indicating a homogenous mixture. The radioactivity of the sample was then determined using a scintillation counter.

Activities of ODC were determined as described above for ADC, except that [1-^{14}C]-L-ornithine (Armersham, specific activity 2.18 GBq/mmol) was used. The labelled ornithine was diluted with non-radioactive L-ornithine-HCl (Sigma) resulting in a 10 mM stock with specific activity of 22 MBq/mmol.

2.5.2.2 PMT

Extraction and assay procedures were modified from the methods of Robins *et al.* (1990) and Walton *et al.* (1994). Tissues were harvested, weighed into samples of approximately 2.5 g, and immediately frozen in liquid nitrogen before storage at -70°C until required for enzyme activity determinations. Frozen root tissue was ground to a fine powder under liquid nitrogen using a mortar and pestle. The frozen power was transferred into a screw-topped centrifuge tube and three times the volume of extraction buffer (20 mM Tris base, 12.5% (w/v) glucose, 10 mM 2-mercaptoethanol, 2 mM Na_2EDTA, pH = 7.8) was added. The tube was briefly vortexed to homogenise the mixture, followed by centrifugation at 14000 rpm for 5 minutes. The supernatant was removed to a new tube and the centrifugation repeated. 100 µl of supernatant was mixed with 100 µl of incubation mixture containing 20 µl of 20 mM putrescine, 20 µl of 25 mM 2-mercaptoethanol, 40 µl of 1 M KPi buffer (pH = 8), 2 µl of 10 mM *S*-adenosyl-L-[$^{14}CH_3$] methionine (specific activity 18 MBq/mmol), and 18 µl water. The reaction mixtures were incubated at 30°C for 30 minutes. Control reaction mixtures lacking putrescine were included. Reactions were terminated by addition of 100 µl of 10% (w/v) NaOH saturated with NaCl. The product, *N*-methylputrescine, was extracted into 1 ml of toluene:isoamylalcohol (3:2) (v/v) by thorough mixing and brief centrifugation. 0.8 ml of the organic phase was taken and the radioactivity determined by liquid scintillation counting.

2.5.3 Alkaloid analysis

2.5.3.1 Alkaloid extraction

Extraction of alkaloids was performed essentially as described by Saunders and Blume (1981). Approximately 250 mg of plant tissue was homogenised in extraction buffer (40% (v/v) methanol, 0.1% (v/v) 1 M HCl) at a proportion of 10 ml of buffer per g fresh weight of plant tissue, using a Kinematica AG Polytron PT1200 homoginiser (Selby). The homogenate was centrifuged at 2,500 rpm for 3 minutes. Fine particles were removed by filtration of the supernatant through a 0.45 μm Sartorius RC filter and stored at -20°C until the determination of alkaloid level by HPLC (high-performance liquid chromatography).

2.5.3.2 Alkaloid determination

Following extraction, alkaloids were separated on a Bondapak C18 reverse phase column (3.9 mm x 300 mm, particle size 10 μm) using a HPLC integrated system comprising of a Waters 600E (pump/HPLC unit) and a Waters 717plus Autosampler. The system was operated at room temperature with a helium-sparged (20 ml/min) mobile phase of 50% (v/v) methanol and 0.2% (v/v) phosphoric acid buffered to a pH of 7.25 with triethylamine. 20 μl of sample was eluted with an isocratic flow rate of 1 ml/min. The mobile phase was filtered through a 0.45 μm Sartorious filter (RC45) prior to use. Alkaloids were detected with a Waters tunable 486 absorbance detector set at 260 ηm. Comparisons were made with authentic standards of nicotine, nornicotine, anabasine (all from Sigma) and anatabine (a gift from Dr. Patrick M. Lippiello and Dr Elisa Lovette, Pharmacology Laboratory Research & Development, R.J. Reynolds Tobacco Company, USA). Samples of plant extract were also 'spiked' with standards to confirm alkaloid peak identifications on the chromatogram. In most cases, nornicotine and anabasine levels were very low and were not quantified. Amounts of nicotine and anatabine present in samples were determined from standard graphs constructed using known amounts of authentic standards of nicotine and anatabine.

Chapter 3

Effects of Down-regulating *ADC* in *N. tabacum*

3.1 Using 460 bp fragment of *N. rustica ADC* coding sequence

3.1.1 Binary vector construction and transformation of bacteria

To produce transformed root tissues of *N. tabacum* with down-regulated *ADC*, it was necessary to first generate *Agrobacterium rhizogenes* carrying a binary vector containing *Nicotiana ADC* gene sequence in an antisense orientation with transcription driven by a strong promoter. pFIH10 was chosen as a suitable vector as it is a pBIN19 based vector which functions efficiently when placed in *A. rhizogenes* to produce transformed roots of *Nicotiana* species containing binary vector T-DNA (Hamill *et al.*, 1987a). pFIH10 is an expression vector that enables a foreign gene to be expressed under control of the CaMV35S promoter with an upstream duplicated enhancer, reported to increase the transcriptional strength of the promoter in transgenic plants (Kay *et al.*. 1987), and the CaMV35S terminator sequence (Hamill *et al.*, 1987a).

3.1.1.1 Cloning a 460 bp fragment of N. rustica ADC *sequence into pBluescript (Construction of pYC1B)*

At the commencement of this project, the full-length coding sequence for *ADC* was not available from *Nicotiana* species. However, a 460 bp genomic fragment from the *ADC* coding sequence of the species *N. rustica* was available in this laboratory as an *Xba*I fragment cloned into pGEM3Z (Doblin, 1993). This was thought highly likely to possess sufficient nucleotide homology to the *N. tabacum ADC* sequence to be effective as an antisense sequence, particularly as Carron *et al.*, (1994) reported the production of hairy root lines from the forage legume *Lotus corniculatus* which contained a portion of the *Antirhinum majus* dihydroflavonol reductase (*DFR*) gene in the antisense orientation under the transcriptional control of the CaMV35S promoter. Using stringency washes,

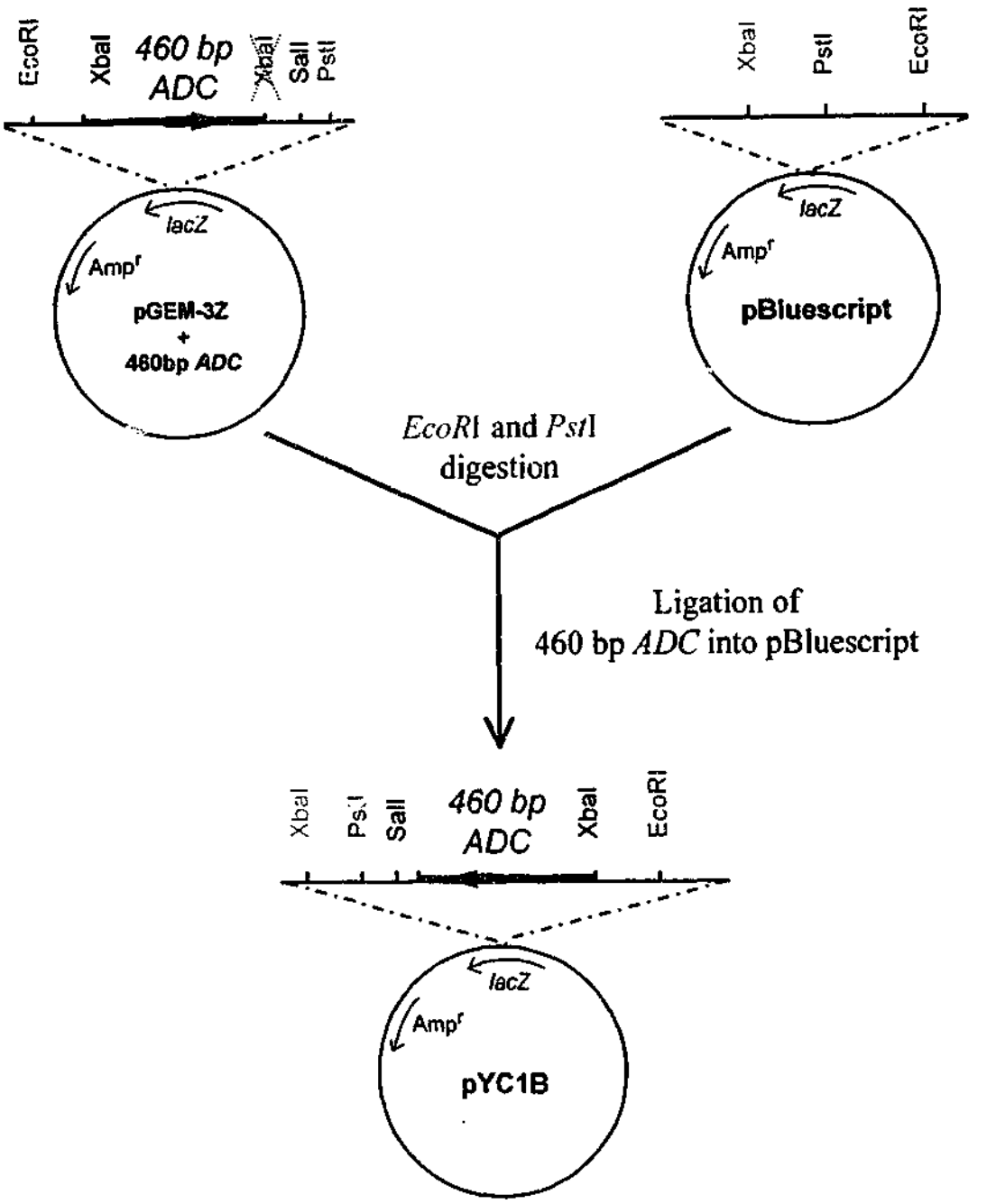

Fig. 3-1 **Construction of pYC1B.** 460 bp *N. rustica ADC* fragment was previously cloned into plasmid pGEM3Z (Doblin, 1993). With one damaged *Xba*I site, the *ADC* fragment was excised from the plasmid and ligated into pBluescript at *Eco*RI and *Pst*I sites. This enabled the excision of the *ADC* fragment at the *Xba*I sites in pYC1B. Blue arrows indicate orientation 5'→3' of the *ADC* fragment with respect to the coding sequence. (Only selected restriction sites in the plasmids are illustrated.)

it was estimated that the *A. majus DRF* gene shared about 80% nucleotide homology with sequences in the *L. corniculatus* genome (Carron *et al.*, 1994). Several of the antisense *DFR* transformed root lines that were recovered in this study showed up to 80% reduction in levels of condensed tannins compared to controls. Previous reports had also noted that a partial gene sequence was effective in down-regulating gene expression in plants when expressed in an antisense orientation. For example, Cannon *et al.* (1990) showed that expression of an antisense fragment of the GUS gene with as little as 41-base paring homology was sufficient to give up to a 100% inhibition of GUS activity in leaves of 8/16 plants previously transformed with the *uidA* (GUS) gene. Bachem *et al.* (1994) demonstrated the inhibition of *PPO* (polyphenol oxidase) expression in transgenic potato plants by expressing a series of antisense *PPO* gene constructs, the length of which varied from 500 bp to 1.9 kb. They found no significant differences in the effectiveness of the constructs with regards to their capacity to reduce PPO enzyme activity. Kuipers *et al.* (1995) compared *GBSS* (granule-bound starch synthase) gene expression in a large number of potato plants transformed with antisense constructs of *GBSS* genomic DNA (3 kb) and a 0.6 kb fragment representing the 3' end of the coding sequence, both under transcriptional control of the *GBSS* promoter. They found that similar numbers of completely inhibited, partially inhibited and non-inhibited GBSS plants were present in the population of transgenic plants expressing either the full-length or partial antisense sequences. Thus, it was concluded that the size of the antisense RNA does not determine the efficacy of inhibition.

In the current project, initial efforts attempted to directly clone the 460 bp *N. rustica ADC* fragment into the *Xba*I site of pFIH10 in an antisense orientation. However, it was found that the *Xba*I site at the 3' end of the *ADC* fragment in pGEM3Z was damaged (Fig. 3-1) leading to an inability to excise the fragment from the plasmid at the *Xba*I site. To enable the *ADC* fragment to be placed into pFIH10 in the antisense orientation, it was first subcloned into pBluescript to create pYC1B (Fig. 3-1). This allowed the fragment to be recovered as a *Xba*I fragment of *ca* 470 kb which was ligated into *Xba*I digested pFIH10.

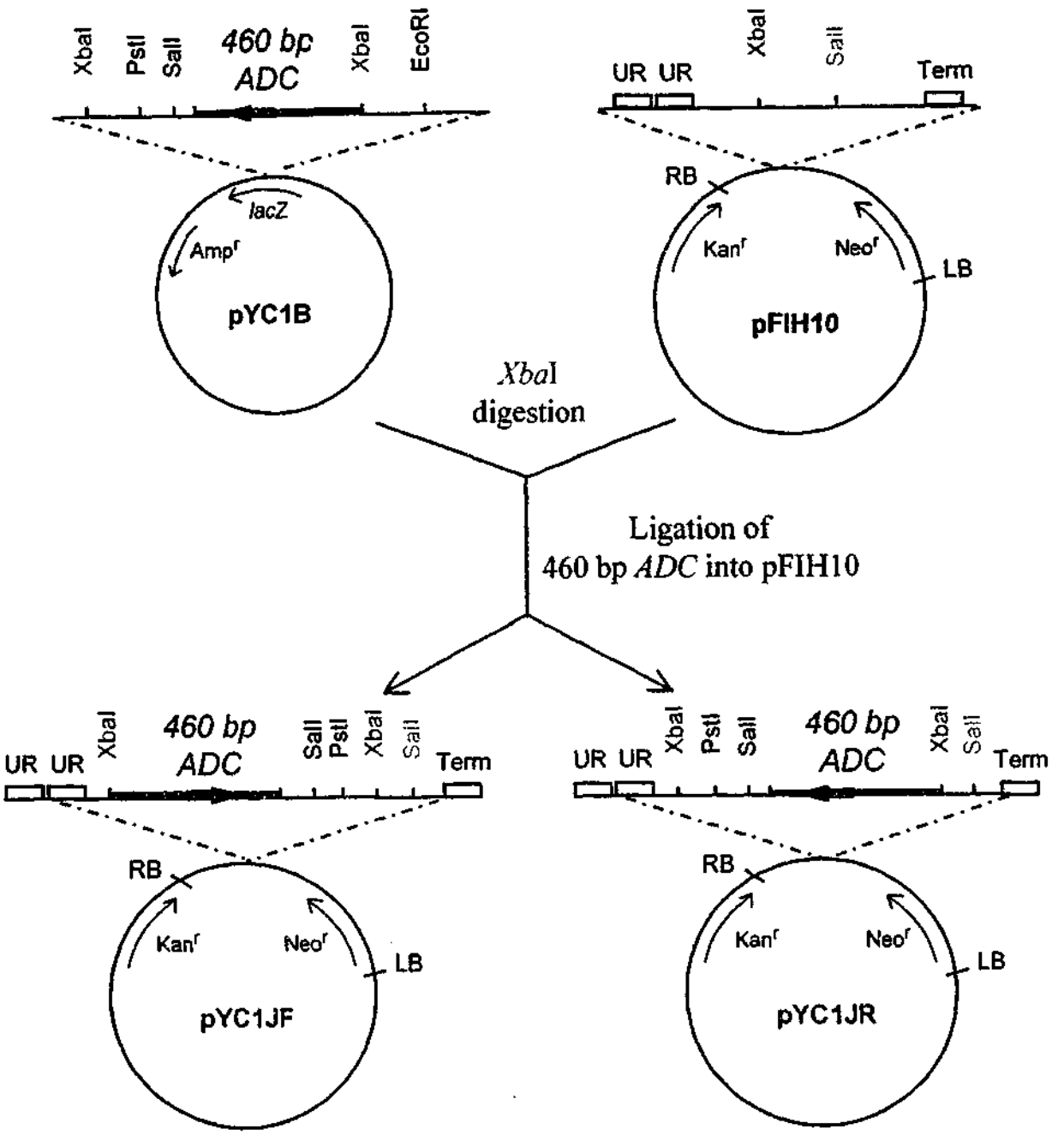

UR = Upsteam enhancer of CaMV35S promoter
Term = CaMV35S terminator

Fig.3-2 **Construction of pYC1JF and pYC1JR.** The *ADC* fragment was excised from pYC1B and ligated into pFIH10 at the *Xba*I site. pYC1JR contained the 460bp *ADC* fragment in an antisense orientation, whilst pYC1JF contained the 460bp *ADC* fragment in a sense orientation. Blue arrows indicate orientation 5'→ 3' of the *ADC* fragment with respect to the coding sequence. (Only selected restriction sites in the plasmids are illustrated.) As pFIH10 is derived from pBIN19 (Bevan, 1984), Kan^r confers resistance to kanamycin in bacteria whilst Neo^r confers resistance to kanamycin in transgenic plant cells (Hamill *et al.*, 1987a).

3.1.1.2 Cloning the 460 bp ADC *fragment from pYC1B into pFIH10 in an antisense orientation (Construction of pYC1JR)*

The 460 bp fragment of *ADC* coding sequence was excised as a *Xba*I fragment from pYC1B, ligated into the *Xba*I site of pFIH10 and transformed into *E. coli* (Fig. 3-2). After screening colony blots and probing with the *ADC* fragment, 13 positive colonies were recovered, from a total of 116 kanamycin resistant colonies. The orientation of the inserted fragment in the plasmid of the selected colonies was analyzed using a colony boil PCR procedure in conjunction with forward oligonucleotides (PW1-35S and MADC-IIIF) and reverse oligonucleotides (PW1-term and MADC-VR) (oligonucleotide sequence of these primers are recorded in Appendix 1). PCR was undertaken using various combinations of these primers and revealed the orientation of the cassette in the plasmid as showed in Table 3-1 and depicted in Fig. 3-3. PCR products were confirmed to contain *ADC* gene sequence by Southern hybridization.

Table 3-1 Results of PCR amplification using various combinations of oligonucleotide primers to elucidate the orientation of the 460 bp *ADC* fragment in the plasmid.

Primer combination	PW1-35S	PW1-term	MADC-IIIF	MADC-VR	Expected size of the band (bp)	Band of expected size obtained	Confirmed by Southern blotting to be *ADC*	Interpretation
A	✓	✓			830	✓	✓	Presence of insert of appropriate size in binary vector, pFIH10.
B			✓	✓	460	✓	✓	Presence of the fragment of *ADC* coding sequence.
C	✓			✓	590	✓	✓	Fragment of *ADC* coding sequence in pFIH10 in sense orientation.
D	✓		✓		590	✓	✓	Fragment of *ADC* coding sequence in pFIH10 in antisense orientation.

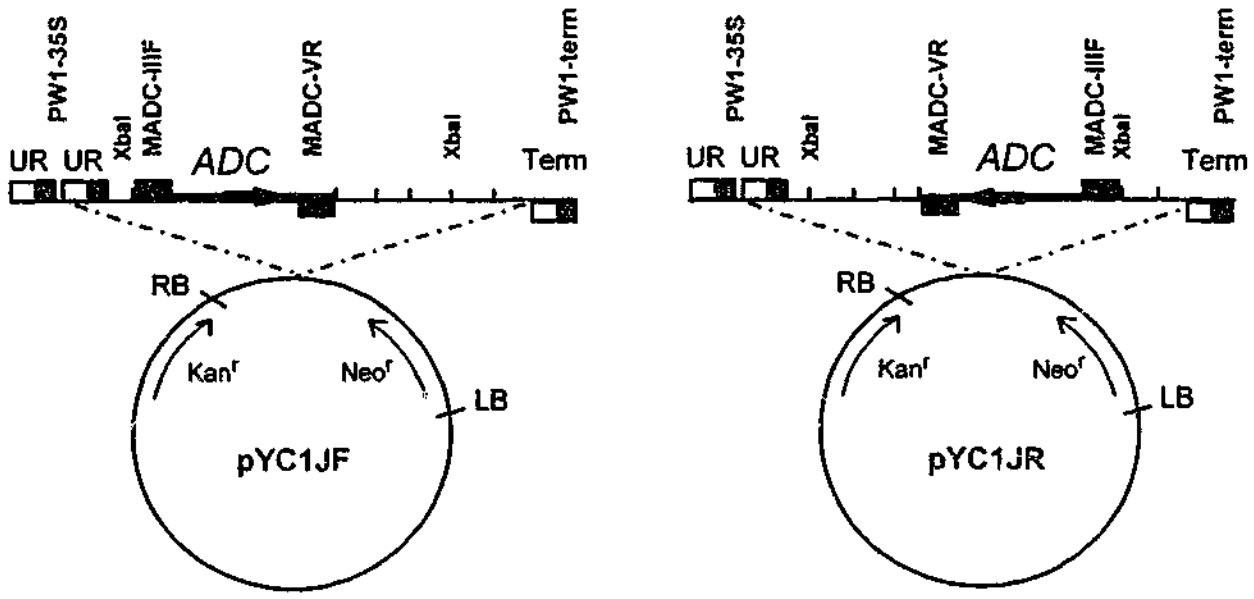

Fig. 3-3 Diagram of pYC1JF and pYC1JR constructs showing the orientation of the *ADC* fragment together with the location of the oligonucleotide primers. Blue arrows indicate orientation 5'→ 3' of the *ADC* fragment with respect to the coding sequence. PW1-35S and PW1-term are forward and reverse oligonucleotide primers of CaMV35S promoter and terminator, respectively, whilst MADC-IIIF and MADC-VR are forward and reverse primers of the 460 bp *N. rustica ADC* fragment. (Only selected restriction sites in the plasmids are illustrated.)

As anticipated, two classes of plasmid were identified amongst transformed *E. coli* colonies. One contained the sense oriented fragment of *ADC* sequence resulting positive bands in the PCR with the primer combination sets A, B and C, and was designated as pYC1JF. The other class was designated pYC1JR which contained the *ADC* fragment in an antisense orientation in the pFIH10 vector and generated positive bands from the primer combination sets A, B, and D in the PCR. Digestion of the plasmids with several restriction enzymes was also undertaken to confirm the orientation of the *ADC* fragment in these two classes.

3.1.1.3 Introduction of pYC1JR into A. rhizogenes

Plasmid pYC1JR was transformed into *A. rhizogenes* strain LBA9402 by triparental mating. Single *A. rhizogenes* colonies which were resistant to kanamycin were screened for the presence of pYC1JR initially using the colony boil PCR procedure and then confirmed using restriction enzyme digestion as previously undertaken in *E. coli*.

A.

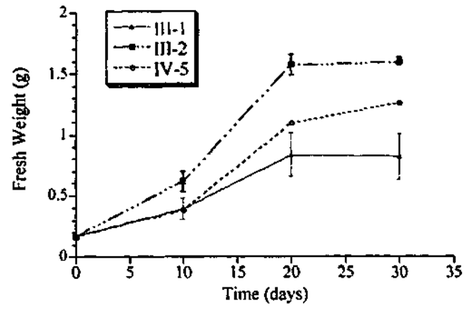

B.

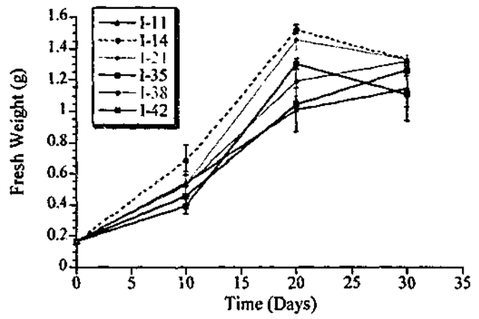

Fig. 3-4 Growth curves of control lines (A) and 460 bp antisense *ADC* lines (B). Each growth curve represents the mean (±s.e.) fresh weight (g) of triplicate samples harvested at day 10 and duplicate samples harvested at day 20 and 30 (except line IV-5, the data of which was from one sample).

I = Antisense *ADC* (CaMV35S-460 bp *ADC*)
III = Control LBA9402 (*A. rhizogenes* T-DNA only)
IV = Control pBI121 (CaMV35S-GUS)

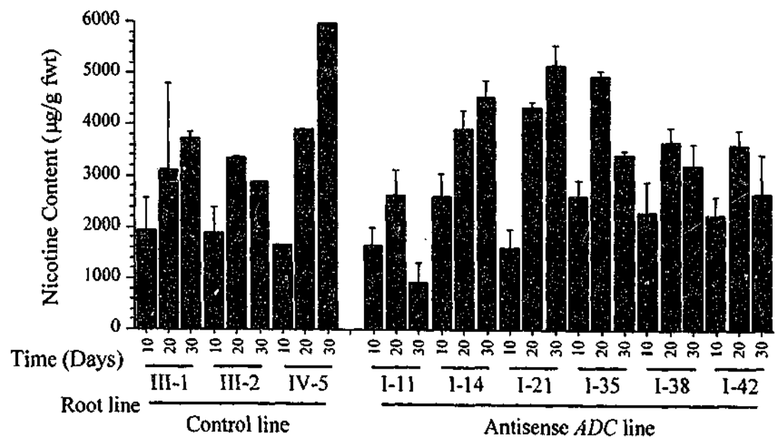

Fig. 3-5 Nicotine content in control and 460 bp antisense *ADC* root lines. Each histogram represents the mean (±s.e.) nicotine content (µg/g fwt) of triplicate samples at day 10, and duplicate samples at days 20 and 30 (except line IV-5, the data of which was from one sample).

3.1.2 Establishment and analysis of transformed root lines containing 460 bp antisense *ADC* fragment

Using established methodology as described (Chapter 2; Hamill *et al.*, 1987b; Hamill and Lidgett, 1997), three groups of transformed root lines of the high alkaloid variety of *N. tabacum*, NC95 (Moore *et al.*, 1962), were established following *A. rhizogenes* infection (Table 3-2).

Table 3-2 Designated groups of the transgenic root lines generated using LBA9402/pYC1JR.

Root line group	*A. rhizogenes* var. LBA9402	Key feature
I	plus pYC1JR	Transformed root lines containing 460 bp *N. rustica ADC* antisense construct.
III	Wild type	Control transformed root lines containing T-DNA only.
IV	plus pBI121	Control transformed root lines containing the CaMV35S-GUS gene construct

NB Group II lines were generated subsequently from *N. tabacum* var. NC95 containing a larger antisense *ADC* fragment. (see section 3.2 below.)

3.1.2.1 Growth characteristics of 460 bp antisense ADC *transformed root lines*

The growth of control and manipulated antisense *ADC* root lines was monitored over a 30 day period of culture with fresh weights being recorded at days 10, 20 and 30. The growth curves of control and antisense *ADC* root lines are shown in Fig. 3-4-A and B, respectively. Although minor differences between the growth of separate antisense *ADC* lines were observed, the extent of these differences was in the same range as was observed in control root lines.

3.1.2.2 Nicotine content of 460 bp antisense ADC *transformed root lines*

Nicotine content of the root cultures harvested for growth assessment at each time point was determined. Fig. 3-5 shows the mean nicotine levels in the control and 460 bp antisense *ADC* transformed root lines at three time points representing early (day

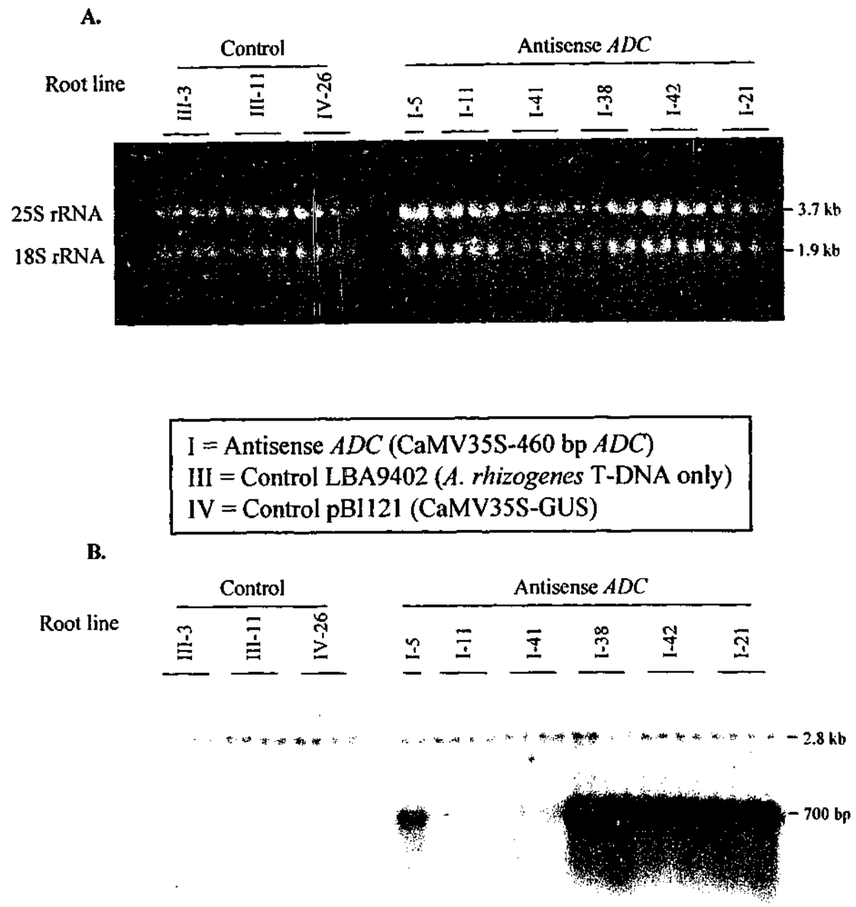

Fig. 3-6 Northern blot hybridisation of 460 bp antisense *ADC* root lines and controls with independent, duplicate samples analysed at day 12 of growth cycle, except line I-5. Each lane contains 20 µg of total RNA extracted from tissues in separate culture vessels.

(A) Bands of the 18S and 25S ribosomal RNA visible after staining with ethidium bromide illustrate a relatively equal amount of RNA loading in each well.

(B) Autoradiograph of the Northern blot probed with the 460 bp *ADC* fragment shows an endogenous 2.8 kb *ADC* transcript in all root lines and a transcript representing the introduced *ADC* fragment at 700 bp in most of the antisense *ADC* lines analysed. It is clear that despite a very strong antisense *ADC* signal in lines I-5, I-38, I-42 and I-21, the transcript level of endogenous *ADC* are not markedly altered from controls.

10), mid (day 20) and late (day 30) stages in the growth cycle. Consistent with previous observations in this laboratory for high alkaloid varieties of *N. tabacum* (Lidgett, 1997), the nicotine levels of each control root line was lower when analysed at day 10 of the growth cycle, compared to tissues of the same line when analysed at days 20 and 30.

Examination of the data overall indicates that the nicotine content of transformed root lines containing the 460 bp *ADC* fragment in an antisense orientation was similar to that possessed by controls - with the possible exception of line I-11 which had rather low level of nicotine at day 30 of the growth cycle. This raised the question as to whether the antisense manipulation had any effect upon endogenous *ADC* transcript levels in these transformed lines. Northern blot analysis was undertaken to address this question.

3.1.2.3 Northern blot of 460 bp antisense ADC *transformed root lines*

Total RNA from three control lines and six 460 bp antisense *ADC* root lines was extracted at day 12 of the growth cycle. This represented a stage when each line was in the early part of the active growth stage. Previous work in this laboratory has indicated that *ADC* is actively expressed in *N. tabacum* root cultures at this stage of growth (Lidgett, 1997). A Northern blot was set up using RNA from each extract (Fig. 3-6) and probed with a double-strand DNA probe of the 460 bp *ADC* coding sequence. Endogenous *ADC* transcripts were detected in both control and antisense *ADC* lines while a signal, at about 700 bp, presumed to be the transgenic antisense *ADC* coding sequence was detected only in antisense *ADC* lines (Fig. 3-6-B). For three of the antisense lines (I-21, I-38, I-42), the intensity of the 700 bp transcript was very strong (Fig. 3-6-B).

As has been noted in section 1.4.1.3, Borrell *et al.* (1995) showed that ADC protein was not detectable in roots of oat seedlings. Analogously, in young plants of *A. thaliana* transcripts of *ADC1* and *ADC2* were both found to be barely detectable in root tissue (Soyka and Heyer, 1999). Results from the present study in which expression of *ADC* was detected in transformed roots of *N. tabacum* (Fig. 3-6-B), however, are in

agreement with similar findings from other plants, such as cultured roots of *H. albus* (Hashimoto *et al.*, 1989a), transformed roots of *N. rustica* (Hamill *et al.*, 1990), and *D. stramonium* (Robins *et al.*, 1991a, 1991c; Michael *et al.*, 1996). Interestingly, these latter species all produce alkaloids derived from putrescine, and hence, the expression of *ADC* in such roots may be a function of increased flux through the *ADC* arm of the polyamine biosynthesis pathway leading to secondary metabolism.

To confirm that the 700 bp *ADC* signal in the Northern blot did indeed represent the antisense transcript, an asymmetric PCR was set up to synthesise single-strand probes to detect either sense or antisense *ADC* transcript. To avoid the possibility of interference from any trace signals that may remain on the blot after stripping, a new Northern blot was set up and was hybridized with the probe synthesized using asymmetric PCR. The sense-strand probe was generated from asymmetric PCR using the forward nucleotide primer, MADC-IIIF, in the labelling reaction (Fig. 3-7). The antisense *ADC* transcript of the manipulated lines, I-38, I-42 and I-21 was clearly detected using this asymmetric PCR product in addition to that of line I-5 which was detected as a weaker signal (Fig. 3-8-A). In contrast the endogenous sense *ADC* transcript of both control and manipulated lines were barely detectable (Fig. 3-8-A). This confirms that the foreign *ADC* fragment was transcribed in the antisense orientation in root lines I-5, I-38, I-42 and I-21. Though antisense mRNA transcripts have been reported to be difficult to detect in some transgenic tissues expressing the sense message (van der Krol *et al.*, 1988; Smith *et al.*, 1988), other studies involving transformed roots have reported antisense mRNA to be readily detectable (Carron *et al.*, 1994).

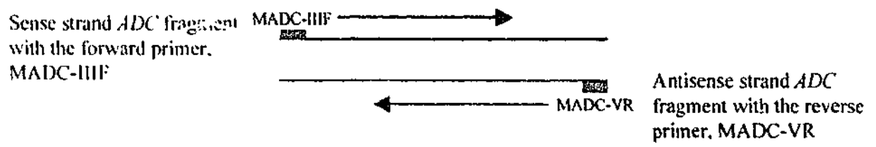

Fig. 3-7 Diagram illustrates double-strand *ADC* fragment with the forward primer (MADC-IIIF) and the reverse primer (MADC-VR). Using MADC-IIIF as a primer in the labelling reaction in asymmetric PCR, a sense-strand probe is amplified (blue). Thus, this PCR probe binds and detects the antisense transcript on the Northern blot. On the other hand, when MADC-VR was used as a primer in the reaction, an antisense-strand is amplified (green). Therefore, the sense transcription on the blot will be detected by this probe.

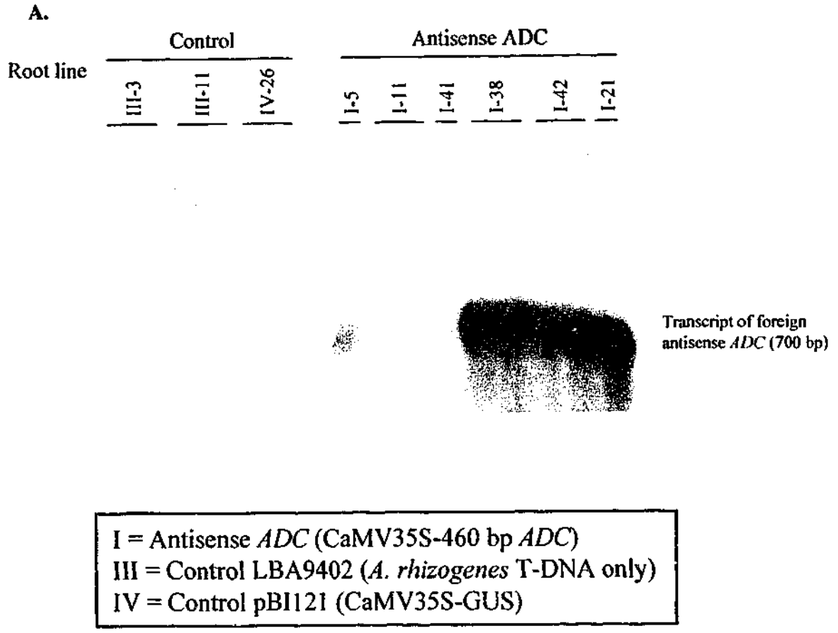

Fig. 3-8 Autoradiographs of Northern blot analysis of antisense 460 bp *ADC* root lines and controls with duplicate samples (except lines I-5, I-41 and I-21). Each lane contains 20 µg of total RNA extracted from tissues in separate culture vessels.

(A) Autoradiograph of the blot probed with sense strand DNA of the 460 bp *ADC* fragment to detect antisense transcript of the introduced *ADC* fragment.

(B) Autoradiograph of the blot probed with antisense strand DNA of the 460 bp *ADC* fragment to detect sense transcript of the endogenous *ADC*.

A similar procedure was employed to detect the sense transcript of the endogenous gene except that a reverse primer, MADC-VR oligonucleotide, was used to produce an antisense-strand probe in the labelling reaction (Fig. 3-7). Fig. 3-8-B shows the hybridisation of this antisense-strand probe to the blot. Both antisense and sense *ADC* transcripts were detected using this probe. However, when compared to Fig. 3-6-B and 3-8-A where the blots were probed with double-strand and sense-strand probes, respectively, the sense *ADC* transcript in Fig. 3-8-B shows a much stronger signal whereas the antisense transcript was revealed as a much weaker signal.

3.1.3 Conclusions regarding the efficacy of using the 460 bp fragment of *N. rustica ADC* coding sequence to down-regulate *ADC* in *N. tabacum*

Examination of Fig. 3-6 to 3-8 demonstrates that several root lines containing the 460 bp antisense *ADC* fragment accumulated antisense transcript to a high level (particularly lines I-21, I-38 and I-42) but this did not lead to a reduction in the level of endogenous *ADC* transcript compared to control lines (III-3, III-11 and IV-26) or lines in which the antisense transcript is either not expressed, or is expressed at lower levels (lines I-11, I-5, I-41).

Although the results of others indicated that an antisense fragment as little as 41 bp can down-regulate gene expression (Cannon *et al.*, 1990), the present study clearly indicates that expression of this 460 bp fragment was insufficient to reduce transcript levels of endogenous *ADC* in transformed roots of *N. tabacum* var. NC95 (Fig. 3-6 and Fig. 3-8).

To test whether a longer *ADC* antisense fragment would be more effective at down-regulating *ADC*, it was thus decided to make a larger antisense construct comprising approximately the first half of the tobacco coding sequence.

3.2 1.2 kb *ADC* coding sequence of *N. tabacum*

3.2.1 Cloning 1.2 kb *ADC* coding sequence

At the time this experiment was initiated, the *ADC* coding sequence of the most closely related species to tobacco in the GenBank/EMBL databases was a cDNA from tomato. This was reported as being 2.05 kb in length and consisting of an open reading frame of 1.5 kb and 530 bp of 3' untranslated region (Rastogi *et al.*, 1993). To identify an oligonucleotide primer that would enable the recovery, via PCR, of DNA sequence for *N. tabacum* as close to the 5' end of the coding sequence of *ADC* as possible, primer YC1F (forward primer) (sequence presented in Appendix 1) was designed based on the conserved regions between tomato and pea *ADC* sequences, the only other full-length dicotyledon *ADC* sequence available in the Genbank/EMBL databases at that time (Rastogi *et al.*, 1993; Perez-Amador *et al.*, 1995; accession numbers L16582 and Z37540 respectively). Oligonucleotide EY1R (reverse primer)* (sequence given in Appendix 1) was designed based on the conserved regions between tomato and pea. A putative fragment of *Arabidopsis ADC* sequence, available also in the database at that time (accession number Z37204), was also utilised in the design of this oligonucleotide primer. These forward and reverse primers respectively represented the tomato *ADC* nucleotide transcript positions 31 – 50 and 1255 – 1275 (amino acid positions 2 – 7 and 411 – 417 in the ADC protein) (Fig. 3-9) reported by Rastogi *et al.* (1993). An *Xba*I restriction enzyme recognition site was placed at the 5' end of each primer to facilitate the subsequent cloning of the DNA fragment into pFIH10.

* Reverse primer was designed together with E. Fredericks, a fellow postgraduate in the laboratory.

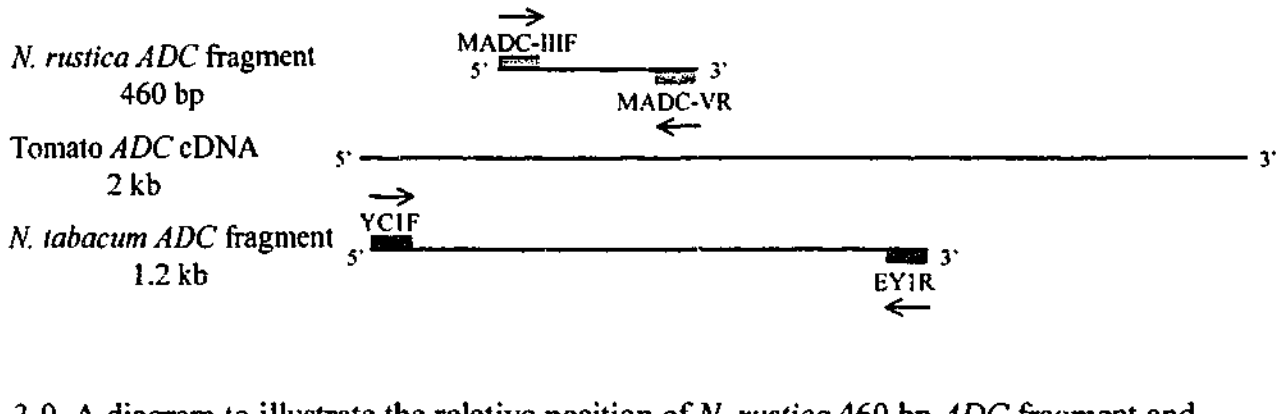

Fig. 3-9 A diagram to illustrate the relative position of *N. rustica* 460 bp *ADC* fragment and the *N. tabacum* 1.2 kb *ADC* fragment obtained from PCR with corresponding region in the tomato *ADC* cDNA. Arrows indicate direction of oligonucleotides 5'→ 3'.

Using YC1F and EY1R, a strong band of the expected size, 1.2 kb and also a faint band at a smaller size were amplified from *N. tabacum* genomic DNA. A Southern blot of the purified amplified fragment was conducted and probing with the *N. rustica* 460 bp fragment noted above confirmed that the 1.2 kb fragment was indeed from within the *ADC* gene sequence.

3.2.1.1 Cloning the 1.2 kb ADC *fragment into pGEM-T vector (Construction of pYC2T)*

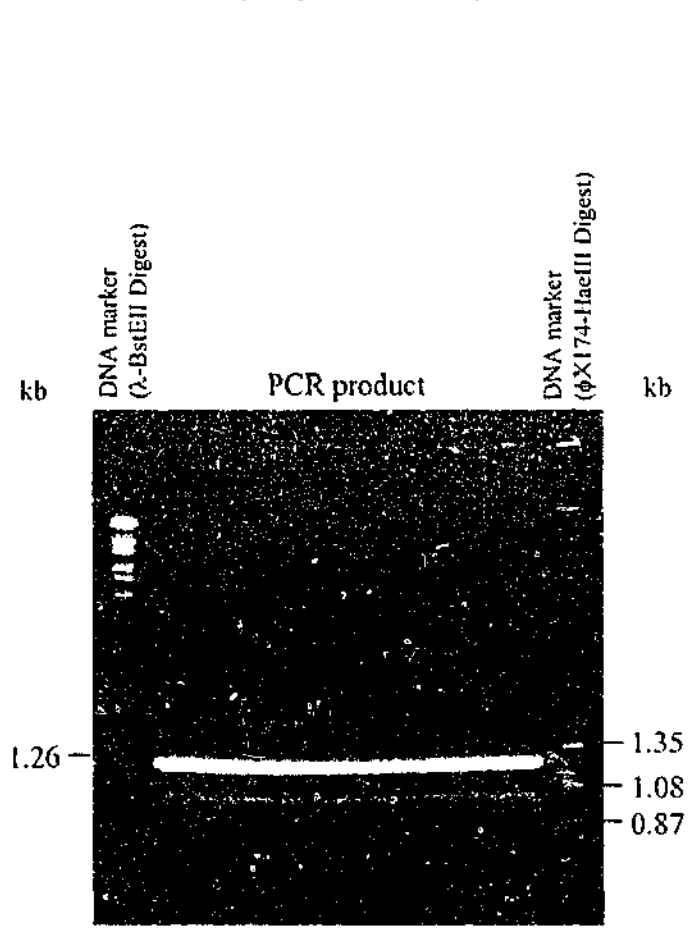

Fig. 3-10 Preparative agarose gel showing successful PCR amplification of a 1.2 kb *N. tabacum ADC* fragment.

The products of several PCR reactions were pooled (Fig. 3-10). The 1.2 kb *ADC* fragment was purified from the agarose gel, using the phenol freeze method and was ligated into a commercially-produced vector, pGEM-T (Fig. 3-11). The plasmid was subsequently transformed into *E. coli* cells and was isolated from two white colonies, using a miniprep method. When analysed by agarose gel electrophoresis, digestion of the plasmid with *Xba*I produced an insert fragment of 1.2 kb, in addition to the 3 kb band of pGEM-T, whilst *Sal*I digestion linearised the plasmid to produce a DNA fragment of 4.2 kb (Fig. 3-12). One of the plasmids was designated pYC2T (Fig. 3-11) and was used subsequently as a source of 1.2kb *ADC* DNA.

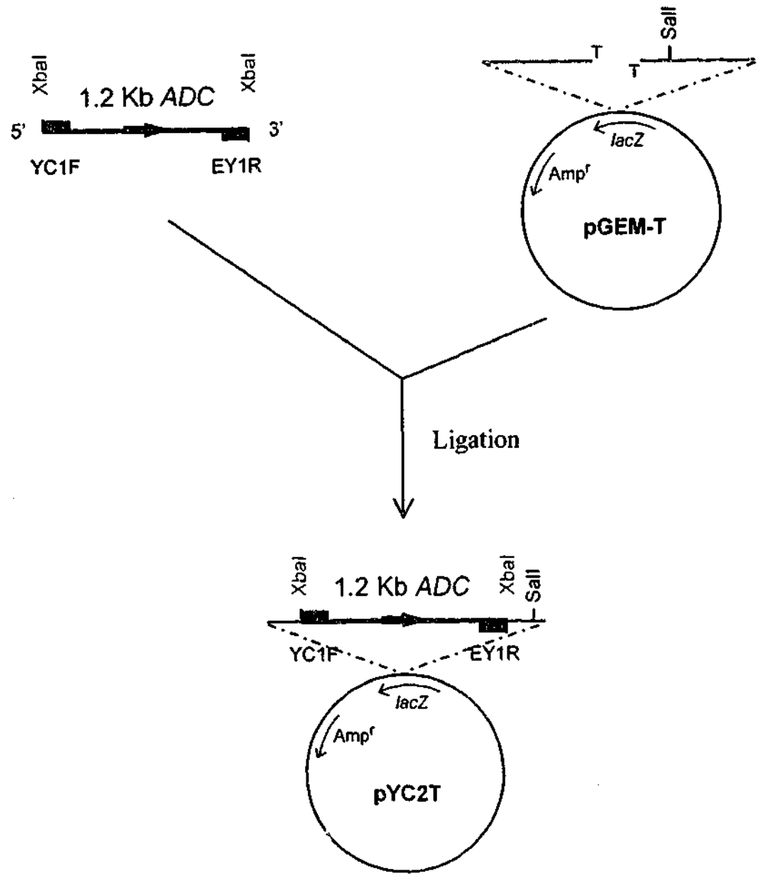

Fig. 3-11 **Construction of pYC2T.** Using YC1F and EY1R as forward and reverse primers, respectively, a 1.2 kb *ADC* fragment was amplified by PCR from *N. tabacum* var. NC95 genomic DNA and was ligated into pGEM-T. Blue arrows indicate orientation 5'→ 3' of the *ADC* fragment with respect to the coding sequence. (Only relevant restriction sites are illustrated.)

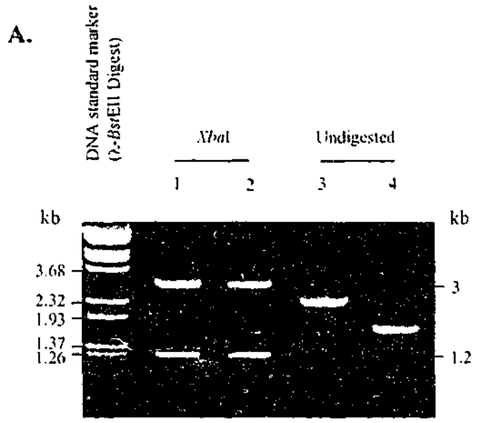

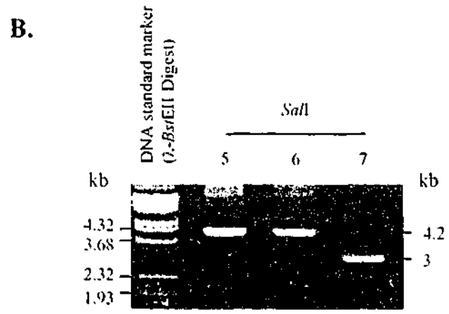

Fig. 3-12 Digestion of pYC2T with *Xba*I (A) and *Sal*I (B).

(A) Lane 1 and 2 : Plasmids from two positive colonies were digested with *Xba*I yielding two bands representing the 1.2 kb *ADC* fragment and 3 kb pGEM-T vector.
Lane 3 : Undigested plasmid from one positive colonies.
Lane 4 : Undigested plasmid from a negative colony.

(B) Lane 5 and 6 : Plasmids from the positive colonies were digested with *Sal*I yielding a 4.2 kb band corresponding to the linearised pYC2T.
Lane 7 : Plasmid from negative colony digested with *Sal*I, yielding a 3 kb band corresponding to the linearised pGEM-T.

3.2.1.2 Sequencing of the 5' and 3' ends of the 1.2 kb fragment of N. tabacum ADC *coding sequence*

GAP analysis of the deduced protein representing the 5' and 3' ends of tomato *ADC* cDNA against the corresponding regions in the 1.2 kb DNA fragment recovered from tobacco via PCR is illustrated in Fig. 3-13. Sequencing analysis of the 5' and 3' ends of the insert in pYC2T revealed that the deduced amino acid similarity and identity are 97.04% and 86.39%, respectively, to the tomato *ADC* sequence. The 1.2 kb size and homology with appropriate regions of the tomato *ADC* cDNA indicated that intronic sequences were absent (or at least were minimal in size) within the 1.2 kb *N. tabacum ADC* fragment.

```
Percent Similarity: 97.238   Percent Identity: 86.740

 Tomato ADC x Both ends of tobacco ADC fragment

Tomato    10 ..........LVVRFPDVLKNRLETLQSAFDMAINSQGYEAHYQGVYPVK 50
                       ||||:||||||||||.||||||:|::|||||:||||||||||
Tobacco    1 ..........LVVRLPDVLKNRLESLQSAFDLAVHSQGYGAHYQGVYPVK 40
Tomato    51 CNQDRFVVEDIVKFGSPYRFGLEAGSKPELLLAMNCL..............  86
             ||||||||||||||||||:|||||||||||||||.||
Tobacco   41 CNQDRFVVEDIVKFGSPFRFGLEAGSKPELLLAMSCL..............  77


Tomato   321 .....................LQSLVETLNEDARADYRNLSAAAVRGEYDT 350
                                  |||:.|||||||  ||||||||||||||:|
Tobacco   78 .....................LQSMAETLNEDALADYRNLSAAAVRGEYET 107


Tomato   351 CLIYSDQLKQRCVEQFKDGSLDIEQLAAVDSICDWVSKAIGVADPVRTYH 400
             |::|||||||||||||||:|||:||:|||||||||:|||||:|.|||||||||
Tobacco  108 CVLYSDQLKQRCVEQFKEGSLGIEHLAAVDSICDFVSKAMGAADPVRTYH 157
Tomato   401 VNLSVFTSIPDFWGFSQLFPIVPI.........................  424
             ||||:|||||||::|:|||||||||
Tobacco  158 VNLSIFTSIPDFLAFGQLFPIVPI.........................  181
```

Fig.3-13 A comparison of deduced amino acid sequences of tomato *ADC* (Rastogi *et al.*, 1993) and deduced amino acid sequences at both ends of *N. tabacum ADC* fragment using the ANGIS program GAP. Deduced amino acid sequences of the forward primer, YC1F, and the reverse primer, EY1R, in *N. tabacum ADC* fragment are illustrated in blue and green, respectively.

Nucleotide sequence of the 5′ end of the 1.2 kb fragment *ADC*.

```
ADC2        2458 .......CTTGTTGTTCGCTTCCCTGATGTGTTGAAAAACCGGTTGGAAT 2500
                         |||||||| ||| | ||||||||||||||||||||||||||
1.2kb ADC      1 .......CTTGTTGTCCGCCTTCCTGATGTGTTGAAAAACCGGTTGGAAT 43

ADC2        2501 CTCTGCAATCGGCTTTTGATCTCGCGGTTCATTCCCAGGGCTATGGGGCC 2550
                 ||||||||||||||||||||||||||||||||||||||||||||||||||
1.2kb ADC     44 CTCTGCAATCGGCTTTTGATCTCGCGGTTCATTCCCAGGGCTATGGGGCC 93

ADC2        2551 CACTACCAAGGTGTTTATCCCGTGAAATGCAATCAAGACAGGTTCGTGGT 2600
                 ||||||||||||||||||||||||||||||||||||||||||||||||||
1.2kb ADC     94 CACTACCAAGGTGTTTATCCCGTGAAATGCAATCAAGACAGGTTCGTGGT 143

ADC2        2601 GGAAGATATCGTGAAATTCGGGTCGCCATTCCGGTTCGGGTTGGAAGCCG 2650
                 ||||||||||||||||||||||||||||||||||||||||||||||||||
1.2kb ADC    144 GGAAGATATCGTGAAATTCGGGTCGCCATTCCGGTTCGGGTTGGAAGCCG 193

ADC2        2651 GGTCTAAACCCGAGCTCCTGTTAGCCATGAGCTGTCTCT..........  2689
                 |||||||||||||||||||||||||||||||||||||
1.2kb ADC    194 GGTCTAAACCCGAGCTCCTGTTAGCCATGAGCTGTCTCT..........  232
```

Nucleotide sequence of the 3′ end of the 1.2 kb fragment *ADC*.

```
ADC2        3390 ..........................................CCTCCAATCCA 3400
                                                           ||||||||||
1.2kb ADC      1 ..........................................CCTCCAATCCA 11

ADC2        3401 TGGCGGAGACGCTCAACGAAGATGCCCTTGCTGATTACCGCAATTTATCT 3450
                 ||||||||||||||||||||||||||||||||||||||||||||||||||
1.2kb ADC     12 TGGCGGAGACGCTCAACGAAGATGCCCTTGCTGATTACCGCAATTTATCT 61

ADC2        3451 GCTGCTGCAGTTCGTGGAGAGTATGAGACATGTGTACTTTACTCTGATCA 3500
                 ||||||||||||||||||||||||||||||||||||||||||||||||||
1.2kb ADC     62 GCTGCTGCAGTTCGTGGAGAGTATGAGACATGTGTACTTTACTCTGATCA 111

ADC2        3501 GTTGAAACAGAGATGTGTGGATCAGTTTAAAGAAGGGTCCTTGGGTATTG 3550
                 |||||||||||||||||||| ||||||||||||||||||||||||||||
1.2kb ADC    112 GTTGAAACAGAGATGTGTGGAGCAGTTTAAAGAAGGGTCCTTGGGTATTG 161

ADC2        3551 AACATCTTGCTGCTGTTGATAGCATCTGTGATTTTGTATCAAAGGCTATG 3600
                 |||||||||||||||||||||||||| ||||||||||||||||||||||
1.2kb ADC    162 AACATCTTGCTGCTGTTGATAGCATCTGTGACTTTGTATCAAAGGCTATG 211

ADC2        3601 GGGGCTGCTGATCCTGTCCGCACTTACCATGTGAATCTGTCAATTTTCAC 3650
                 ||||||||||||||||||||||||||||||||||||||||||||||||||
1.2kb ADC    212 GGGGCTGCTGATCCTGTCCGCACTTACCATGTGAATCTGTCAATTTTCAC 261

ADC2        3651 TTCAATTCCTGATTTTTGGGCCTTTGGTCAATTGTTTCCGATTGTTCCAA 3700
                 |||||||||||||||| |||||||||||||||||| ||||||||||
1.2kb ADC    262 TTCAATTCCTGATTTTTTGGCCTTTGGTCAATTGTTTCCTATTGTTCCAA 311

ADC2        3701 TTCA                                              3704
                 | ||
1.2kb ADC    312 TCCA                                              315
```

Fig.3-14 A comparison of nucleotide sequences of *ADC2* from *N. tabacum* var. Xanthi (accession number AF127241 in GenBank) and nucleotide sequences at both ends of the *ADC* fragment from *N. tabacum* var. NC95 using the ANGIS program GAP. Nucleotide sequences of the forward primer, YC1F, and the reverse primer, EY1R, in the *ADC* fragment are illustrated in blue and green, respectively.

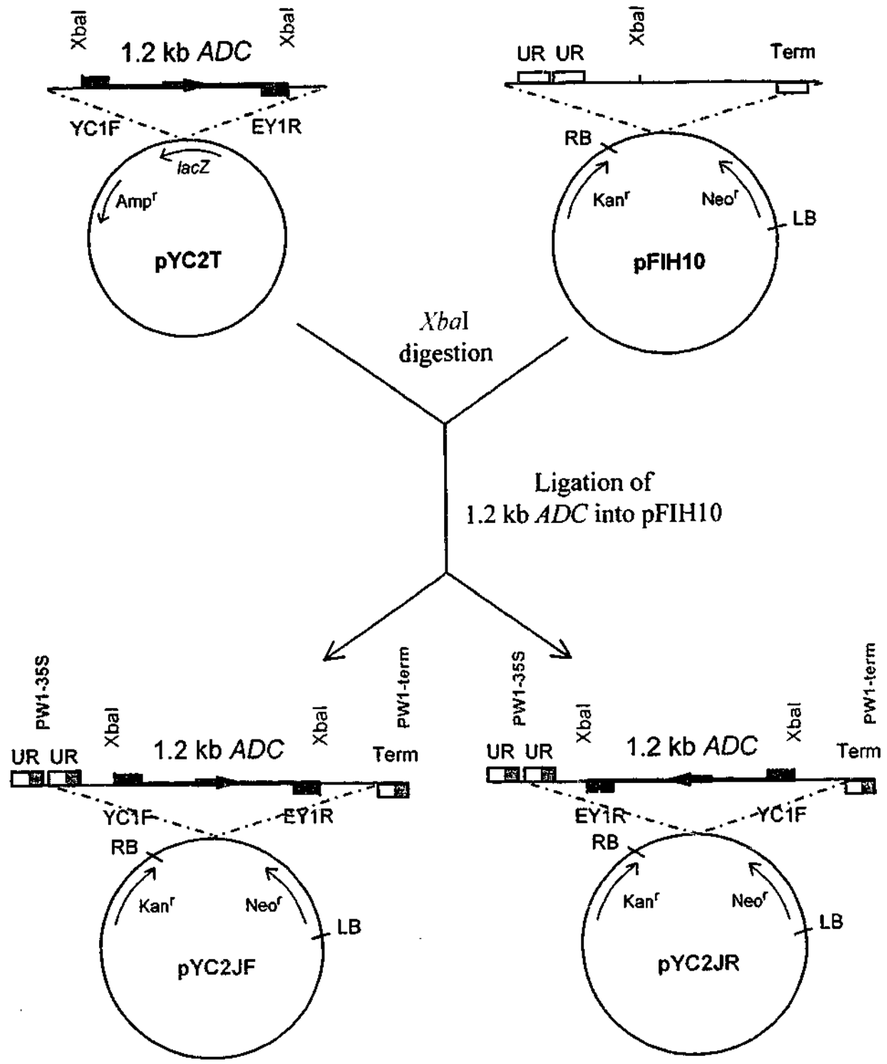

UR = Upsteam enhancer of CaMV35S promoter
Term = CaMV35S terminator

Fig. 3-15 Constructions of pYC2JF and pYC2JR. *ADC* fragment was excised from pYC2T and ligated into pFIH10 at the *Xba*I site. Blue arrows indicate orientation 5'→ 3' of the *ADC* fragment with respect to coding sequence. (Only relevant restriction sites are illustrated.)

It is noteworthy that two *ADC* genomic DNA sequences from *N. tabacum* var. Xanthi were subsequently reported in the GenBank database (accession number AF127240 [*NtADC1*] and AF127241 [*NtADC2*], Wang *et al.*, 2000). Comparison with the sequence of the 1.2 kb *N. tabacum ADC* recovered in this study shows that homology at the 5' end is 96% and 99% for *NtADC1* and *NtADC2*, respectively, over 232 nucleotides, whilst homology over 315 nucleotides at the 3' end is 97% and 98% for *NtADC1* and *NtADC2*, respectively. This suggests that the 1.2 kb fragment cloned in pYC2T was probably amplified from *NtADC2* (Fig. 3-14).

3.2.1.3 Cloning the 1.2 kb ADC *fragment from pYC2T into pFIH10 in the antisense orientation (Construction of pYC2JR)*

The 1.2 kb fragment of *ADC* coding sequence was excised from pYC2T as an *Xba*I fragment, and ligated into pFIH10 at the *Xba*I site (Fig. 3-15). Colony blots probed with the 460 bp fragment of *N. rustica ADC* sequence revealed three putative positive transformed clones from a total of 74 kanamycin resistant colonies. The orientation of the insert fragment in the plasmid of the selected clones was determined using the colony boil-PCR procedure as described previously in section 3.1.1.2. The oligo-nucleotide primers YC1F and EY1R were used in primer combination, instead of MADC-IIIF and MADC-VR (Table 3-3).

Table 3-3 Results of PCR amplification using various combinations of oligonucleotide primers to elucidate the orientation of the 1.2 kb *ADC* fragment in the plasmid in transformed *E. coli*.

Primer combination	PW1-35S	PW1-term	YC1F	EY1R	Expected size of the band (kb)	Band of expected size obtained	Interpretation
B			✓	✓	1.2	✓	Presence of the *ADC* fragment..
C	✓			✓	1.3	✓	Presence of 1.2 kb fragment of *ADC* sequence in the sense orientation relative to CaMV35S promoter.
D		✓	✓		1.4	✓	
E	✓		✓		1.3	✓	Presence of 1.2 kb fragment of *ADC* sequence in the antisense orientation relative to the CaMV35S promoter.
F		✓		✓	1.4	✓	

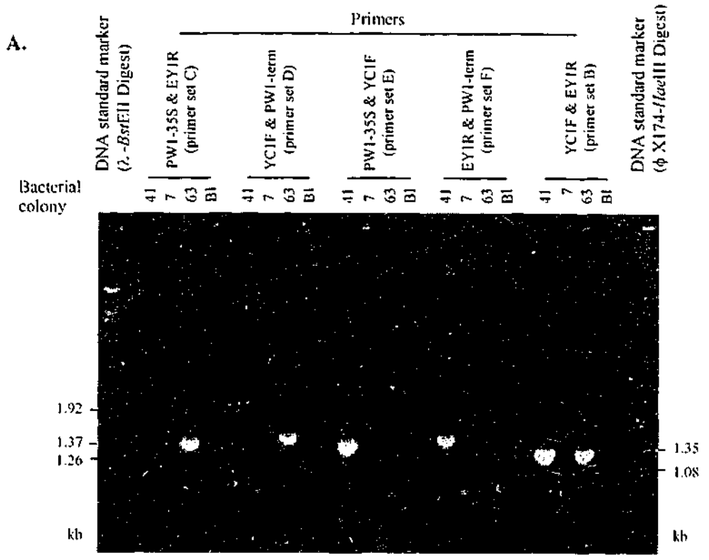

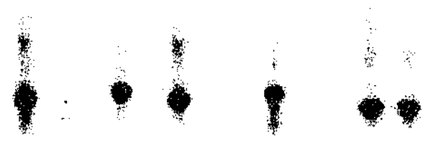

Fig. 3-16 Colony boil PCR of transformed *E. coli* with various sets of primers to determine the orientation of the insert, 1.2 kb *ADC* fragment, in the vector pFIH10. PW1-35S and PW1-term are forward and reverse oligonucleotide primers of CaMV35S promoter and terminator, respectively, whilst YC1F and EY1R are forward and reverse oligonucleotide primers of the 1.2 kb tobacco *ADC* fragment.

A) Gel electrophoresis of the PCR products from :

41 = colony containing antisense *ADC* construct in pFIH10.
7 = colony containing pFIH10 without *ADC* construct.
63 = colony containing sense *ADC* construct in pFIH10.
Bl = blank without *E. coli* colony as a PCR negative control.

B) Southern blot of the gel probed with 460 bp *N. rustica ADC* fragment.

Southern analysis of products from all amplifications yielded no hybridisation in PCR samples 7 and Bl. In contrast, the PCR set from the positive colonies, 41 and 63, yielded products of the expected sizes corresponding to the primers used (Table 3-3). Using primer set C and D in the PCR, only colony number 63 produced a signal, whilst colony number 41 produced signal when the primer set E and F were used. Thus, the *ADC* fragment in colonies number 63 and 41 are in sense and antisense orientation relative to the CaMV35S promoter, respectively.

Gel electrophoresis of the PCR products together with the results from the subsequent Southern blot probed with the fragment of *N. rustica ADC* sequence confirmed the orientation of the inserted fragment in the plasmid of two clones (Fig. 3-16-A and B). The sense orientated fragment of *ADC* sequence in the vector was designated pYC2JF. The antisense orientated fragment of *ADC* was designated pYC2JR. Digestion of both plasmids separately with several enzymes and probing the Southern blot was also undertaken to confirm the integrity and orientation of the 1.2 kb *ADC* fragment in the plasmids.

3.2.1.4 Introduction of pYC2JR into A. rhizogenes

Plasmid pYC2JR and pYC2JF were separately transformed into *A. rhizogenes* strain LBA9402 as described previously in section 3.1.1.3. Single *A. rhizogenes* colonies resistant to kanamycin were analysed for the presence and the orientation of the inserted fragment in the plasmid by the colony boil-PCR technique as in the Table 3-4. The presence of *ADC* sequences in the PCR products were also confirmed by Southern hybridization probing with the 460 bp fragment of *N. rustica ADC* sequence.

Table 3-4 Results of PCR amplification using various combinations of oligonucleotide primers to elucidate the orientation of the 1.2 kb *ADC* fragment in the *A. rhizogenes* plasmid.

Primer combination	PW1-35S	PW1-term	YC1F	Expected size of the band (kb)	Band of expected size obtained	Confirmed by Southern blotting to be *ADC*	Interpretation
A	✓	✓		1.5	✓	✓	Presence (integration) of the binary vector, pFIH10, and the insert *ADC* fragment.
D		✓	✓	1.4	✓	✓	Presence of 1.2 kb fragment of *ADC* sequence in the sense orientation relative to CaMV35S promoter.
E	✓		✓	1.3	✓	✓	Presence of 1.2 kb fragment of *ADC* sequence in the antisense orientation relative to the CaMV35S promoter.

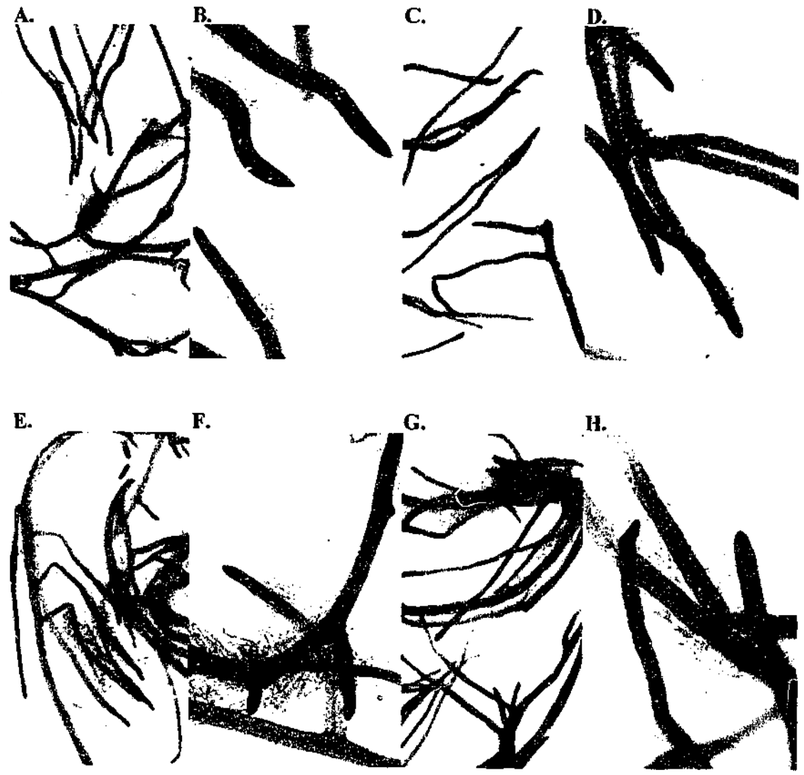

A. and B. = IV-3
C. and D. = IV-9
E. and F. = IV-10
G. and H. = IV-13
I. and J. = IV-15
K. = III-8 (negative control for GUS staining)

Fig. 3-17 GUS staining in control root line groups IV and III. Gus staining was visible in all five lines of control group IV, containing pBI121 (Panels A-J). In contrast, the control line in group III (III-8) which was generated from wild type *A. rhizogenes* LBA9402 was not stained (Panel K).

3.2.2 Establishment and screening of the transformed root lines containing 1.2 kb antisense *ADC* fragment

Transformed root lines of *N. tabacum* var. NC95 were established using *A. rhizogenes* infection as summarized in Table 3-5. More than ten transformed root lines containing the 1.2 kb antisense *ADC* construct were generated.

Table 3-5 Designated groups of the generated transgenic root lines.

Root line group	*A. rhizogenes* var. LBA9402	Key features
II	plus pYC2JR	Transformed root lines containing 1.2 kb *N. tabacum ADC* antisense construct.
III	Wild type	Control transformed root lines containing T-DNA only.
IV	plus pBI121	Control transformed root lines containing CaMV35S::GUS gene construct.

3.2.2.1 GUS staining of root tissues from control root lines of N. tabacum var NC95 (Group IV)

Root lines of *N. tabacum* var. NC95 from group IV, which contained the GUS gene under the control of the CaMV35S promoter, were established as a control group to assess effects of manipulating gene expression in alkaloid metabolism. Five independent lines in this group, each established from a single root tip, were chosen at random and stained for GUS activity. All stained indigo blue (Fig. 3-17) indicating the presence of GUS activity in each of these root lines.

3.2.2.2 Preliminary screen to assess the nicotine content of 1.2 kb antisense ADC root lines

Following establishment of transformed root lines *in vitro* from single root tips, the nicotine content of five control and eleven antisense root lines was determined at day 20 of the growth cycle. Mean levels of nicotine in control root lines were in the expected

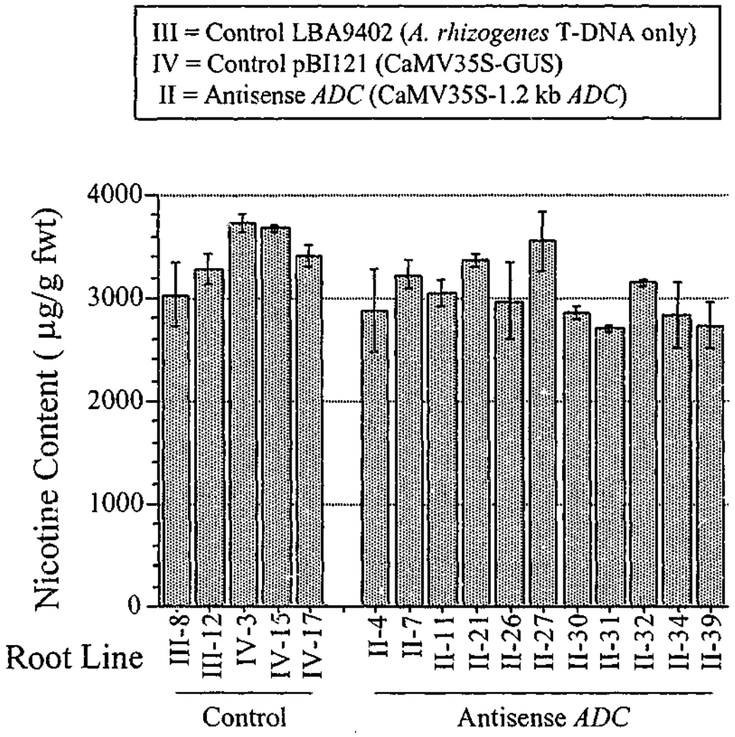

Fig. 3-18 Nicotine content in control and 1.2 kb antisense *ADC* transformed root lines of *N. tabacum* var. NC95 at day 20 of the growth cycle. Each histogram represents the mean (± s.e.) nicotine content of duplicate samples.

range of 3000 µg/g to 3750 µg/g fwt while mean levels of nicotine in eleven antisense *ADC* lines were in the range of 2700 µg/g to 3550 µg/g fwt (Fig. 3-18). An analysis of variance indicates a significant difference ($p = 0.018$) between the nicotine content of the control group (Mean 3420, Std. Dev. 122.60) and that of the antisense *ADC* group (Mean 3025, Std. Dev. 82.66). A Dunnett's statistical test of this data, however, does not show any significant difference ($p > 0.05$) between the nicotine content of any individual antisense *ADC* root line and that which is characteristic of the control group. Together, these results suggest, therefore, that although the expression of the 1.2 kb antisense *ADC* fragment did not markedly reduce the nicotine content of transformed root lines, however, the slight reductions were observed in some antisense *ADC* lines relative to controls were real, at least at day 20 of the growth cycle.

3.2.2.3 *Analysis of transcript levels of ADC and also other genes associated with putrescine metabolism in 1.2 kb antisense* ADC *transformed root lines*

Time course studies of *ADC* transcript accumulation during growth of *N. tabacum*, *A. belladonna*, *H. muticus* and *D. stramonium* transformed root cultures have revealed that in these species *ADC* transcript was highest during the early-mid stages of the growth cycle (from days 4 to 15) (Michael *et al.*, 1996; Lidgett, 1997). Thus, root tissues of antisense *ADC* lines and controls were screened for *ADC* transcript levels at day 9 of the growth cycle. Two Northern blots (Fig. 3-19-A and O) were set up using RNA extracted from nine antisense *ADC* lines (five with duplicate samples) and also four control lines. The first blot was probed with the antisense-strand of 1.2 kb *ADC* synthesised using asymmetric PCR, to detect the endogenous *ADC* transcripts (Fig. 3-19-B). The same blot was reprobed, separately (with all signals stripped between probings), with double-strand DNA sequences representing tobacco *ODC*, *SAMDC*, *SAMS*, *SPDS* and *PMT* (Fig. 3-19-C to G) (details of these probes are recorded in the Appendix 2).

The levels of *ADC* and other gene transcripts in control and antisense *ADC* root lines were determined relative to the levels of ubiquitin transcripts in each line (Fig. 3-

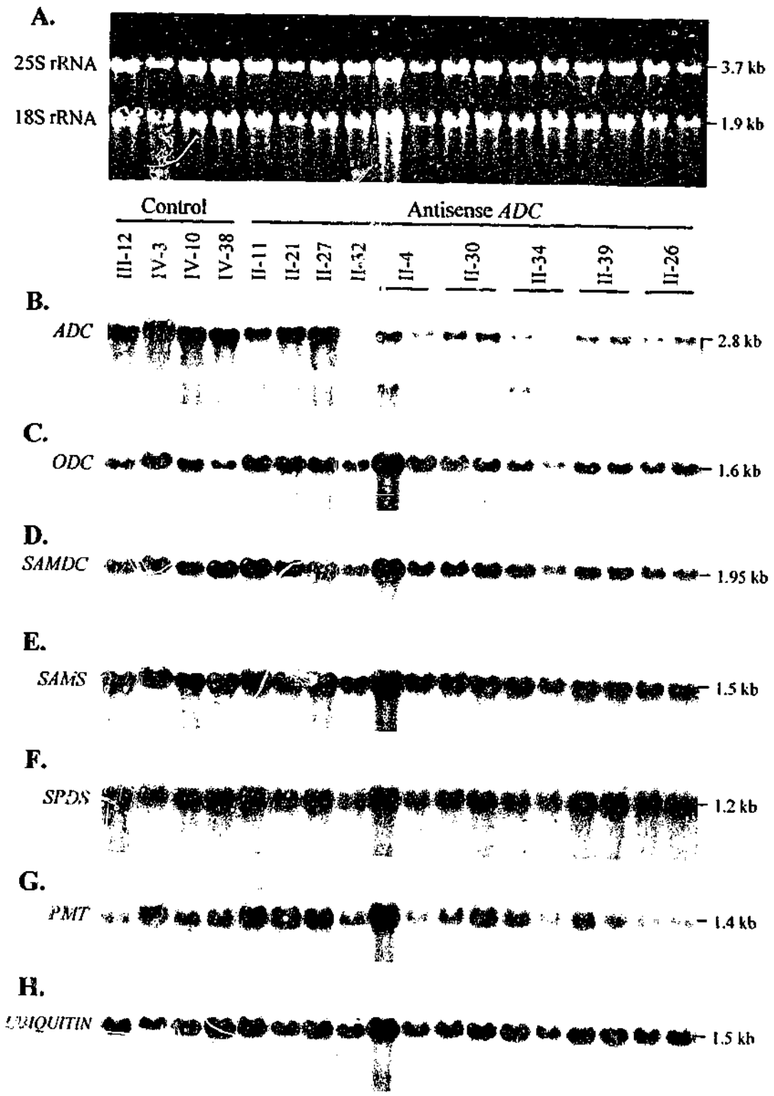

Fig. 3-19 Northern blot analysis of 1.2 kb antisense *ADC* root lines and controls. Each lane contains 20 μg of total RNA extracted from root tissues at day 9 of the growth cycle. RNA in duplicate lanes of lines II-4, II-30, II-34, II-39 and II-26 were extracted from tissues grown in separate culture vessels.
(A) The 18S and 25S ribosomal bands visible after staining with ethidium bromide illustrate a relatively equal amount of RNA loaded in each well.
(B) The blot was probed with antisense strand DNA of 1.2 kb *ADC* to detect the endogenous *ADC* transcript. Then the blot was reprobed separately with double-strand DNA of *ODC*, *SAMDC*, *SAMS*, *SPDS*, *PMT* and *UBIQUITIN* (C to H). Between each probe, the blot was stripped and exposed to a phosphorimager cassette to ensure the clearing of the previous signals on the blot.

19-I to N). In Fig. 3-19-I, the relative *ADC* transcript level in line IV-38 was lowest among the controls and was designed as 1. The relative *ADC* transcript levels in two other control lines, IV-10 and III-12, were 1.4 and 1.6, respectively. However, for unknown reason the relative *ADC* transcript levels in control line IV-3 was rather high at 4.6. In most of the antisense *ADC* root lines, the relative *ADC* transcript levels were below 1, with 6/9 lines analysed having *ADC* transcript levels of 0.5 or less. Only two out of nine antisense *ADC* lines analysed (II-21 and II-27) had levels of *ADC* transcript comparable to the controls (Fig. 3-19-I).

The relative *ODC* transcript levels in controls were in the range of 1 (IV-38) to 3.2 (IV-3) (Fig. 3-19-J) with the mean of these *ODC* transcript levels being 1.9. The level of ODC transcript in antisense *ADC* lines varied from 1.2 to 3 indicating that the antisense *ADC* lines had relative *ODC* transcript levels comparable to those of the control group (Fig. 3-19-J). Similarly, the levels of other transcript analysed in antisense *ADC* lines, namely *SAMDC*, *SAMS*, *SPDS* and *PMT*, were comparable to the levels of these transcripts observed in controls (Fig. 3-19-K to N).

Antisense *ADC* signals were observed in all manipulated root lines, except line II-27 (Fig. 3-19-P) which produced a reading that was slightly greater than background readings observed in controls (Fig. 3-19-R). A negative correlation between the levels of antisense *ADC* transcript and the endogenous *ADC* transcript was observed in most of the manipulated lines. For example, line II-27 had a very low level of antisense *ADC* transcript that was similar to the background level seen in controls (Fig. 3-19-R), and possessed a level of endogenous *ADC* transcript comparable to that of controls (Fig. 3-19-I). In comparison, lines II-11, II-4, II-32, II-30, II-34, II-39 and II-26 had high levels of antisense *ADC* transcript (Fig. 3-19-R), but low levels of the endogenous transcript (Fig. 3-19-I). In contrast to these general observations, however line II-21 had a normal level of endogenous *ADC* transcript (Fig. 3-19-I) despite having a rather high level of the antisense transcript (Fig. 3-19-R).

I.

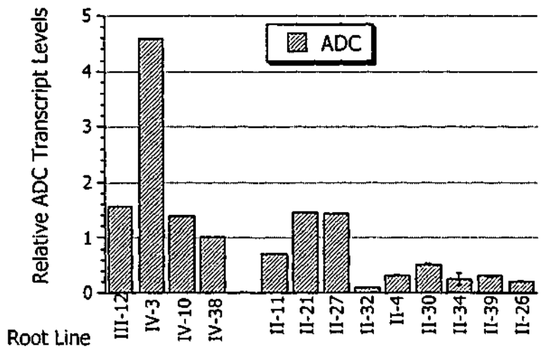

J.

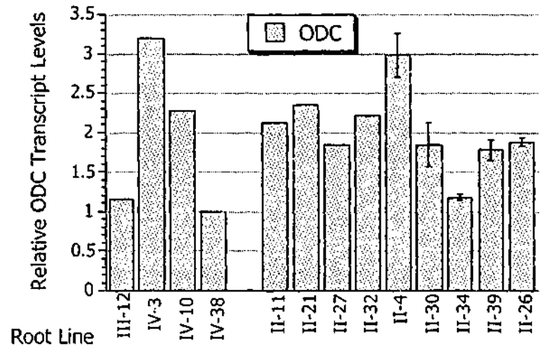

K.

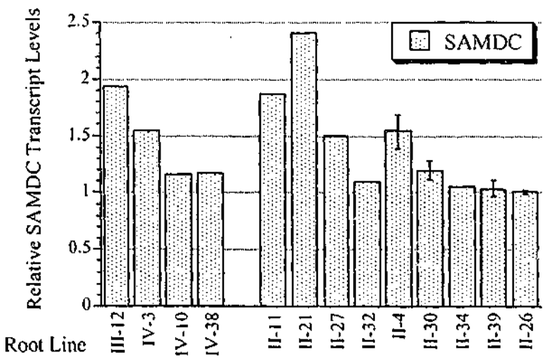

L.

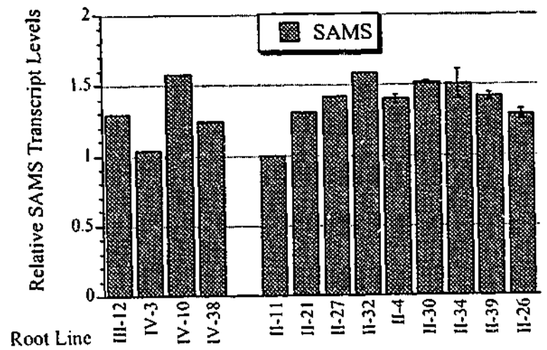

M.

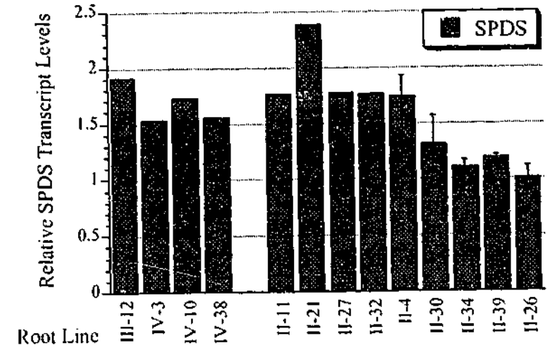

N.

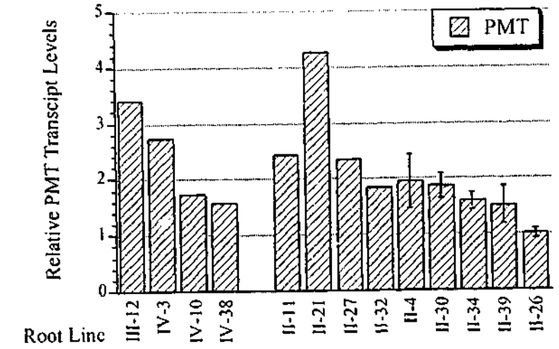

Fig. 3-19 (I to N) Relative transcript level of *ADC*, *ODC*, *SAMDC*, *SAMS*, *SPDS* and *PMT* illustrated in histograms. Levels of transcripts were quantified relative to the levels of *UBIQUITIN* transcripts in each lane. The lowest relative level of each transcript was assigned a value of 1, except panel I in which the relative *ADC* transcript level of 1 was assigned to line IV-38; the control root line that possessed the lowest transcript level. Histograms of lines II-4, II-30, II-34, II-39 and II-26 represent the mean relative transcript level (±s.e.) of duplicate samples whilst the remaining histograms represent that of single sample.

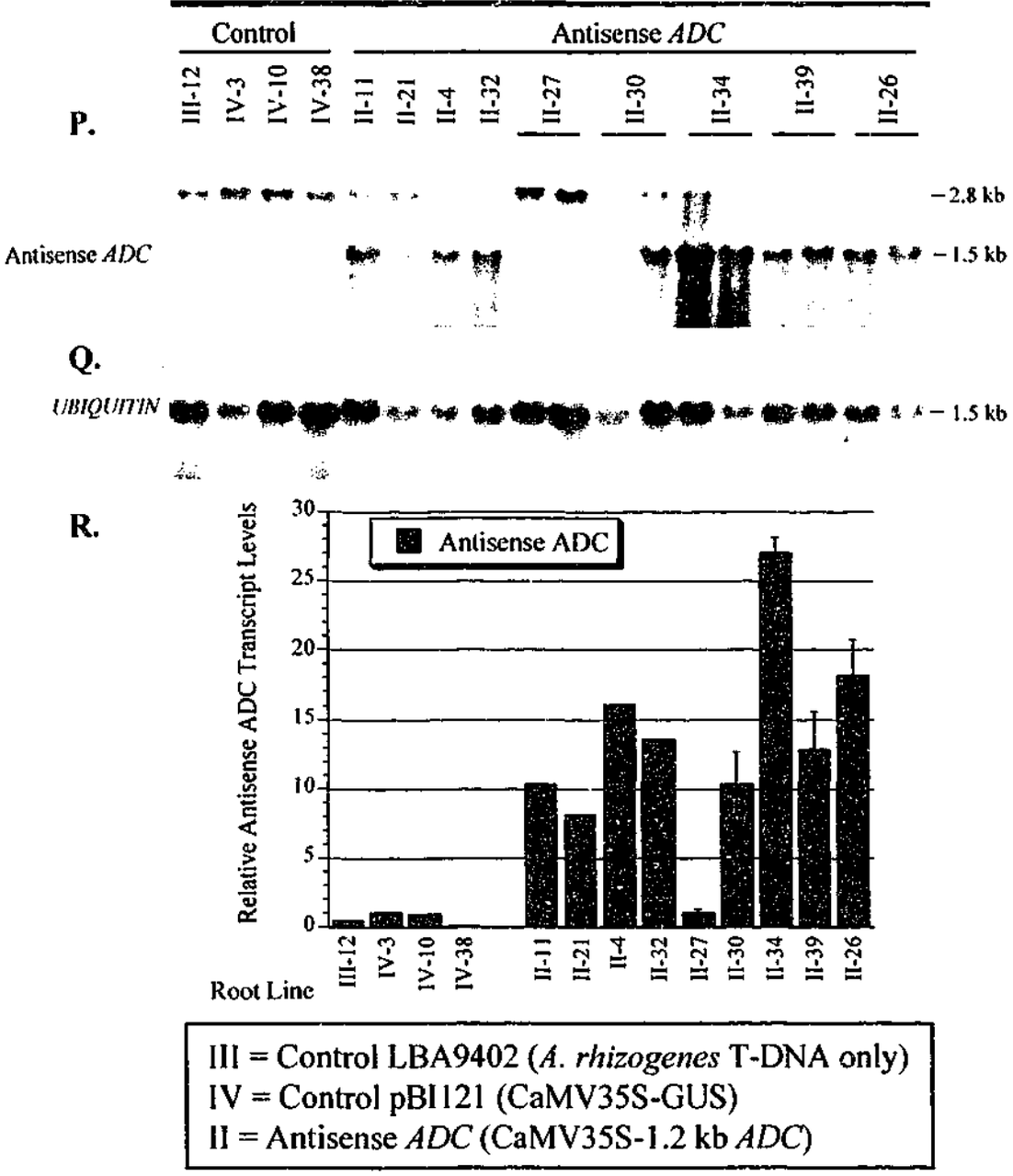

Fig. 3-19 (O) RNA gel blot run parallel with Fig. 3-19-A. (P) The blot was probed with sense strand DNA of 1.2 kb *ADC* fragment synthesised by asymmetric PCR to detect an antisense transcript of the introduced *ADC* fragment as a hybridisation band in the size range of 1.5 kb. Endogenous *ADC* transcripts were also detected as a hybridisation band in the size range of 2.8 kb, however, since traces of the antisense strand probe were synthesised in the asymmetric PCR. (Q) The blot was stripped and reprobed with a double-stranded DNA fragment of *UBIQUITIN*. (R) Relative antisense *ADC* transcript levels are illustrated in histograms. As mention in Fig. 3-19- I to N, levels of transcripts were quantified relative to the levels of *UBIQUITIN* transcripts in each lane. The lowest relative level of the transcript detected in antisense lines (II-27) was assigned a value of 1. Histograms of lines II-27, II-30, II-34, II-39 and II-26 represent the mean (±s.e.) relative transcript level of duplicate samples, whilst the remaining samples represent those from a single sample. The relative antisense *ADC* transcript levels in control lines III-12, IV-3 and IV-10 represent background reading obtained after quantification using the Image Quant system.

3.2.2.4 Screening of transformed root lines for ADC *activity*

Six antisense *ADC* lines possessing low levels of endogenous *ADC* transcript, (II-32, II-4, II-30, II-34, II-39 and II-26), together with another two antisense *ADC* lines not previously analysed for *ADC* transcript levels (II-7 and II-35) and three controls (III-12, IV-3 and IV-9) were analysed for ADC activity. The histograms in Fig. 3-20 show the mean ADC activity at day 14 of the growth cycle.

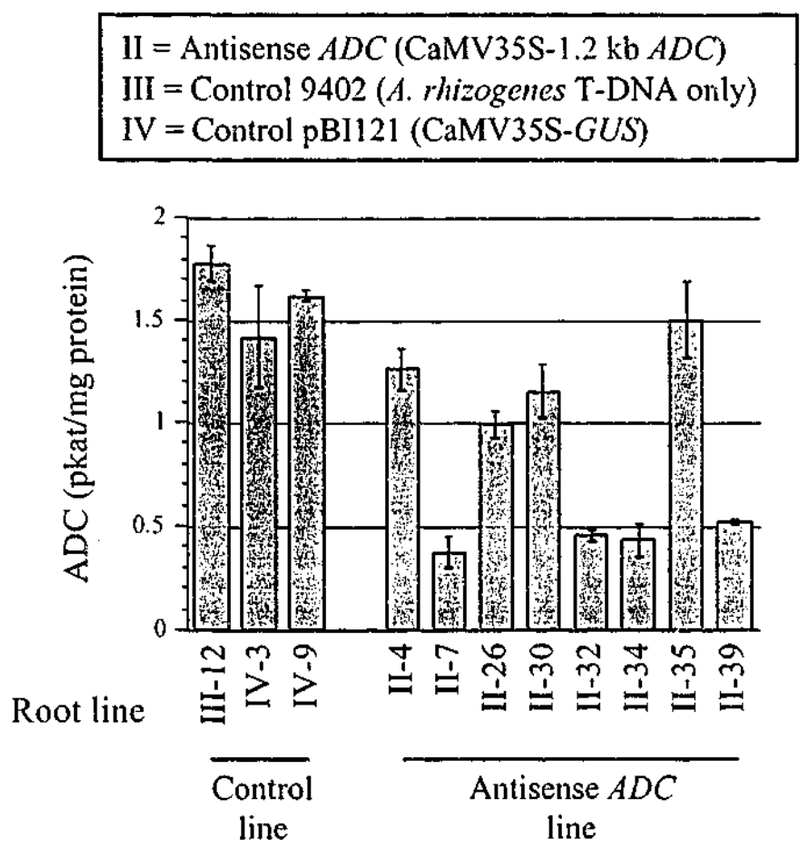

Fig. 3-20 ADC activities were determined from root tissues harvested from duplicate culture vessels at day 14 of the growth cycle. The extract from each vessel was subjected to duplicate samples for the enzyme assay. Each histogram represents the mean ADC activity (± s.e.).

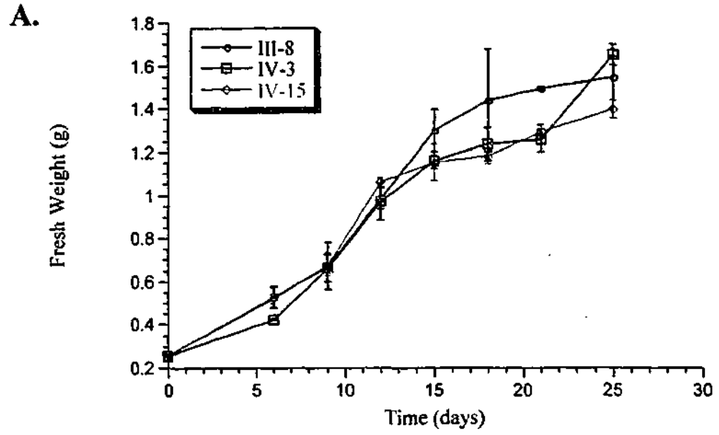

III = Control LBA9402 (*A. rhizogenes* T-DNA only)
IV = Control pBI121 (CaMV35S-*GUS*)
II = Antisense *ADC* (CaMV35S-1.2 kb *ADC*)

Fig. 3-21 Growth curves of controls (A) and 1.2 kb antisense *ADC* root lines (B) over a 25 day period. Each data point represents the mean (±s.e.) fresh weight (g) of four samples (or two samples for line III-8) harvested at days 6, 9, 12, 15, 18, 21 and 25 of the growth cycle.

One-way ANOVA revealed a significant difference between the ADC activity of the antisense root lines and the control group ($P < 0.05$). Mean activity of ADC in the three control lines was 1.61 pkat/mg protein (Std. Dev. = 0.23). When ADC activity in individual manipulated lines was compared with the mean ADC activity in the control group, a Dunnett's statistical test showed significant differences ($P < 0.05$) between the average activity observed in the controls and the activity of several antisense lines, namely lines II-7, II-26, II-32, II-34 and II-39. Four of these antisense lines (II-7, II-32, II-34 and II-39) had ADC activity which was less than 30% of control values (Fig. 3-20). Among the root lines analysed, line II-7 exhibited lowest ADC activity and was only 20% of the mean ADC activity exhibited by controls. This finding is similar to the report of Watson *et al.* (1998) in which an *ADC* mutant of *A. thaliana* was isolated and found to exhibit low activity of ADC, which was only 18% of the activity of wild type. It is perhaps noteworthy that none of the antisense *ADC* root lines analysed in this study had close to zero ADC activity, possibly due to the essential nature of this enzyme for the growth of plant tissues (Martin-Tanguy, 1997).

3.2.3 Detailed analysis of selected 1.2 kb antisense *ADC* root lines

3.2.3.1 Growth, nicotine and anatabine profiles

As was noted in Fig. 3-18, preliminary analysis of 1.2 kb antisense *ADC* root lines suggested a slight reduction in the nicotine content of some transformants. To examine the relationship between ADC activity and alkaloid content further, a detailed analysis was undertaken on three selected lines with low *ADC* transcript levels and ADC activities (II-32, II-34 and II-39) to examine nicotine content throughout the growth cycle. In addition, line II-26 was analysed. This line possessed reduced *ADC* transcript levels compared to those of controls (Fig. 3-19-I), however ADC activity in this line was closer to that which was typical of controls (Fig. 3-20).

For practical purposes, the experiment was set up as two parallel groups on successive days. Group one was composed of control root line IV-3 and antisense root line II-26 and II-32, whilst group two consisted of control root line III-12 and IV-15 as

well as antisense root line II-34 and II-39. Apart from the setting up and harvesting dates which were one day apart, all other conditions, such as the batch of media used, the growth environment and the time points used for harvest were exactly the same.

Growth of three control and four antisense *ADC* root lines was analysed at three day intervals (except for the last time point) from day 6 to day 25 of the growth cycle. At each time point the fresh weight of four replicate samples of the root lines were determined (except line III-8 of which the fresh weight was determined from duplicate samples). Analysis of data showed that control and 1.2 kb antisense *ADC* transformed root lines grew at similar rates as each other (Fig. 3-21-A and B). The growth pattern of each line was composed of an initial lag phase, lasting about five days, a period of rapid growth in the mid phase lasting about ten days, and a slower phase (*ca* 10 days) toward the end of the cycle.

Alkaloid content of the root lines was determined from the tissues at each time point (Fig. 3-22). Nicotine levels of controls were in the range 1500 µg/g fwt – 5800 µg/g fwt throughout the growth cycle, whereas nicotine in 1.2 kb antisense *ADC* lines ranged from 1100 µg/g fwt – 4200 µg/g fwt. Most of the root lines seemed to have the highest nicotine accumulation at day 21.

Closer examination of the data showed that whilst the nicotine content of all 1.2 kb antisense *ADC* root lines analysed at days 6 to 15 was quite comparable to that of controls, there was a reduced capacity in all four antisense lines to accumulate the high levels of nicotine typically found in control tissues during the latter phase of the growth cycle. This difference was most marked in lines II-26 and II-34 with levels of nicotine reaching a maximum of about 4000 µg/g fwt, compared to 5200 µg/g fwt – 5800 µg/g fwt in control tissues (Fig. 3-22).

The other main pyridine alkaloid produced by *N. tabacum* transformed roots is anatabine, being usually 10-20% of the total alkaloid pool (Hamill *et al.*, 1986; Parr and Hamill, 1987). Analysis of anatabine levels in 1.2 kb antisense *ADC* lines was also undertaken to determine whether any difference existed between the levels of this alkaloid in antisense *ADC* lines and controls (also Chapter 4). Data presented in Fig. 3-

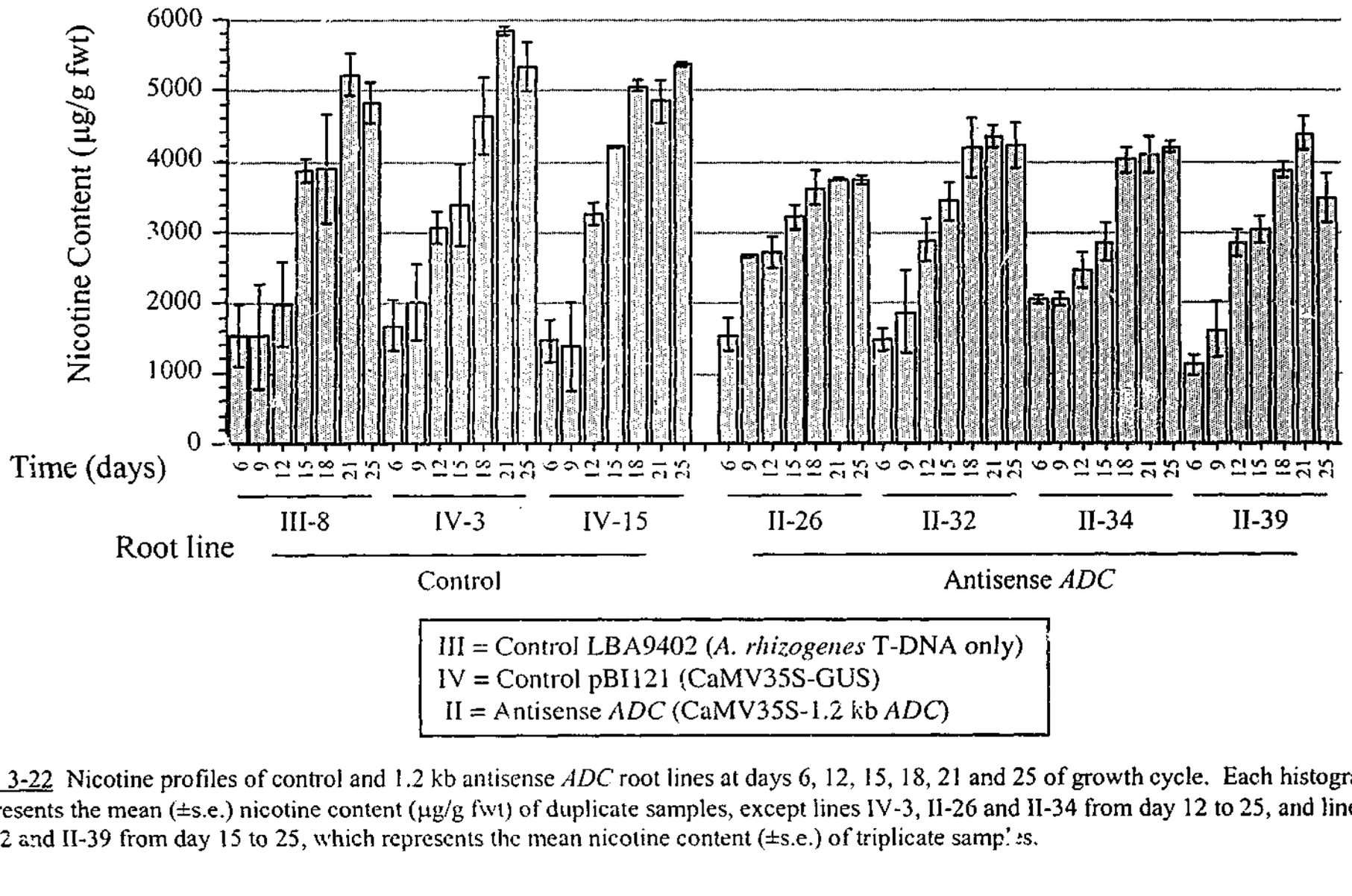

Fig. 3-22 Nicotine profiles of control and 1.2 kb antisense *ADC* root lines at days 6, 12, 15, 18, 21 and 25 of growth cycle. Each histogram represents the mean (±s.e.) nicotine content (µg/g fwt) of duplicate samples, except lines IV-3, II-26 and II-34 from day 12 to 25, and lines IV-15, II-32 and II-39 from day 15 to 25, which represents the mean nicotine content (±s.e.) of triplicate samples.

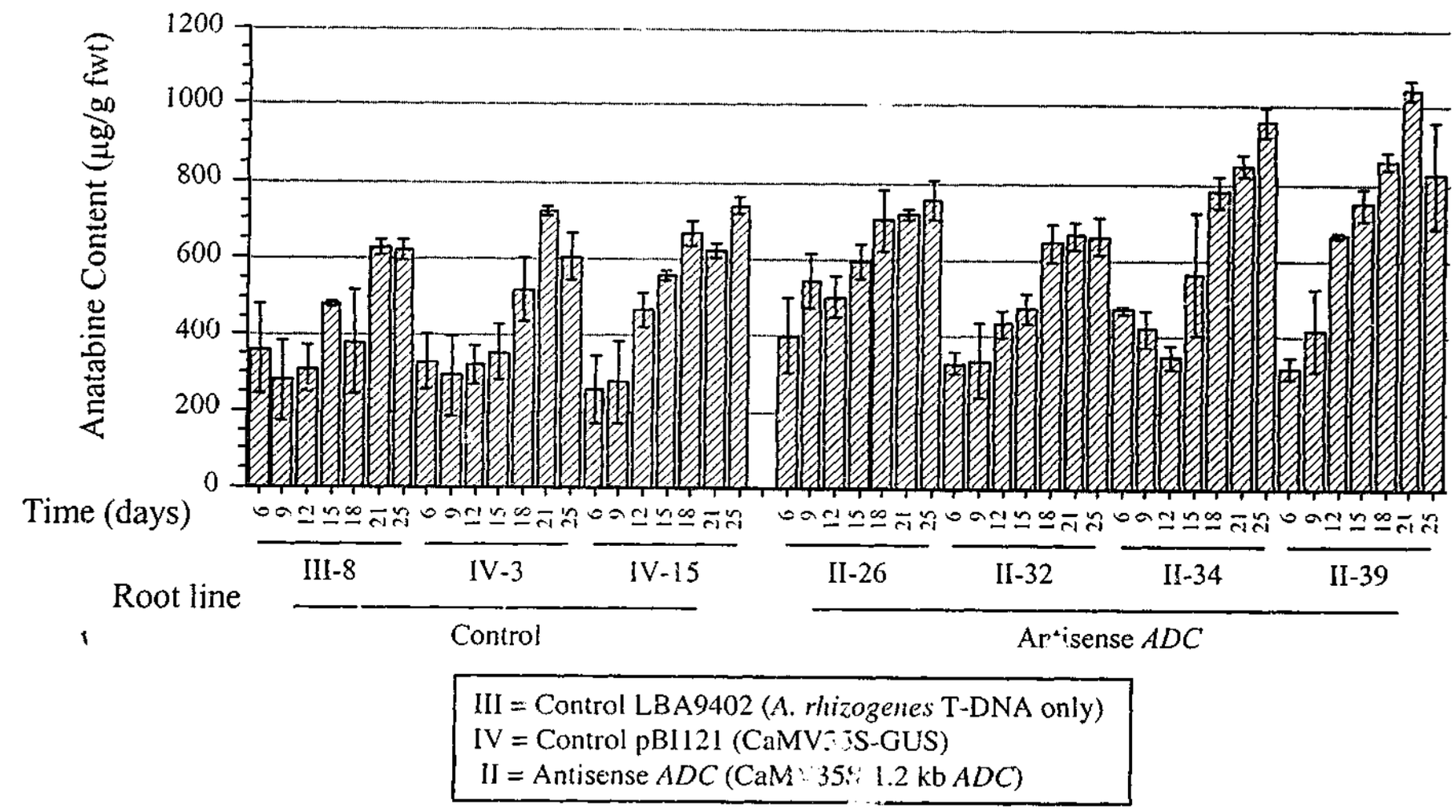

Fig. 3-23 Anatabine profiles of control and 1.2 kb antisense *ADC* root lines at days 6, 12, 15, 18, 21 and 25 of growth cycle. Each histogram represents the mean (±s.e.) anatabine content (µg/g fwt) of duplicate samples, except lines IV-3, II-26 and II-34 from day 12 to 25, and lines IV-15, II-32 and II-39 from day 15 to 25, which represents the mean anatabine content (±s.e.) of triplicate samples.

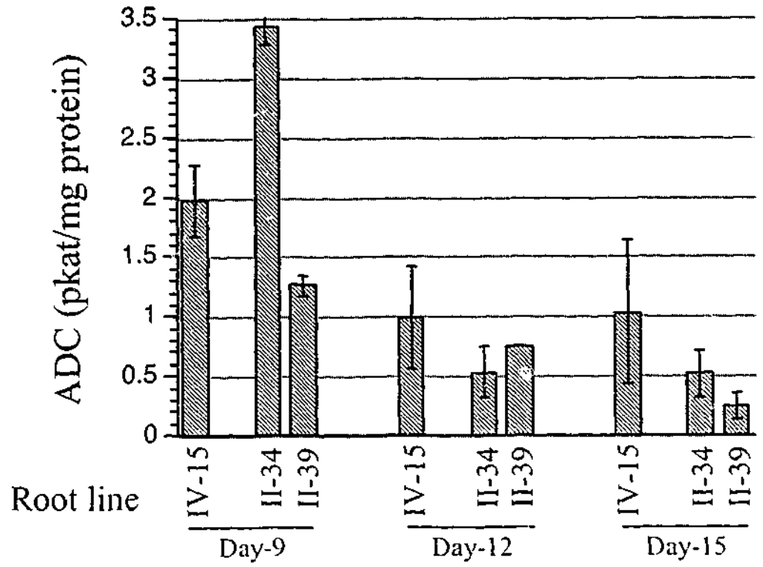

Fig. 3-24 The ADC activity of a control root line, IV-15, and 1.2 kb antisense *ADC* root lines, II-34 and II-39, at days 9, 12 and 15 of the growth cycle. Each histogram represents the mean (±s.e.) ADC activity (pkat/mg protein) of duplicate samples, except line II-39 at day 12.

IV = Control pBI121 (CaMV35S-GUS)
II = Antisense *ADC* (CaMV35S-1.2 kb *ADC*)

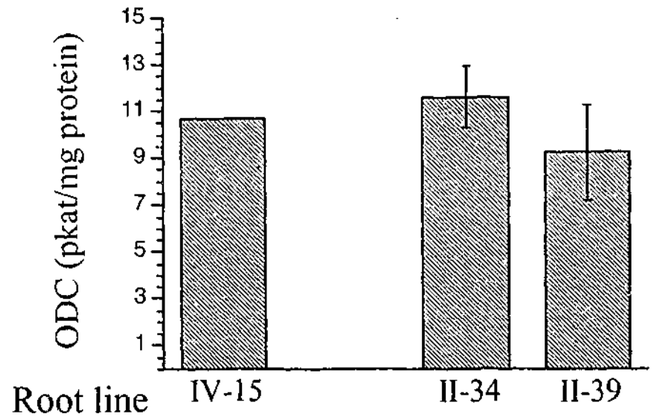

Fig. 3-25 The ODC activity of a control root line, IV-15, and 1.2 kb antisense *ADC* root lines, II-34 and II-39, at day 9 of the growth cycle. Each histogram represents the mean (±s.e.) ODC activity (pkat/mg protein) of duplicate samples, except line IV-15.

23 show mean levels of anatabine in the range of 250 µg/g fwt – 720 µg/g fwt for control lines with a slightly higher range being observed in 1.2 kb antisense *ADC* lines (300 µg/g fwt – 1020 µg/g fwt).

Relative to levels found in control tissues, a slight increase in anatabine levels was most noticeable in two lines (II-34 and II-39), with levels reaching about 900 µg/g fwt – 1000 µg/g fwt at days 21 to 25 of culture as opposed to about 700 µg/g fwt in control tissues. However, anatabine levels in lines II-26 and II-32 were not noticeably different from controls.

3.2.3.2 ADC activity during the growth cycle

ADC activity in a control root line, IV-15, together with 1.2 kb antisense *ADC* root lines, II-34 and II-39, at days 9, 12 and 15 of the growth cycle were determined (Fig. 3-24). Using the same protein extract, the ODC activities in root tissues at day 9 were also determined (Fig. 3-25).

In the present study of *N. tabacum* transformed roots, levels of ADC activity in controls are comparable with results previously reported in transformed roots of *N. rustica* (Hamill *et al.*, 1990). In that study, Hamill *et al.* (1990) reported ADC activities in control transformed *N. rustica* root lines of approximately 3 pkat/mg protein at day 7 of the growth cycle. In the present study, the average ADC activity of control lines at day 9 of growth was in the range of 1 pkat/mg protein – 2 pkat/mg protein (Fig. 3-24). In this study, the majority of root lines transformed with the 1.2 kb antisense *ADC* fragment exhibited activities in the range of 0.3 pkat/mg protein –1.3 pkat/mg protein. One antisense line, II-34, when analysed at day 9 of the growth cycle, however, possessed an ADC activity of 3.4 pkat/mg protein.

Over the course of the growth cycle, activities of ADC in the control root line (IV-15) and the antisense *ADC* root lines (II-34 and II-39) were found to be highest during the early phase of growth (Fig. 3-24). Such a pattern is also consistent with the activity of ADC in *N. rustica* root cultures transformed with either the *yODC* or *CAT* genes as reported by Hamill *et al.* (1990).

A.

Plant line IV-3 II-39 II-26

B.

Plant line IV-15 II-26 II-32

IV = Control pBI121 (CaMV35S-*GUS*)
II = Antisense *ADC* (CaMV35S-1.2 kb *ADC*)

C. IV-3 D. II-39

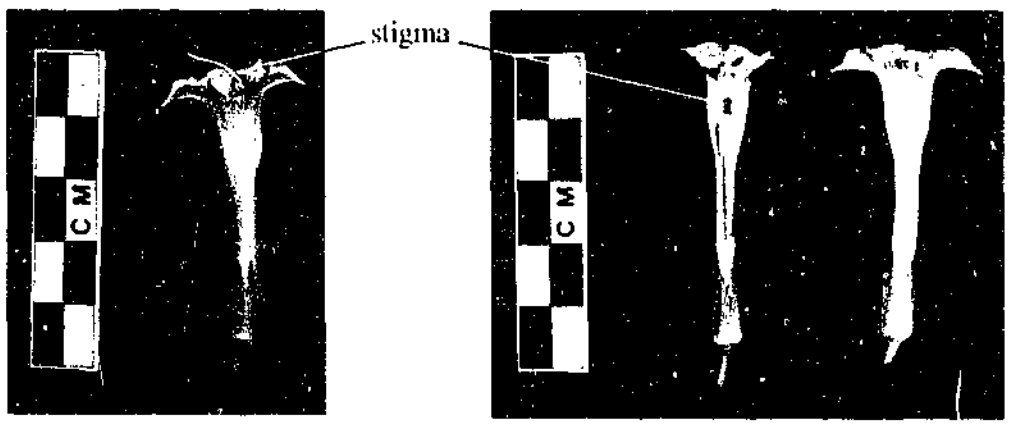

Fig. 3-26 Phenotype of regenerants.

(A and B) 1.2 kb antisense *ADC* plant lines II-26, II-32 and II-39 as well as control lines IV-3 and IV-15 were regenerated from root lines and grown under identical green house conditions. All regenerants exhibited wrinkled leaves and reduced internodal distances.

(C and D) Differences in the length of styles and filaments relative to flower tubes occur between the control, IV-3 and the 1.2 kb antisense *ADC* line, II-39. The control IV-3 has a longer style which lift the stigma above the flower tube, whereas line II-39 has longer filament lifting anthers above the flower tube.

Despite the variation in ADC activity among root lines IV-15, II-34, and II-39 harvested at day 9 of growth, the ODC activity of these tissues remained similar across all three lines (Fig. 3-25) and the absolute values were comparable to those reported by Hamill *et al.* (1990). In that report, ODC activities in control cultures of *N. rustica* roots were observed to range between 10 pkat/mg protein to 22 pkat/mg protein (Hamill *et al.*, 1990), whilst in the present study ODC activities were found to be approximately 10 pkat/mg protein in all lines. Therefore, together with the Northern data presented in Fig. 3-19-J, it seems likely that decreased activity of ADC, due to expression of a 1.2 kb antisense *ADC* fragment, does not markedly alter expression of ODC in *N. tabacum* root lines when measured at the levels of transcript accumulation (Fig. 3-19-J) and enzyme activity (Fig. 3-25). In addition, effects of this down-regulation upon the expression of genes in associated areas of polyamine metabolism appear to be minimal (Figs. 3-19-K to 3-19-N). These results contrast with the observation of Capell *et al.* (2000) who reported that rice cell lines transformed with oat *ADC* cDNA in an antisense orientation under the control of the CaMV35S promoter, exhibited down-regulation of both ADC and ODC activities, compared to wild type and controls transformed only with the selectable marker (*htp*). In that study, eight out of twelve lines showed a significant reduction in endogenous ADC activity, although it is worth noting that only three of these eight lines exhibited a corresponding reduction in activity of ODC (Capell *et al.*, 2000).

3.2.4 Plants regenerated from 1.2 kb antisense *ADC* root lines

To determine whether the expression of 1.2 kb *ADC* fragment in the antisense orientation had any obvious effect on growth, morphology and nicotine content of intact plants grown in soil, plants were regenerated from transformed root lines as described in Chapter 2. Antisense *ADC* root lines, II-26, II-32 and II-39, and the control root lines, III-8, IV-3 and IV-15 produced plantlets when roots were cultured on regeneration medium. Rooted plants of 3-4 cm in height were transferred to soil and grown under identical conditions in a PC2 greenhouse as described in Chapter 2.

All regenerated plants, control and antisense 1.2 kb *ADC* lines, were healthy and grew vigorously in soil. All plants exhibited shorter internode and slight wrinkling of leaf tissue compared to seed derived plants of var. NC95 (Fig. 3-26-A and B). This phenotype (T phenotype) is typical of plants containing Ri T-DNA (Tepfer, 1984). No clear difference in vegetative phenotype between controls and *ADC* antisense transformants was apparent.

One different feature between the regenerant control IV-15 and the 1.2 kb antisense *ADC* line II-39 was observed in the reproductive organs. The flower of the control IV-15 was 4.1 cm in length, whilst that of the 1.2 kb antisense *ADC* line II-39 was slightly longer at 4.4 cm. However, the relative length of the style and the filament of both flowers was quite different. The control IV-15 had short filaments (3.6 cm) and a longer style (3.9 cm) which lifted the stigma above the corolla (Fig. 3-26-C). In contrast, the 1.2 kb antisense *ADC* line II-39 had a short style (3.6 cm) and longer filaments (4.3 cm) lifting anthers above the corolla (Fig. 3-26-D).

As has been noted, during the late phase of root culture growth, significant differences were noted in the alkaloid content between the 1.2 kb antisense *ADC* root lines, II-26, II-32, and II-39, and the control root lines (Fig. 3-22 and Fig. 3-23). When regenerated into plants however, no such differences were apparent between the antisense and control lines. Plants regenerated from the control root lines possessed nicotine and anatabine titres within the range of 1300 µg/g fwt – 2200 µg/g fwt and 80 µg/g fwt – 140 µg/g fwt, respectively (Fig. 3-27). The alkaloid titres of the antisense regenerants were similar, and ranged between 1200 µg/g fwt – 2200 µg/g fwt for nicotine and 140 µg/g fwt – 220 µg/g fwt for anatabine, respectively. A Dunnett's statistical test indicated that none of the 1.2 kb antisense *ADC* lines were significantly different from the control group with respect to nicotine or anatabine levels.

A.

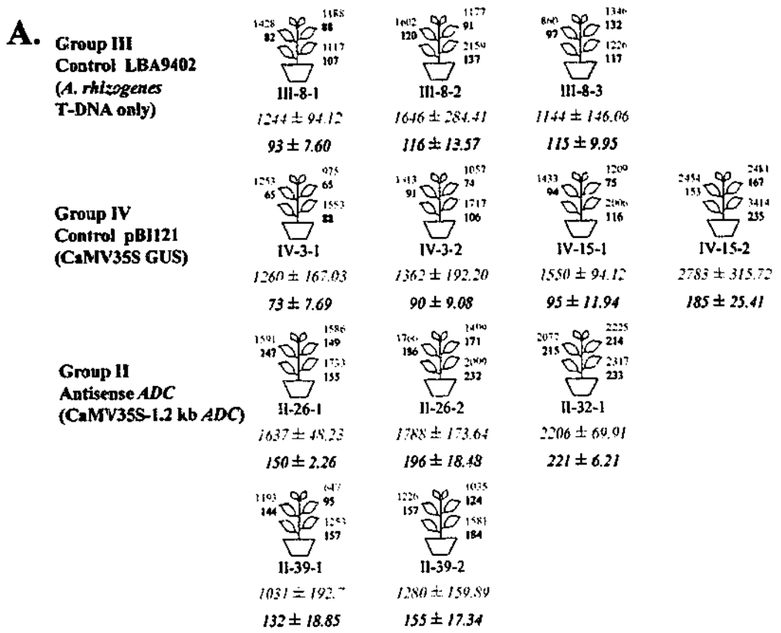

B.

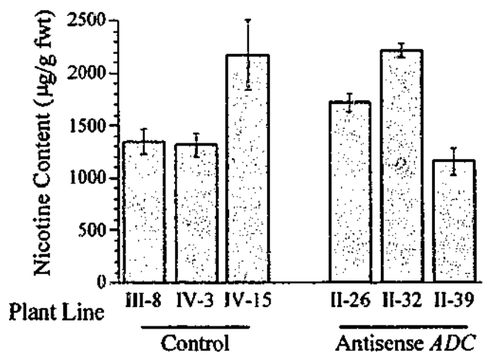

C.

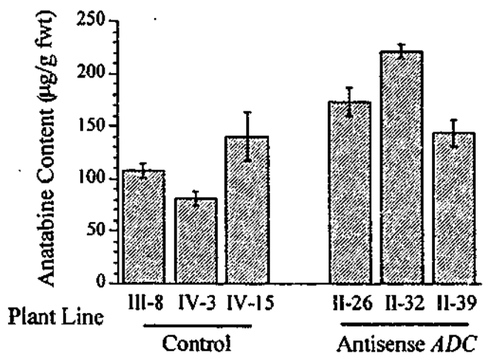

Fig. 3-27 (A) Schematic representation of plants regenerated from 1.2 kb antisense *ADC* root lines showing leaf-specific alkaloid titres. The numbers following each line represents the number of samples. Nicotine and anatabine titres of leaves numbered 6, 7 and 8 from the apex are illustrated in red and blue, respectively. Mean (±s.e.) titres of nicotine (µg/g fwt) and anatabine (µg/g fwt) from these leaves on each plant are presented under the icons. The average nicotine content (±s.e.) (B) and the average anatabine content (±s.e.) (C) per line are presented as histograms.

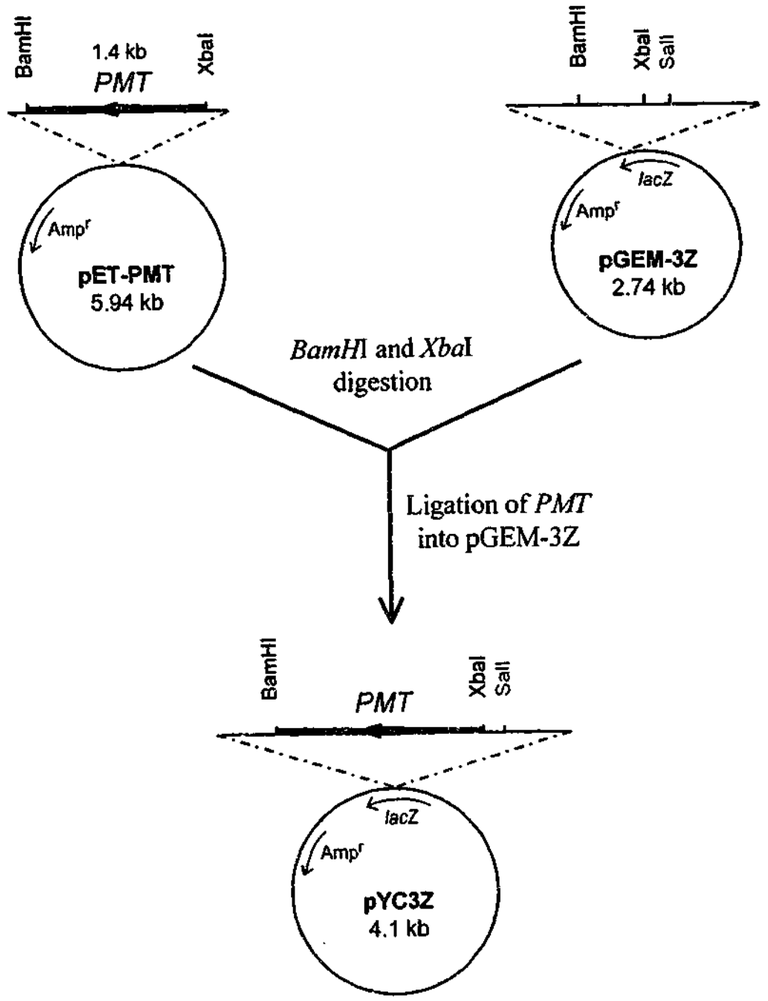

Fig. 4-1 **Construction of pYC3Z.** *PMT* in the pET-PMT was excised and ligated into pGEM-3Z at *Bam*HI and *Xba*I sites. Blue arrows indicate orientation 5'→ 3' of the *PMT* coding sequence. (Only selected restriction sites in the plasmids are illustrated.)

Chapter 4

Effects of Down-regulating PMT in *N. tabacum*.

4.1 Binary vector construction and transformation of bacteria

The purpose of experiments to be described in this section was to generate transgenic tissues of *N. tabacum* expressing *PMT* in an antisense orientation with the aim of studying effects upon their alkaloid composition and growth characteristics. The coding sequence of *PMT* (Hibi *et al.*, 1994) was kindly supplied by Assoc. Professor T. Hashimoto in a pET vector. It was not possible to subclone the *PMT* sequence directly into the binary expression vector, pFIH10 (Hamill *et al.*, 1987a), in the antisense orientation due to the lack of convenient cloning sites. Thus, the *PMT* sequence was first subcloned into pGEM3Z prior to be being excised as a *Bam*HI/*Sal*I fragment of 1.4 kb and cloned into the pFIH10 plasmid.

4.1.1 Cloning *PMT* sequence from pET-PMT into pGEM3Z (Construction of pYC3Z)

The *PMT* coding sequence was cleaved from pET-*PMT* at *Xba*I and *Bam*HI sites. The excised fragment showed the expected size at 1.4 kb and was ligated into the unique *Xba*I and *Bam*HI sites of the vector pGEM3Z (Fig. 4-1). Plasmid was isolated from seven transformed *E. coli* colonies and six showed an insert of appropriate size. Digestion of the plasmid from one selected positive colony with various restriction enzymes and analysis by gel electrophoresis confirmed the presence of the insert, *PMT*. The resulting construct was designated pYC3Z.

4.1.2 Cloning *PMT* sequence from pYC3Z into pFIH10 (Construction of pYC3JR)

The *PMT* coding sequence was isolated from pYC3Z using *Bam*HI and *Sal*I restriction enzymes, ligated into the unique *Bam*HI and *Sal*I sites of pFIH10 which are

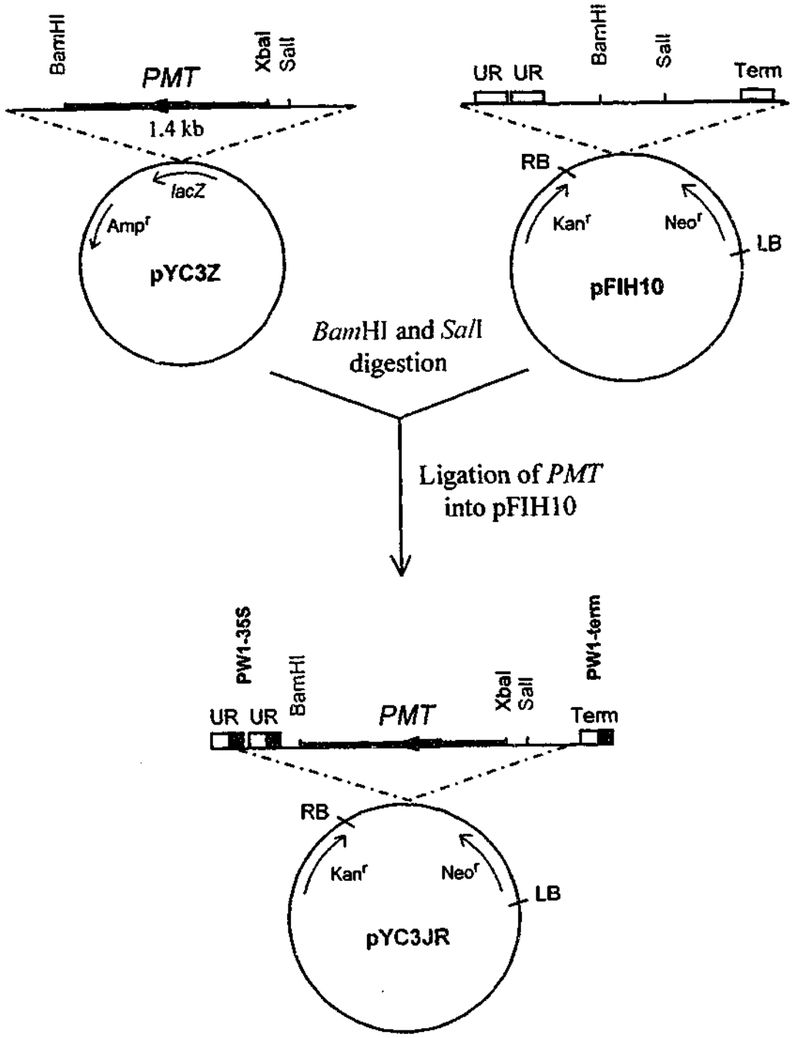

UR = Upsteam enhancer of CaMV35S promoter
Term = CaMV35S terminator

Fig. 4-2 **Construction of pYC3JR.** *PMT* was excised from pYC3Z and ligated into pFIH10 at *Bam*HI and *Sal*I sites. Blue arrows indicate orientation 5'→ 3' of the *PMT* coding sequence. (Only selected restriction sites in the plasmids are illustrated.) As pFIH10 is derived from pBIN19, Kan^r confers resistance to kanamycin in bacteria whilst Neo^r confers resistance to kanamycin in transgenic plant cells (Hamill *et al.*, 1987a).

located between the CaMV35S promoter and terminator sequences (Fig. 4-2) and transformed into *E. coli*. Bacterial colonies capable of growth on LB with kanamycin were screened for the presence of the *PMT* coding sequence by colony blot hybridisation. Of 107 colonies analysed, three produced a positive signal on an autoradiograph. The presence of *PMT* in these plasmids was confirmed by the colony-boil PCR procedure using primers PW1-35S and PW1-term which containing recognition sites within the CaMV35S promoter and the polyadenylation signal respectively. A colony containing a plasmid producing a band of the expected size was selected for further work and the plasmid was designated pYC3JR.

The orientation of the *PMT* coding sequence in pYC3JR was confirmed using restriction enzyme digestions and Southern blot hybridisation (Fig. 4-3 and Table 4-1). Digestion with *Bam*HI and *Sal*I yielded an expected 1.4 kb fragment representing the *PMT* sequence, whilst digestion with *Eco*RI yielded a 1.45 kb fragment which was consistent with the antisense orientation. In contrast, the sense-oriented fragment would have yielded a fragment of 0.3 kb when digested with *Eco*RI. As further confirmation, digestion with *Pst*I yielded a fragment hybridising to the *PMT* probe at 1.3 kb, as expected for plasmid containing antisense oriented *PMT*. An autoradiograph of the Southern blot probed with the *PMT* coding sequence confirmed the presence of the positive hybridisation signal of appropriate size in each digestion.

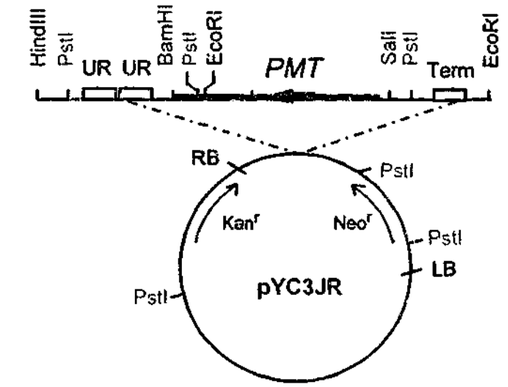

Fig. 4-3 Illustration of the selected restriction sites, *Bam*HI, *Sal*I, *Eco*RI, and *Pst*I, in pYC3JR which contains *PMT* coding sequence in the antisense orientation. Blue arrow indicates orientation 5'→ 3' of the *PMT* coding sequence.

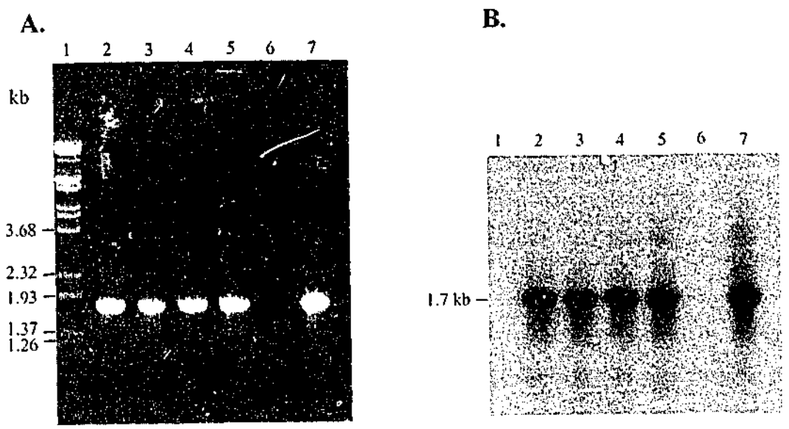

Lanes
1. DNA standard (λ -*Bst*EII digest)
2. to 5. Colony boiled PCR products from four single positive colonies of *A. rhizogenes* containing pYC3JR.
6. Colony boiled PCR product from a colony of wild type *A. rhizogenes* (negative control).
7. Colony boiled PCR product from a colony of *E. coli* containing pYC3JR (positive control).

Fig. 4-4 Preliminary analysis of pYC3JR in *A. rhizogenes*.

(A) Gel electrophoresis of the colony boiled PCR product of four single positive *A. rhizogenes* colonies containing pYC3JR, a negative control, and a positive control.
(B) Autoradiograph of the blot probed with *PMT* coding sequence from *N. tabacum*.

Table 4-1 Summary of the analysis of pYC3JR with restriction enzyme digestion and Southern blot hybridisation.

Restriction enzyme digestion	Expected size of band hybridised with *PMT* coding sequence (kb)	Band of expected size obtained	Interpretation
*Bam*HI and *Sal*I	1.4	✓	Presence of *PMT* coding sequence
*Eco*RI	1.45	✓	Presence of *PMT* coding sequence in the plasmid in antisense orientation
*Pst*I	1.3	✓	

4.1.3 Cloning of pYC3JR into *A. rhizogenes*

Plasmid pYC3JR was transformed into *A. rhizogenes* strain LBA9402 by triparental mating. Single *A. rhizogenes* colonies, growing on YMB medium containing kanamycin, were identified by screening for the presence of pYC3JR, using a colony boil PCR procedure and employing the primers PW1-35S and PW1-term as described previously. DNA bands at the size of about 1.7 kb were indicative of the presence of pYC3JR (Fig. 4-4a). An autoradiograph of a Southern blot, probed with the *PMT* coding sequence, showed strong hybridisation with these DNA molecules of about 1.7 kb (Fig. 4-4b).

The antisense orientation of the *PMT* sequence in *A. rhizogenes* was confirmed by restriction enzyme analysis of total DNA extracted from *A. rhizogenes* containing pYC3JR, followed by Southern hybridisation using ^{32}P-labelled *PMT* coding sequence as a probe (Fig. 4-5).

4.2 Establishment and preliminary analysis of transformed root lines containing antisense *PMT*

Seven groups of transformed root lines were established initially to assess the effects of introducing *PMT* sequence in an antisense orientation into *Nicotiana* following *A.*

A.

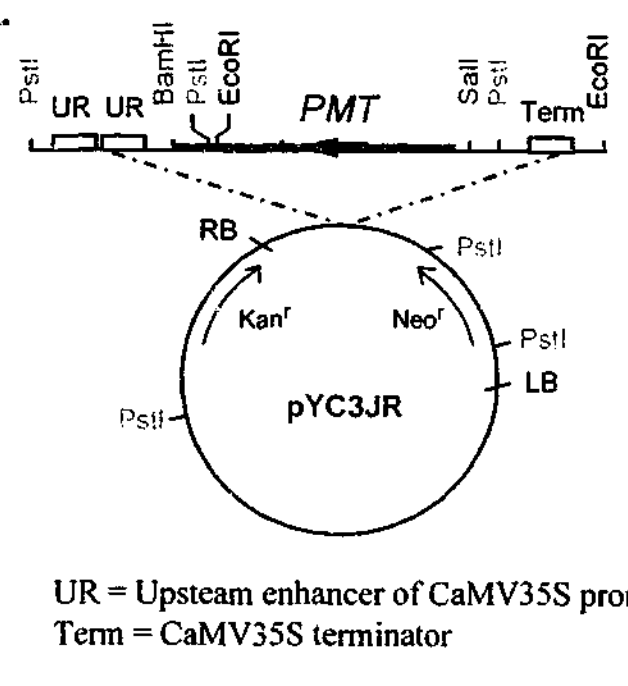

UR = Upsteam enhancer of CaMV35S promoter
Term = CaMV35S terminator

B.

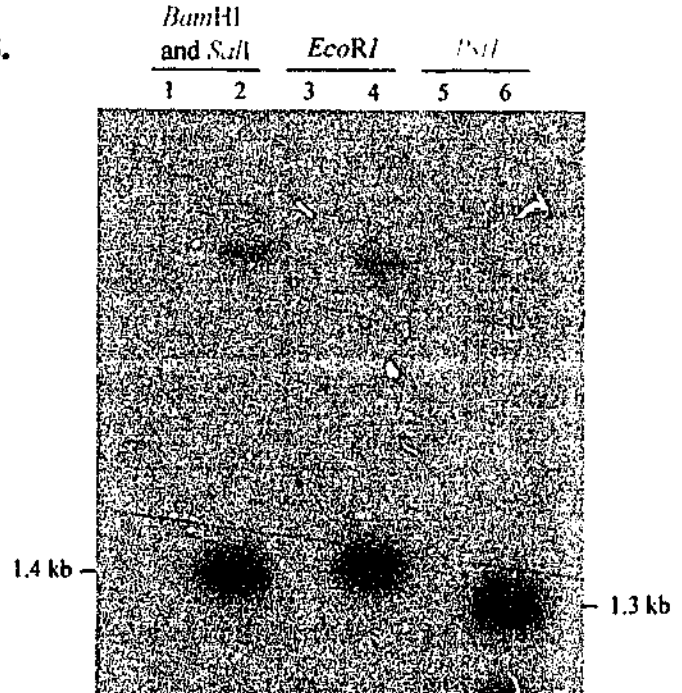

Lanes
1, 3 and 5 = Total DNA from *A. rhizogenes* containing pFIH10 digested with *Bam*HI + *Sal*I, *Eco*RI and *Pst*I, respectively (negative controls).
2, 4 and 6 = Total DNA from the positive colony of *A. rhizogenes* containing pYC3JR digested with *Bam*HI + *Sal*I, *Eco*RI and *Pst*I, respectively.

Fig. 4-5 Further analysis of pYC3JR in *A. rhizogenes*.
(A) Diagram of the construct pYC3JR showing useful diagnostic restriction sites. Blue arrow indicates orientation 5'→ 3' of the *PMT* coding sequence.
(B) Autoradiograph of the blot probed with *PMT* coding sequence.

rhizogenes infection of leaf tissues. The details of these transformed root lines are summarised in Table 4.2.

Table 4-2 Summary of properties of established root lines containing *PMT* sequence in an antisense orientation.

Root line	Plant species and variety	*A. rhizogenes*	Key feature
III	*N. tabacum* var. NC95	LBA9402	Control transformed root lines of high nicotine tobacco variety – without binary vector T-DNA.
IV	*N. tabacum* var. NC95	LBA9402 + pBI121	Control transformed root lines of high nicotine tobacco variety– with binary vector T-DNA (CaMV35S-GUS)
V	*N. tabacum* var. NC95	LBA9402 + pYC3JR	CaMV35S - antisense *PMT* transformed root lines of high nicotine tobacco variety
VI	*N. tabacum* var. LAFC 53	LBA9402 + pBI121	Control transformed root lines of low nicotine tobacco variety with binary vector T-DNA (CaMV35S-GUS)
IX	*N. tabacum* var. LAFC 53	LBA9402 + pYC3JR	CaMV35S - antisense *PMT* transformed root lines of low nicotine tobacco variety
XI	*N. sylvestris*	LBA9402 + pBI121	Control transformed root lines of *N. sylvestris* with binary vector T-DNA (CaMV35S-GUS)
XII	*N. sylvestris*	LBA9402 + pYC3JR	CaMV35S - Antisense *PMT* transformed root lines of *N. sylvestris*

4.2.1 Analysis of alkaloid content by HPLC

The main pyridine alkaloids produced by *Nicotiana* species, which are available commercially, are nornicotine, anabasine and nicotine. The retention times of authentic alkaloid standards, nornicotine, anabasine and nicotine, in a 50% methanol running buffer, were 7.15, 8.37 and 14.9 mins, respectively (Fig. 4-6).

In most varieties of *N. tabacum*, levels of nornicotine are very low, due to breeding programs aimed at reducing the capacity of plants to produce this alkaloid. Anabasine levels are usually also very low, being only 0.3-1.7% in both root and leaf tissues of *N. tabacum* analysed by Saitoh *et al.* (1985) and in leaf tissues of *N. tabacum* analysed by Sisson and Severson (1990). An additional alkaloid is anatabine which constitutes 10 -

20% of the alkaloid pool in *N. tabacum* leaves and also roots (Saitoh *et al.*, 1985; Parr and Hamill, 1987). Anatabine is not readily available from any commercial source. According to the data of Saunders and Blume (1981), the retention time of anatabine would be expected to be slightly greater than that of anabasine under the HPLC conditions used here.

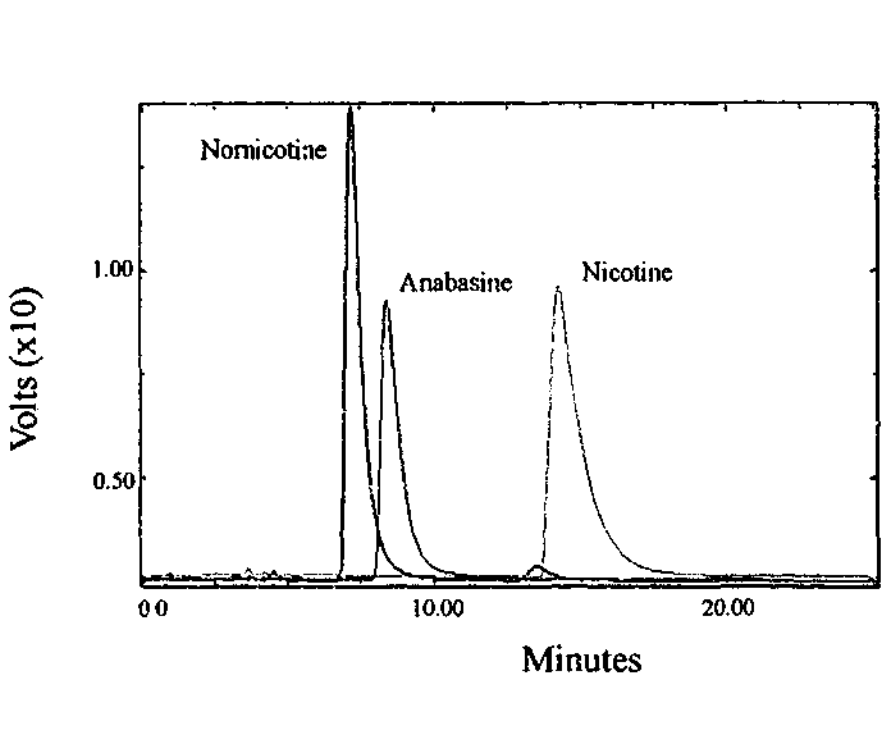

Fig. 4-6 HPLC chromatogram of standard nornicotine, anabasine, and nicotine which were run separately showed the retention times at 7.15, 8.37 and 14.9 minutes, respectively.

HPLC analysis of control root lines from NC95 and LAFC53 reveals qualitatively similar patterns, with the nicotine content of the high alkaloid variety NC95 being about three times that of the low alkaloid variety LAFC53 (Fig. 4-7-A). Initial analysis of antisense *PMT* transformed root lines of *N. tabacum* var. NC95 revealed a different profile from that which is characteristic of control lines. Fig 4-7-B illustrates a HPLC chromatogram, comparing a control root line of *N. tabacum* var. NC95 (IV-15) and one of these antisense *PMT* root lines of *N. tabacum* NC95, line V-26. The difference between the chromatograms of these lines is a substantial reduction of the nicotine peak in the antisense *PMT* line and a large increase in the peak of a second constituent at the RT 8.9 mins. A small peak at this time point was also detected in the control transformed root line generated from low nicotine producing tobacco, LAFC53 (Fig. 4-7-A). It was thought likely that this peak represented the alkaloid anatabine due to: a) its slightly different retention time (8.9 mins) (Fig. 4-7) from that of anabasine (8.4

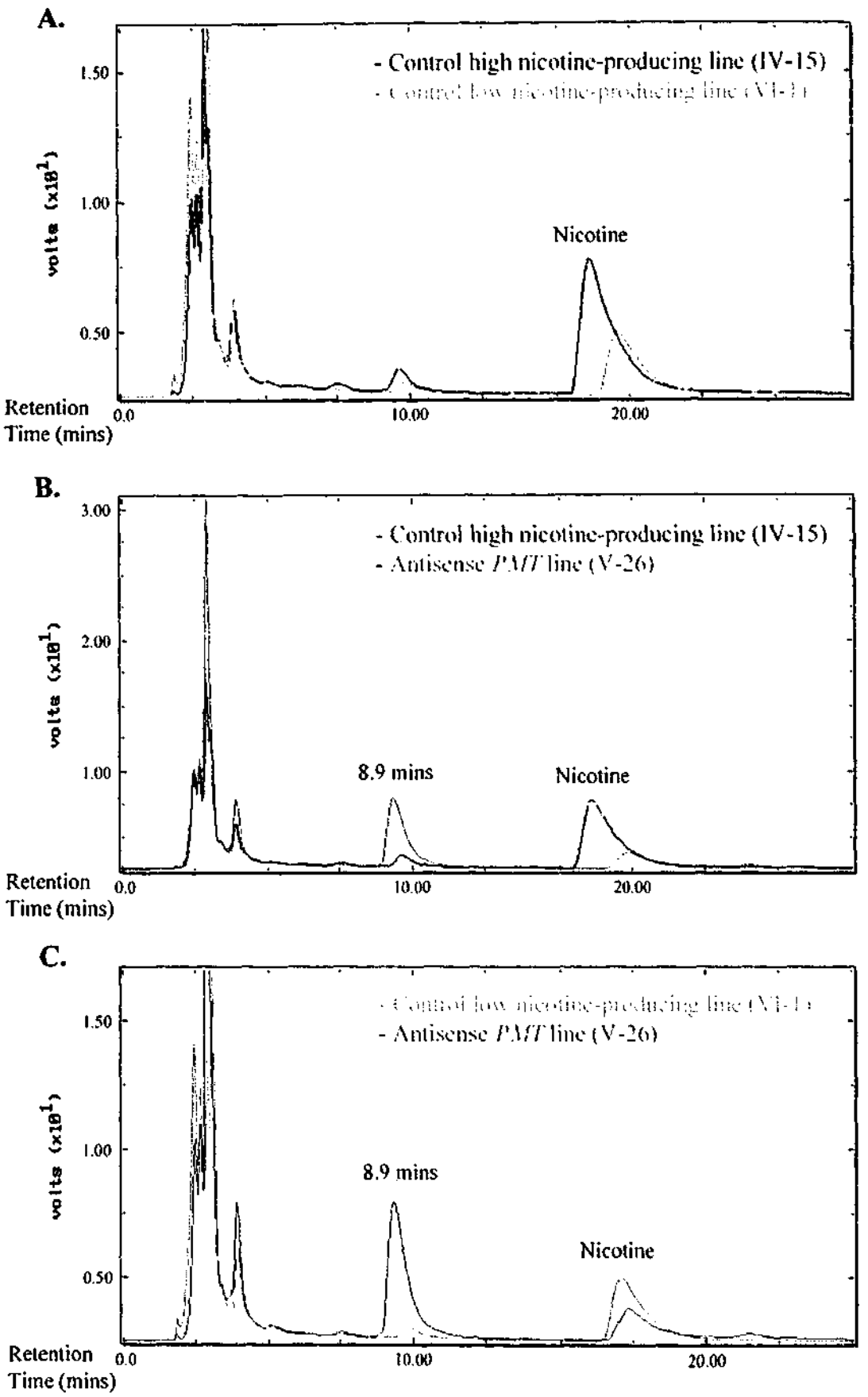

Fig. 4-7 Overlay HPLC chromatograms showing characteristic alkaloid patterns from various types of transformed root cultures.
(A) Control root lines, IV-15 and VI-1, generated from high and low nicotine-producing varieties of tobacco (*N. tabacum* NC95 and *N. tabacum* LAFC53), respectively.
(B) Control root line, IV-15, and antisense *PMT* root line, V-26, generated from a high nicotine-producing variety of tobacco (*N. tabacum* NC95).
(C) Antisense *PMT* root line, V-26, generated from a high nicotine-producing variety of tobacco (*N. tabacum* NC95), and a control root line, VI-1, generated from a low nicotine-producing variety of tobacco (*N. tabacum* LAFC53).

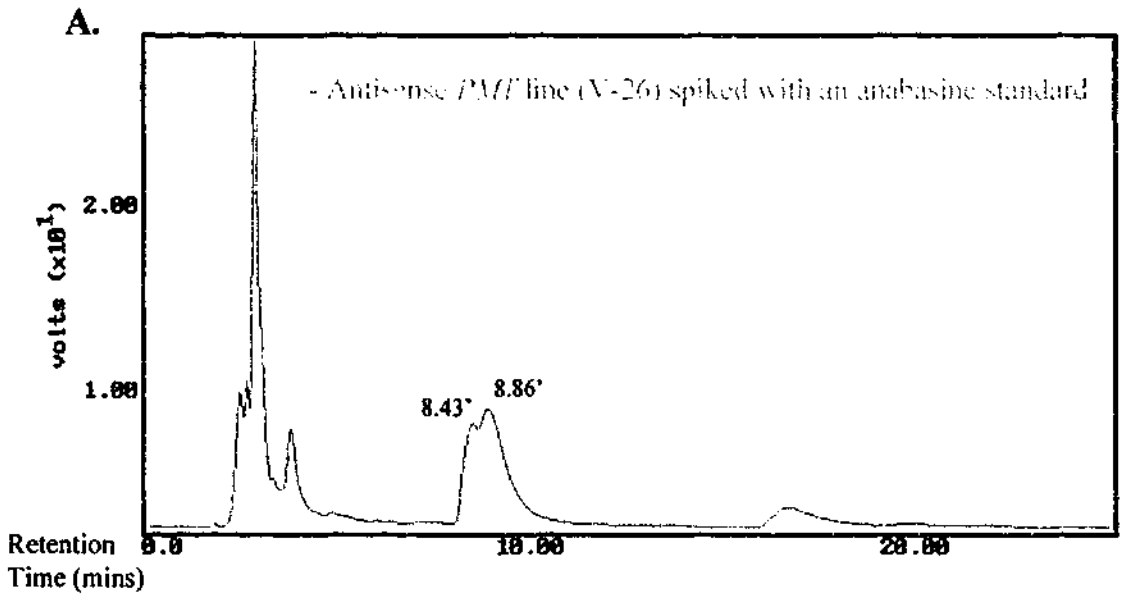

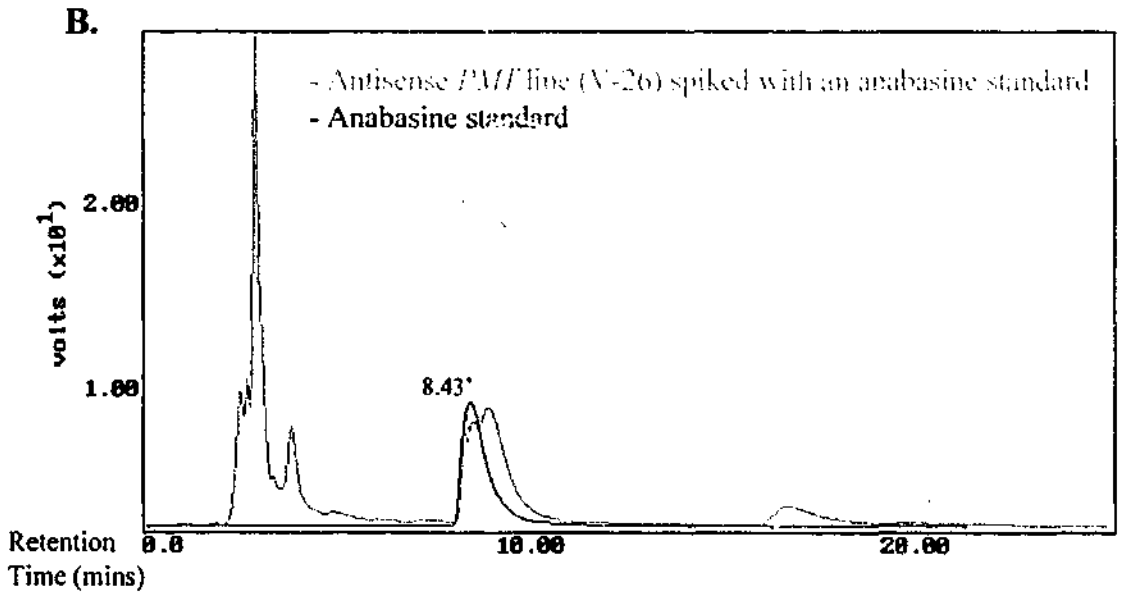

Fig. 4-8 (A) HPLC chromatogram of alkaloids extracted from the antisense *PMT* line V-26, spiked with an anabasine standard.

(B) The original chromatogram overlayed with the chromatogram of an anabasine standard.

mins) (Fig 4-6) and b) the observation that it was the second predominant alkaloid/metabolite present in root extracts of *N. tabacum*. However, as anabasine has a similar retention time (Fig. 4-6), it was deemed important to determine experimentally whether the 8.9 mins peak on the HPLC chromatogram was anabasine or anatabine. A sample of the antisense *PMT* root line extract (V-26) was spiked with anabasine standard and subjected to HPLC analysis. The chromatogram showed 0.43 minutes difference in the retention times of two peaks eluted at 8.43 and 8.86 mins (Fig. 4-8-A), whereas the anabasine standard alone produced only one peak at the earlier time point (Fig. 4-8-B). This result indicated that the 8.9 mins peak in the chromatogram, which was elevated in antisense *PMT* root lines relative to control tissues, was not anabasine.

The identity of this constituent was therefore suspected to be anatabine. An authentic standard of anatabine was obtained, after considerable searching for a supplier, from Dr. Patrick M. Lippiello and Dr Elisa Lovette (Pharmacology Laboratory Research & Development, RJ Reynolds Tobacco Company, USA). HPLC analysis showed that the authentic anatabine sample had a retention time corresponding to that of the elevated peak present in the antisense *PMT* lines (Fig. 4-9).

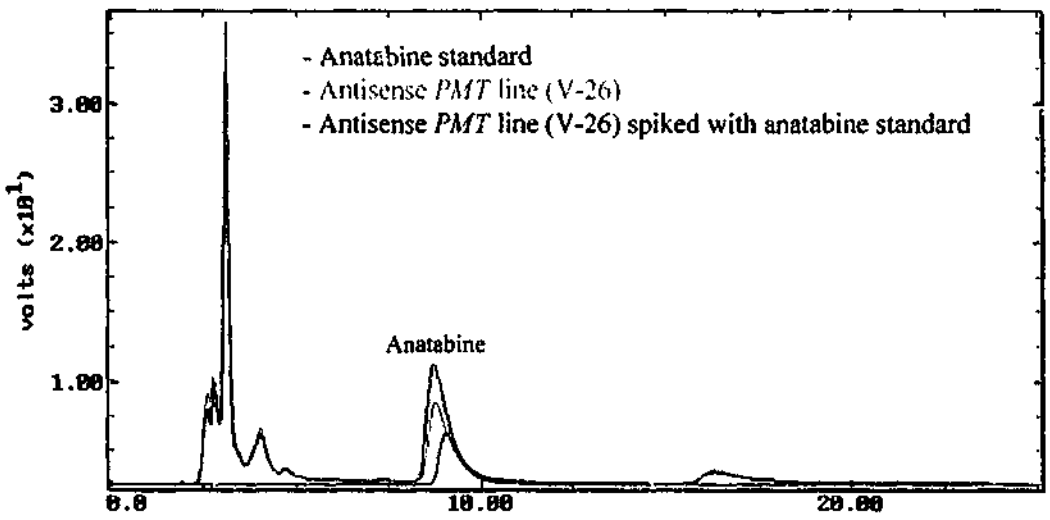

Fig. 4-9 Overlay of three separate HPLC chromatograms of anatabine standard, the alkaloid extract from antisense *PMT* line V-26, and the same extract spiked with anatabine standard. Note that the chromatograms show some tailing of peaks in this buffer (Saunders and Blume, 1981). If the amount of anatabine in the spike is reduced, then a perfect overlay is observed with the 8.9 mins peak present in the V-26 extract.

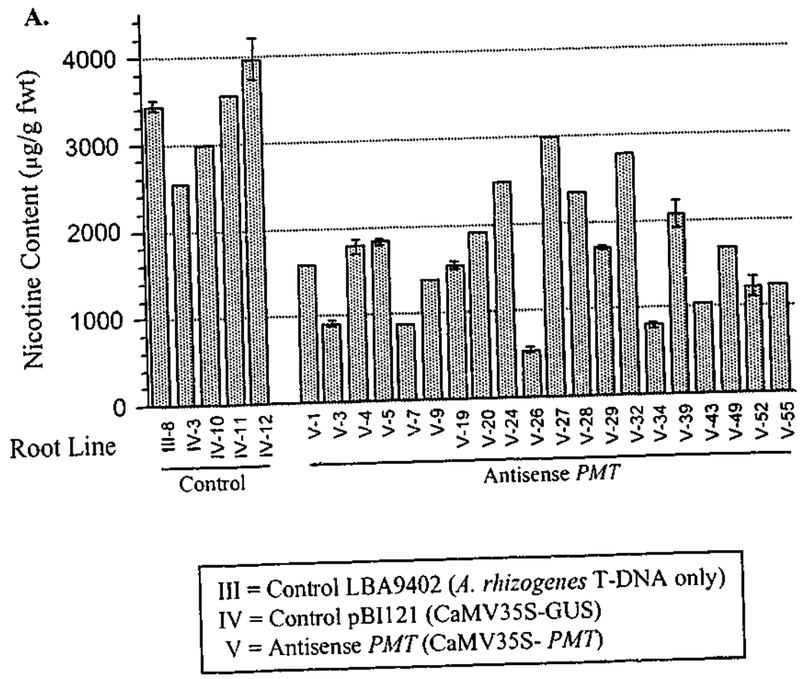

Fig. 4-10 Screening of 20 antisense *PMT* root lines, from an *N. tabacum* var. NC95 background, for unusual nicotine and anatabine levels at day 20 of the growth cycle. Where duplicate samples were available for analysis, data were presented as histograms with error bars representing either the mean (±s.e.) nicotine (A) or anatabine (B) content (µg/g fwt).

As a final confirmation, analysis of alkaloids in the antisense *PMT* line (V-26) and the control line (IV-10) was undertaken using GC-MS and revealed an elevated level of anatabine in line V-26 relative to that in line IV-10 (Appendix 3).

4.2.2 Initial alkaloid analysis of antisense *PMT* root lines generated from *N. tabacum* var. NC95 (high alkaloid variety)

Using the sample of authentic anatabine, it was possible to quantify the levels of anatabine in control and antisense *PMT* lines by HPLC analysis. The accumulation of nicotine and anatabine in five control lines and 20 antisense *PMT* lines of *N. tabacum* NC95 at day 20 of the growth cycle are illustrated in Fig. 4-10-A and B. Where duplicate samples were available for analysis, data were presented as histograms with error bars representing the mean (±s.e.) nicotine or anatabine content of samples.

It is clear from data presented in Fig. 4-10-A that the nicotine content of control lines at this time point ranged from about 2500 - 4000 µg/g fwt with an average of 3287 µg/g fwt. The nicotine content of most of the manipulated lines was lower. Analysis of variance for nicotine levels showed that there was a significant difference between the nicotine content of these two groups ($p<0.001$). In half of the antisense *PMT* lines examined, the nicotine content was less than 50% of the average level observed in controls. Moreover, several lines (V-3, V-7, V-26 and V-34) had less than 1000 µg/g fwt nicotine (approximating to the level observed in transformed root lines generated from the low nicotine producing variety of *N. tabacum,* LAFC53). The mean nicotine content of root line V-26 was only 537 µg/g fwt, indicating approximately a 6-fold reduction in the nicotine content of this line compared to that of controls.

Levels of anatabine were quite similar in all of the control root lines ranging from 489 - 673 µg/g fwt with a mean anatabine content of 447 µg/g fwt. In contrast, almost all of the antisense *PMT* lines accumulated anatabine at levels which were greater than the highest level found in the controls. 15 out of 20 antisense *PMT* lines analysed accumulated anatabine at a level more than 2-fold greater than the mean levels of anatabine in the controls. Interestingly, root line V-26 which had the lowest nicotine content amongst the antisense *PMT* lines also had the highest level of anatabine (1850

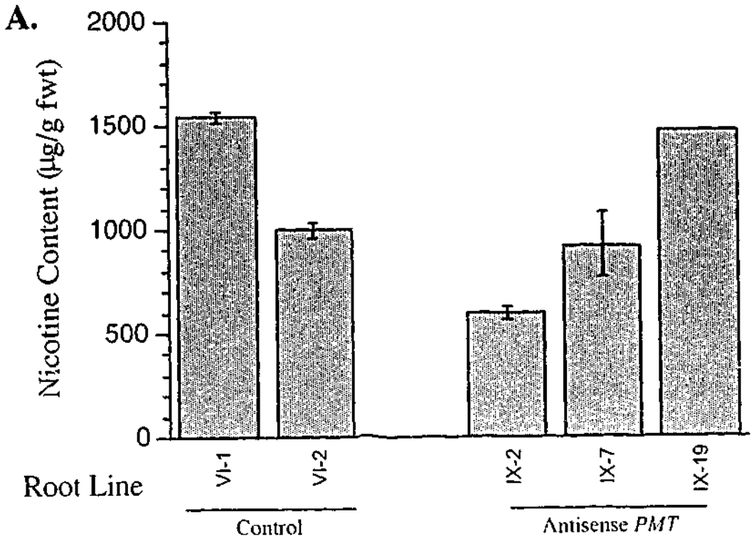

VI = Control pBI121 (CaMV35S-GUS) from *N. tabacum* var LAFC53, low nicotine producing variety.
IX = Antisense *PMT* (CaMV35S-*PMT*) from *N. tabacum* var LAFC53, low nicotine producing variety.

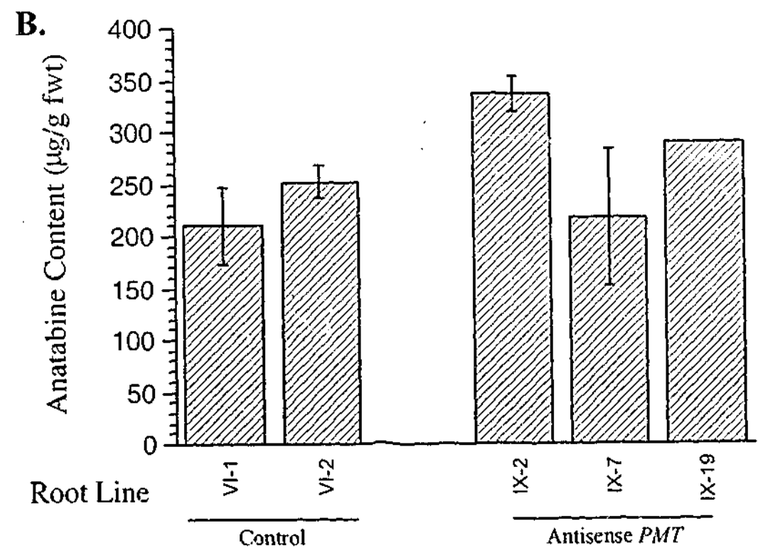

Fig. 4-11 Nicotine and anatabine contents at day 21 of the growth cycle in control and antisense *PMT* root lines generated from *N. tabacum* var. LAFC53 (low nicotine variety). Each histogram represents mean (± se) nicotine (A) or anatabine (B) from duplicate samples, except that of line IX-19 which represents one sample.

µg/g fwt). However, there was not a strict inverse correlation between nicotine content and anatabine content of antisense *PMT* lines. For example, line V-9 and V-55 had similar nicotine levels (1350 µg/g fwt and 1250 µg/g fwt, respectively) but showed about a 3-fold difference in their anatabine levels (1600 µg/g fwt for V-9 and 550 µg/g fwt for V-55).

Several of the screened antisense *PMT* root lines exhibited significantly lower median alkaloid levels, based on 95% confidence intervals, compared to those of control lines. Four of these lines, V-7, V-26, V-34 and V-43, were chosen for further characterisation, as described in section 4.4.

4.2.3 Preliminary alkaloid analysis of a limited number of antisense *PMT* transformed root lines generated from *N. tabacum* var. LAFC53 (low alkaloid variety)

A limited number of control and antisense *PMT* root lines generated from the low alkaloid variety, *N. tabacum* var. LAFC53 were analysed for nicotine and anatabine contents. Initial analyses of root lines at day 21 of the growth cycle are illustrated in Fig. 4-11-A and B.

One of the three antisense LAFC53 *PMT* lines analysed (IX-2) had a lower level of nicotine (600 µg/g fwt) and also a higher level of anatabine (340 µg/g fwt) than those found in LAFC53 controls (1000 – 1540 µg/g fwt for nicotine and 210 – 250 µg/g fwt for anatabine). Though the nicotine level was similar to that of lines V-26 and V-34 noted above in section 4.2.2, the anatabine level of line IX-2 was not elevated, being in fact much less than that observed in control lines of the high nicotine genotype, NC95 (490 – 670 µg/g fwt, Fig. 4-10-B).

4.2.4 Preliminary alkaloid analysis of a limited number of antisense *PMT* transformed root lines generated from *N.* sylvestris

N. sylvestris is the maternal progenitor species of the allotetraphoid *N. tabacum* (Riechers and Timko, 1999; Murad *et al*, 2002) and, like *N. tabacum*, has an alkaloid profile in which nicotine predominants in roots and anatabine is the second alkaloid (Saitoh *et al.*, 1985; Sisson and Severson, 1990). It was decided to generate several antisense *PMT* root lines of *N. sylvestris* to observe whether the same trends as noted above in *N. tabacum* were also evident in this species. Two control and five antisense *PMT* transformed root lines from *N. sylvestris* were analysed for nicotine and anatabine contents at day 21 of the growth cycle (Fig. 4-12-A and B).

One of the antisense *PMT* lines XII-14 had a significant reduction in nicotine content compared to that found in controls ($p<0.05$). The nicotine content of root line XII-14 (560 µg/g fwt) was about 3-fold lower than levels found in controls (1340 µg/g fwt – 1800 µg/g fwt) (Fig. 4-12-A). The highest anatabine level observed in these root lines was also in antisense *PMT* line XII-14 (760 µg/g fwt), being 3.7 times greater than the average level of anatabine in controls (210 µg/g fwt) (Fig. 4-12-B). Analysis of variance for the anatabine level in line XII-14 showed that this elevation was significant at $p<0.05$, compared to levels observed in controls. Another antisense *PMT* line, XII-20, also had markedly increased anatabine content of more than twice the controls (Fig. 4-12-B), even though its nicotine content was only slightly less than controls (Fig. 4-12-A).

In these preliminary experiments, therefore, it was observed that in several antisense *PMT* lines generated from *N. tabacum* var. NC95 and LAFC53, and *N. sylvestris*, a reduction in titres of nicotine appeared to coincide with an increase in the titres of anatabine at days 20/21 of the growth cycle (Fig. 4-10, Fig. 4-11, and Fig. 4-12). To further examine this phenomenon in tissues throughout the growth cycle, and in intact transgenic plants, alkaloid quantifications form several antisense *PMT* root lines of *N. tabacum* were undertaken.

A.

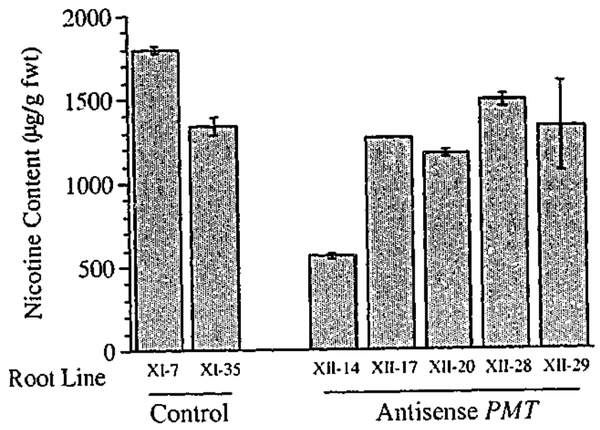

XI = Control pBI121 (CaMV35S-GUS) generated from *N. sylvestris*
XII = Antisense *PMT* (CaMV35S-*PMT*) generated from *N. sylvestris*

B.

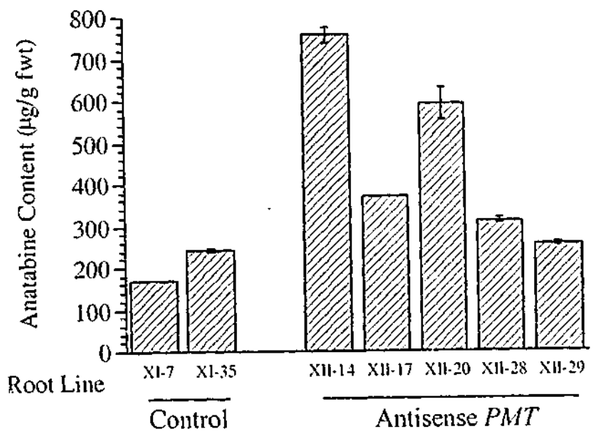

Fig. 4-12 Nicotine and anatabine content at day 21 of the growth cycle in control and antisense *PMT* root lines generated from *N. sylvestris*. Each histogram represents mean (±s.e.) nicotine (A) or anatabine (B) content (µg/g fwt) of duplicate samples, except that of line XII-17 which represents one sample.

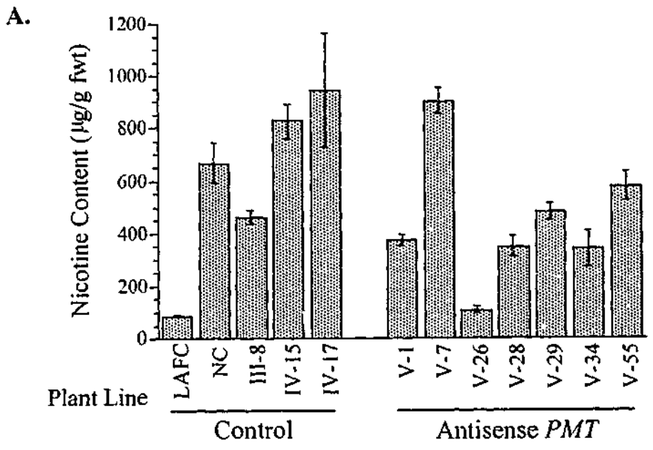

LAFC = *N. tabacum* var. LAFC53; low nicotine variety tobacco.
NC = *N. tabacum* var. NC95; high nicotine variety tobacco.
III = Control LBA9402 (*A. rhizogenes* T-DNA only) generated from high nicotine variety tobacco, NC95.
IV = Control pBI121 (CaMV35S-GUS) generated from high nicotine variety tobacco, NC95.
V = Antisense *PMT* (CaMV35S-*PMT*) generated from high nicotine variety tobacco, NC95.

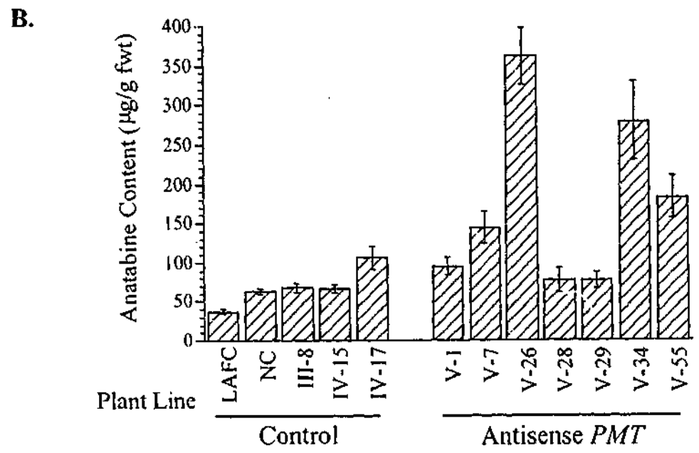

Fig. 4-13 Preliminary analysis of nicotine and anatabine content in leaves of regenerated plants from transformed root lines and also parental varieties grown from seed. Each histogram represents mean (±s.e.) nicotine (A) or anatabine (B) content (µg/g fwt) of two fully expanded leaves, 3rd and 4th from the apex, from duplicate plants, except those of lines V-7, V-29, and the parental varieties, which are derived from one plant.

4.3 Plants regenerated from antisense *PMT* root lines

4.3.1 Initial analysis of regenerants

Plants were regenerated from three control root lines (III-8, IV-15 and IV-17) and seven antisense *PMT* root lines (V-1, V-7, V-26, V-28, V-29, V-34 and V-55) all of which represented *N. tabacum* var. NC95, the high nicotine producing variety. All regenerated plants grew vigorously in soil and exhibited a slight wrinkling of leaves and a more compact growth habit than seed-derived plants, characteristics which are typical of the T phenotype caused by the presence of Ri T-DNA from *A. rhizogenes* (Tepfer, 1984). Whilst there was slight variation between plants regenerated from different transformed lines, no particular phenotype was characteristic of antisense *PMT* plants compared to controls.

Nicotine and anatabine levels were determined using leaf tissue of regenerated plants at a similar stage of development (plants having about 12-15 leaves, and no signs of floral buds). In addition, parental *N. tabacum* var. NC95 and var. LAFC53 plants were also analysed which were grown alongside the transformed plants and harvested at a comparable stage of development. Fig. 4-13 illustrates the nicotine and anatabine levels in these plants. Nicotine levels in transformed control plants of group III and IV, together with tissues from seed-derived parental plant NC95, were in the range of 460 µg/g fwt – 950 µg/g fwt, with an average of ~ 700 µg/g fwt (Fig. 4-13-A). Six of the antisense *PMT* plant lines had a lower nicotine content that the average of controls, with four antisense *PMT* lines, V-1, V-26, V-28 and V-34, containing less than 400 µg/g fwt nicotine. Thus, whilst the difference in nicotine content of antisense *PMT* transformants, relative to controls, was less marked than that of corresponding root lines, it was nevertheless evident in most of the antisense *PMT* lines. Interestingly, the nicotine level in antisense *PMT* plant line V-26 was very comparable to that of the LAFC53 variety.

Anatabine levels in control lines of group III and IV were in the range of 70 µg/g fwt – 100 µg/g fwt which were very similar to levels observed in seed-derived plants of

NC95 variety (Fig. 4-13-B). Four antisense *PMT* plant lines, V-1, V-7, V-28 and V-29, contained levels of anatabine comparable to control plants in group III and IV. In contrast, anatabine levels in plant line V-26, V-34 and V-55 were elevated relative to those controls, being up to 4.5-fold greater in line V-26 than the average levels found in controls.

4.3.2 Detailed analysis of regenerants

To confirm the observations noted above and to analyse alkaloid content from several leaves taken from around the plant, a second analysis was undertaken. Plants were regenerated again from three control and four antisense *PMT* root lines, grown together in the glasshouse. All alkaloid levels were determined using three mature leaves taken from the middle portion of preflowering plants (6th, 7th and 8th from the apex), each being approximately 50 cm in height. The nicotine and anatabine contents in control lines were higher than before and ranged between 1300-2200 µg/g fwt and 80-140 µg/g fwt, respectively (Fig. 4-14-B and C). The nicotine levels in three antisense *PMT* lines (V-26, V-34 and V-43) were 2- to 3.7-fold lower than those in controls (Fig. 4-14-B). Also the anatabine levels in these lines were 3- to 5-fold greater than those in controls (Fig. 4-14-C). Plant tissue of line V-7 contained normal levels of nicotine and anatabine even though detailed analysis of transformed roots from which it was regenerated had reduced nicotine and elevated anatabine levels (sections 4.2.2 and 4.4.1). The reasons for this are unclear at present (also see section 5.2), but it is noteworthy that plant tissue of line V-7 from the first batch of regenerants also had normal levels of nicotine and anatabine (Fig. 4-13).

Whilst all plants regenerated from transformed roots had a T-phenotype, there was no significant difference in the vegetative morphology between the controls and the antisense *PMT* lines (Fig. 4-15-A). A difference in the morphology of reproductive organs of some plants was observed (Fig. 4-15-B to D). For example, the length of the flower of control IV-15 was 4.1 cm, whilst that of the antisense *PMT* line V-26 was 4.8 cm. In addition, flowers of line V-26, had an elongated style (5.2 cm) relative to the pBI121 control (3.9 cm) whilst the length of filaments of V-26 and IV 15 were 4.2 cm

A.

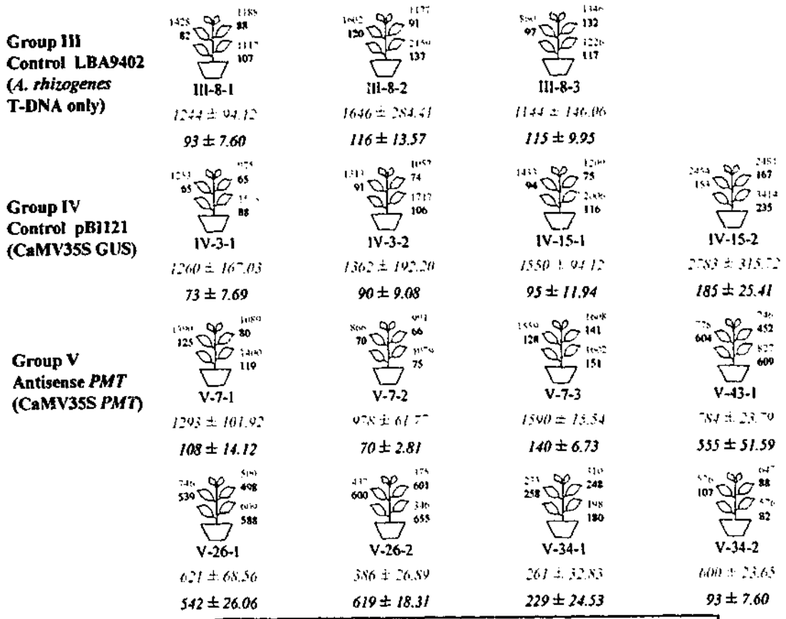

B.

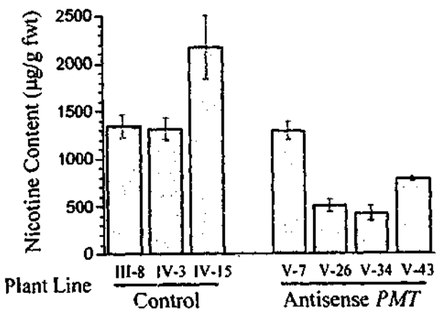

C.

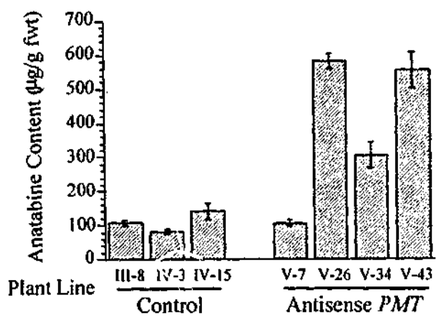

Fig. 4-14 (A) Schematic representation of plants regenerated from root lines showing leaf-specific alkaloid titres. The numbers following each line represents the number of samples. Nicotine and anatabine titres of leaves numbered 6, 7 and 8 from the apex are illustrated in red and blue, respectively. Mean (±s.e.) titres of nicotine and anatabine (in µg/g fwt) from these leaves on each plant are presented under the icons.
The average nicotine content (±s.e.) (B) and the average anatabine content (±s.e.) (C) per line are presented as histograms.

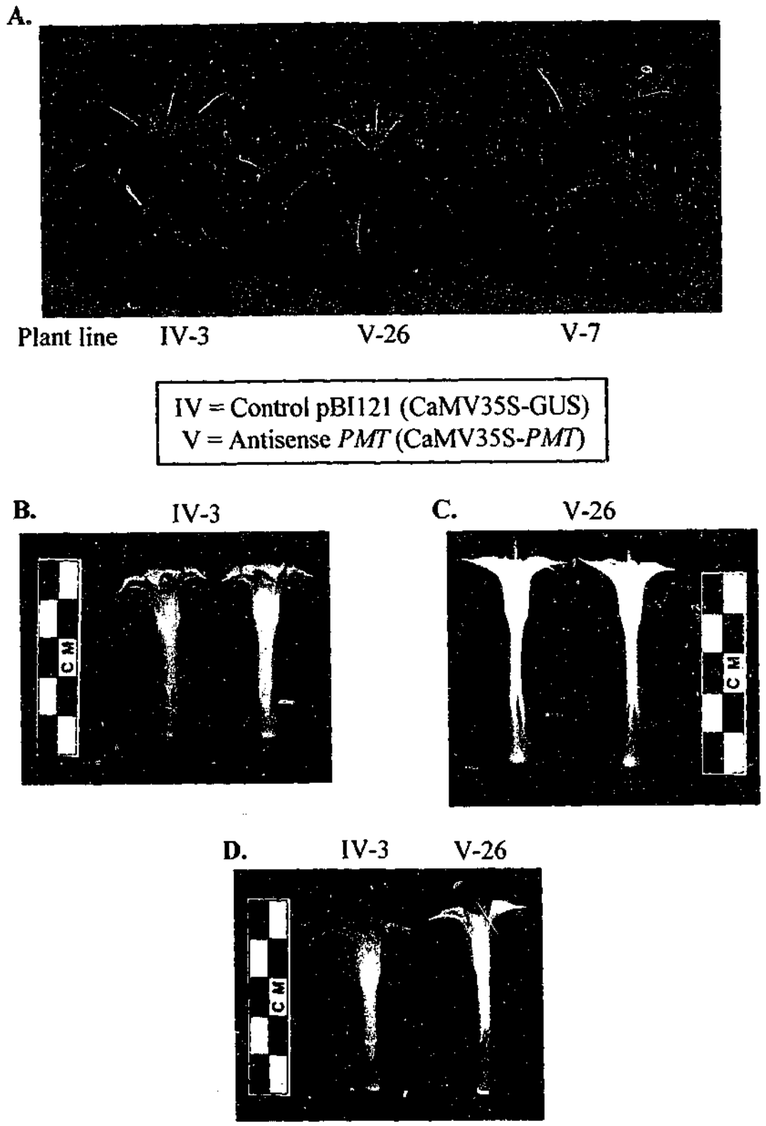

Fig. 4-15 Phenotype of regenerants.

(A) Antisense plant lines V-7 and V-26, and control plant line IV-3 were regenerated from root lines and grown under identical green house conditions. All regenerants exhibited slightly wrinkled leaves and a compact appearance, consistent with the transformed (T) phenotype as described by Tepfer (1984).

(B to D) Flowers from regenerants, control line IV-3 and antisense *PMT* line 26. Antisense *PMT* line 26 has a longer flower tube and style relative to the control line IV-3. Change in flower size and heterostyly also have been reported in regenerated plants from Ri T-DNA-transformed roots (Tepfer, 1984).

and 3.6 cm, respectively. These differences could possibly be caused by alterations in gene expression affecting primary metabolism, particularly polyamine metabolism. However, as heterostyly has been previously reported in plants containing Ri T-DNA (Tepfer, 1984), it is difficult to ascertain whether it was related to antisense expression of *PMT* in line V-26. Experimentation with a greater number of independent transformants would be needed to investigate this further.

4.3.3 Segregation ratios of the transformants.

Seed set in regenerated plants was poor, consistent with the observations of reduced pollen viability in Ri T-DNA transformants (Tepfer, 1984). Following manual fertilisation with their own pollen, however, most antisense *PMT* lines and controls produced some seeds. A small sample of seeds from the plant lines regenerated in the preliminary analysis, except line III-8 and V-34 which did not set seed, was surface sterilised and sown on MS medium without kanamycin to check for viability (Table 4-3). Up to 270 seeds from each plant line were then sown on medium containing 100 µg/ml kanamycin to check for binary vector T-DNA segregation ratios (Table 4-4). Seeds from the parental variety, *N. tabacum* var. NC95, were also sown as a negative control.

Table 4-3 Germination of the seeds on MS media without kanamycin

Plant line	Number of parental transgenic plants that produced seeds upon selfing	Number of seeds tested	Number of seeds germinated	Number of seeds failed to germinate
N. tabacum var.NC95	1	150	148	2
IV-15	2	35	32	3
IV-17	2	25	25	0
V-1	1	13	7	6
V-7	1	24	22	2
V-26	2	37	36	1
V-28	1	12	12	0
V-29	1	13	9	4
V-55	1	12	12	0

A.

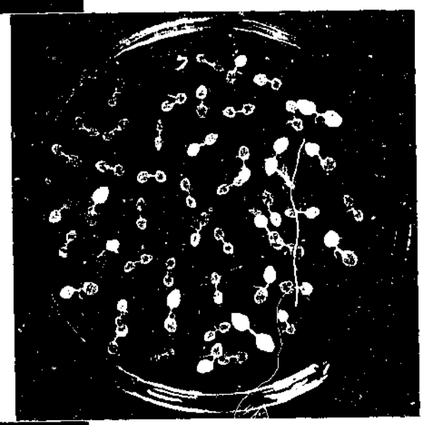

B.

C.

Fig. 4-16 Seed germination on MS phytagel containing 3% sucrose and grown under direct light at 25°C for 17 days.

A) Example of seedlings following germination of transformed seeds on media without kanamycin. All seedlings exhibited healthy growth (positive control).
B) Example of seedlings following germination of *N. tabacum* var. NC95 seeds on media containing 100 mg/l kanamycin. All seedlings exhibited kanamycin sensitive characteristics, bleached cotyledons and lack of root growth (negative control).
C) Example of seedlings following germination of transformed seeds on media containing 100 mg/l kanamycin. Both kanamycin resistant and kanamycin sensitive seedlings were identified in the population.

After germination, seedlings of every line grew and were healthy on control plates containing medium without kanamycin (Fig. 4-16-A and Table 4-3). On medium with kanamycin, all parental NC95 seedlings exhibited kanamycin sensitive characteristics (Fig. 4-16-B), whilst segregation for resistance:sensitivity was observed in seedlings from binary vector transformants (Fig. 4-16-C).

Table 4-4 Sensitive to resistant ratios of T_1 progeny seedlings following self fertilisation of transgenic parental plants. Seeds were germinated and grown on MS media containing 100 mg/L kanamycin.

Plant lines	Number of parental transgenic plants that produced seeds upon selfing	Observed numbers $kan^r : kan^s$	Predicted kan^r transgene copy number	Expected ratios $kan^r : kan^s$	$\Sigma\chi^2_{[1]}$	p-value
N. tabacum var. NC95	1	0 : 267	0	S	-	-
IV-15	2	482 : 22	2	15 : 1	3.056	$0.05 < p < 0.10$
IV-17	2	449 : 28	2	15 : 1	0.118	$0.70 < p < 0.80$
V-1	1	206 : 20	2	15 : 1	2.607	$0.10 < p < 0.20$
V-7	1	119 : 142	-	1 : 1	2.029	$0.10 < p < 0.20$
V-26	2	495 : 8	3	63 : 1	0.003	$p > 0.90$
V-28	1	269 : 0	-	R	-	-
V-29	1	104 : 7	2	15 : 1	0.057	$0.80 < p < 0.90$
V-55	1	269 : 0	-	R	-	-

kan^r = kanamycin resistant seedlings.; kan^s = kanamycin sensitive seedlings.;
S = All were sensitive to kanamycin.; R = All were resistant to kanamycin.

From these results, most of the antisense *PMT* lines appear to have more than one separately segregating locus for kanamycin resistance, indicating multiple integrations of the binary vector T-DNA, and thus quite likely the *PMT* gene. The ability of *A. rhizogenes* to transfer several copies of both Ri and binary vector T-DNA into a plant genome was previously reported by Hamill *et al.* (1987b). From Table 4-4, it appears that each of the plant lines IV-15, IV-17 V-1 and V-29 contained two separately segregating loci for the kanamycin-resistance gene. The antisense *PMT* line V-26, which showed the greatest difference in nicotine and anatabine relative to that of controls, appears to have contained three independently segregating copies of the

kanamycin-resistance gene. The reason for the apparent 1:1 segregation pattern observed in line V-7 is not clear. It may be indicative of some instability in expression of the *NPT II* gene conferring kanamycin resistance. It is noteworthy that this line, unlike the others, showed a reduced nicotine/high anatabine profile in transformed root tissues but a normal alkaloid profile in regenerated plant tissues. This could be due to instability of expression of the antisense *PMT* gene, possibly caused by methylation of the binary vector T-DNA in regenerated plants.

Further analyses of the offspring of these plants was not pursued due to the likelihood of complex inheritance patterns, relating to the antisense *PMT* gene, leading to a substantial degree of variation in alkaloid content. An interesting area for future investigation may be to examine the stability of changes in alkaloid content of transgenic tissues over several generations.

4.4 Detailed analysis of selected antisense *PMT* root lines.

4.4.1 Growth, nicotine and anatabine profiles

Four antisense *PMT* transformed root lines with low nicotine content, V-7, V-26, V-34 and V-43, from the population of root lines in which preliminary analysis was undertaken (Fig. 4-10) and two transformed control root lines (III-8 and IV-15), were analysed for growth, nicotine and anatabine content throughout a 26 day culture period. All these root lines were generated from *N. tabacum* var. NC95. A low alkaloid transformed root line from *N. tabacum* var. LAFC53 which was analysed previously (VI-1) was included as a comparison.

As described in section 3.2.3.1, for logistical reasons, the experiment was set up as two parallel groups on successive days. Group one was composed of root line IV-15, V-7, V-26 and V-34, whilst group two consisted of root line VI-1, III-8 and V-43. Apart from the setting up and harvesting dates, which were one day apart, all other conditions, such as the batch of media, the growth environment, and time points for harvesting material, were exactly the same.

A.

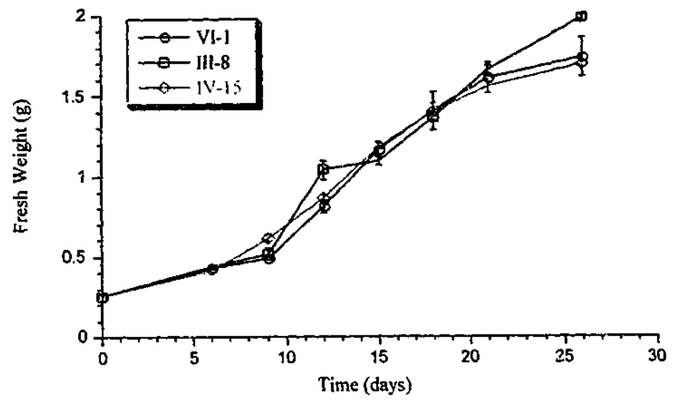

VI = Control pBI121 (CaMV35S-GUS) generated from low alkaloid variety tobacco, LAFC53.
III = Control LBA9402 (*A. rhizogenes* T-DNA only) generated from high alkaloid variety tobacco, NC95.
IV = Control pBI121 (CaMV35S-GUS) generated from high alkaloid variety tobacco, NC95.
V = Antisense *PMT* (CaMV35S-*PMT*) generated from high alkaloid variety tobacco, NC95.

B.

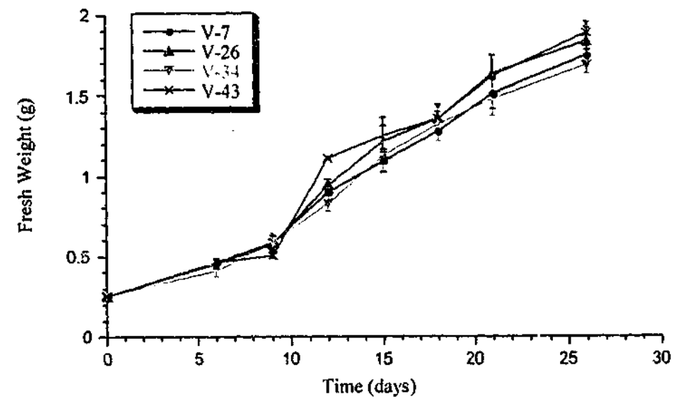

Fig. 4-17 Growth curves of control (A) and antisense *PMT* root lines (B) over a 26 day period. Each data point represents the mean (±s.e.) fresh weight (g) of triplicate root samples harvested at days 6, 9, 12, 15, 18, 21 and 26.

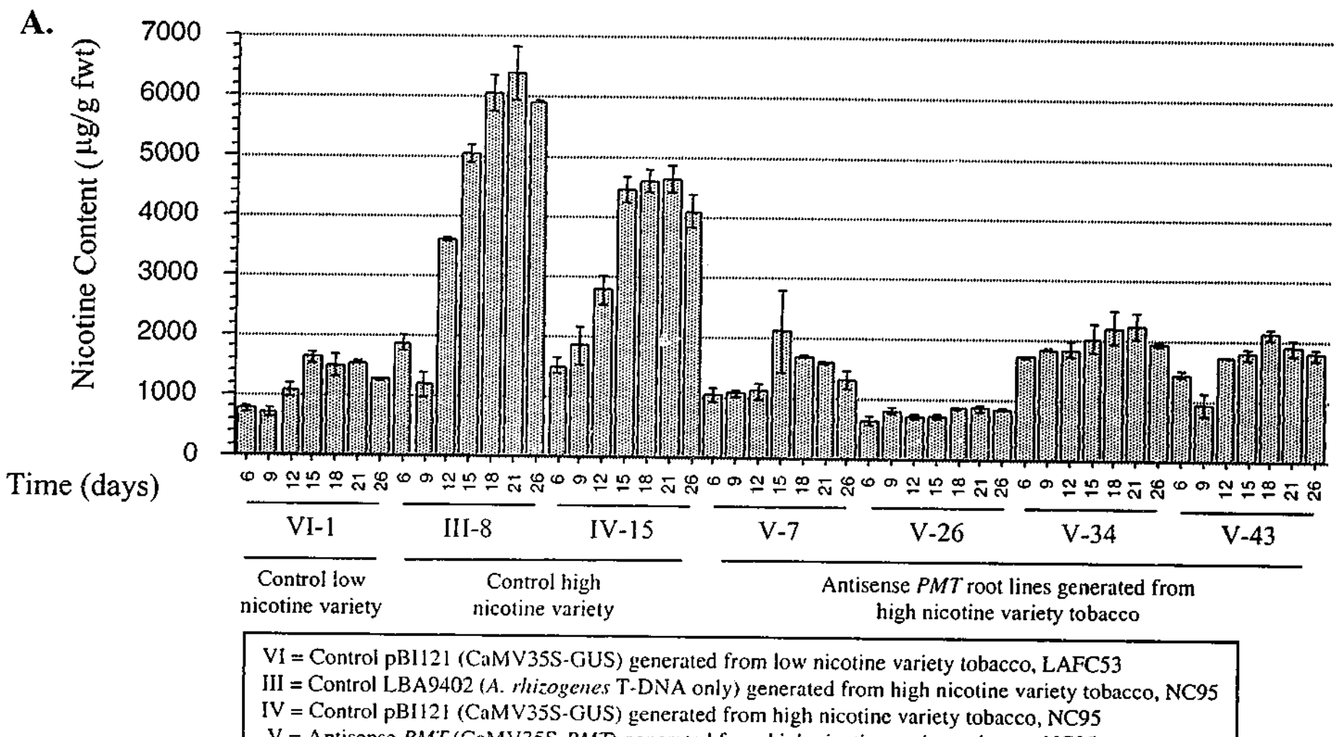

Fig. 4-18 Nicotine profiles of control and antisense *PMT* root lines at days 6, 12, 15, 18, 21 and 26 of the growth cycle. Each histogram represents the mean (±s.e.) nicotine content (µg/g fwt) of duplicate samples.

Fig. 4-17-A and B illustrated the growth of the control and antisense *PMT* lines, respectively. Similar to the data presented in Fig. 3-21, the growth pattern of each line was composed of an initial lag phase of 5-7 days, a period of rapid growth in the mid phase of about 10 days and a slower growth phase toward the end of the cycle. As is clear, from this data, no differences between the growth of high and low alkaloid root lines or between that of the controls and antisense *PMT* lines were observed. Thus, any differences in the alkaloid profiles of lines is likely to due to differences in capacity to produce alkaloids as opposed to growth-related alterations.

Nicotine titres within root lines were determined from tissues harvested at each time point (Fig. 4-18). The level of nicotine in roots of the low alkaloid variety, line VI-1, was lower than that of root lines derived from the high alkaloid variety, lines III-8 and IV-15, at all time points throughout the growth cycle. Mean nicotine levels in control root lines of the high alkaloid variety, III-8 and IV-15, ranged from 1500 µg/g fwt during early growth to 5500 µg/g fwt during the latter part of the growth cycle. In contrast, the mean nicotine titre in transformed roots of line VI-1 was 700 µg/g fwt during early growth, increasing to 1500 µg/g fwt as growth progressed. Such patterns and levels of alkaloid accumulation are typical of numerous transformed root lines generated from these varieties of *N. tabacum* and analysed in this laboratory (Lidgett, 1997). Moreover, a reproducible feature of transformed roots from these varieties is that at about days 12 to15 of the growth cycle, the high alkaloid tissues begin to accumulate much higher levels of nicotine, leading to the characteristic 2.5- to 3-fold difference in the nicotine content of root lines from each variety by the end of the growth cycle. In contrast, patterns of alkaloid accumulation in antisense *PMT* root lines more closely resembled cultures of the LAFC53 variety, rather than the NC95 variety from which they were derived. Thus, whilst each line had a low-normal nicotine content at the beginning of the growth cycle, levels failed to rise substantially in the mid/late phases of the growth cycle, leading to large differences in alkaloid content compared to controls, by the end of the culture period. The most dramatic difference in nicotine accumulation patterns from that of control NC95 root lines, was exhibited by line V-26 which had a very low level of nicotine throughout the growth cycle (Fig. 4-18).

Nicotine levels in antisense *PMT* lines analysed in this study were between 640-2200 µg/g fwt. Statistical analyses using a two-way ANOVA showed significant differences ($p<0.001$) in nicotine levels among groups of root lines and between time points. Subsequently, a Tukey's statistical test indicated that the differences between the mean levels of nicotine in the NC95 control group and those in each of antisense *PMT* lines, as well as the LAFC53 line, begin to become statistically significant ($p < 0.05$) at day 12 of the growth cycle and remained so until the end of the cycle. However, at day 6 of the growth cycle, the nicotine levels in line V-26 and also VI-1 (LAFC53 line) were significantly different ($p<0.05$) from the mean level of nicotine in the NC95 control group (group IV). As expected, significant differences in nicotine content were not observed between NC95 control lines, III-8 and IV-15, or between any pair of antisense *PMT* root lines in group V, or between any group V line and the LAFC53 line VI-1.

Fig. 4-19 illustrates the anatabine content of these root lines. As anticipated, the LAFC53 line VI-1 not only had a low nicotine content but exhibited also a low anatabine content relative to that of the NC95 control lines III-8 and IV-15 at all stages throughout the growth cycle. Thus, anatabine levels in line VI-1 ranged from 150–240 µg/g fwt over the growth cycle, whilst levels in NC95 control lines ranged from 220 µg/g fwt early in the growth cycle to 900 µg/g fwt later in the growth cycle. Thus, analogous to the situation involving nicotine, anatabine levels tended to increase by a factor of 2-3 in roots of the NC95 variety during the latter part of the growth cycle (Fig 4-19). In contrast, the anatabine levels in all antisense *PMT* lines was much higher, ranging from a low of *ca* 1000–1500 µg/g fwt in the early stages of the cycle to levels of *ca* 2000 µg/g fwt to > 2500 µg/g fwt in the latter parts of the cycle. As was the situation regarding nicotine, line V-26 showed the greatest difference in anatabine content when compared to controls with levels reaching 2850 µg/g fwt in tissues harvested at day 21 of the growth cycle (Fig 4-19). The anatabine levels in this line were up to 6 times higher than those in NC95 control lines harvested at comparable time points. Analysis of variance followed by either a Tukey's or Dunnett's statistical test showed that anatabine levels in every antisense *PMT* root lines at every time point were

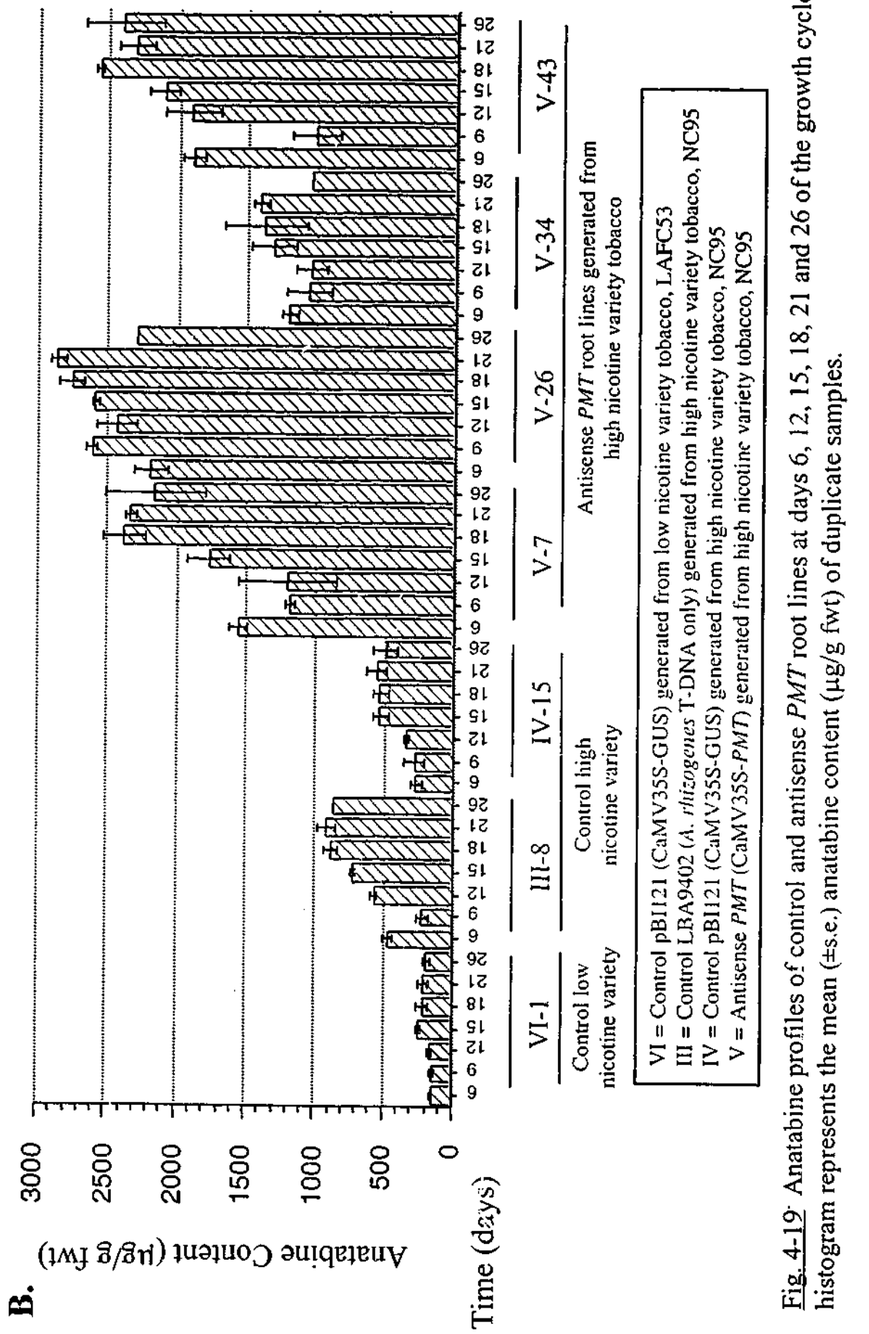

Fig. 4-19 Anatabine profiles of control and antisense *PMT* root lines at days 6, 12, 15, 18, 21 and 26 of the growth cycle. Each histogram represents the mean (±s.e.) anatabine content (µg/g fwt) of duplicate samples.

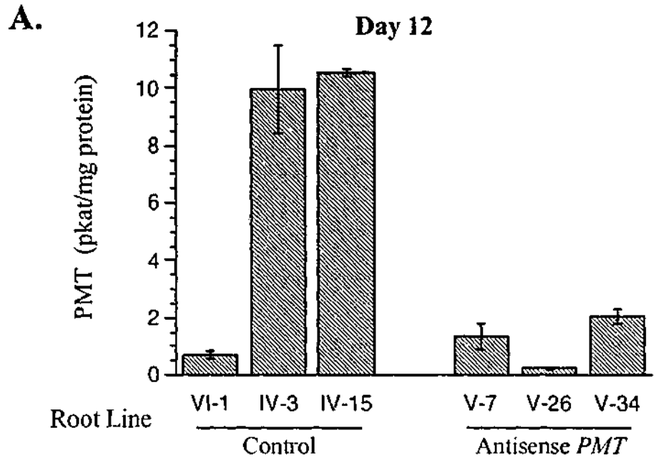

VI = Control pBI121 (CaMV35S-GUS)
generated from low nicotine variety tobacco, LAFC53
IV = Control pBI121 (CaMV35S-GUS)
generated from high nicotine variety tobacco, NC95
V = Antisense *PMT* (CaMV35S-*PMT*)
generated from high nicotine variety tobacco, NC95

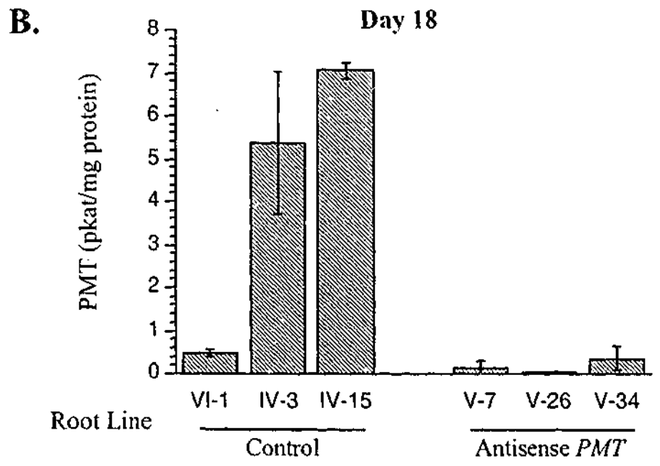

Fig. 4-20 PMT activities of control and antisense *PMT* root lines at day 12 (A) and day 18 (B) of the growth cycle. The activities were determined from three separate cultures. The extract from each culture was subjected to triplicate samples for the enzyme assay. Each histogram represents mean (±s.e.) PMT activity of each line in pkat/mg protein.

significantly different from those in NC95 control root lines and also the LAFC53 root line, harvested at comparable time points.

4.4.2 PMT activity

PMT activity of three antisense *PMT* lines analysed above (V-7, V-26 and V-34) together with two high nicotine-producing control lines from variety NC95 (IV-3 and IV-15) and a low nicotine-producing control line from variety LAFC53 (VI-1) were determined from three replicated samples taken at two time points in the mid stage of the growth cycle, day 12 and day 18. Data is presented in Fig. 4-20-A and B.

At day 12, PMT activities in the NC95 control lines IV-3 and IV-15 were 10 pkat/mg protein and 10.5 pkat/mg protein, respectively (Fig. 4-20-A). These values are close to the expected values for actively growing root cultures of wild type *N. tabacum* (Wagner *et al.*, 1986c; Hibi *et al.*, 1994). In contrast, PMT activity in the low alkaloid line, LAFC53, (line VI-1) was 0.7 pkat/mg protein - a reduction compared to those in the high alkaloid control lines (NC95) by a factor of approximately 15. PMT activity at day 12 of the growth cycle was dramatically reduced in each of the three antisense *PMT* lines that were examined averaging 1.3 pkat/mg protein, 0.2 pkat/mg protein, and 2.1 pkat/mg protein for lines V-7, V-26 and V-34, respectively. It is noteworthy that in root line V-26, PMT activity was reduced by a factor of more than 40 compared to levels found in NC95 controls.

At day 18 of the culture cycle, the PMT activities of all root lines were reduced compared to those observed at day 12, which is in agreement with previous observation regarding PMT activity in transformed roots of *N. rustica* (Hamill *et al.*, 1990). However, the reduction in PMT activity at day 18 was much more marked for antisense *PMT* lines compared to controls (Fig. 4-20-B). At this time point, mean PMT activities in the NC95 control lines IV-3 and IV-15 were 5.4 pkat/mg protein and 7.0 pkat/mg protein, respectively, whilst those in antisense *PMT* lines V-7, V-26 and V-34 were 0.1 pkat/mg protein, 0.04 pkat/mg protein and 0.4 pkat/mg protein, respectively.

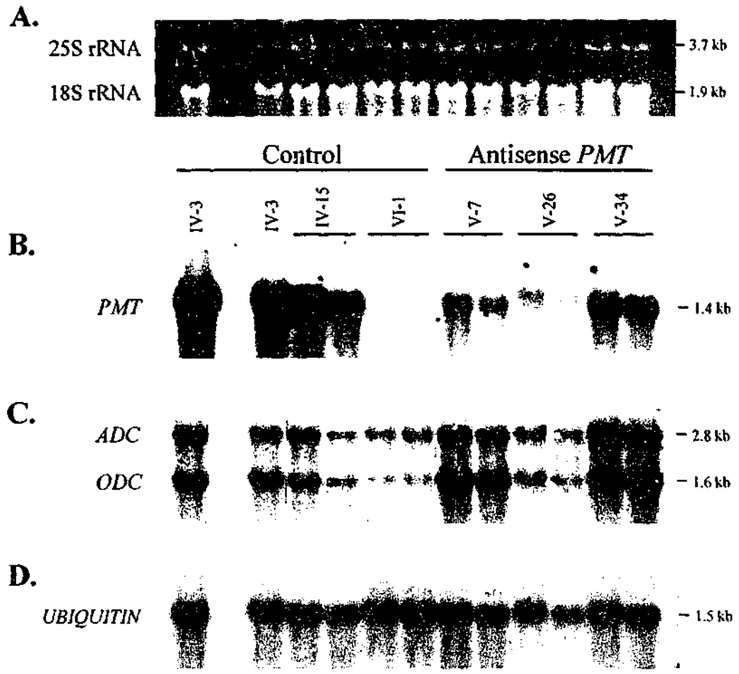

IV = CaMV35S GUS (control pBI121) in high alkaloid variety of *N. tabacum*.
VI = CaMV35S GUS (control pBI121) in low alkaloid variety of *N. tabacum*.
V = CaMV35S-*PMT* (antisense *PMT*) in high alkaloid variety of *N. tabacum*.

Fig. 4-21 Northern blot analysis of antisense *PMT* root lines and controls. Each lane contains 20 μg of total RNA extracted from separate root cultures at day 12 of the growth cycle.

(A) Bands of 18S and 25S ribosomal RNAs visible after staining with ethidium bromide illustrate a relatively equal amount of RNA loaded in each well. The blot was probed with the *PMT* coding sequence from *N. tabacum* (B). After stripping, the blot was reprobed with the fragments of *ADC* and *ODC* coding sequences both from *N. tabacum* (C). At the end of the experiment, the blot was probed with the *UBIQUITIN* coding sequence, after stripping (D).

Thus, at both time points the PMT activities in antisense *PMT* root lines were markedly reduced compared to those in controls. In particular, the activity of antisense *PMT* line V-26 (which consistently had lowest nicotine and highest anatabine levels) was more than 100-fold lower than levels observed in control transformed roots of *N. tabacum* var. NC 95 at day 18. It is interesting to note that PMT levels were also more than 10-fold lower in antisense *PMT* line V-26 than in transformed root line VI-1, established from low alkaloid variety, LAFC53, at day 18 of the culture cycle.

As PMT is a key enzyme in the biosynthesis of nicotine, it may be expected that the reduction in PMT activity observed at day 18 of growth, compared to day 12, would also result in reduced nicotine biosynthesis. The nicotine titres measured at day 18, however, were not markedly reduced compared to those at day 12 (Fig. 4-18). Similarly, a comparison of the nicotine levels at days 15 and 21 did not reveal any marked differences. Such responses may be a function of the difference between the rate of nicotine depletion and the rate of nicotine biosynthesis within growing root tissues cultured *in vitro*. That is, the rate of nicotine turnover or secretion into the medium may be slower than the rate of nicotine synthesis. Consequently, higher titres of nicotine were observed in root lines at days 18 or 21 of growth, compared to days 12 or 15, despite the reduction in PMT activities. An alternative possibility may be that not only is the activity of PMT, or the rate of nicotine synthesis, slowed at day 18, but the rates of nicotine depletion are also reduced at day 18 compared to those at day 12 of growth.

4.4.3 Analysis of transcript levels of *PMT* and other genes encoding alkaloid biosynthesis enzymes in *Nicotiana*

Transcript levels of *PMT* and other genes encoding enzymes of alkaloid biosynthesis was determined at day 12 of the growth cycle. Total RNA was extracted from the antisense *PMT* lines, V-7, V-26 and V-34, as well as the low alkaloid LAFC53 control line, VI-1. NC95 root lines IV-3 and IV-15 were used as high alkaloid producing control lines. Three parallel Northern blots were set up using the same RNA extracts. The first Northern blot was probed with *PMT*, then after stripping, with

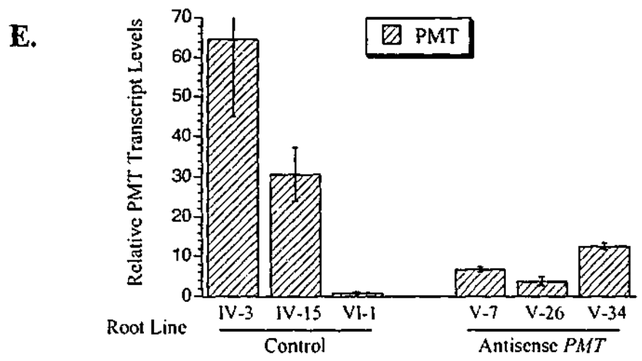

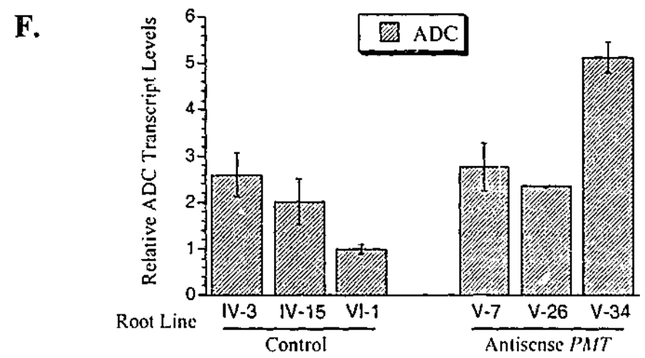

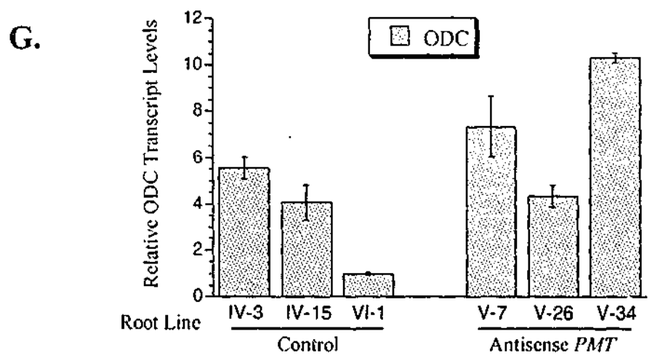

IV = CaMV35S GUS (control pBI121) in high alkaloid variety of *N. tabacum*.
VI = CaMV35S GUS (control pBI121) in low alkaloid variety of *N. tabacum*.
V = CaMV35S-*PMT* (antisense *PMT*) in high alkaloid variety of *N. tabacum*.

Fig 4-21 (continued) The intensities of *PMT*, *ADC*, *ODC* and *UBIQUITIN* transcripts were quantified using a phosphoimager. Transcript levels of *PMT*, *ADC* and *ODC* respectively, are illustrated relative to the levels of *UBIQUITIN* transcript in each lane (E to G). Each histogram represents mean (±s.e.) transcript level in each root line. The lowest relative level of each transcript was assigned a value of 1.

fragments of *ODC* and *ADC* together (Fig. 4-21-A). (Preliminary experiments had already determined that *ODC* and *ADC* probes did not cross hybridise to each other's transcript on Northern blots.) The second blot was probed, separately after stripping between hybridisations, with fragments of *SAMDC*, *SAMS* and *SPDS* (Fig. 4-21-B). The third blot was probed, separately, with *QPT* and *PMT* (Fig. 4-21-C). At the end of the experiments, each blot was probed separately with the *Antirrhinum* ubiquitin coding sequence to check for evenness of loading and to quantify the signal in each lane relative to that of ubiquitin (details of all probes used are recorded in Appendix 2).

Fig. 4-21-B, E, Q and T clearly shows that the transcript level of *PMT* in the antisense *PMT* lines was lower than in the high nicotine producing NC95 controls. However, *PMT* transcript in each of these lines was higher than that observed for the low alkaloid LAFC53 line VI-1, even though in root line V-26, the PMT activity is less than that observed in extracts of root line VI-1 (section 4.4.2). This apparent discrepancy between *PMT* transcript signal and enzyme activity may be explained by the fact that a double-strand probe was used to detect *PMT* transcript. Thus, in the antisense *PMT* lines, the signals obtained may be due to a mixture of sense and antisense mRNA molecules hybridising to the probes. Nevertheless, the overall pattern of the *PMT* transcript abundance observed in antisense *PMT* lines was broadly comparable to the pattern of enzyme activity. Line V-26 had the lowest level of enzyme activity and also *PMT* transcript abundance, while line V-34 had the highest PMT activity and transcript level of the antisense *PMT* lines that were analysed in details.

The transcript levels of *ADC* and *ODC* which encode upstream enzymes contributing to the putrescine pool seem not to have been altered in antisense *PMT* lines V-7 and V-26 compared to the control lines IV-3 and IV-15 (Figs. 4-21-C, 4-21-F and 4-21-G). The *ADC* and *ODC* transcript levels in both of these antisense *PMT* lines were quite similar and comparable to the controls, IV-3 and IV-15. However, the transcript levels of both genes in line V-34 were somewhat greater than in the controls. Interestingly, transcript levels of both *ADC* and *ODC* were lower in roots of LAFC53 line VI-1 than in roots of NC95 control lines IV-3 and IV-15. Whilst differences in transcript abundance between control NC95 and control LAFC53 transformed root lines were not as marked as for *PMT*, where differences were up to 30-fold, they were

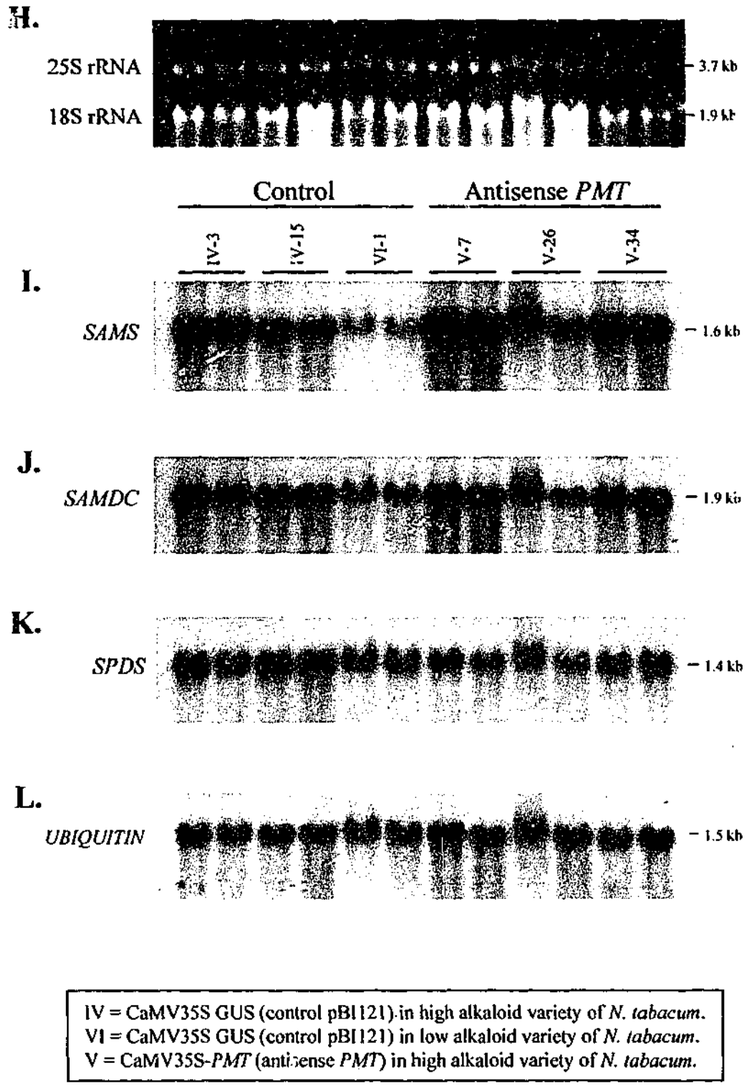

IV = CaMV35S GUS (control pBI121) in high alkaloid variety of *N. tabacum*.
VI = CaMV35S GUS (control pBI121) in low alkaloid variety of *N. tabacum*.
V = CaMV35S-*PMT* (antisense *PMT*) in high alkaloid variety of *N. tabacum*.

Fig. 4-21 (continued) Further Northern blot analysis of antisense *PMT* root lines and controls. Each lane contains the same 20 µg of total RNA as shown in the previous blot (Fig. 4-21-A).
(H) Bands of 18S and 25S ribosomal RNA visible after staining with ethidium bromide illustrate a relatively equal amount of RNA loaded in each well. The blot was probed with *SAMS, SAMDC* and *SPDS* coding sequences separately (I to K). At the end of the experiment, the blot was probed with *UBIQUITIN* coding sequence after stripping (L).

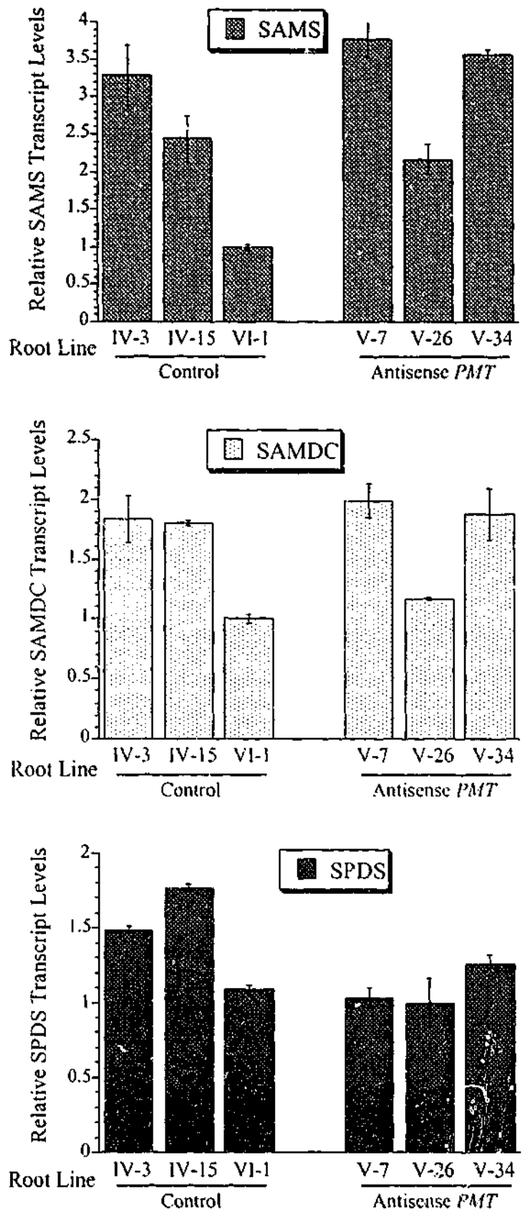

IV = CaMV35S GUS (control pBI121) in high alkaloid variety of *N. tabacum*.
VI = CaMV35S GUS (control pBI121) in low alkaloid variety of *N. tabacum*.
V = CaMV35S-*PMT* (antisense *PMT*) in high alkaloid variety of *N. tabacum*.

Fig 4-21 (continued) (M to O) Transcript levels of *SAMS, SAMDC* and *SPDS* respectively, are illustrated relative to the levels of *UBIQUITIN* transcript in each lane. Each histogram represents mean (±s.e.) transcript level in each root line. The lowest relative level of each transcript was assigned a value of 1.

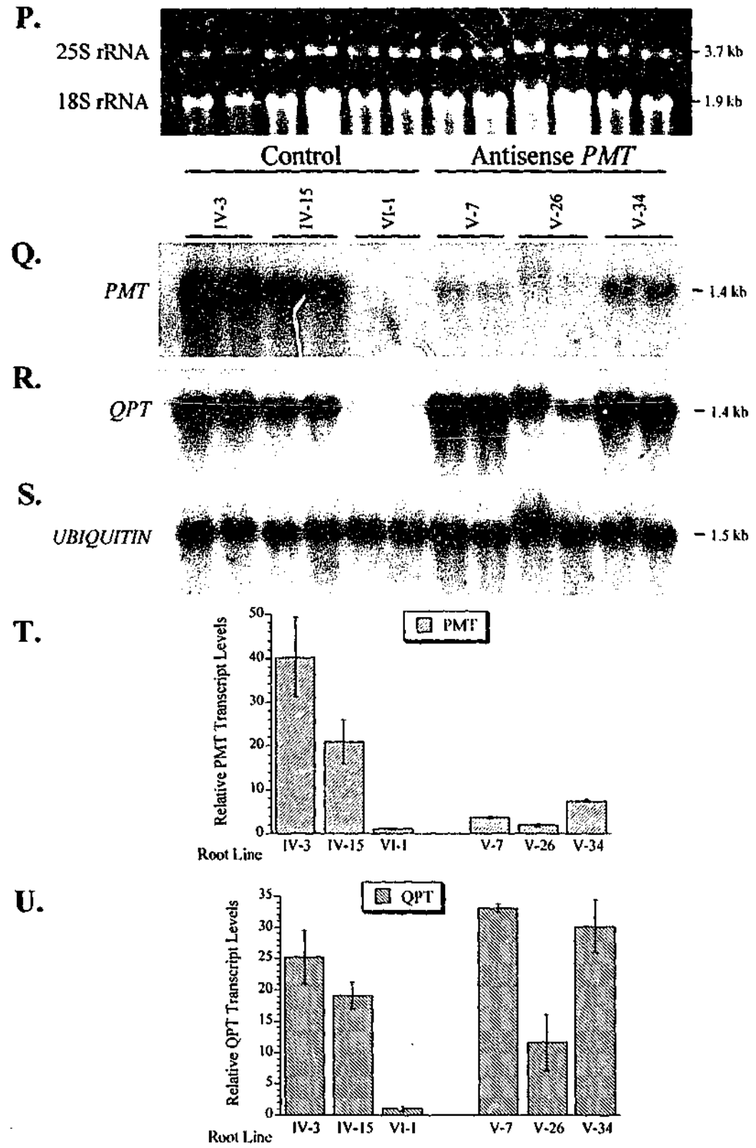

IV = CaMV35S GUS (control pBI121) in high alkaloid variety of *N. tabacum*.
VI = CaMV35S GUS (control pBI121) in low alkaloid variety of *N. tabacum*.
V = CaMV35S-*PMT* (antisense *PMT*) in high alkaloid variety of *N. tabacum*.

Fig. 4-21 (continued) Further Northern blot analysis of antisense *PMT* root lines and controls. Each lane contains the same 20 µg of total RNA as shown in the first blot (Fig. 4-21-A).
(P) Bands of 18S and 25S ribosomal RNA visible after staining with ethidium bromide illustrate a relatively equal amount of RNA loaded in each well. The blot was probed with *PMT*, *QPT* and *UBIQUITIN* coding sequences separately (Q to S). The transcript levels of *PMT* and *QPT* are illustrated relative to the level of *UBIQUITIN* transcript in each lane (T and U). Each histogram represents mean (±s.e.) transcript level in each root line. The lowest relative level of each transcript was assigned a value of 1.

nevertheless substantial, being approximately 2- to 2.5-fold for *ADC* and 4- to 5-fold for *ODC*.

The transcript levels of *SAMS*, *SAMDC* and *SPDS* in antisense *PMT* root lines were broadly comparable to levels observed in the control lines IV-3 and IV-15 (Figs. 4-21-H to 4-21-O). Line V-26 did show a reduced level of transcript for *SAMDC*, being about 60% that of other lines. In this respect it was similar to line VI-1, which had reduced transcript levels of each gene relative to those found in high alkaloid controls. The transcript level of *SPDS* in all antisense lines was reduced relative to the controls but as differences were only in the order of about 30%, it is difficult to be confident that these differences were real without further analyses being undertaken.

QPT plays a key role in providing nicotinic acid required for pyridine alkaloid synthesis. *QPT* transcript, like *PMT* transcript, was consistently present at markedly different levels between high alkaloid and low alkaloid transformed root lines (Figs 4-21-Q to 4-21-U). This is in agreement with observation of Sinclair *et al.* (2000) who suggest that expression of *PMT* and *QPT* are co-ordinately regulated in *N. tabacum* and that both are negatively affected by *nic1* and/or *nic2* mutations which are present in LAFC53 (Chaplin, 1975). In support of this suggestion, it is interesting to note that the control root line VI-1, generated from a low alkaloid variety tobacco, possessed low levels of *PMT* and *QPT* transcript compared to those of high alkaloid controls. Furthermore, this low alkaloid variety root line also exhibited reduced levels of other transcripts encoding enzymes providing substrates for alkaloid biosynthesis, notably *ODC*, *ADC* and *SAMS*.

QPT transcript levels in two of three antisense *PMT* lines (V-7 and V-34) are slightly elevated relative to NC95 controls, whilst *QPT* levels in line V-26 was about half of that observed ,on average, in NC95 controls (Figs. 4-21-R and 4-21-U). Overall, the level of *QPT* transcript in each antisense *PMT* line was at least 10 times that observed in transformed roots of the low alkaloid variety line VI-1.

Thus, in the antisense *PMT* root lines, apart from a significant reduction in the level of *PMT* transcript, the overall effects of down-regulating PMT upon the expression of

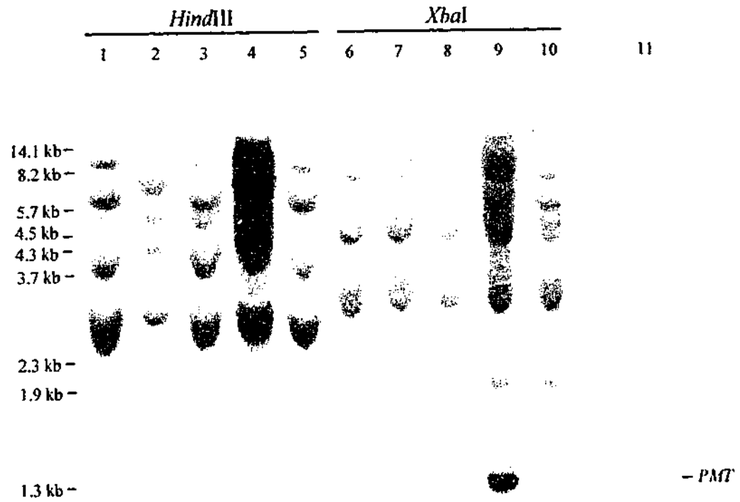

Lane 1 and 6 = VI-15 (control pBI121 root line generated from *N. tabacum* NC95
Lane 2 and 7 = V-7 (antisense *PMT* root line)
Lane 3 and 8 = V-26 (antisense *PMT* root line)
Lane 4 and 9 = V-34 (antisense *PMT* root line)
Lane 5 and 10 = Intact root from *N. tabacum* NC95 plant
Lane 11 = *PMT* and pYC3Z (positive control)

Fig. 4-22 Southern blot analysis of the *PMT* gene in control and antisense *PMT* root lines. A blot of genomic DNA (20 µg per lane) digested with either *Hind*III or *Xba*I was hybridised with *PMT* probe from *N. tabacum*. All antisense *PMT* lines showed additional band(s) compared to controls.

genes in associated areas of primary metabolism appear to be minimal. It is perhaps noteworthy, however, the line showing the greatest reduction in the levels of *PMT* transcript and enzyme, V-26, did show generally diminished transcript levels of several genes (such as *QPT* and *SAMDC*). Whether this is as a direct result of *PMT* down-regulation remains unclear at this time.

4.4.4 Southern blot analysis

Genomic DNA from three antisense *PMT* root lines (V-7, V-26 and V-34) and one control line (IV-15), in addition to intact root tissue from *N. tabacum* var. NC95 plants, was isolated and digested with either *Xba*I or *Hind*III. Gel blot analysis of the digested DNA, hybridised to ^{32}P-labelled *PMT* encoding sequence, revealed extra copies of *PMT* gene sequence in each of the manipulated lines (Fig. 4-22).

Digestion of genomic DNA from transgenic tissues with *Hind*III was designed to assist with the estimation of copy number of foreign gene sequences. A *Hind*III site is present to the 5' side of the *PMT* coding sequence in pFIH10 (Fig. 4-3). However, as no sites are present in the *PMT* coding sequence, or in the remainder of the construct, the next *Hind*III site to be encountered will be in genomic DNA, 3' to the insertion site of the binary vector T-DNA. Thus, after Southern hybridisation, each band on the resulting autoradiograph is generally representative of a separate insertion. Analysis of genomic DNA digested with *Hind*III showed 4 clear bands in control tissues. In antisense *PMT* line V-7, 1-2 additional *PMT* bands were apparent whilst in line V-34, 3-4 additional bands were apparent (Fig. 4-22). It is interesting to note that whilst the Southern data shown here suggest the presence of one additional *PMT* copy in root line V-26, data presented in Table 4-4 suggest the presence of three independently segregating kanamycin-resistance genes in plants regenerated from this root line. The reason(s) for this apparent discrepancy are not clear at the present time.

PMT is a member of a multigene family. Following Southern blot analyses, Hashimoto *et al.* (1998a) demonstrated that five *Hind*III genomic DNA fragments of *N. tabacum* cv. Burley 21 hybridized to a full-length *PMT* probe. A subsequent report by Riecherss and Timko (1999) similarly demonstrated the presence of five *PMT*-related

DNA sequences in the genome of *N. tabacum* cv. Xanthi. In contrast, Southern analyses performed with *N. tabacum* var. NC95 using DNA from the control root line, IV-15, and from the intact root of the parent plant revealed that only four *Hin*dIII genomic fragments hybridized to the *PMT* probe (section 4.4.4, Fig. 4-22). Such a discrepancy may be attributable to the different *N. tabacum* cultivars used in the experiment.

Analysis of *Xba*I-digested DNA of all three antisense *PMT* lines showed an additional band of 1.4 kb in each of the antisense *PMT* lines. As the *PMT* coding sequence was inserted as a 1.4 kb molecule at the *Xba*I site of pFIH10, this suggests that the construct was present in a structurally intact form in each of these manipulated lines.

Chapter 5

Discussion

Experiments described in this thesis were concerned with using the approach of antisense-mediated down-regulation of gene expression to investigate the molecular control of pyridine alkaloid metabolism in *N. tabacum*. Transformed roots of *N. tabacum*, cultured *in vitro*, were used as the main experimental tissue. These cultures are regarded as being much more genetically stable than disorganised cell cultures (Aird *et al*., 1988). If care is taken to ensure appropriate tissue culture conditions are maintained, they provide a robust experimental system to study effects of gene manipulation upon pyridine alkaloid metabolism (Hamill *et al*., 1986; 1990; Hamill and Lidgett, 1997). An added advantage of using transformed roots is that intact plants can be recovered from selected root lines which, although they often have slightly altered phenotypes due to the presence of Ri T-DNA from *A. rhizogenes* (Tepfer, 1984), do enable effects of gene manipulation to be assessed in transgenic plants with respect to alkaloid metabolism. Furthermore, the use of transformed roots is an integral component of a diverse array of experimental programs concerned with the biotechnological production of biologically active metabolites and proteins (Doran, 1997).

5.1 Down-regulation of *ADC*

In Chapter 3 of this thesis, the focus of the study was the down-regulation of *ADC* gene expression. As was noted in section 1.7.1, it was thought that this approach may provide useful information relating to the involvement of ADC in pyridine alkaloid biosynthesis in *Nicotiana* which biochemical inhibitor experiments have not been totally resolved. *ADC* antisense experiments were undertaken with the aim of producing transformed root lines with diminished ADC activity in order to compare alkaloid levels in such lines with that of wild type lines. Two constructs were assessed with respect to their ability to down-regulate *ADC* expression in transformed roots of *N. tabacum*. A

460 bp fragment of the *N. rustica ADC* coding sequence was successfully expressed in the antisense orientation in *N. tabacum* transformed root cultures. However, this did not produce any detectable reduction in endogenous *ADC* transcript levels in these tissues. In contrast, expression of a 1.2 kb *N. tabacum ADC* coding sequence in an antisense orientation did lead to a significant decrease in the levels of *ADC* transcript and also enzyme activity of antisense transformed lines (section 3.2.2.3 and 3.2.2.4). The different capacity of both fragments to down-regulate *ADC* gene expression may be due to one or more possibilities. One important parameter to consider is the degree of homology between the antisense transcript and that of the endogenous *ADC* genes. Although the 460 bp fragment was sourced from the related species *N. rustica*, as opposed to the 1.2 kb fragment which was recovered from *N. tabacum*, it is unlikely that interspecies sequence divergence rendered the 460 bp fragment ineffective. Many experiments have confirmed that heterologous genes can be used to achieve antisense effects (e.g. Carron *et al.*, 1994; reviewed in Bourque, 1995). Murray and Crockett (1992) concluded that antisense down-regulation can be successfully achieved if the transgene and target sequences are more than 80% homologous. The percentage identity of the 460 bp *N. rustica ADC* coding sequence to *N. tabacum ADC1* and *ADC2* are 92.7% and 90.3%, respectively (Appendix 4 and 5). Thus, insufficient homology between both *ADC* sequences seems unlikely to explain why the 460 bp fragment was not effective in reducing *ADC* transcript whereas the 1.2 kb fragment was effective.

Different lengths of antisense RNA transcripts may have contributed to their different capacities to down-regulate *ADC* expression, although it is noteworthy that most naturally occurring antisense RNAs in prokaryotes are relatively short (Takayama and Inouye, 1990; Murray and Crockett, 1992). At least two suggestions have been put forward to explain the effectiveness of short anti-mRNA transcripts (Murray and Crockett, 1992). First, at least in bacteria, it appears that short mRNA transcripts are produced at a faster rate than larger mRNA transcripts. Secondly, the rate of hybridisation of a larger antisense transcript to its target will tend to be slower than that of a shorter molecule. In bacteria also, the region of the gene represented by the antisense transcript can affect its capacity to down-regulate gene expression. Daugherty *et al.* (1989) and Hirashima *et al.* (1989) reported that relatively short antisense RNA

molecules (381 bp and 33 bp, respectively) which overlapped the ribosome binding sites were the most effective for down-regulation of gene expression in bacteria.

In higher plants several groups have experimented with the expression of constructs representing various regions of target genes in an antisense orientation, however no consensus has been established as to the efficacy of any particular region of a gene's coding sequence (reviewed in Bourque, 1995). A number of experiments have been conducted to examine the capacity of various regions of reporter genes to down-regulate gene expression in transgenic plants previously transformed with that reporter gene. In an experiment involving the retransformation of transgenic tobacco plants containing the chloramphenicol acetyltransferase (*CAT*) gene, it was shown that expression of the 5'-terminal 172 bp of the *CAT* gene in the antisense direction was less effective than expression of the full-length *CAT* gene sequence (Delauney *et al.*, 1988). Sandler *et al.*, (1988) investigated the effect of *nos* antisense sequences from different regions of the gene on the expression of nopaline synthase (*nos*) in transgenic containing the *nos* gene. They found that inhibition of *nos* expression varied with the region of *nos* antisense that was used and that antisense sequences from the 3' region of *nos* were even more effective than the full-length coding region.

In a comparable experiment involving the retransformation of GUS positive *N. plumbaginifolia*, Cannon *et al.* (1990) showed up to 100% inhibition of *GUS* gene expression in transgenic plants using an antisense RNA with a 41-base homology spanning the translation start codon of the gene. In experiments aimed at down-regulating an endogenous gene, a comparison of the effectiveness of antisense chalcone synthase (*CHS*) fragments in petunia showed that antisense constructs representing the 3' portion of the *CHS* gene were more effective in decreasing floral pigmentation than constructs representing the 5' portion of the gene (Mol *et al.*, 1989; van der Krol *et al.*, 1990).

The differences in levels of inhibition brought about by the various fragments used to produce antisense sequences may indicate that the optimal region and size of an effective antisense sequence can be influenced by secondary structure of the target RNAs or the antisense RNAs, or both. In the present study, it seems that a 460 bp

fragment representing the mid portion of the *ADC* coding sequence, although capable of producing antisense mRNA as confirmed by Northern analysis using strand-specific probes, is ineffective as an antisense sequence in down-regulating gene expression – at least in *N. tabacum*. On the other hand, a 1.2 kb fragment from the mid-5' region of the coding sequence is quite effective in down-regulating gene expression. Further experiments would be required to establish whether full-length antisense transcripts, or shorter transcripts targeted to particular regions of the coding sequence such as the translation start point, would be more effective than the 1.2 kb fragment used in this study.

Using the 1.2 kb antisense *ADC* construct, several transformed root lines were recovered in this study with < ~ 25% of wild type *ADC* transcript remaining (Fig. 3-19-I). Assessment of these lines for ADC activity showed that compared to controls, ADC activity was reduced by 50 – 60% (Fig. 3-20). As was noted in chapter 1 (section 1.4.1.3), an apparent lack of a direct correlation between transcript abundance and enzyme activity may be explained by the observation that ADC has been reported to be subject to considerable post-transcriptional regulation and/or post-translational controls (Malmberg *et al.*, 1992; Rastogi *et al.*, 1993; Malmberg and Cellino, 1994). Studies in transgenic tobacco and rice over-expressing oat *ADC* also noted that the relationship between oat *ADC* transcript level and ADC activity was not directly proportional (Masgrau *et al.*, 1997; Carpell *et al.*, 1998). Thus it is possible that a 90% or greater reduction of ADC activity, using a conventional antisense approach, may be difficult or impossible as it is likely that even a few mRNA molecules "escaping" inactivation by antisense sequences are likely to be translated efficiently to produce disproportionately elevated levels of active ADC enzyme.

Examination of the growth kinetics of 1.2 kb antisense *ADC* transformed root lines showed that there was no significant difference between them and controls. No published reports exist which correlate the diminution of ADC activity by biochemical inhibitors and the effects on growth of tobacco root cultures. However, the combined reports of Walton *et al.*, (1990) and Robins *et al.*, (1991b), noted that even though *D. stramonium* transformed root cultures treated with 1-2.5 mM DFMA possess very low levels of residual ADC activity and approximately 40-50% of residual ODC activity,

their growth was not significantly reduced relative to untreated controls. Thus it is probably not surprising that no alteration in the growth kinetics of antisense *ADC* tobacco transformed root lines was observed relative to controls in the present study.

Initial examination of the 1.2 kb antisense *ADC* transformed roots generated in this study also suggested that they had a similar alkaloid content as control lines. However, careful analysis over the course of a growth cycle of several transformed root lines containing down-regulated *ADC* (lines II 26, II 32, II 34 and II 39) showed that whilst they had close to normal levels of alkaloid during the early and mid-phases of the growth cycle, they had reduced nicotine levels relative to controls by the end of the growth cycle. Two of these lines (II-34 and II 39) also had slightly elevated levels of anatabine at the end of their growth cycle relative to control lines. This stage of the growth cycle is typically characterised by relatively low levels of ODC and ADC activity in transformed roots of *Nicotiana* (Hamill *et al.*, 1990) and also *Datura* (Robins *et al.*, 1990,1991c; Michael *et al.*, 1996). Such a relative decrease in the nicotine content of *N. tabacum* transformed root lines, together with a relative increase in the levels of anatabine, suggests that the antisense *ADC* manipulation may have reduced the supply of putrescine-derived metabolites destined for nicotine biosynthesis at this late stage of the growth cycle whilst the supply of nicotinic acid continued as per normal via the QPT route (see also results in chapter 4 and discussion in 5.2 below). Towards the end of the growth cycle, reduced ADC activity due to the antisense manipulation may have produced a reduced pool of putrescine that was used preferentially for growth as opposed to alkaloid production. These observations do not, however, rule out the possibility that a low level of ADC activity is sufficient to maintain a pool of putrescine used exclusively or mainly for alkaloid biosynthesis which, in antisense lines, becomes somewhat limiting in the latter part of the growth phase of transformed roots when expression of endogenous *ADC* is reduced.

In conclusion, the current study represents the first attempt to quantify accurately the effects on pyridine alkaloid metabolism by reducing the supply of putrescine in tobacco tissues using an antisense approach to diminish ADC activity. Some evidence was produced that a ~50% reduction in ADC activity can decrease the nicotine content of transformed roots, together with a slight increase in anatabine levels, toward the end

of the growth cycle. In contrast to biochemical inhibitor feeding experiments involving DFMA, where negative effects upon ODC can not be ruled out, evidence from the current study suggests that reductions in *ADC* transcript/enzyme levels as a result of the antisense manipulation do not cause alterations in *ODC* transcript/enzyme levels (Figs. 3-19, 3-20, 3-24 and 3-25). Clearly, however, many further experiments are required to enable definitive statements to be made regarding the relative contributions of ODC vs ADC to the synthesis of putrescine used to synthesise nicotine in *N. tabacum* transformed roots. Some of the more obvious experiments that could be usefully undertaken are outlined below.

1. Using the antisense *ADC* lines created in this study, it would be interesting to also undertake a detailed analysis of polyamines, free and conjugated, at all stages of growth and development in root lines and regenerated plants. Though technically demanding, such studies could provide valuable insights into both the role(s) of these metabolites *in vivo* and their capacity to be altered by down-regulation of *ADC* gene expression.

2. A detailed analysis of regenerated transgenic plants containing the 1.2 kb antisense *ADC* construct (or possibly a more effective one) to determine if reduced ADC activity enabled normal growth and alkaloid production under all conceivable growth conditions, particularly under conditions of limited nitrogen availability or herbivore attack which are known to place substantial burdens on the alkaloid biosynthetic capacity of *Nicotiana* plants (Baldwin *et al.*, 1994). The present study may provide a clue that under such conditions, such plants may in fact show a reduced capacity to elicit a wild type chemical response to such environmental stresses.

3. Recovery of transformants (both transformed roots and plants) with strongly down-regulated ODC expression/activity. If such lines were viable, and contained normal ADC activity, an analysis of their growth, alkaloid and polyamine (both conjugated and free) profiles may enable deductions to be made as to the contribution of the ODC route to putrescine pools used for alkaloid biosynthesis – particularly, as noted above, under conditions of environmental stress such as wounding or in the latter part of the growth cycle when any limitations in biosynthetic capacity are likely to be most pronounced.

4. Sexual crossing of transgenic plants with down-regulated *ODC* and *ADC* to determine whether combined or even synergistic interactions between both antisense transgenes occurs with regards to putrescine synthesis and, if so, whether this affects growth/ development or alkaloid biosynthesis or both. Feeding radioactive ornithine/arginine to ODC/ADC-deficient lines may also be useful to determine whether each route to putrescine is differentially utilised in antisense lines relative to the situation in normal, wild type lines.

5.2 Down-regulation of PMT

In Chapter 4 of this thesis, the focus of experiments was the down-regulation of PMT using an antisense approach. The main conceptual difference between these experiments and those discussed above involving ADC, is of course that PMT is considered to belong exclusively to secondary metabolism as it catalyses the first committed step in providing putrescine-derived intermediates for nicotine biosynthesis in *N. tabacum*. As such, we predicted that it should both be possible to recover viable lines with strongly down-regulated PMT activity and that such lines should have a severely reduced capacity to synthesise nicotine. This proved to be the case, with several transformed root lines being recovered that possessed very low levels of *PMT* transcript compared to controls. Such lines also had markedly reduced enzyme activity with one antisense *PMT* line in particular (line V-26) exhibiting PMT activity about 10% of wild type and about half of that found in transformed roots of a low alkaloid variety of *N. tabacum* (LAFC53). Levels of PMT activity in wild type and low alkaloid variety transformed roots were comparable to activities reported previously for non-transformed roots of wild type and low alkaloid varieties of *N. tabacum*, respectively, which were maintained *in vitro* in medium containing auxin to stimulate growth (Hibi *et al.*, 1994).

The capacity to down-regulate *PMT* appeared to be independent of the number of copies of the foreign antisense *PMT* sequence. Several reports in the literature have also not observed a correlation between antisense transcript levels or antisense gene copy number and the level of phenotypic alteration caused by the presence of the

antisense sequence (reviewed in Bourque, 1995). For example, van der Krol *et al.* (1988), working with transgenic petunia, observed no correlation between the number of antisense chalcone synthase gene copies and the steady state level of antisense RNA found in transgenic plants. Also, Carron *et al.*, (1994) observed that no correlation existed between antisense copy number of an antisense *DFR* sequence and its capacity to diminish condensed tannin levels in transformed roots of *L. corniculatus*. The wide variations observed in the effectiveness of antisense sequences in suppressing gene activity may be attributed to differences in the relative positions of the antisense gene within the genome of the transgenic cell – the so called 'position effect' phenomenon (Bourque, 1995). In over-expression experiments, transgene copy number and transcript levels have also been found to be not necessarily strongly correlated. For example Leech *et al.* (1998) studied transgenic tobacco expressing two consecutive genes, encoding tryptophan decarboxylase and strictosidine synthase, in the monoterprenoid alkaloid biosynthesis pathway of *Catharanthus roseus*. No clear correlation between the number of integration events of a specific transgene and the levels of accumulated transcript was observed in this case.

Effects of down regulated *PMT* expression upon alkaloid profiles of transformed root lines were, in part, predictable but also provided some new insights into the control of alkaloid biosynthesis in *N. tabacum*. As was predicted, reduced PMT activity was associated with reduced nicotine levels of transformants, with concentrations falling to levels at or below that of roots of the low alkaloid variety, LAFC53 (Fig. 4-18). Transformed roots of *N. tabacum* var. NC95 with reduced PMT activity and reduced nicotine levels were also correlated with increased anatabine content. This alkaloid is present at 10-20% of the levels of nicotine in intact root of *N. tabacum* (Saitoh *et al.*, 1985; Sisson and Severson, 1990) and also in root cultures of *N. rustica* (Hamill *et al.*, 1986). Anatabine, in fact, is not found at high levels in any *Nicotiana* species studies to date (Saitoh *et al.*, 1985; Sisson and Severson 1990) and appears to have been largely ignored in studies into pyridine alkaloid metabolism. A comprehensive search of available literary databases reveals only a small number of references where anatabine is the primary focus of the article. In concurrence with this, it is not commercially

available and considerable effort was required during this study to obtain a sample to authenticate and quantify the elevated levels seen in several antisense *PMT* lines.

At a mechanistic level, the explanation for elevated anatabine levels in antisense *PMT* transgenic root lines of *N. tabacum* appears relatively straightforward. Though the supply of intermediates required to synthesise the *N*-methylpyrrolidine ring of nicotine is diminished, the supply of nicotinic acid is likely to be maintained as per normal and thus excess nicotinic acid is used to synthesise anatabine. This hypothesis suggests the lack of a feedback mechanism to prevent over-production of nicotinic acid. The results of the Northern experiments suggests this is true, at least to a considerable extent, as several antisense *PMT* lines had *QPT* transcript levels that were comparable with controls. It may be noteworthy, however, that the most severely affected line, V-26, did have lower *QPT* transcript levels than controls or other antisense lines raising the possibility that some degree of feedback inhibition of *QPT* transcription in transgenic root lines with very reduced PMT activity may occur. The enzyme responsible for anatabine synthesis has not been positively identified, but it may be the same enzyme that is responsible for the final step in nicotine synthesis. This enzyme has also been implicated in causing increased anabasine levels in *N. hesperis, N. rustica* and *N. tabacum* tissues following exposure to elevated cadaverine (Fig. 1-3) (Walton and Belshaw, 1988; Walton *et al.*, 1988; Fecker *et al.*, 1993). It is possible that the capacity of *Nicotiana* root tissues to convert excess nicotinic acid to anatabine represents a detoxification mechanism whereby the plant roots can effectively rid themselves of excess nicotinic acid which may be otherwise inhibitory to growth. Previous experiments have shown that feeding nicotinic acid to root cultures of *N. rustica* was phytostatic at 1 mM (Robins *et al.*, 1987). Interestingly in the study of Robins *et al.* (1987) and also in a subsequent report by Friesen *et al.* (1992) working with *N. alata* root cultures, feeding of nicotinic acid was found to lead to uncharacteristically high levels of anatabine in extracts of these tissues.

Polyamine levels of the antisense *PMT* root lines produced in this study were not assessed and thus additional studies would be necessary to investigate whether polyamine metabolism was unduly disturbed by the down-regulation of PMT in such root lines. It is quite possible that the antisense lines did have elevated putrescine

and/or polyamine levels as gene transcripts encoding ODC, ADC, SAMDC, SPDS and SPMS were comparable between antisense *PMT* root lines and wild type. As antisense *PMT* root lines exhibited comparable growth cycle characteristics to transformed roots of both the wild type (NC95) and low alkaloid variety (LAFC 53), it is clear that any alterations in polyamine metabolism resulting from the down-regulation of PMT did not affect root growth *in vitro*.

In the present study, as expected, regenerated plants from several antisense *PMT* root lines of *N. tabacum* also showed, for the most part, reduced nicotine levels throughout the plant. Similar observations have been made in transgenic *N. sylvestris* in which *PMT* levels were reduced by either co-suppression (Sato *et al.*, 2001) or by antisense experiments (Voelckel *et al.*, 2001). However, one line (V-7) in which plants were recovered from two separate regeneration experiments, possessed nicotine levels comparable to those in control regenerated plants of the high alkaloid variety NC95. The reasons for this are not clear but a similar phenomenon has been reported by Robbins *et al*, (1998) who analysed condensed tannins (CT) in plants regenerated from hairy roots of *L. corniculatus*, CT levels had been reduced by up to 80 % due to antisense expression of the *A. majus DFR* gene (Carron *et al.*, 1994). In that study, it was observed that only one of the antisense root lines produced a corresponding CT phenotype in regenerated shoot tissues leading to the conclusion that it is not possible to accurately predict the biochemical phenotype of an antisense regenerated plant by screening at the transformed root level (Robbins *et al.*, 1998). It is possible that a gene silencing process, such as methylation of the antisense transcript, occurred during or shortly after the regeneration process in these cases thereby inactivating the transgene. Inactivation or silencing of transgene expression by methylation or other processes has been reported in transgenic plants by previous workers (Matzke *et al.*, 1989; Mallory *et al.*, 2001; Kloti *et al.*, 2002).

In contrast to the reports of Sato *et al.* (2001) and Voelckel *et al.* (2001), this study also found significantly elevated levels of anatabine to be present in leaf tissues of plants with reduced nicotine that were regenerated from antisense *PMT* root lines. As *QPT* is expressed predominantly in roots of *N. tabacum* (Sinclair *et al*, 2001), it seems likely this is as a result of translocation of anatabine from roots to shoot as in the case of

nicotine. The production of viable, rapidly growing and, as far as can be judged, normal plant *N. tabacum* tissues with markedly elevated anatabine levels raises the question as to why this alkaloid is not found at high levels in any natural *Nicotiana* species. As was noted in chapter 1, nicotine, or its similarly toxic demethylated derivative nornicotine, predominate in most *Nicotiana* species. In some species however, appreciable levels of anabasine are found and in one species, *N. glauca*, anabasine predominates and nicotine represents less than 15% of the alkaloid fraction in leaf tissues (Saitoh *et al.*, 1985; Sisson and Seversson 1990). It is possible that anatabine is not as toxic to predators, or is less stable *in vivo*, than these other alkaloids – no toxicity data appears to be available in the scientific literature. Given its close structural similarities to anabasine (Fig. 1-1) however, which is toxic to both mammals and insects (Budavari *et al.*, 1996), the biological properties of anatabine might be predicted to be similar. Future experiments could perhaps test the capacity of *N. tabacum* plants possessing low level of nicotine and high levels of anatabine to repel or prove toxic to herbivores/insect pests as opposed to plants possessing characteristically high levels of nicotine and low levels of anatabine. Suitable insects to test such ideas may include larvae of generalist herbivores such as species in the *Helicoverpa* genus and also the specialist, nicotine-adapted herbivore *Manduca sexta* (tobacco hornworm) (Voelckel *et al.*, 2001).

In the present study, all regenerated plants exhibited a somewhat bushy appearance with slightly wrinkled leaves – a phenotype typical of that described previously for transgenic *N. tabacum* containing Ri T-DNA (Tepfer, 1984). Antisense *PMT* transgenic plants were not noticeably different from Ri T-DNA control plants, however, though it is of course possible that subtle differences in phenotype between these plants and controls existed but were masked by the T phenotype. To investigate this area further, studies involving the generation of transgenic plants containing the antisense construct utilised in the present study should be undertaken with disarmed *A. tumefaciens* rather than wild type *A. rhizogenes* for transformation. In a recent report, Sato *et al.* (2001) reported on the results of experiments involving disarmed *A. tumefaciens* to recover transformed *N. sylvestris* plants containing a construct in which the *PMT* coding sequence was placed under transcriptional control of the CaMV35S promoter. Transgenic plants containing *PMT* transcript levels elevated, relative to wild type, were

phenotypically normal, whereas a cosuppression line with *PMT* transcript levels only 16% that of wild type exhibited several distinct phenotypes. Abnormalities included a branched inflorescence stem, a continuous spiral sheet of leaf-like tissues along the stem caused by neighbouring leaves fusing at the basal region and a small seed set from self-pollinated flowers. Sato *et al.* (2001) suggested that these morphological changes may be caused by the increased accumulation of pathway intermediates, especially putrescine and spermidine.

5.3 Future directions

In conclusion, this thesis makes a contribution to our understanding of the control of pyridine alkaloid metabolism in *Nicotiana tabacum*, using the technique of antisense down-regulation of gene expression to target genes encoding ADC and PMT. Since many of the other genes encoding enzymes in this area of metabolism, and in ancillary areas of primary metabolism, have been cloned and characterised in recent years (Table 1-2), additional experiments may be warranted in future to explore the effects of down-regulating these genes also, both individually and in combination. As a result of recent improvements in our understanding of the mechanisms by which double-stranded RNA leads to down-regulation of specific gene activity (Waterhouse *et al.*, 1998, 2001; Vance and Vaucheret, 2001; Jones *et al.*, 2001; Hutvagner and Zamore, 2002), improved vectors have been developed that specifically produce double-stranded RNA corresponding to a given cDNA sequence, e.g. the pHANNIBAL vector (Wesley *et al.*, 2001). Future use of such vectors may allow the identification of *N. tabacum* transformants with very low or essentially zero activity of genes where translational control may enable even small amounts of mRNA to produce significant levels of enzyme activity, as appears to be the case for ADC in *N. tabacum*. Such experiments will contribute, in an iterative manner, to a greater appreciation of the complexities of secondary metabolite production in plants.

Appendices

MADCIIIF 5' T C T A G A G T A/C/T T G C/T A A C/T G G C/T T A C/T A A A/G G A 3'
Xbal

MADCVR 5' G G T C T A G A T C G/A T A G/A T C I A C I C C I A/G I C C A/G C C 3'
Xbal

PW1-35S 5' G G G G G T A C C G A A T T C C T G A C G T A A G G G A T G A C G C A C 3'
KpnI EcoRI

PW1-term 5' G G G T C T A G A A A G G T T A C T G G A T T T T G G T T T T A G G A 3'
Xbal HindIII

YCIF 5' G G T C T A G A C T T G T T G T C C G T T T T C C T G A 3'
Xbal

EYIR 5' G G T C T A G A T G G/A A T T G G A A C A A T A G G A A A 3'
Xbal

Appendix 1 Oligonucleotide primers used in this study.

Appendix 2 Probes used in this study.

Gene	Source
ADC	1.) For section 3.1 and 3.2.1 Plasmid pYC1B (chapter 3) contains a 460 bp DNA insert representing 460 bp of *N. rustica ADC* cloned into pBluescript (Fig. 3-1). The PCR fragment was recovered from *N. rustica* genomic DNA using oligonucleotide primers MADCIIIF and MADCVR (Doblin, 1993). The 460 bp insert is released by digestion with *Xba*I. 2.) For section 3.2.2.3 and section 4.4.3 Plasmid pYC2T (chapter 3) contains a 1.2 kb DNA insert representing the mid portion of *N. tabacum ADC* cloned into pGEM-T (Fig. 3-11). The PCR fragment was recovered from *N. tabacum* root genomic DNA using oligonucleotide primers YC1F and EYIR (section 3.2.1). The 1.2 kb insert is released by digestion with *Xba*I.
ODC	Plasmid pODC#8 contains a 800 bp DNA insert, cloned into pBluescript, representing the 5' portion of *N. tabacum ODC* cDNA (Lidgett 1997; accession no Y110472). An 800 bp fragment suitable as a molecular probe is released by digestion with *Xba*I and *Bam*HI.
PMT	Plasmid pETPMT contains the full-length *PMT* coding sequence *of N. tabacum* (Hibi *et al.*, 1994; accession no D28506) kindly supplied by A/Prof T. Hashimoto, Nara Institute of Technology, Japan. The coding sequence is released as a 1.4 kb fragment by digestion with B*am*HI and E*co*RI.
QPT	Plasmid pRQPT1 contains the coding sequence of *N. rustica QPT* in pBluescript (Sinclair *et al.*, 2000; accession no AJ243436) and released as a 1.3 kb fragment by digestion with E*co*RI and X*ho*I.
SAMDC	Plasmid pTSmDC1 (kindly supplied by Dr. A. Michael, BBSRC Institute Food Research, UK) contains a DNA insert cloned into pBluescript which represents approximately half of *N. tabacum SAMDC* coding sequence. The insert is highly homologous to the 5' portion of the *N. sylvestris* cDNA representing *SAMDC* (accesion no AB015609) and is released from pTSmDC1 as an 800 bp fragment by digestion with X*ba*I and *Kpn*I.
SPDS	Plasmid pDsSS2 (kindly supplied by Dr. A. Michael, BBSRC Institute Food Research, UK) contains *D. stramonium* spermidine synthase (*SS2*) cDNA sequence (accession no Y08253) in pBluescript. The 1.2 kb DNA insert possesses 90.5% nucleotide homology with the *N. sylvestris* spermidine synthase genes (accession no AB006692; Hashimoto *et al.*, 1998b). The insert in pDsSS2 is released by digestion with *Xba*I and *Kpn*I.
SAMS	A purified PCR product was used as a probe (identity confirmed by sequence analysis; accession no AB006187) representing the *N. tabacum* SAM synthase coding sequence. The PCR product was amplified from *N. tabacum* root mRNA/cDNA using oligonucleotides representing approximately 1 kb of tobacco SAM synthase coding sequence (Forward oligonucleotide position = 64-84: 5' CAAGCTCTGTGACCAGGTCTC3'; reverse oligonucleotide position =1027-1047: 5'GACGGCCTGAAGTCAAAGTTCTCC3').
Ubiquitin	Plasmid pJAM293 contains a cDNA insert, representing the coding sequence of the *Antirhinum majus* ubiqitin gene cloned into pBluescript which was kindly supplied by Dr. Cathie Martin, John Innes Institute, UK. The 1.8 kb DNA insert is released by digestion with *Eco*R1.

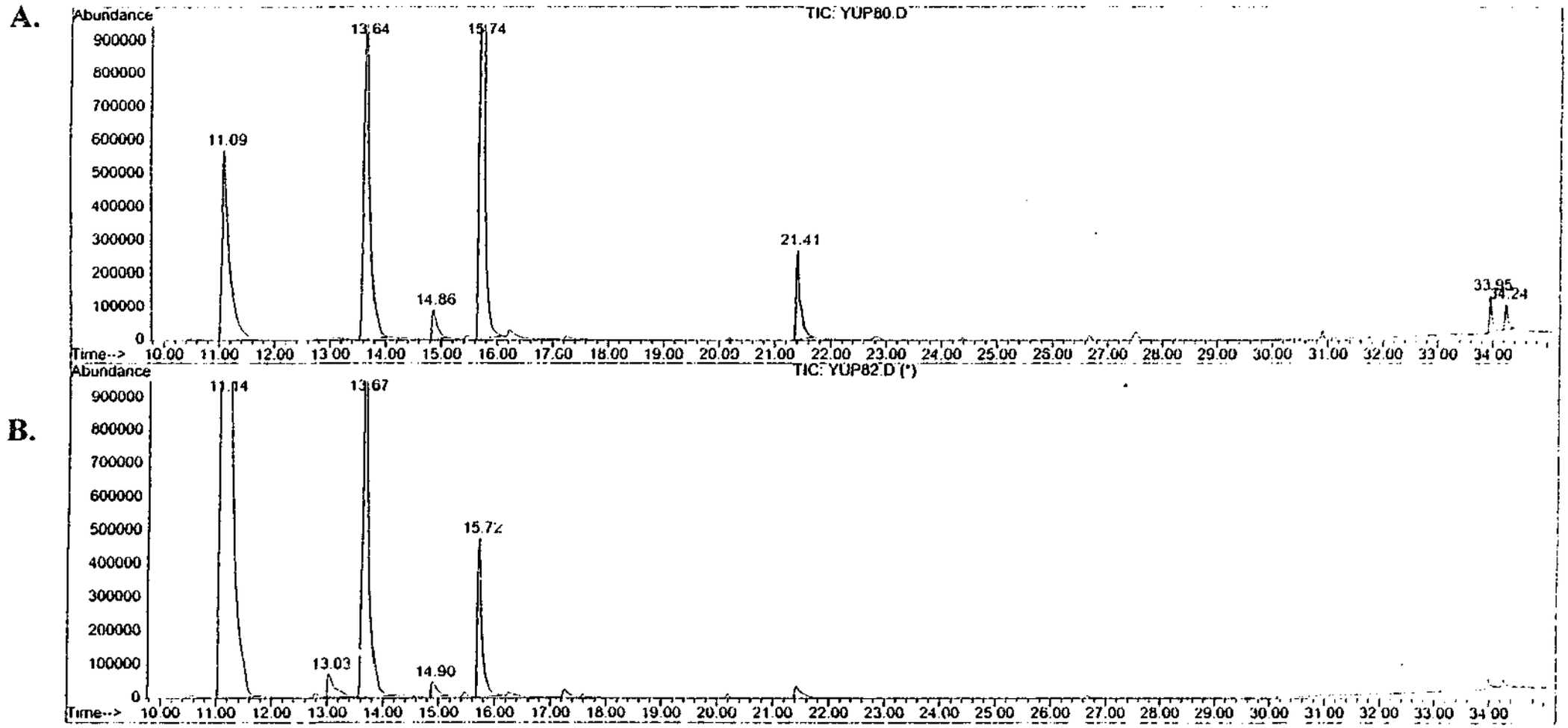

Appendix 3 GC-MS analysis

GC chromatograms comparing alkaloid extracts of antisense *PMT* root line V-26 (A) with control root line IV-10 (B) at day 20 of the growth cycle (Fig. 4-10). The abundance of the internal standard (2, 2'-dipyridyl) at RT 13.6 mins was quantitatively similar in both samples. The peaks at RT 11.1 and 15.7 mins were identified as nicotine and anatabine by MS (Appendices 3-C and D). The antisense line (A) contained a much lower level of nicotine (RT 11.1 mins) relative to the control line (B). Conversely, the antisense root line contained a considerably higher level of anatabine (RT 15.7 mins). It is also noteworthy that the antisense line possessed higher levels of metabolites with RTs at 21.4, 33.9 and 34.2 mins, compared to the control line. One of these (RT = 33.9 mins) was tentatively identified as 3,3'-(2,4-piperidinediyl) bis-pyridine suggesting that the antisense line also possessed higher levels of other pyridine nucleotide derivatives than the control line.

C.

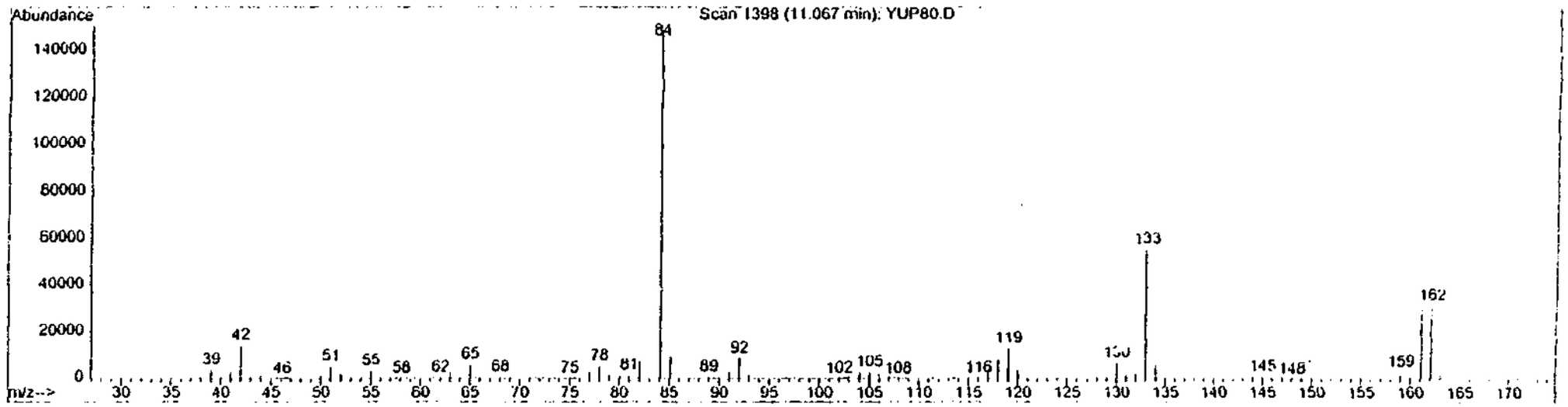

D.

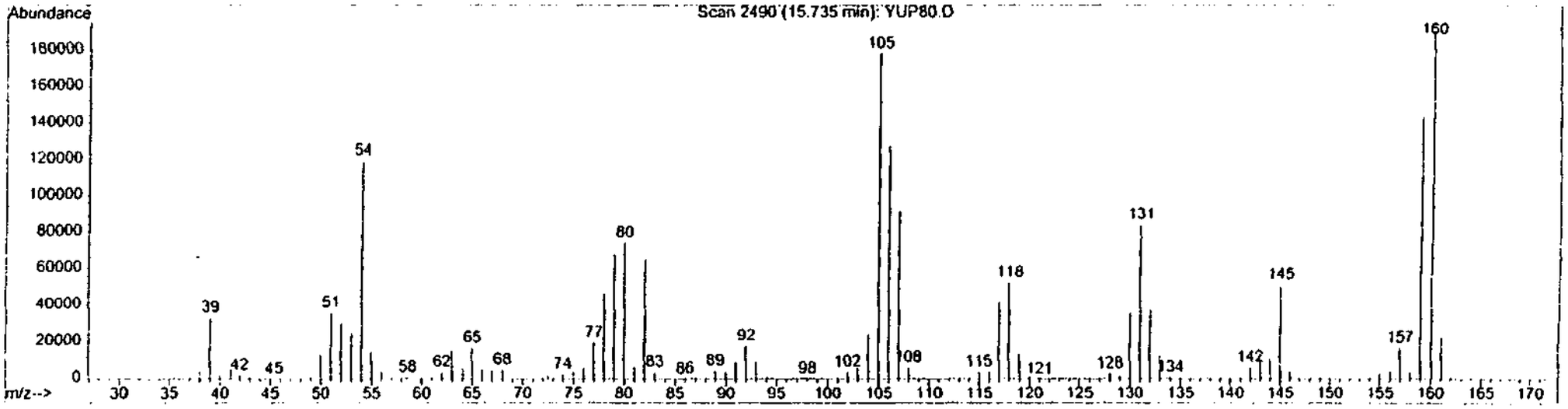

Appendix 3 (continued)

(C) Mass spectrum of metabolite RT 11.1 mins identified as nicotine by comparison with the HP library database.

(D) Mass spectrum of metabolite RT 15.7 mins identified as anatabine by comparison with the mass spectrum of the authentic standard (not shown).

Appendix 3 E i : Mass Spectrum of the Anatabine standard supplied by Dr Patrick Lipiello - p85)

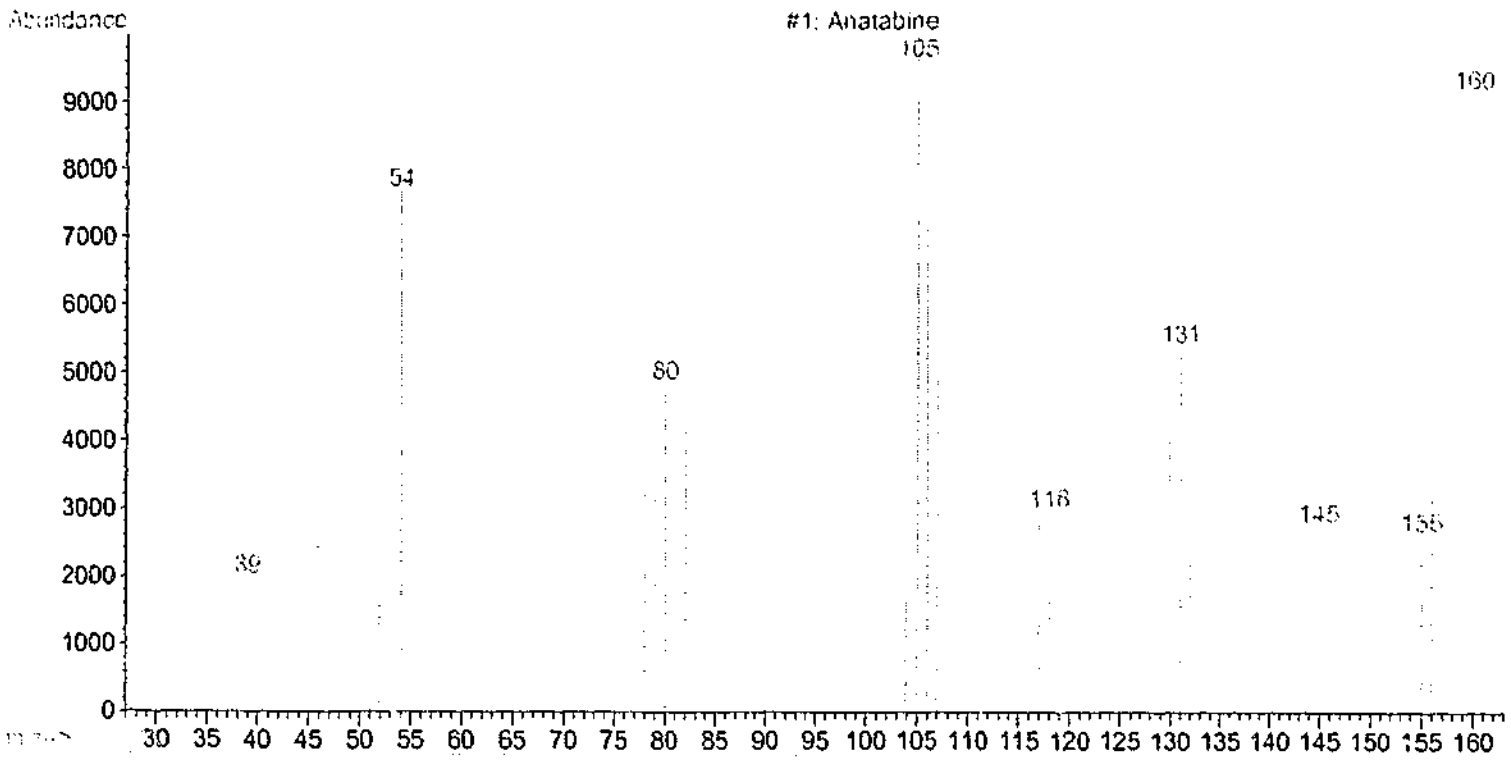

Appendix 3E ii : Mass Spectrum of Anatabine
(courtesy of Dr Mike Zimmermann, Philip Morris RD &E Center, Richmond, USA)

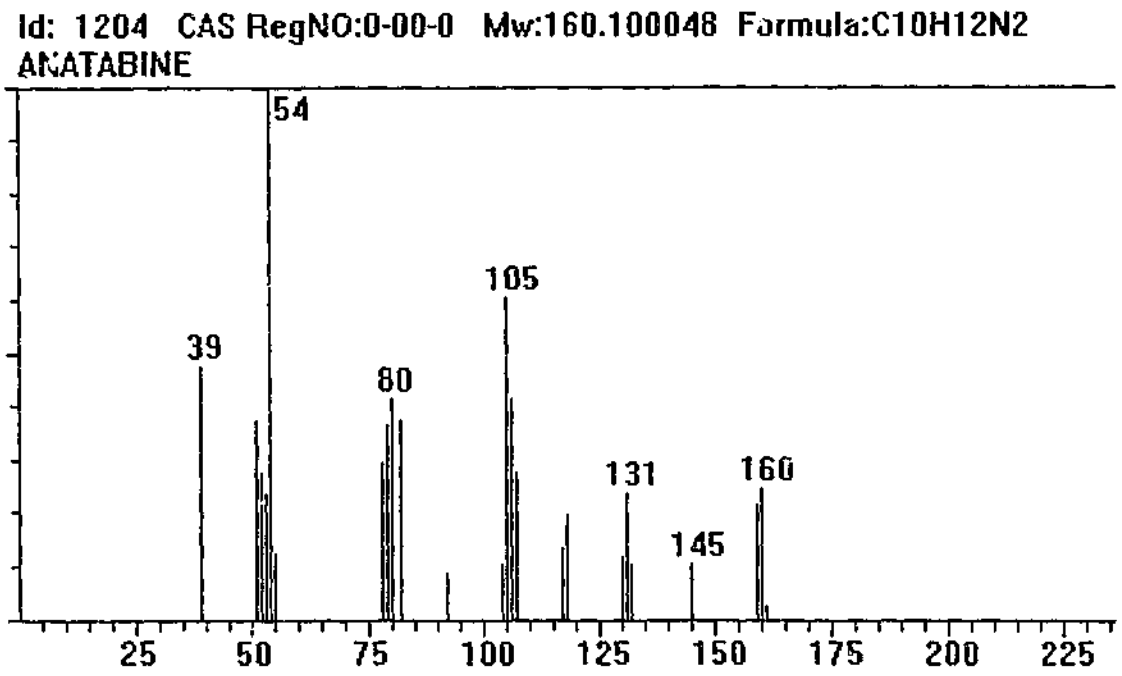

Appendix 3 F: Mass Spectrum of Nicotine (Mizrachi *et al.*, 2000)

REFERENCE: Mizrachi N, Levy S, Goren Z. Fatal poisoning from nicotiana glauca leaves: identification of anabasine by gas-chromatography/mass spectrometry. J Forensic Sci 2000;45(3): 736–741.

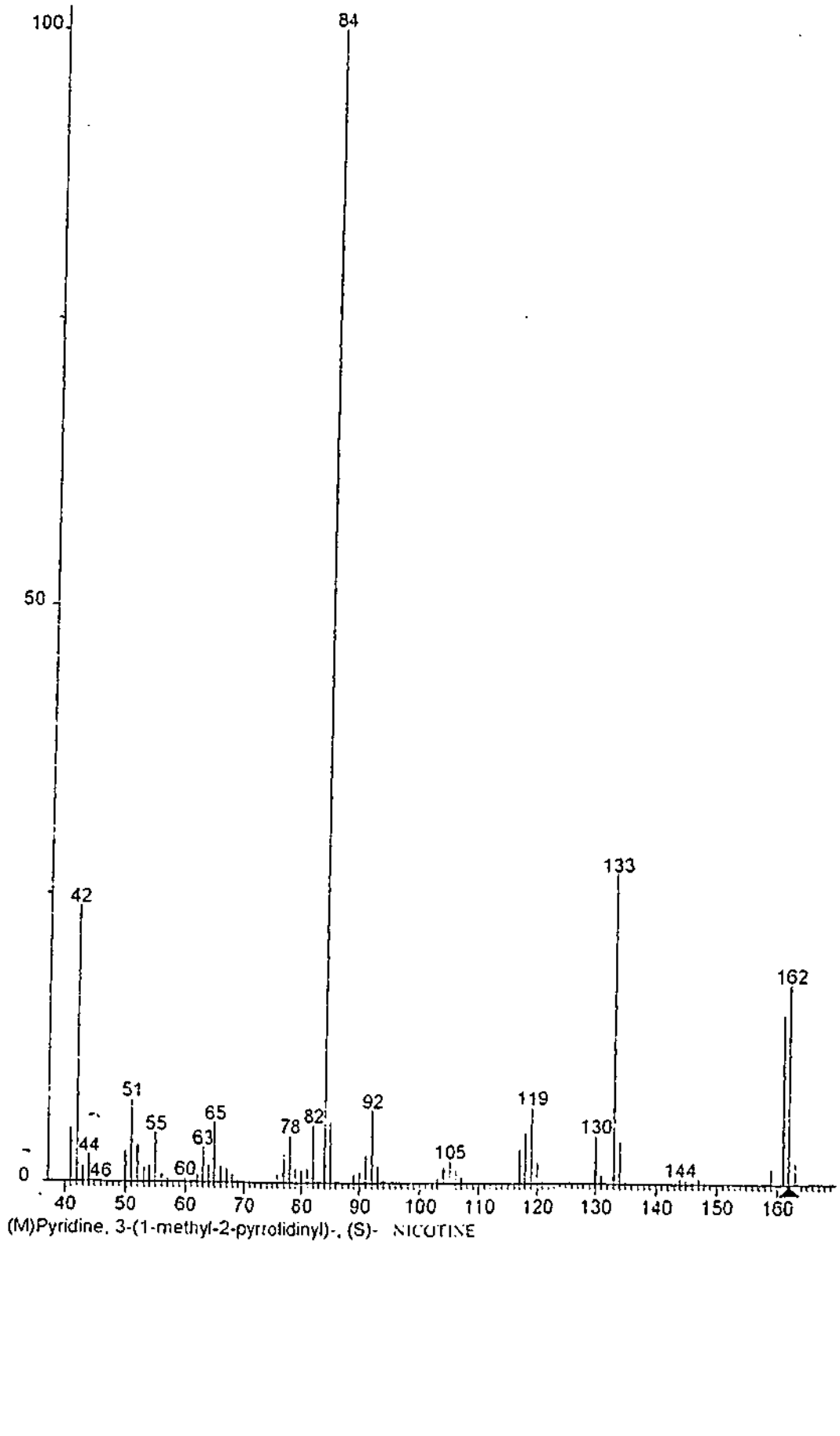

Appendix 3 G i: Mass Spectrum of Anabasine (Mizrachi *et al*., 2000)

REFERENCE: Mizrachi N, Levy S, Goren Z. Fatal poisoning from nicotiana glauca leaves: identification of anabasine by gas-chromatography/mass spectrometry. J Forensic Sci 2000;45(3): 736-741.

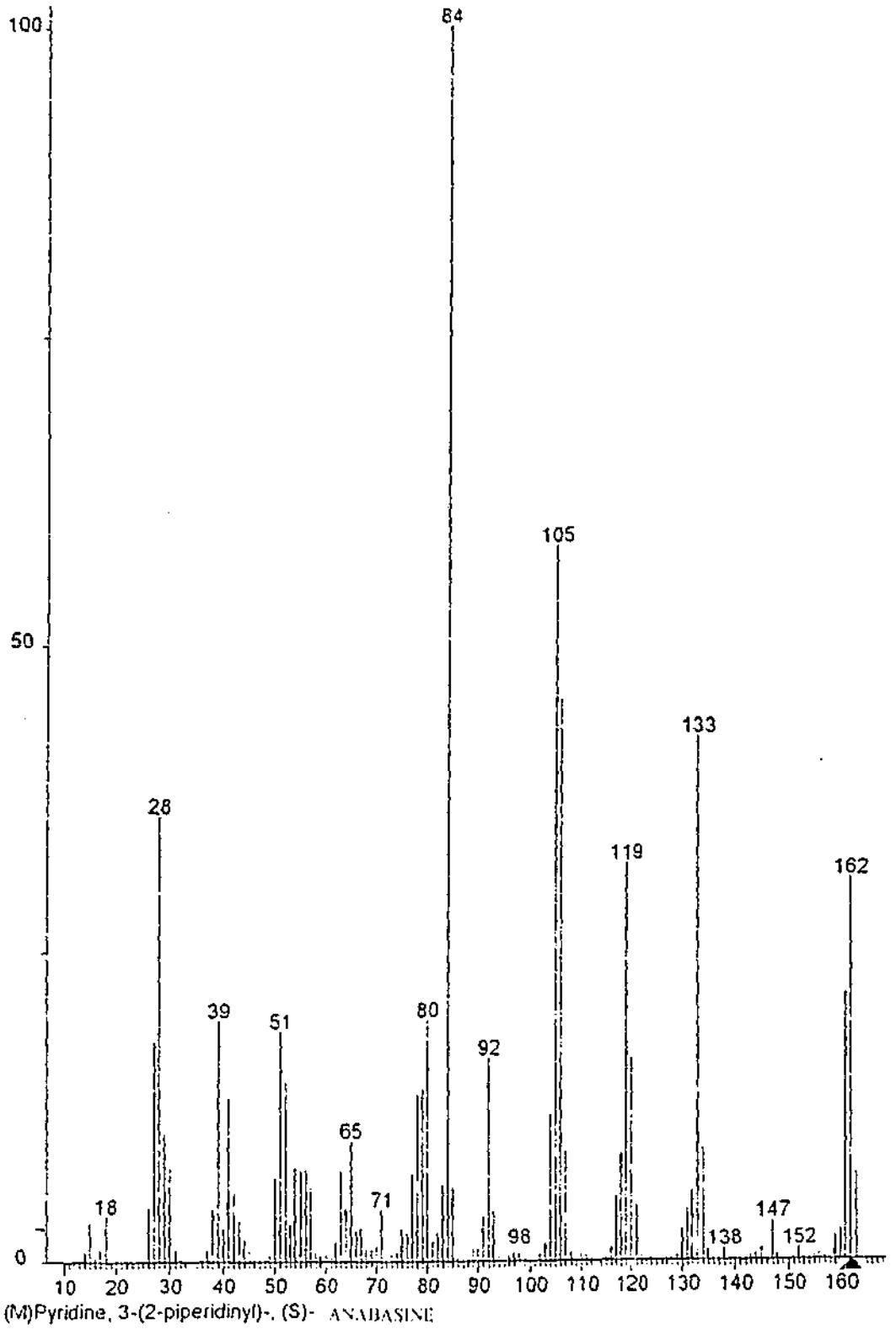

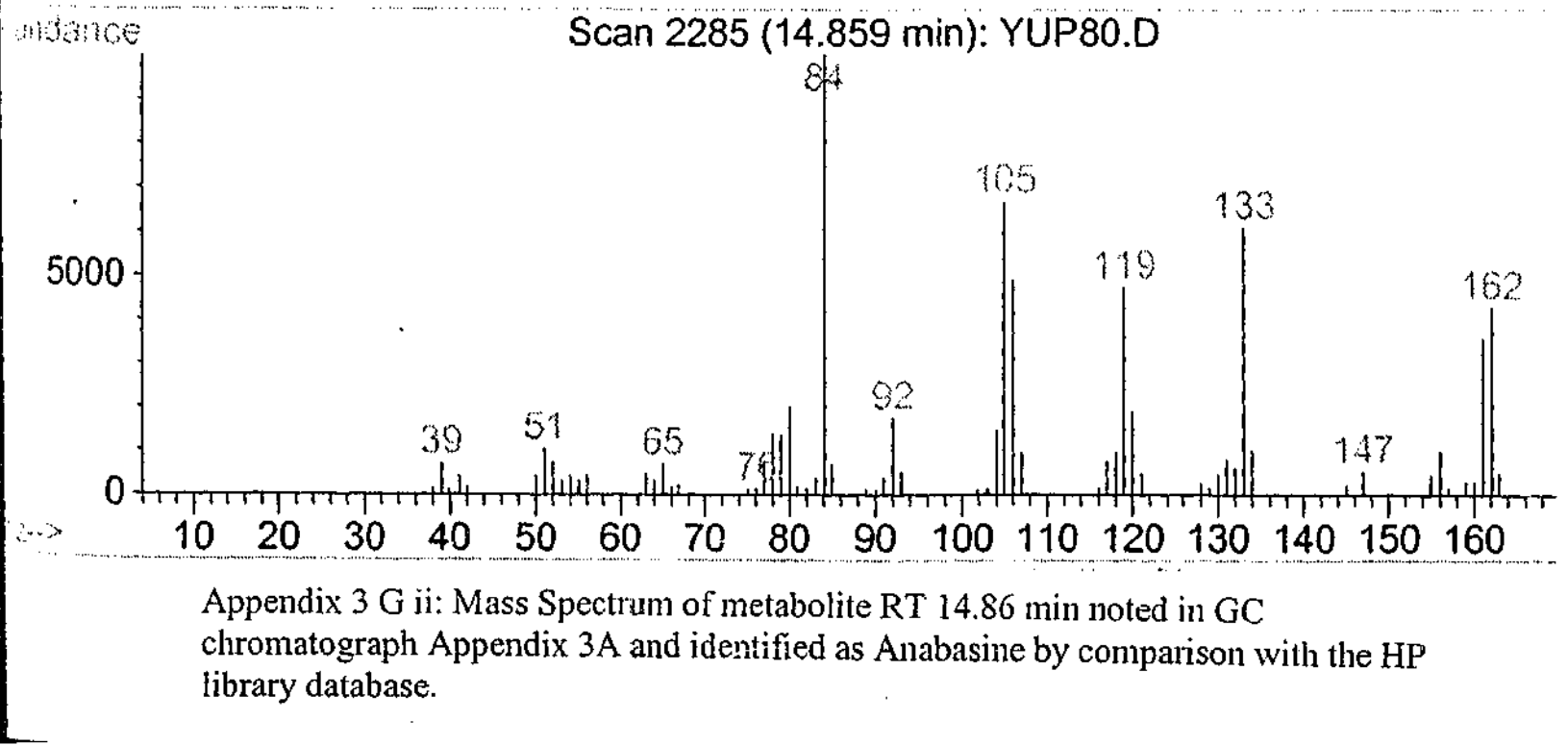

Appendix 3 G ii: Mass Spectrum of metabolite RT 14.86 min noted in GC chromatograph Appendix 3A and identified as Anabasine by comparison with the HP library database.

```
GAP of: N. tabacum ADC1 to: N. rustica 460bp ADC

        Gap Weight:  5.000      Average Match:  1.000
     Length Weight:  0.300   Average Mismatch:  0.000

           Quality:  383.0            Length:   4321
             Ratio:  0.927             Gaps:      0
Percent Similarity: 92.736   Percent Identity: 92.736
```

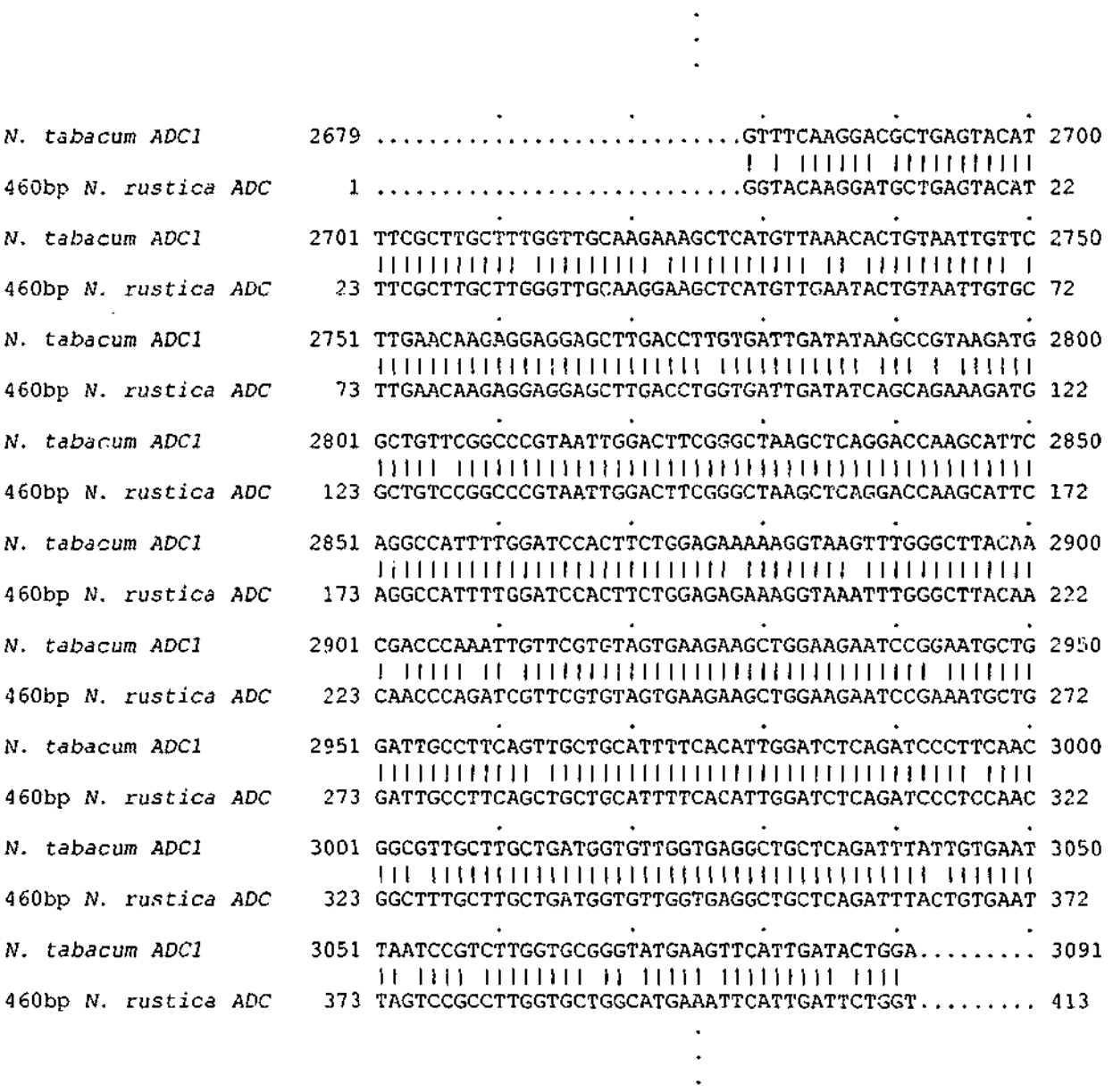

Appendix 4 A comparison of coding sequences of *N. tabacum ADC1* and coding sequences of the 460 bp *N. rustica ADC* using ANGIS program GAP. The percentage identity of both sequences is 92.7%.

```
GAP of: N. tabacum ADC2 to: N. rustica 460bp ADC

        Gap Weight:  5.000     Average Match:  1.000
     Length Weight:  0.300  Average Mismatch:  0.000

           Quality:  373.0            Length:   4368
             Ratio:  0.903              Gaps:      0
Percent Similarity: 90.315  Percent Identity: 90.315
```

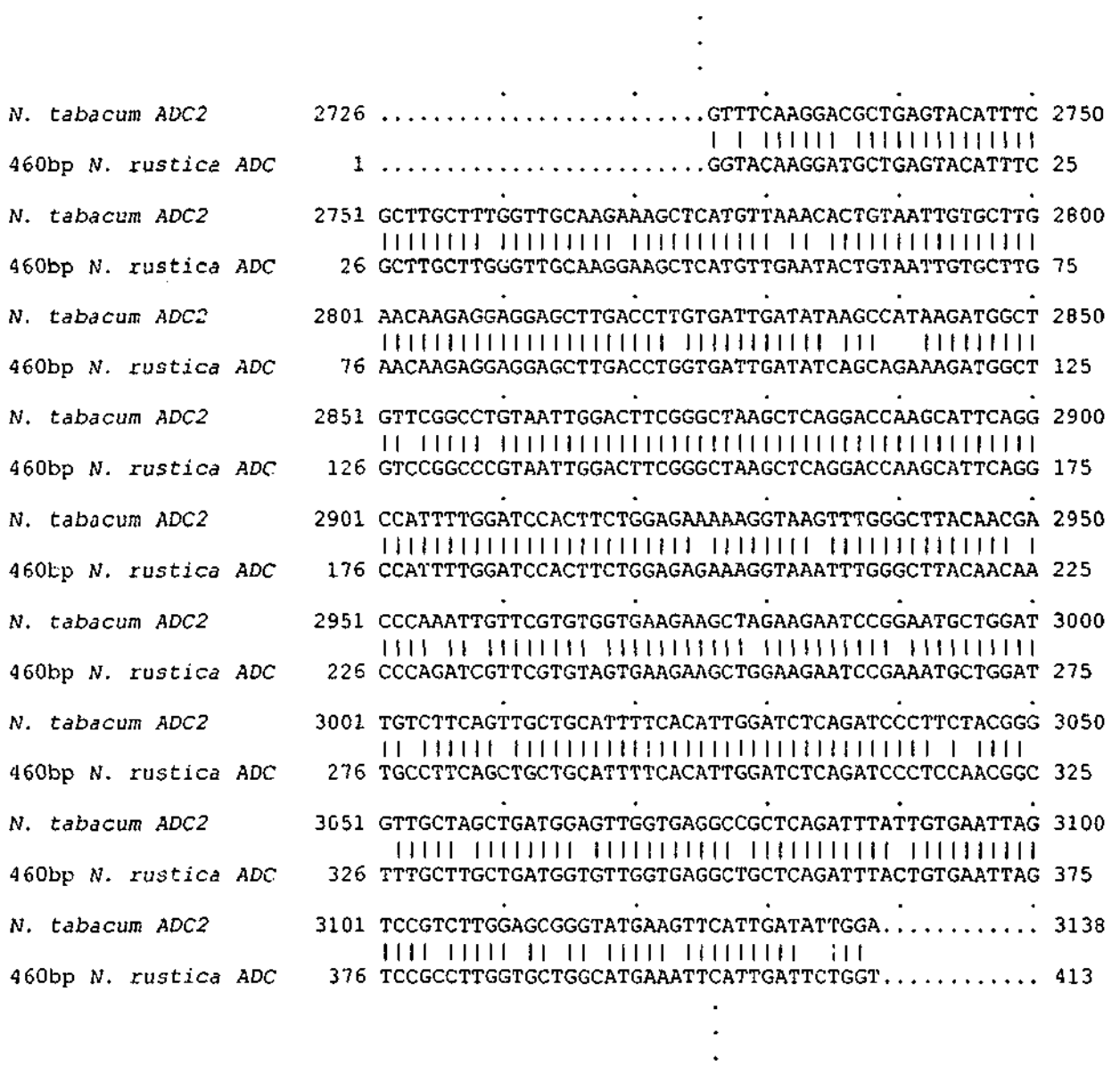

Appendix 5 A comparison of coding sequences of *N. tabacum ADC2* and coding sequences of the 460 bp *N. rustica ADC* using ANGIS program GAP. The percentage identity of both sequences is 90.3%.

References

Aerts, R. J., De Waal, A., Pennings, E. J. M., and Verpoorte, R. (1991). The distribution of strictosidine synthase activity and alkaloids in *Cinchona* plants. *Planta* **183**: 536-541.

Aird, E. L. H., Hamill, J. D., Robins, R. J., and Rhodes, M. J. C. (1988). Chromosome stability in transformed hairy root cultures and the properties of variant lines of *Nicotiana rustica* hairy root. In R. J. Robins, and M. J. C. Rhodes (eds), *Manipulating Secondary Metabolism in Culture*, pp: 137-144. Cambridge: Cambridge University Press.

Alabadi, D., and Carbonell, J. (1998). Expression of ornithine decarboxylase is transiently increased by pollination, 2,4-dichlorophenoxyacetic acid, and gibberellic acid in tomato ovaries. *Plant Physiology* **118**: 323-328.

Andersen, S. E., Bastola, D. R., and Minocha, S. C. (1998). Metabolism of polyamines in transgenic cells of carrot expressing a mouse ornithine decarboxylase cDNA. *Plant Physiology* **116**: 299-307.

Bachem, C. W. B., Speckmann, G., van der Linde, P. C. G., Verheggen, F. T. M., Hunt, M. D., Steffens, J.C., and Zabeau, M. (1994). Antisense expression of polyphenol oxidase genes inhibits enzymatic browning in potato tubers. *Biotechnology* **12**: 1101-1105.

Baldwin, I. T., and Huh, S. (1994). Primary function for a chemical defense- Nicotine does not protect *Datura stramonium* L. from UV damage. *Oecologia* **97**: 243-247.

Baldwin, I. T., Schmelz, E. A., and Ohnmeiss, T. E. (1994). Wound-induced changes in root and shoot jasmonic acid pools correlate with induced nicotine synthesis in *Nicotiana sylvestris* Spegazzini and Comes. *Journal of Chemical Ecology* **20**: 2139-2157.

Baldwin, I. T., Zhang, Z., Diab, N., Ohnmeiss, T. E., McCloud, E. S., Lynds, G. Y., and Schmelz, E. A. (1997). Quantification, correlations and manipulations of wound-induced changes in jasmonic acid and nicotine in *Nicotiana sylvestris*. *Planta* **201**: 397-404.

Bastola, D. R., and Minocha, S. C. (1995). Increased putrescine biosynthesis through transfer of mouse ornithine decarboxylase cDNA in carrot promotes somatic embryogenesis. *Plant Physiology* **109**: 63-71.

Bell, E., and Malmberg, R. L. (1990). Analysis of a cDNA encoding arginine decarboxylase from oat reveals similarity to the *Escherichia coli* arginine decarboxylase and evidence of protein processing. *Molecular & General Genetics* **224**: 431-436.

Berlin, J. (1981). Formation of putrescine and cinnamoyl putrescines in tobacco cell cultures. *Phytochemistry* **20**: 53-55.

Berlin, J., Rugenhagen, C., Dietze, P., Fecker, L. F., Goddijn, O. J. M., and Hoge, J. H. C. (1993). Increased production of serotonin by suspension and root cultures of *Peganum harmala* transformed with a tryptophan decarboxylase cDNA clone from *Catharanthus roseus*. *Transgenic Research* **2**: 336-344.

Berlin, J., Mollenschott, C., Herminghaus, S., and Fecker, L. F. (1998). Lysine decarboxylase transgenic tobacco root cultures biosynthesize novel hydroxycinnamoylcadaverines. *Phytochemistry* **48**: 79-84.

Bernet, E., Claparols, I., Santos, M. A., and Torne, J. M. (1998). Role of putrescine metabolic pathways in the differentiation process of maize meristematic callus. *Plant Physiology & Biochemistry* **36**: 759-766.

Bevan, M. (1984). Binary *Agrobacterium* vectors for plant transformation. *Nucleic Acids Research* **12**: 8711-8723.

Birecka, H., Birecki, M., and Frohlich, M. W. (1987). Evidence for arginine as the endogenous precursor of necines in *Heliotropium*. *Plant Physiology* **84**: 42-46.

Birecka, H., Birecki, M., Cohen, E. J., Bitonti, A. J., and McCann, P. P. (1988). Ornithine decarboxylase, polyamines, and pyrrolizidine alkaloids in *Senecio* and *Crotalaria*. *Plant Physiology* **86**: 224-230.

Bohlmann, J., De Luca, V., Eilert, U., and Martin, W. (1995). Purification and cDNA cloning of anthranilate synthase from *Ruta graveolens*: modes of expression and properties of native and recombinant enzymes. *The Plant Journal* **7**: 491-501.

Borrell, A., Culianez-Macia, F. A., Altabella, T., Besford, R. T., Flores, D., and Tiburcio, A. F. (1995). Arginine decarboxylase is localized in chloroplasts. *Plant Physiology* **109**: 771-776.

Borrell, A., Besford, R. T., Altabella, T., Masgrau, C., and Tiburcio, A. F. (1996). Regulation of arginine decarboxylase by spermine in osmotically-stressed oat leaves. *Physiologia Plantarum* **98**: 105-110.

Bourque, J. E. (1995). Antisense strategies for genetic manipulations in plants. *Plant Science* **105**: 125-149.

Bracher, D., and Kutchan, T. M. (1992). Strictosidine synthase from *Rauvolfia serpentina* analysis of a gene involved in indole alkaloid biosynthesis. *Archives of Biochemistry & Biophysics* **294**: 717-723.

Bradford, M. M. (1976). A rapid and sensitive method for the quantitation of microgram quantities of protein utilizing the principle of protein-dye binding. *Analytical Biochemistry* **72**: 248-254.

Braekman, J. C., Daloze, D., and Pasteels, J. M. (1998). Alkaloids in animals. In M. F. Roberts, and M. Wink (eds), *Alkaloids: Biochemistry, Ecology, and Medicinal Applications*, pp. 349-378. New York: Plenum Press.

Bruneton, J. (1995). *Pharmacognosy, Phytochemistry, Medicinal Plants*. Hampshire, England: Intercept.

Budavari, S., O'Neil, M. J., Smith, A., Heckelman, P. E., and Kinneary, J. F. (eds) (1996). The Merck Index. 12th ed. New Jersey: Whitehouse Station.

Burtin, D., and Michael, A. J. (1997). Overexpression of arginine decarboxylase in transgenic plants. *Biochemical Journal* **325**: 331-337.

Canel, C., Lopes-Cardoso, M. I., Whitmer, S., van der Fits, L., Pasquali, G., van der Heijden, R., Hoge, J. H. C., and Verpoorte, R. (1998). Effects of over-expression of strictosidine synthase and tryptophan decarboxylase on alkaloid production by cell cultures of *Catharanthus roseus*. *Planta* **205**: 414-419.

Cannon, M., Platz, J., Oleary, M., Sookdeo, C., and Cannon, F. (1990). Organ-specific modulation of gene expression in transgenic plants using antisense RNA. *Plant Molecular Biology* **15**: 39-47.

Capell, T., Escobar, C., Liu, H., Burtin, D., Lepri, O., and Christou, P. (1998). Over-expression of the oat arginine decarboxylase cDNA in transgenic rice (*Oryza sativa* L.) affects normal development patterns *in vitro* and results in putrescine accumulation in transgenic plants. *Theoretical & Applied Genetics* **97**: 246-254.

Capell, T., Bassie, L., Topsom, L., Hitchin, E., and Christou, P. (2000). Simultaneous reduction of the activity of two related enzymes, involved in early steps of the polyamine biosynthetic pathway, by a single antisense cDNA in transgenic rice. *Molecular & General Genetics* **264**: 470-476.

Carron, T. R., Robbins, M. P., and Morris, P. (1994). Genetic modification of condensed tannin biosynthesis in *Lotus corniculatus*. 1. Heterologous antisense dihydroflavonol reductase down-regulates tannin accumulation in "hairy root" cultures. *Theoretical & Applied Genetics* **87**:1006-1015.

Chang, K. S., Lee, S. H., Hwang, S. B., and Park, K. Y. (2000). Characterization and translational regulation of the arginine decarboxylase gene in carnation (*Dianthus caryophyllus* L.). *The Plant Journal* **24**: 45-56.

Chaplin, J. F. (1975). Registration of LAFC 53 tobacco germplasm (reg. no. GP 13). *Crop Science* **15**: 282.

Chavadej, S., Brisson, N., McNeil, J. N., and De Luca, V. (1994). Redirection of tryptophan leads to production of low indole glucosinolate canola. *Proceedings of the National Academy of Sciences of the United States of America* **91**: 2166-2170.

Chelvarajan, R. L., Fannin, F. F., and Bush, L. P. (1993). Study of nicotine demethylation in *Nicotiana otophora*. *Journal of Agricultural & Food Chemistry* **41**: 858-862.

Choi, K. B., Morishige, T., Shitan, N., Yazaki, K., and Sato, F. (2002). Molecular cloning and characterization of coclaurine N-methyltransferase from cultured cells of *Coptis japonica*. *The Journal of Biological Chemistry* **277**: 830-835.

Chowdhury, K. (1991). One step 'miniprep' method for the isolation of plasmid DNA. *Nucleic Acids Research* **19**: 2792-2793.

Chung, C. T., Miller, R. H. (1988). A rapid and convenient method for the preparation and storage of competent bacterial cells. *Nucleic Acids Research* **16**: 3580.

Daugherty, B. L., Hotta, K., Kumar, C., Ahn, Y. H., Zhu, J. D., and Pestka, S. (1989). Antisense RNA: Effect of ribosome binding sites, target location, size, and concentration on the translation of specific mRNA molecules. *Gene Anal Tech.* **6**: 1-16.

Davies, H. M., Hawkins, D. J., and Smith, L. A. (1989). Quinoprotein characteristics of *N*-methyl-putrescine oxidase from tobacco roots. *Phytochemistry* **28**: 1573-1578.

Dawson, R. F. (1962). Biosynthesis of the *Nicotiana* alkaloids. In W. R. Brode (ed), *Science in Progress*, vol. 12, pp. 117-143. New Haven: Yale University Press.

De Luca, V., and St Pierre, B. (2000). The cell and developmental biology of alkaloid biosynthesis. *Trends in Plant Science* **5**: 168-173.

De Luca, V., Marineau, C., and Brisson, N. (1989). Molecular cloning and analysis of cDNA encoding a plant tryptophan decarboxylase: Comparison with animal dopa decarboxylases. *Proceedings of the National Academy of Sciences of the United States of America* **86**: 2582-2586.

Delauney, A. J., Tabaeizadeh, Z., and Verma, D. P. S. (1988). A stable bifunctional antisense transcript inhibiting gene expression in transgenic plants. *Proceedings of the National Academy of Sciences of the United States of America* **85**: 4300-4304.

DeScenzo, R. A., and Minocha, S. C. (1993). Modulation of cellular polyamines in tobacco by transfer and expression of mouse ornithine decarboxylase cDNA. *Plant Molecular Biology* **22**: 113-127.

Di Fiore, S., Li, Q. R., Leech, M. J., Schuster, F., Emans, N., Fischer, R., and Schillberg, S. (2002). Targeting tryptophan decarboxylase to selected subcellular compartments of tobacco plants affects enzyme stability and in vivo function and leads to a lesion-mimic phenotype. *Plant Physiology* **129**: 1160-1169.

Dittrich, H., and Kutchan, T. M. (1991). Molecular cloning, expression, and induction of berberine bridge enzyme, an enzyme essential to the formation of benzophenanthridine alkaloids in the response of plants to pathogenic attack. *Proceedings of the National Academy of Sciences of the United States of America* **88**: 9969-9973.

Doblin, M. (1993). The role of putrescine biosynthesis in the control of polyamine and alkaloid metabolism in plants. Bachelor of Science Honours thesis. Department of Genetics and Developmental Biology, Monash University, Australia.

Dogru, E., Warzecha, H., Seibel, F., Haebel, S., Lottspeich, F., and Stockigt, J. (2000). The gene encoding polyneuridine aldehyde esterase of monoterpenoid indole alkaloid biosynthesis in plants is an ortholog of the α/β hydrolase super family. *European Journal of Biochemistry* **267**: 1397-1406.

Doran, P. M. (ed) (1997). *Hairy Roots: Culture and Application*. Amsterdam: Overseas Publishers Association.

El Hadrami, I., and D' Auzac, J. (1992). Effects of polyamine biosynthetic inhibitors on somatic embryogenesis and cellular polyamines in *Hevea brasiliensis*. *Journal of Plant Physiology* **140**: 33-36.

Espartero, J., Pintor-Toro, J. A., and Pardo, J. M. (1994). Differential accumulation of *S*-adenosylmethionine synthetase transcripts in response to salt stress. *Plant Molecular Biology* **25**: 217-227.

Evans, P. T., and Malmberg, R. L. (1989). Do polyamines have roles in plant development? *Annual Review of Plant Physiology & Plant Molecular Biology* **40**: 235-269.

Facchini, P. J., and De Luca, V. (1994). Differential and tissue-specific expression of a gene family for tyrosine/dopa decarboxylase in opium poppy. *The Journal of Biological Chemistry* **269**: 26684-26690.

Facchini, P. J., Penzes, C., Johnson, A. G., and Bull, D. (1996). Molecular characterization of berberine bridge enzyme genes from opium poppy. *Plant Physiology* **112**: 1669-1677.

Fecker, L. F., Hillebrandt, S., Ruegenhagen, C., Herminghaus, S., Landsmann, J., and Berlin, J. (1992). Metabolic effects of a bacterial lysine decarboxylase gene expressed in a hairy root culture of *Nicotiana glauca*. *Biotechnology Letters* **14**: 1035-1040.

Fecker, L. F., Rugenhagen, C., and Berlin, J. (1993). Increased production of cadaverine and anabasine in hairy root cultures of *Nicotiana tabacum* expressing a bacterial lysine decarboxylase gene. *Plant Molecular Biology* **23**: 11-21.

Feth, F., and Wagner, K. G. (1989). Determination of ornithine, putrescine, *N*-methylputrescine and *N*-methylpyrroline pools in tobacco tissue by high-performance liquid chromatography. *Physiologia Plantarum* **75**: 71-74.

Feth, F., Arfmann, H. A., Wray, V., and Wagner, K. G. (1985). Determination of putrescine-*N*-methyltransferase by high-performance liquid chromatography. *Phytochemistry* **24**: 921-923.

Feth, F., Wagner, R., and Wagner, K. G. (1986). Regulation in tobacco callus of enzyme activities of the nicotine pathway I. The route ornithine to methylpyrroline. *Planta* **168**: 402-407.

Flores, H. E. (1991). Changes in polyamine metabolism in response to abiotic stress. In R. Slocum and H. E. Flores (eds), *The Biochemistry and Physiology of Polyamines in Plants*, pp: 215-225. Boca Raton, FL: CRC Press.

Flores, H. E., and Galston, A. W. (1982). Polyamines and plant stress: Activation of putrescine biosynthesis by osmotic shock. *Science* **217**: 1259-1261.

Flores, H. E., Protacio, C. M. and Signs, M. W. (1989). Primary and secondary metabolism of polyamines in plants. In J. E. Poulton, J. T. Romeo, and E. E. Conn (eds), *Recent Advances in Phytochemistry*; vol. 23: Plant Nitrogen Metabolism, pp: 329-393. New York: Plenum Press.

Ford, Y. Y., Ratcliffe, R. G., and Robins, R. J. (1998). *In vivo* nuclear-magnetic-resonance analysis of polyamine and alkaloid metabolism in transformed root cultures of *Datura stramonium* L.: evidence for the involvement of putrescine in phytohormone-induced de-differentiation. *Planta* **205**: 205-213.

Friesen, J. B., and Leete, E. (1990). Nicotine synthase – An enzyme from *Nicotiana* species which catalyzes the formation of (*S*)-nicotine from nicotinic acid and 1-methyl-Δ'-pyrrolinium chloride. *Tetrahedron Letters* **131**: 6295-6298.

Friesen, J. B., Burkhouse, P. C., Biesboer, D. D., and Leete, E. (1992). Influence of alkaloid precursors on the alkaloid content of *Nicotiana alata* root cultures. *Phytochemistry* **31**: 3059-3063.

Galloway, G. L., Malmberg, R. L., and Price, R A. (1998). Phylogenetic utility of the nuclear gene arginine decarboxylase: An example from Brassicaceae. *Molecular Biology & Evolution* **15**: 1312-1320.

Galston, A. W., and Kaur-Sawhney, R. (1995). Polyamines as endogenous growth regulations. In P. J. Davies (ed), *Plant Hormones: Physiology, Biochemistry and Molecular Biology* (2nd ed.), pp: 158-178. Dordrecht: Kluwer Academic Publishers.

Galston, A. W., Kaursawhney, R., Altabella, T., and Tiburcio, A. F. (1997). Plant polyamines in reproductive activity and response to abiotic stress. *Botanica Acta* **110**: 197-207.

Gamborg, O. L., Miller, R. A., and Ojima, K. (1968). Nutrient requirements of suspension cultures of soy bean root cells. *Experimental Cell Research* **50**: 151-158.

Geerlings, A., Hallard, D., Caballero, A. M., Cardoso, I. L., van der Heijden, R., and Verpoorte, R. (1999). Alkaloid production by a *Cinchona officinalis* 'Ledgeriana' hairy root culture containing constitutive expression constructs of tryptophan decarboxylase and strictosidine synthase cDNAs from *Catharanthus roseus*. *Plant Cell Reports* **19**: 191-196.

Geerlings, A., Ibanez, M. M. L., Memelink, J., van der Heijden, R., and Verpoorte, R. (2000). Molecular cloning and analysis of strictosidine β-d-glucosidase, an enzyme in terpenoid indole alkaloid biosynthesis in *Catharanthus roseus*. *The Journal of Biological Chemistry* **275**: 3051-3056.

Goddijn, O. J. M., Lohman, F. P., De Kam, R. J., Schileperoort, R. A., and Hoge, J. H. C. (1994). Nucleotide sequence of the tryptophan decarboxylase gene of *Catharanthus roseus* and expression of *tdc-gus*A gene fusions in *Nicotiana tabacum*. *Molecular & General Genetics* **242**: 217-225.

Goddijn, O. J. M., Pennings, E. J. M., van der Helm, P., Schilperoort, R. A., Verpoorte, R., and Hoge, J. H. C. (1995). Overexpression of a tryptophan decarboxylase cDNA in *Catharanthus roseus* crown gall calluses results in increased tryptamine levels but not in increased terpenoid indole alkaloid production. *Transgenic Research* 4: 315-323.

Greenberg, M. L., and Cohen, S. S. (1985). Dicyclohexylamine-induced shift of biosynthesis from spermidine to spermine in plant protoplasts. *Plant Physiology* **78**: 568-575.

Griffith, G. D., and Griffith, T. (1964). Metabolism of the methyl group of nicotine in *Nicotiana rustica*. *Plant Physiology* **39**: 970-973.

Hallard, D., van der Heijden, R., Verpoorte, R., Cardoso, M. I. L., Pasquali, G., Memelink, J., and Hoge, J. H. C. (1997). Suspension cultured transgenic cells of *Nicotiana tabacum* expressing tryptophan decarboxylase and strictosidine synthase cDNAs from *Catharanthus roseus* produce strictosidine upon secologanin feeding. *Plant Cell Reports* **17**: 50-54.

Hamill, J. D., and Lidgett, A. J. (1997). Hairy root cultures – Opportunities and key protocols for studies in metabolic engineering. In P. M. Doran (ed), *Hairy Roots: Culture and Application*, pp 1-29. Amsterdam: Overseas Publishers Association.

Hamill, J. D., Parr, A. J., Robins, R. J., and Rhodes, M. J. C. (1986). Secondary product formation by cultures of *Beta vulgaris* and *Nicotiana rustica* transformed with *Agrobacterium rhizogenes*. *Plant Cell Reports* **5**: 111-114.

Hamill, J. D., Evans, D. M., Robins, R. J., Rhodes, M. J. C., Martin, C., and Prescott, A. (1987a). Foreign gene insertion into transformed roots with binary vectors and *Agrobacterium rhizogenes*

– potential for genetic manipulation of plant secondary metabolism. In R. J. Robins, and M. J. C. Rhodes (eds), *Manipulating Secondary Metabolism in Culture*, pp: 145-153. Cambridge: Cambridge University Press.

Hamill, J. D., Prescott, A., and Martin, C. (1987b). Assessment of the efficiency of co-transformation by the T-DNA of disarmed binary vectors derived from *Agrobacterium tumefaciens* and the T-DNA from *A. rhizogenes*. *Plant Molecular Biology* **9**: 573-584.

Hamill, J. D., Robins, R. J., Parr, A. J., Evans, D. M., Furze, J. M., and Rhodes, M. J. C. (1990). Over-expressing a yeast ornithine decarboxylase gene in transgenic roots of *Nicotiana rustica* can lead to enhanced nicotine accumulation. *Plant Molecular Biology* **15**: 27-38.

Hanfrey, C., Sommer, S., Mayer, M. J., Burtin, D., and Michael, A. J. (2001). *Arabidopsis* polyamine biosynthesis: absence of ornithine decarboxylase and the mechanism of arginine decarboxylase activity. *The Plant Journal* **27**: 551-560.

Hao, D. Y., and Yeoman, M. M. (1996). Nicotine *N*-demethylase in cell-free preparations from tobacco cell cultures. *Phytochemistry* **42**: 325-329.

Hao, D. Y., and Yeoman, M. M. (1998). Evidence in favour of an oxidative *N*-demethylation of nicotine to nornicotine in tobacco cell cultures. *Journal of Plant Physiology* **152**: 420-426.

Hartmann, T. (1991). Alkaloids. In G. A. Rosenthal and M. R. Berebaum (eds), *Herbivores: Their Interactions with Secondary Plant Metabolites* (2nd ed.), vol. 1: The Chemical Participants, pp: 79-121. San Diego: Academic Press.

Hartmann, T., Sander, H., Adolph, R., and Toppel, G. (1988). Metabolic links between the biosynthesis of pyrrolizidine alkaloids and polyamines in root cultures of *Senecio vulgaris*. *Planta* **175**: 82-90.

Hashimoto, T., and Yamada, Y. (1994). Alkaloid biogenesis: Molecular aspects. *Annual Review of Plant Physiology & Plant Molecular Biology* **45**: 257-285.

Hashimoto, T., Yukimune, Y., and Yamada, Y. (1986). Tropane alkaloid production in *Hyoscyamus* root cultures. *Journal of Plant Physiology* **124**: 61-75.

Hashimoto, T., Yukimune, Y., and Yamada, Y. (1989a). Putrescine and putrescine *N*-methyltransferase in the biosynthesis of tropane alkaloids in cultured roots of *Hyoscyamus albus* I. Biochemical studies. *Planta* **178**: 123-130.

Hashimoto, T., Yukimune, Y., and Yamada, Y. (1989b). Putrescine and putrescine *N*-Methyltransferase in the biosynthesis of tropane alkaloids in cultured roots of *Hyoscyamus albus* II. Incorporation of labeled precursors. *Planta* **178**: 131-137.

Hashimoto, T., Yun, D., and Yamada, Y. (1993). Production of tropane alkaloids in genetically engineered root cultures. *Phytochemistry* **32**: 713-718.

Hashimoto, T., Shoji, T., Mihara, T., Oguri, H., Tamaki, K., Suzuki, K., and Yamada, Y. (1998a). Intraspecific variability of the tandem repeats in *Nicotiana* putrescine *N*-methyltransferases. *Plant Molecular Biology* **37**: 25-37.

Hashimoto, T., Tamaki, K., Suzuki, K., and Yamada, Y. (1998b). Molecular cloning of plant spermidine synthases. *Plant & Cell Physiology* **39**: 73-79.

Hauschild, K., Pauli, H. H., and Kutchan, T. M. (1998). Isolation and analysis of a gene *bbe1* encoding the berberine bridge enzyme from the California poppy *Eschscholzia californica*. *Plant Molecular Biology* **36**: 473-478.

Hayashi, S. I., and Murakami, Y. (1995). Rapid and regulated degradation of ornithine decarboxylase. *Biochemical Journal* **306**: 1-10.

Herminghaus, S., Schreier, P. H., McCarthy, J. E. G., Landsmann, J., Botterman, J., and Berlin, J. (1991). Expression of a bacterial lysine decarboxylase gene and transport of the protein into chloroplasts of transgenic tobacco. *Plant Molecular Biology* **17**: 475-486.

Herminghaus, S., Tholl, D., Rugenhagen, C., Fecker, L. F., Leuschner, C., and Berlin, J. (1996). Improved metabolic action of a bacterial lysine decarboxylase gene in tobacco hairy root cultures by its fusion to a *rbcS* transit peptide coding sequence. *Transgenic Research* **5**: 193-201.

Hiatt, A. C., McIndoo, J., and Malmberg, R. L. (1986). Regulation of polyamine biosynthesis in tobacco; effects of inhibitors and exogenous polyamines on arginine decarboxylase, ornithine decarboxylase, and *S*-adenosylmethionine decarboxylase. *The Journal of Biological Chemistry* **261**: 1293-1298.

Hibi, N., Fujita, T., Hatano, M., Hashimoto, T., and Yamada, Y. (1992). Putrescine *N*-methyltransferase in cultured roots of *Hyoscyamus albus*: n-Butylamine as a potent inhibitor of the transferase both *in vitro* and *in vivo*. *Plant Physiology* **100**: 826-835.

Hibi, N., Higashiguchi, S., Hashimoto, T., and Yamada, Y. (1994). Gene expression in tobacco low-nicotine mutants. *Plant Cell* **6**: 723-735.

Hirashima, A., Sawaki, S., Mizuno, T., Houba-Herin, N., and Inouye, M. (1989). Artificial immune system against viral infection involving antisense RNA targeted to the 5'-terminal noncoding region of coliphage SP RNA. *Journal of Biochemistry Tokyo* **106**: 163-166.

Huang, F., and Kutchan, T. M. (2000). Distribution of morphinan and benzo[c]phenanthridine alkaloid gene transcript accumulation in *Papaver somniferum*. *Phytochemistry* **53**: 555-564.

Hutvagner, H., and Zamore, P. D. (2002). RNAi: nature abhors a double strand. *Current Opinion in Genetics and Development* **12**: 225 – 232.

Imanishi, S., Hashizume, K., Kojima, H., Ichihara, A., and Nakamura, K. (1998a). An mRNA of tobacco cell, which is rapidly inducible by methyl jasmonate in the presence of cycloheximide, codes for a putative glycosyltransferase. *Plant & Cell Physiology* **39**: 202-211.

Imanishi, S., Hashizume, K., Nakakita, M., Kojima, H., Matsubayashi, Y., Hashimoto, T., Sakagami, Y., Yamada, Y., and Nakamura, K. (1998b). Differential induction by methyl jasmonate of genes encoding ornithine decarboxylase and other enzymes involved in nicotine biosynthesis in tobacco cell cultures. *Plant Molecular Biology* **38**: 1101-1111.

Imanishi, S., Nakakita, M., Yamashita, K., Furuta, A., Utsuno, K., Muramoto, N., Kojima, H., and Nakamura, K. (2000). Aspirin and salicylic acid do not inhibit methyl jasmonate-inducible expression of a gene for ornithine decarboxylase in tobacco BY-2 cells. *Bioscience Biotechnology & Biochemistry* **64**: 125-133.

Jones, L., Ratcliff, F., and Baulcombe, D.C. (2001). RNA-directed transcriptional gene silencing in plants can be inherited independently of the RNA trigger. *Current Biology* **11**: 47–757.

Junghanns, K. T., Kneusel, R. E., Baumert, A., Maier, W., Groger, D., and Matern, U. (1995). Molecular cloning and heterologous expression of acridone synthase from elicited *Ruta graveolens* L cell suspension cultures. *Plant Molecular Biology* **27**: 681-692.

Kaiser, A. (1999). Cloning and expression of a cDNA encoding homospermidine synthase from *Senecio vulgaris* (Asteraceae) in *Escherichia coli*. *The Plant Journal* **19**: 195-201.

Kaiser, A., Sell, S., and Hehl, R. (2002). Heterologous expression of a bacterial homospermidine synthase gene in transgenic tobacco: Effects on the polyamine pathway. *Archiv der Pharmazie* **335**: 143-151.

Kanegae, T., Kajiya, H., Amano, Y., Hashimoto, T., and Yamada, Y. (1994). Species-dependent expression of the hyoscyamine 6β-hydroxylase gene in the pericycle. *Plant Physiology* **105**: 483-490.

Kay, R., Chan, A., Daly, M., and McPherson, J. (1987). Duplication of CaMV35S promoter sequences creates a stronger enhancer for plant genes. *Science* **236**: 1299-1302.

Kenton, A., Parokonny, A. S., Gleba, Y. Y., and Bennett, M. D. (1993). Characterization of the *Nicotiana tabacum* L. genome by molecular cytogenetics. *Molecular & General Genetics* **240**: 159-169.

Khan, M. B., and Harborne, J. B. (1991). Potassium deficiency increases tropane alkaloid synthesis in *Atropa acuminata* via arginine and ornithine decarboxylase levels. *Phytochemistry* **30**: 3559-3564.

Kloti, A., He, X., Potrykus, I., Hohn, T., and Futterer, J. (2002). Tissue-specific silencing of a transgene in rice. *Proceedings of the National Academy of Sciences of the United States of America* **99**: 10881-10886.

Kraus, P. F. X., and Kutchan, T. M. (1995). Molecular cloning and heterologous expression of a cDNA encoding berbamunine synthase, a C-O phenol-coupling cytochrome P450 from the higher plant *Berberis stolonifera*. *Proceedings of the National Academy of Sciences of the United States of America* **92**: 2071-2075.

Kuipers, A. G. J., Soppe, W. J. J., Jacobsen, E., and Visser, R. G. F. (1995). Factors affecting the inhibition by antisense RNA of granule-bound starch synthase gene expression in potato. *Molecular & General Genetics* **246**: 745-755.

Kumar, A., Altabella, T., Taylor, M. A., and Tiburcio, A. F. (1997). Recent advances in polyamine research. *Trends in Plant Science* **2**: 124-130.

Kutchan, T. M. (1995). Alkaloid biosynthesis - The basis for metabolic engineering of medicinal plants. *Plant Cell* **7**: 1059-1070.

Kutchan, T. M. (1998). Molecular genetics of plant alkaloid biosynthesis. In G. A. Cordell (ed), *The Alkaloids, Chemistry and Pharmacology*, vol. 50: 257-316. San Diego: Academic Press.

Kutchan, T. M., Hampp, N., Lottspeich, F., Beyreuther, K., and Zenk, M. H. (1988). The cDNA clone for strictocidine synthase from *Rauvolfia serpentina*. *FEBS Letters* **237**: 40-44.

Lambers, H., Chapin, F. S., and Pons, T. L. (1998). *Plant Physiological Ecology*. New York: Springer-Verlag.

Leech, M. J., May, K., Hallard, D., Verpoorte, R., De Luca, V., and Christou, P. (1998). Expression of two consecutive genes of a secondary metabolic pathway in transgenic tobacco: Molecular diversity influences levels of expression and product accumulation. *Plant Molecular Biology* **38**: 765-774.

Leete, E. (1979). Alkaloids derived from ornithine, lysine, and nicotinic acid. In E. A. Bell, and B. V. Chariwood (eds), *Secondary Plant Products*, pp: 65-91. Berlin: Springer-Verlag. (Encyclopedia of Plant Physiology; new series, vol. 8).

Leete, E. (1983). Biosynthesis and metabolism of tobacco alkaloids. In S. W. Pelletier (ed), *Alakloids: Chemical and Biological Perspectives*, pp: 86-152. New York: John Wiley & Sons.

Leete, E., and Slattery, S. A. (1976). Incorporation of [2-^{14}C]- and [6-^{14}C]nicotinic acid into the tobacco alkaloids. Biosynthesis of anatabine and α,β-dipyridyl. *Journal of the American Chemical Society* **98**: 6326-6330.

Legg, P. D., and Collins, G. B. (1971). Inheritance of percent total alkaloids in *Nicotiana tabacum* L. II. Genetic effects of two loci in Burley 21 x LA Burley 21 populations. *Canadian Journal of Genetics and Cytology* **13**: 287-291.

Legg, P. D., Chaplin, J. F., and Collins, G. B. (1969). Inheritance of percent total alkaloids in *Nicotiana tabacum* L. Populations derived from crosses of low alkaloid lines with burley and flue-cured varieties. *Journal of Heredity* **60**: 213-217.

Lepri, O., Bassie, L., Safwat, G., Thu-Hang, P., Trung-Nghia, P., Holtta, E., Christou, P., and Capell,T. (2001). Over-expression of a cDNA for human ornithine decarboxylase in transgenic rice plants alters the polyamine pool in a tissue-specific manner. *Molecular Genetics and Genomics* 266: 303-312.

Lidgett, A. (1997). Molecular Characterisation of Polyamine Biosynthetic Genes and Effects of Genetic Manipulation on Alkaloid Metabolism in *Nicotiana tabacum*. Doctoral dissertation. Department of Genetics and Developmental Biology, Monash University, Australia.

Lin, X., Kaul, S., Rounsley, S., Shea, T. P., Benito, M. I., Town, C. D., Fujil, C. Y., Mason, T., Bowman, C. L., Barnstead, M., Feldblum, T. V., Buell, C. R., Ketchum, K. A., Lee, J., Ronning, C. M., Koo, H. L., Moffat, K. S., Cronin, L. A., Shen, M., Pai, G., van Aken, S., Umayam, L., Tallon, L. J., Gill, J. E., Adams, M. D., Carrera, A. J., Creasy, T. H., Goodman, H. M., Somerville, C. R., Copenhaver, G. P., Preuss, D., Nierman, W. C., White, O., Eisen, J. A., Salzburg, S. L., Fraser, C. M., and Venter, J. C. (1999). Sequence and analysis of chromosome 2 of the plant *Arabidopsis thaliana*. *Nature* **402**: 761-768.

Lopez-Meyer, M., and Nessler, C. L. (1997). Tryptophan decarboxylase is encoded by two autonomously regulated genes in *Camptotheca acuminata* which are differentially expressed during development and stress. *The Plant Journal* **11**: 1167-1175.

Lovett, J. V., and Hoult, A. H. C. (1998). Allelopathy in plants. In M. F. Roberts, and M. Wink (eds), *Alkaloids: Biochemistry, Ecology, and Medicinal Applications*, pp. 337-347. New York: Plenum Press.

Luckner, M. (1990). *Secondary Metabolism in Microorganisms, Plants, and Animals* (3rd edn). Berlin: Springer-Verlag.

Lukacin, R., Springob, K., Urbanke, C., Ernwein, C., Schroder, G., Schroder, J., and Matern, U. (1999). Native acridone synthases I and II from *Ruta graveolens* L. form homodimers. *FEBS Letters* **448**: 135-140.

Mad Arif, S. A., Taylor, M. A., George, L. A., Butler, A. R., Burch, L. R., Davies, H. V., Stark, M. J. R., and Kumar, A. (1994). Characterisation of the *S*-adenosylmethionine decarboxylase (SAMDC) gene of potato. *Plant Molecular Biology* **26**: 327-338.

Maldonado-Mendoza, I. E., Burnett, R. J., and Nessler, C. L. (1992). Nucleotide sequence of a cDNA encoding 3-hydroxy-3-methylglutaryl coenzyme A reductase from *Catharanthus roseus*. *Plant Physiology* **100**: 1613-1614.

Maldonado-Mendoza, I. E., Lopez-Meyer, M., Galef, J. R., Burnett, R. J., and Nessler, C. L. (1996). Molecular analysis of a new member of the opium poppy tyrosine/3,4-dihydroxyphenylalanine decarboxylase gene family. *Plant Physiology* **110**: 43-49.

Mallory, A. C., Ely, L., Smith, T. H., Marathe, R., Anandalakshmi, R., Vaucheret, H., Pruss, G., Bowman, L., Vance, V. B. (2001). HC-Pro transgene silencing eliminates the small RNAs but not trans methylation or the mobile signal. *Plant Cell* **13**: 571-583.

Malmberg, R. L., and Cellino, M. L. (1994). Arginine decarboxylase of oats is activated by enzymatic cleavage into 2 polypeptides. *The Journal of Biological Chemistry* **269**: 2703-2706.

Malmberg, R. L., Smith, K. E., Bell, E., and Cellino, M. L. (1992). Arginine decarboxylase of oats is clipped from a precursor into two polypeptides found in the soluble enzyme. *Plant Physiology* **100**: 146-152.

Malmberg, R. L., Watson, M. B., Galloway, G. L., and Yu, W. (1998). Molecular genetic analyses of plant polyamines. *Critical Reviews in Plant Sciences* **17**: 199-224.

Manceau, F., Fliniaux, M. A., and Jacquin Dubreuil, A. (1989). Ability of a *Nicotiana plumbaginifolia* cell suspension to demethylate nicotine into nornicotine. *Phytochemistry* **28**: 2671-2674.

Mangold, U., Eichel, J., Batschauer, A., Lanz, T., Kaiser, T., Spangenberg, G., Werck-Reichhart, D., and Schroder, J. (1994). Gene and cDNA for plant cytochrome P450 proteins (CYP72 family) from *Catharanthus roseus*, and transgenic expression of the gene and a cDNA in tobacco and *Arabidopsis thaliana*. *Plant Science* **96**: 129-136.

Mann, D. F., and Byerrum, R. U. (1974). Activation of the *de novo* pathway for pyridine nucleotide biosynthesis prior to ricinine biosynthesis in castor beans. *Plant Physiology* **53**: 603-609.

Martin-Tanguy, J. (1985). The occurrence and possible function of hydroxycinnamoyl acid amides in plants. *Plant Growth Regulation* **3**: 381-399.

Martin-Tanguy, J. (1997). Conjugated polyamines and reproductive development: Biochemical, molecular and physiological approaches. *Physiologia Plantarum* **100**: 675-688.

Masgrau, C., Altabella, T., Farras, R., Flores, D., Thompson, A. J., Besford, R. T., and Tiburcio, A. F. (1997). Inducible overexpression of oat arginine decarboxylase in transgenic tobacco plants. *The Plant Journal* **11**: 465-473.

Matsuda, J., Okabe, S., Hashimoto, T., and Yamada, Y. (1991). Molecular cloning of hyoscyamine 6β-hydroxylase, a 2-oxoglutarate-dependent dioxygenase, from cultured roots of *Hyoscyamus niger*. *The Journal of Biological Chemistry* **266**: 9460-9464.

Matzke, M. A., Primig, M., Trnovsky, J., and Matzke, A. J. M. (1989). Reversible methylation and inactivation of marker genes in sequentially transformed tobacco plants. *The EMBO Journal* **8**:643-649.

McKnight, T. D., Roessner, C. A., Devagupta, R., Scott, A. I., and Nessler, C. L. (1990). Nucleotide sequence of a cDNA encoding the vascular protein strictosidine synthase from *Catharanthus roseus*. *Nucleic Acids Research* **18**: 4939.

McKnight, T. D., Bergey, D. R., Burnett, R. J., and Nessler, C. L. (1991). Expression of enzymatically active and correctly targeted strictosidine synthase in transgenic tobacco plants. *Planta* **185**: 148-152.

Meijer, A., H., Cardoso, M., I., L., Voskuilen, J. T., de Waal, A., Verpoorte, R., and Hoge, J., H., C. (1993a). Isolation and characterization of a cDNA clone from *Catharanthus roseus* encoding NADPH:cytochrome P_{450} reductase, an enzyme essential for reactions catalyzes by cytochrome P_{450} mono-oxygenases in plants. *The Plant Journal* **4**: 47-60.

Meijer, A., H., Souer, E., Verpoorte, R., and Hoge, J., H., C. (1993b). Isolation of cytochrome P_{450} cDNA clones from the higher plant *Catharanthus roseus* by a PCR strategy. *Plant Molecular Biology* **22**: 379-383.

Michael, A. J., Furze, J. M., Rhodes, M. J. C., and Burtin, D. (1996). Molecular cloning and functional identification of a plant ornithine decarboxylase cDNA. *Biochemical Journal* **314**: 241-248.

Mizusaki, S., Tanabe, Y., Noguchi, M., and Tamaki, E. (1971). Phytochemical studies on tobacco alkaloids XIV. The occurrence and properties of putrescine *N*-methyltransferase in tobacco roots. *Plant & Cell Physiology* **12**: 633-640.

Mizusaki, S., Tanabe, Y., Noguchi, M., and Tamaki, E. (1972). *N*-methylputrescine oxidase from tobacco roots. *Phytochemistry* **11**: 2757-2762.

Mizusaki, S., Tanabe, Y., Noguchi, M., and Tamaki, E. (1973). Changes in the activities of ornithine decarboxylase, putrescine *N*-methyltransferase and *N*-methylputrescine oxidase in tobacco roots in relation to nicotine biosynthesis. *Plant & Cell Physiology* **14**: 103-110.

Mol, J. N. M., Stuitje, A. R., and van der Krol, A. (1989). Genetic manipulation of floral pigmentation genes. *Plant Molecular Biology* **13**: 287-294.

Moore, E. L., Powell, N. T., Jones, G. L., and Gwynn, G. R. (1962). Flue-cured tobacco variety NC95; Resistant to root-knot, black shank and the wilt diseases. In *Agricultural Experiment Station*, Bulletin **419**, pp, 3-18. North Carolina, Raleigh: North Carolina State College.

Morishige, T., Tsujita, T., Yamada, Y., and Sato, F. (2000). Molecular characterization of the *S*-adenosyl-L-methionine:3'-hydroxy-*N*-methylcoclaurine 4'-*O*-methyltransferase involved in isoquinoline alkaloid biosynthesis in *Coptis japonica*. *The Journal of Biological Chemistry* **275**: 23398-23405.

Murad, L., Lim, K. Y., Christopodulou, V., Matyasek, R., Lichtenstein, C. P., Kovarik, A., and Leitch, A. R. (2002). The origin of tobacco's T genome is traced to a particular lineage within *Nicotiana tomentosiformis* (Solanaceae). *American Journal of Botany* **89**: 921-928.

Murashige, T., and Skoog, F. (1962). A revised medium for rapid growth and bioassays with tobacco tissue cultures. *Physiologia Plantarum* **15**: 473-479.

Murray, J. A. H., and Crockett, N. (1992). Antisnese techniques: An overview. In J. A. H. Murray (ed), *Antisense RNA and DNA*, *Modern Cell Biology*; vol. 11: 1-49. New York: Willey-Liss.

Nakai, K., and Kanehisa, M. (1992). A knowledge base for predicting protein localization sites in eukaryotic cells. *Genomics* **14**: 897-911.

Nakajima, K., Hashimoto, T., and Yamada, Y. (1993a). Two tropinone reductases with different stereospecificities are short-chain dehydrogenase evolved from a common ancestor. *Proceedings of the National Academy of Sciences of the United States of America* **90**: 9591-9595.

Nakajima, K., Hashimoto, T., and Yamada, Y. (1993b). cDNA encoding tropinone reductases-II from *Hyoscyamus niger*. *Plant Physiology* **103**: 1465-1466.

Nakajima, K., Oshita, Y., Yamada, Y., and Hashimoto, T. (1999). Insight into the molecular evolution of two tropinone reductases. *Bioscience Biotechnology & Biochemistry* **63**: 1819-1822.

Nam, K. H., Lee, S. H., and Lee, J. H. (1996). A cDNA encoding an arginine decarboxylase (accession no. U35367) from soybean hypocotyls (Plant Gene Register 95-142). *Plant Physiology* **110**: 714.

Nam, K. H., Lee, S. H., and Lee, J. H. (1997a). Purification and characterization of arginine decarboxylase from soybean (*Glycine max*) hypocotyls. *Plant & Cell Physiology* **38**: 1150-1155.

Nam, K. H., Lee, S. H., and Lee, J. H. (1997b). Differential expression of ADC mRNA during development and upon acid stress in soybean (*Glycine max*) hypocotyls. *Plant & Cell Physiology* **38**: 1156-1166.

Neuwinger, H. D. (1998). Alkaloids in arrow poisons. In M. F. Roberts, and M. Wink (eds), *Alkaloids: Biochemistry, Ecology, and Medicinal Applications*, pp. 45-84. New York: Plenum Press.

Noji, M., Murakoshi, I., and Saito, K. (1993). Evidence for identity of β–pyrazolealanine synthase with cysteine synthase in watermelon: Formation of β–pyrazolealanine by cloned cysteine synthase *in vitro* and *in vivo*. *Biochemical & Biophysical Research Communications* **197**: 1111-1117.

Noji, M., Murakoshi, I., and Saito, K. (1994). Molecular cloning of a cysteine synthase cDNA from *Citrullus vulgaris* (watermelon) by genetic complementation in an *Escherichia coli* Cys$^-$ auxotroph. *Molecular & General Genetics* **244**: 57-66.

Noury, M., Bassie, L., Lepri, O., Kurek, I., Christou, P., and Capell, T. (2000). A transgenic rice cell lineage expressing the oat arginine decarboxylase (ADC) cDNA constitutively accumulates putrescine in callus and seeds but not in vegetative tissues. *Plant Molecular Biology* **43**: 537-544.

Nyman, S. (1994). Incorporation of arginine, ornithine and phenylalanine into tropane alkaloids in suspension-cultured cells and aseptic roots of intact plants of *Atropa belladonna*. *Journal of Experimental Botany* **45**: 979-986.

Ober, D., and Hartmann, T. (1999). Homospermidine synthase, the first pathway-specific enzyme of pyrrolizidine alkaloid biosynthesis, evolved from deoxyhypusine synthase. *Proceedings of the National Academy of Sciences of the United States of America* **96**: 1477-14782.

Ohta, S., and Yatazawa, M. (1980). Metabolic key step discriminating nicotine producing tobacco callus strain from ineffective one. *Biochemie und Physiologie der Pflanzen* **175**: 382-385.

Park, S. U., Yu, M., and Facchini, P. J. (2002). Antisense RNA-mediated suppression of benzophenanthridine alkaloid biosynthesis in transgenic cell cultures of California poppy. *Plant Physiology* **128**: 696-706.

Parr, A. J., and Hamill, J. D. (1987). Relationship between *Agrobacterium rhizogenes* transformed hairy roots and intact, uninfected *Nicotiana* plants. *Phytochemistry* **26**: 3241-3245.

Pasquali, G., Goddijn, O. J. M., de Waal, A., Verpoorte, R., Schilperoort, R. A., Hoge, J. H. C., and Memelink, J. (1992). Co-ordinated regulation of two indole alkaloid biosynthetic genes from *Catharanthus roseus* by auxin and elicitors. *Plant Molecular Biology* **18**: 1121-1131.

Pasquali, G., Erven, A. S. W., Ouwerkerk, P. B. F., Menke, F. L. H., and Memelink, J. (1999). The promoter of the strictosidine synthase gene from periwinkle confers elicitor-inducible expression in transgenic tobacco and binds nuclear factors GT-1 and GBF. *Plant Molecular Biology* **39**: 1299-1310.

Pauli, H. H., and Kutchan, T. M. (1998). Molecular cloning and functional heterologous expression of two alleles encoding (*S*)-*N*-methylcoclaurine 3'-hydroxylase (CYP80B1), a new methyl jasmonate-inducible cytochrome P450-dependent mono-oxygenase of benzylisoquinoline alkaloid biosynthesis. *The Plant Journal* **13**: 793-801.

Pelletier, S. W. (1983). The nature and definition of an alkaloid. In S. W. Pelletier (ed), *Alkaloids; Chemical and Biological Perspectives*, pp. 1-32. New York: John Wiley & Sons.

Perez-Amador, M. A., Carbonell, J., and Granell, A. (1995). Expression of arginine decarboxylase is induced during early fruit development and in young tissues of *Pisum sativum* (L). *Plant Molecular Biology* **28**: 997-1009.

Pinol, M. T., Palazon, J., Altabella, T., and Serrano, M. (1987). Correlation between K^+ content, activities of arginine and ornithine decarboxylase, and levels of putrescine and nicotine in cultured tobacco callus. *Physiologia Plantarum* **69**: 221-226.

Pinol, M. T., Palazon, J., Cusido, R. M., and Ribo, M. (1999). Influence of calcium ion-concentration in the medium on tropane alkaloid accumulation in *Datura stramonium* hairy roots. *Plant Science* **141**: 41-49.

Poulsen, C., Goddijn, O. J. M., Hoge, J. H. C., and Verpoorte, R. (1994). Anthranilate synthase and chorismate mutase activities in transgenic tobacco plants overexpressing tryptophan decarboxylase from *Catharanthus roseus*. *Transgenic Research* **3**: 43-49.

Primikirios, N. I., and Roubelakis-Angelakis, K. A. (1999). Cloning and expression of an arginine decarboxylase cDNA from *Vitis vinifera* L. cell-suspension cultures. *Planta* **208**: 574-582.

Primikirios, N. I., and Roubelakis-Angelakis, K. A. (2001). Indications for post-translational regulation of *Vitis vinifera* L. arginine decarboxylase. *Plant Molecular Biology* **45**: 669-678.

Proksch, P., and Ebel, R. (1998). Ecological significant of alkaloids from marine invertebrates. In M. F. Roberts, and M. Wink (eds), *Alkaloids: Biochemistry, Ecology, and Medicinal Applications*. New York: Plenum Press.

Rastogi, R., Dulson, J., and Rothstein, S. J. (1993). Cloning of tomato (*Lycopersicon esculentum* Mill) arginine decarboxylase gene and its expression during fruit ripening. *Plant Physiology* **103**: 829-834.

Rhodes, M. J. C., Robins, R. J., Lindsay, E., Aird, H., Payne, A. J., Parr, A. J., and Walton, N. J. (1989). Regulation of secondary metabolism in transformed root cultures. In W. G. W. Kurz (ed), *Primary and Secondary Metabolism of Plant Cell Culture*, pp. 58-72. Berlin: Springer-Verlag.

Riechers, D. E., and Timko, M. P. (1999). Structure and expression of the gene family encoding putrescine *N*-methyltransferase in *Nicotiana tabacum*: new clues to the evolutionary origin of cultivated tobacco. *Plant Molecular Biology* **41**: 387-401.

Robbins, M. P., Bavage, A. D., Strudwicke, C., and Morris, P. (1998). Genetic manipulation of condensed tannins in higher plants. *Plant Physiology* **116**: 1133-1144.

Roberts, M. F., and Wink, M. (1998). Introduction. In M. F. Roberts, and M. Wink (eds), *Alkaloids: Biochemistry, Ecology, and Medicinal Applications*, pp. 1-7. New York: Plenum Press.

Robins, R. J., Hamill, J. D., Parr, A. J., Smith, K., Walton, N. J., and Rhodes, M. J. C. (1987). Potential for use of nicotinic acid as a selective agent for isolation of high nicotine-producing lines of *Nicotiana rustica* hairy root cultures. *Plant Cell Reports* **6**: 122-126.

Robins, R. J., Parr, A. J., Payne, J., Walton, N. J., and Rhodes, M. J. C. (1990). Factors regulating tropane-alkaloid production in a transformed root culture of a *Datura candida* X *Datura aurea* hybrid. *Planta* **181**: 414-422.

Robins, R. J., Bent, E. G., and Rhodes, M. J. C. (1991a). Studies on the biosynthesis of tropane alkaloids by *Datura stramonium* L. transformed root cultures 3. The relationship between morphological integrity and alkaloid biosynthesis. *Planta* **185**: 385-390.

Robins, R. J., Parr, A. J., and Walton, N. J. (1991b). Studies on the biosynthesis of tropane alkaloids in *Datura stramonium* L. transformed root cultures 2. On the relative contributions of L-arginine and L-ornithine to the formation of the tropane ring. *Planta* **183**: 196-201.

Robins, R. J., Parr, A. J., Bent, E. G., and Rhodes, M. J. C. (1991c). Studies on the biosynthesis of tropane alkaloids in *Datura stramonium* L. transformed root cultures 1. The kinetics of alkaloid production and the influence of feeding intermediate metabolites. *Planta* **183**: 185-195.

Robins, R. J., Walton, N. J., Parr, A. J., Lindsay, E., Aird, H., Rhodes, M. J. C., and Hamill, J. D. (1994). Progress in the genetic engineering of the pyridine and tropane alkaloid biosynthetic pathways of Solanaceous plants. In B. E. Ellis, G. W. Kuroki, and H. A. Stafford (eds), *Recent advances in Phytochemistry; Genetic Engineering of Plant Secondary Metabolism* **28**: 1-33.

Romeike, A. (1978). Tropane alkaloids; occurrence and systematic importance in angiosperms. *Botanicle Notices* **131**: 85-96.

Rosco, A., Pauli, H. H., Priesner, W., and Kutchan, T. M. (1997). Cloning and heterologous expression of NADPH-cytochrome P450 reductases from the Papaveraceae. *Archives of Biochemistry & Biophysics* **348**: 369-377.

Roy, M., and Wu, R. (2001). Arginine decarboxylase transgene expression and analysis of environmental stress tolerance in transgenic rice. *Plant Science* **160**: 869-875.

Ruiz, O. A., Bortolotti, C., Masgrau, C., Tiburcio, A. F., and Altabella, T. (2000). Molecular forms of arginine decarboxylase in oat leaves. *Physiologia Plantarum* **108**: 370-375.

Saito, K. and Murakoshi, I. (1998). Genes in alkaloid metabolism. In M. F. Roberts, and M. Wink (eds), *Alkaloids: Biochemistry, Ecology, and Medicinal Applications*, pp. 147-157. New York: Plenum Press.

Saito, K., Murakoshi, I., Inze, D., and Van Montagu, M. (1989). Biotransformation of nicotine alkaloids by tobacco shooty teratomas induced by a Ti plasmid mutant. *Plant Cell Reports* **7**: 607-610.

Saitoh, F., Noma, M., and Kawashima, N. (1985). The alkaloid contents of sixty *Nicotiana* species. *Phytochemistry* **24**: 477-480.

Sambrook, J., Futisch, E. F., and Maniatis, T. (1989). *Molecular Cloning: A Laboratory Manual*. Cold Spring Habor Laboratory Press.

Sandler, S. J., Stayton, M., Townsend, J. A., Ralston, M. L., Bedbrook, J. R., and Dunsmuir, P. (1988). Inhibition of gene expression in transformed plants by antisense RNA. *Plant Molecular Biology* **11**: 301-310.

Sato, F., Hashimoto, T., Hachiya, A., Tamura, K., Choi, K., Morishige, T., Fujimoto, H., and Yamada, Y. (2001). Metabolic engineering of plant alkaloid biosynthesis. *Proceedings of the National Academy of Sciences of the United States of America* **98**: 367-372.

Saunders J. A. and Blume, D. (1981). Quantitation of major tobacco alkaloids by high-performance liquid chromatography. *Journal of Chromatography* **205**: 147-154.

Saunders J. W. and Bush, L. P. (1979). Nicotine biosynthetic enzyme activities in *Nicotiana tabacum* L. genotypes with different alkaloid levels. *Plant Physiology* **64**: 236-240.

Schmeller, T., and Wink, M. (1998). Utilization of alkaloids in modern medicine. In M. F. Roberts, and M. Wink (eds), *Alkaloids: Biochemistry, Ecology, and Medicinal Applications*, pp. 435-459. New York: Plenum Press.

Schroder, G., Unterbusch, E., Kaltenbach, M., Schmidt, J., Strack, D., De Luca, V., and Schroder, J. (1999). Light-induced cytochrome P450-dependent enzyme in indole alkaloid biosynthesis: tabersonine 16-hydroxylase. *FEBS Letters* **458**: 97-102.

Sharma, V., Grubmeyer, C., and Sacchettini, J. C. (1998). Crystal structure of quinolinic acid phosphoribosyltransferase from *Mycobacterium tuberculosis*: a potential drug target. *Structure* **6**: 1587-1599.

Shoji, T., Yamada, Y., and Hashimoto, T. (2000a). Jasmonate induction of putrescine *N*-methyltransferase genes in root of *Nicotiana sylvestris*. *Plant & Cell Physiology* **41**: 831-839.

Shoji, T., Nakajima, K., and Hashimoto, T. (2000b). Ethylene suppresses jasmonate-induced gene expression in nicotine biosynthesis. *Plant & Cell Physiology* **41**: 1072-1076.

Sinclair, S. J., Murphy, K. J., Birch, C. D., and Hamill, J. D. (2000). Molecular characterization of quinolinate phosphoribosyltransferase (QPRTase) in *Nicotiana*. *Plant Molecular Biology* **44**: 603-617.

Sinclair, S. J., and Hamill, J. D. (2002). Wound-responsive regulation of gene expression in *Nicotiana* species suggests novel insights into the control of pyridine alkaloid biosynthesis. *Planta* (under review).

Sisson, V. A., and Severson, R. F. (1990). Alkaloid composition of the *Nicotiana* Species. *Beitrage zur Tabakforschung International* **14**: 327-339.

Sivamani, E., Bassie, L., Christou, P., and Capell, T. (2001). Development of a novel gene transfer system for *Cajanus cajan* and expression of a monocot arginine decarboxylase cDNA in transformed cell lines. *Plant Physiology and Biochemistry* **39**: 575-582.

Slocum, R. D. (1991). Polyamine biosynthesis in plants. In R. D. Slocum, and H. E. Flores (eds), *CRC Biochemistry and Physiology of Polyamines in Plants*, pp: 23-40. Boca Raton: CRC Press.

Slocum, R. D., and Galston, A. W. (1985a). *In-vivo* inhibition of polyamine biosynthesis and growth in tobacco ovary tissues. *Plant & Cell Physiology* **26**: 1519-1526.

Slocum, R. D., and Galston, A. W. (1985b). Arginase-mediated hydrolysis of DFMA to DFMO *in vivo*. *Plant Physiology* **77** Suppl: S45.

Slocum, R. D., Kaur-Sawhney, R., and Galston, A. W. (1984). The physiology and biochemistry of polyamines in plants. *Archives of Biochemistry and Biophysics*. **235**: 283-303.

Slocum, R. D., Bitonti, A. J., McCann, P. P., and Feirer, R. P. (1988). DL-α-difluoromethyl [3,4-^{3}H] arginine metabolism in tobacco and mammalian cells; inhibition of ornithine decarboxylase activity after arginase-mediated hydrolysis of DL-α-difluoromethylarginine to DL-α-difluoromethylornithine. *Biochemical Journal* **255**: 197-202.

Smith, C. J. S., Watson, C. F., Ray, J., Bird, C. R., Morris, P. C., Schuch, W., and Grierson, D. (1988). Antisense RNA inhibition of polygalacturonase gene expression in transgenic tomatoes. *Nature* **334**: 724-726.

Songstad, D. D., De Luca, V., Brisson, N., Kurz, W. G. W., and Nessler, C. L. (1990). High levels of tryptamine accumulation in transgenic tobacco expressing tryptophan decarboxylase. *Plant Physiology* **94**: 1410-1413.

Songstad, D. D., Kurz, W. G. W., and Nessler, C. L. (1991). Tyramine accumulation in *Nicotiana tabacum* transformed with a chimeric tryptophan decarboxylase gene. *Phytochemistry* **30**: 3245-3246.

Southon, I. W., and Buckingham, J. (eds) (1989). *Dictionary of Alkaloids*. London: Chapman and Hall.

Soyka, S., and Heyer, A. G. (1999). *Arabidopsis* knockout mutation of *ADC2* gene reveals inducibility by osmotic stress. *FEBS Letters* **458**: 219-223.

St Pierre, B., Laflamme, P., Alarco, A. M., De Luca, V. (1998). The terminal O-acetyltransferase involved in vindoline biosynthesis defines a new class of proteins responsible for coenzyme A-dependent acyl transfer. *The Plant Journal* **14**: 703-713.

Suzuki, K., Yamada, Y., and Hashimoto, T. (1999). Expression of *Atropa belladonna* putrescine *N*-methyltransferase gene in root pericycle. *Plant & Cell Physiology* **40**: 289-297.

Takayama, K. M., and Inouye, M. (1990). Antisense RNA. *Critical reviews in Biochemical and Molecular Biology* **25**: 155-184.

Takeshita, N., Fujisawa, H., Miura, H., Fitchen, J. H., Yamada, Y., and Sato, F. (1995). Molecular cloning and characterization of *S*-adenosyl-L-methionine:scoulerine-9-O-methyltransferase from cultured *Coptis japonica* cells. *Plant & Cell Physiology* **36**: 29-36.

Taylor, G. R. (1991). Polymerase chain reaction: basic principles and automation. In M. J. McPhersom, P. Quirke and G. R. Taylor (eds), *PCR: A practical Approach*, pp. 1-14. New York: Oxford University Press.

Taylor, M. A., Mad Arif, S. A., Kumar, A., Davies, H. V., Scobie, L. A., Pearce, S. R., and Flavell, A. J. (1992). Expression and sequence analysis of cDNAs induced during the early stages of tuberisation in different organs of the potato plant (*Solanum tuberosum* L.). *Plant Molecular Biology* **20**: 641-651.

Tepfer, D. (1984). Transformation of several species of higher plants by *Agrobacterium rhizogenes*: Sexual transmission of the transformed genotype and phenotype. *Cell* **37**: 959-968.

Thomas, J. C., Adams, D. G., Nessler, C. L., Brown, J. K., and Bohnert, H. J. (1995). Tryptophan decarboxylase, tryptamine, and reproduction of the whitefly. *Plant Physiology* **109**: 717-720.

Tiburcio, A. F., and Galston, A. W. (1986). Arginine decarboxylase as the source of putrescine for tobacco alkaloids. *Phytochemistry* **25**: 107-110.

Tiburcio, A. F., Kaur-Sawhney, R., Ingersoll, R. B., and Galston, A. W. (1985). Correlation between polyamines and pyrrolidine alkaloids in developing tobacco callus. *Plant Physiology* **78**: 323-326.

Tiburcio, A. F., Kaur Sawhney, R., and Galston, A. W. (1987). Effect of polyamine biosynthetic inhibitors on alkaloids and organogenesis in tobacco callus cultures. *Plant Cell Tissue & Organ Culture* **9**: 111-120.

Tiburcio, A. F., Altabella, T., Borrell, A., and Masgrau, C. (1997). Polyamine metabolism and its regulation. *Physiologia Plantarum* **100**: 664-674.

Toth, C., and Coffino, P. (1999). Regulated degradation of yeast ornithine decarboxylase. *The Journal of Biological Chemistry* **274**: 25921-25926.

Tsai, H. F., Wang, H., Gebler, J. C., Poulter, C. D., and Schardl, C. L. (1995). The *Claviceps purpurea* gene encoding dimethylallyltryptophan synthase, the committed step for ergot alkaloid biosynthesis. *Biochemical & Biophysical Research Communications* **216**: 119-125.

Tudzynski, P., Holter, K., Correia, T., Arntz, C., Grammel, N., and Keller, U. (1999). Evidence for an ergot alkaloid gene cluster in *Claviceps purpurea*. *Molecular & General Genetics* **261**: 133-141.

Tyler, V. E., Brady, L. R., and Robbers, J. E. (1981). *Pharmacognosy* (8th edn). Philadelphia: Lea & Febiger.

Unterlinner, B., Lenz, R., and Kutchan, T. M. (1999). Molecular cloning and functional expression of codeinone reductase: the penultimate enzyme in morphine biosynthesis in the opium poppy *Papaver somniferum*. *The Plant Journal* **18**: 465-475.

van der Krol, A. R., Lenting, P. E., Veenstra, J., van der Meer, I. M., Koes, R. E., Gerats, A. G. M., Mol, J. N. M., and Stuitje, A. R. (1988). An antisense chalcone synthase gene in transgenic plants inhibits flower pigmentation. *Nature* **333**: 866-869.

van der Krol, A. R., Mur, L. A., de Lange, P., Mol, J. N. M., and Stuitje, A. (1990). Inhibition of flower pigmentation by antisense CHS genes: promoter and minimal sequence requirements for the antisense effects. *Plant Molecular Biology* **14**: 457-466.

Vance ,V., and Vaucheret, H. (2001). RNA silencing in plants – defense and counter defence. *Science* **292**: 2277–2280.

Vazquez-Flota, F., De Carolis, E., Alarco, A., and De Luca, V. (1997). Molecular cloning and characterization of desacetoxyvindoline-4-hydroxylase, a 2-oxoglutarate dependent-dioxygenase involved in the biosynthesis of vindoline in *Catharanthus roseus* (L.) G. Don. *Plant Molecular Biology* **34**: 935-948.

Verpoorte, R. (1998). Antimicrobially active alkaloids. In M. F. Roberts, and M. Wink (eds), *Alkaloids: Biochemistry, Ecology, and Medicinal Applications*, pp. 397-433. New York: Plenum Press.

Verwoerd, T. C., Dekker, B. M. M., and Hoekema, A. (1989). A small-scale procedure for rapid isolation of plant RNA's. *Nucleic Acids Research* **27**: 2362.

Vetter, H., Mangold, U., Schroder, G., Marner, F., Werck-Reichhart, D., and Schroder, J. (1992). Molecular analysis and heterologous expression of an inducible cytochrome P-450 protein from periwinkle (*Catharanthus roseus* L.). *Plant Physiology* **100**: 998-1007.

Voelckel, C., Krugel, T., Gase, K., Heidrich, N., van Dam, N. M., Winz, R., and Baldwin, I. T. (2001). Antisense expression of putrescine N-methyltransferase confirms defensive role of nicotine in *Nicotiana sylvestris* against *Manduca sexta*. *Chemoecology* **11**: 121-126.

Wagner, R., and Wagner, K. G. (1985). The pyridine-nucleotide cycle in tobacco: Enzyme activities for the *de novo* synthesis of NAD. *Planta* **165**: 532-537.

Wagner, R., Feth, F., and Wagner, K. G. (1986a). The pyridine-nucleotide cycle in tobacco: Enzyme activities for the recycling of NAD. *Planta* **167**: 226-232.

Wagner, R., Feth, F., and Wagner, K. G. (1986b). Regulation in tobacco callus of enzyme activities of the nicotine pathway II. The pyridine-nucleotide cycle. *Planta* **168**: 408-413.

Wagner, R., Feth, F., and Wagner, K. G. (1986c). The regulation of enzyme activities of the nicotine pathway in tobacco. *Physiologia Plantarum* **68**: 667-672.

Walden, R., Cordeiro, A., and Tiburcio, A. F. (1997). Polyamines: small molecules triggering pathways in plant growth and development. *Plant Physiology* **113**: 1009-1013.

Waller, G. R., and Nowacki, E. K. (1978). *Alkaloids Biology and Metabolism in Plants*. New York: Plenum Press.

Wallstrom, E. L., and Persson, L. (1999). No role of the 5' untranslated region of ornithine decarboxylase mRNA in the feedback control of the enzyme. *Molecular & Cellular Biochemistry* **197**: 71-78.

Walton, N. J., and Belshaw, N. J. (1988). The effect of cadaverine on the formation of anabasine from lysine in hairy root cultures of *Nicotiana hesperis*. *Plant Cell Reports* **7**: 115-118.

Walton, N. J., Robins, R. J., and Rhodes, M. J. C. (1988). Perturbation of alkaloid production by cadaverine in hairy root cultures of *Nicotiana rustica*. *Plant Science* **54**: 125-131.

Walton, N. J., Robins, R. J., and Peerless, A. C. J. (1990). Enzymes of *N*-methylputrescine biosynthesis in relation to hyoscyamine formation in transformed root cultures of *Datura stramonium* and *Atropa belladonna*. *Planta* **182**: 136-141.

Walton, N. J., Peerless, A. C. J., Robins, R. J., Rhodes, M. J. C., Boswell, H. D., and Robins, D. J. (1994). Purification and properties of putrescine *N*-methyltransferase from transformed roots of *Datura stramonium* L. *Planta* **193**: 9-15.

Wang, J. M., Sheehan, M., Brookman, H., and Timko, M. P. (2000). Characterization of cDNAs differentially expressed in roots of tobacco (*Nicotiana tabacum* cv. Burley 21) during the early stages of alkaloid biosynthesis. *Plant Science* **158**: 19-32.

Waterhouse, P. M., Graham, M. W., and Wang, M. B. (1998). Virus resistance and gene silencing in plants is induced by double-stranded RNA. *Proceedings of the National Academy of Sciences of the United States of America*. **95**: 13959-13964.

Waterhouse, P. M., Wang M. B., and Lough, T. (2001). Gene silencing as an adaptive defence against viruses. *Nature* **411**: 834–842.

Waterman, P. G. (1998). Chemical taxonomy of alkaloids. In M. F. Roberts, and M. Wink (eds), *Alkaloids: Biochemistry, Ecology, and Medicinal Applications*, pp. 87-107. New York: Plenum Press.

Watson, M. B., and Malmberg, R. L. (1996). Regulation of *Arabidopsis thaliana* (L) Heynh arginine decarboxylase by potassium deficiency stress. *Plant Physiology* **111**: 1077-1083.

Watson, M. B., Yu, W., Galloway, G., and Malmberg, R. L. (1997). Isolation and characterization of a second arginine decarboxylase cDNA from *Arabidopsis* (accession no. AF009647) (PRG 97-114). *Plant Physiology* **114**: 1569.

Watson, M. B., Emory, K. K., Piatak, R. M., and Malmberg, R. L. (1998). Arginine decarboxylase (polyamine synthesis) mutants of *Arabidopsis thaliana* exhibit altered root growth. *The Plant Journal* **13**: 231-239.

Wesley, S. V., Helliwell, C. A., Smith, N. A., Wang, M., Rouse, D. T., Liu, Q., Gooding, P. S., Singh, S. P., Abbott, D., Stoutjesdijk, P. A., Robinson, S. P., Gleave, A P., Green, A. G., and Waterhouse, P. M. (2001). Construct design for efficient, effective and high-throughput gene silencing in plants. *The Plant Journal* **27**: 581-590

Wink, M. (1983a). Inhibition of seed germination by quinolizidine alkaloids; aspects of allelopathy in *Lupinus albus* L. *Planta* **158**: 365-368.

Wink, M. (1983b). Wounding-induced increase of quinolizidine alkaloid accumulation in lupin leaves. *Z. Naturforch.* **38c**: 905-909.

Wink, M. (1997). Special nitrogen metabolism. In P. M. Dey, and J. B. Harborne (eds), *Plant Biochemistry*, pp: 439-486. San Diego: Academic Press.

Wink, M. (1998a). A short history of alkaloids. In M. F. Roberts, and M. Wink (eds), *Alkaloids: Biochemistry, Ecology, and Medicinal Applications*, pp. 11-44. New York: Plenum Press.

Wink, M. (1998b). Chemical ecology of alkaloids. In M. F. Roberts, and M. Wink (eds), *Alkaloids: Biochemistry, Ecology, and Medicinal Applications*, pp. 265-300. New York: Plenum Press.

Wink, M. (1998c). Modes of action of alkaloids. In M. F. Roberts, and M. Wink (eds), *Alkaloids: Biochemistry, Ecology, and Medicinal Applications*, pp. 301-326. New York: Plenum Press.

Wink, M., and Roberts, M. F. (1998). Compartmentation of alkaloid synthesis, transport, and storage. In M. F. Roberts, and M. Wink (eds), *Alkaloids: Biochemistry, Ecology, and Medicinal Applications*, pp. 239-262. New York: Plenum Press.

Wink, M., Heinen, H. J., Vogt, H., and Schiebel, H. M. (1984). Cellular localization of quinolizidine alkaloids by laser desorption mass spectrometry (LAMMA 1000). *Plant Cell Reports* **3**: 230-233.

Wink, M., Schmeller, T., and Latz-Bruning, B. (1998). Modes of action of allelochemical alkaloids: Interaction with neuroreceptors, DNA, and other molecular targets. *Journal of Chemical Ecology* **24**: 1881-1937.

Winz, R. A., and Baldwin, I. T. (2001). Molecular interactions between the specialist herbivore *Manduca sexta* (Lepidoptera, Sphingidae) and its natural host *Nicotiana attenuata*. IV. Insect-induced ethylene reduces jusmonate-induced nicotine accumulation by regulating putrescine N-methyltransferase transcripts. *Plant Physiology* **125**: 2189-2202.

Yao, K., De Luca, V., and Brisson, N. (1995). Creation of a metabolic sink for tryptophan alters the phenylpropanoid pathway and the susceptibility of potato to *Phytophthora infestans*. *Plant Cell* **7**: 1787-1799.

Yoshida, D. (1969). Formation of putrescine from ornithine and arginine in tobacco plants. *Plant & Cell Physiology* **10**: 393-397.

Yoshida, D., and Mitake, T. (1966). Agmatine and *N*-carbamylputrescine as intermediates in the formation of nicotine by tobacco plants. *Plant & Cell Physiology* **7**: 301-305.

Yun, D., Hashimoto, T., and Yamada, Y. (1992). Metabolic engineering of medicinal plants: Transgenic *Atropa belladonna* with an improved alkaloid composition. *Proceedings of the National Academy of Sciences of the United States of America* **89**: 11799-11803.

Yun, D., Hashimoto, T., and Yamada, Y. (1993). Transgenic tobacco plants with two consecutive oxidation reactions catalyzed by hyoscyamine 6β-hydroxylase. *Bioscience Biotechnology & Biochemistry* **57**: 502-503.

Zhang, Z. P., and Baldwin, I. T. (1997). Transport of [2-^{14}C]jasmonic acid from leaves to roots mimics wound-induced changes in endogenous jasmonic acid pools in *Nicotiana sylvestris*. *Planta* **203**: 436-441.